

Abstract:

Background - In the recent wars, 77% of all British casualties received extremity injuries. The critical nature of these injuries resulted in amputations to preserve life, when the limb itself was potentially salvageable. In response, the present research has focussed on development of new technology to reduce amputations by preserving tissue viability.

Materials and Methods - Novel technology was developed including; a dual-bladder pneumatic tourniquet; a cooling sock to reduce tissue temperature; and a perfusion support system to perfuse the limb independently of systemic circulation in hospital. Testing involved laboratory protocols, mimetic of the combat setting. The cooling sock and limb support system were tested using disarticulated porcine and ovine limbs. Techniques were employed to assess the impact of these technologies, including implanted thermistors, doppler flow, infrared scanning and neural stimulation. In ovine limbs histology and blood gas analysis was also studied

Results – Topical CO₂ cooling was associated with deep cooling similar to ice packing, so was utilised while transporting disarticulated porcine limbs reducing deep tissue temperature by between 7.26-15.88°C. The limbs underwent neural stimulation to assess muscle contraction, showing twitch at procedure termination in 2 of the 3 intervention limbs but none of the control limbs. This work was repeated using disarticulated ovine limbs. There were 4 arms in this element; cooled – perfused, non-cooled – perfused, cooled – non-perfused and non-cooled – non-perfused. Deep tissue temperature reduction was very similar between the cooled and non-cooled tests (5.86±3.34°C and 5.23±0.28°C respectively). Baseline nerve stimulation showed that contraction was present in all limbs, however, at the end, contraction was detected only in perfused limbs.

Discussion and Conclusions - Overall, these studies demonstrate that the benefit of cooling was less than expected, but, perfusing the limbs preserved tissue viability. The limb stabilisation technology has a clear tissue preserving effect and offers promise as a technology that can be of benefit to personnel injured in austere situations.



Development of a Novel Multi-Stage Limb Salvage Technology for the optimisation of tissue viability in severely injured limbs

Joanne Morton

PhD Biomedical Engineering

Department of Biomedical Engineering

Primary Supervisor: Professor Terry Gourlay

Secondary Supervisor: Dr Craig Robertson

Year of Submission: 2020

Declaration of Authenticity and Author's Rights:

'This thesis is the result of the author's original research. It has been composed by the author and has not been previously submitted for examination which has led to the award of a degree.'

'The copyright of this thesis belongs to the author under the terms of the United Kingdom Copyright Acts as qualified by University of Strathclyde Regulation 3.50. Due acknowledgement must always be made of the use of any material contained in, or derived from, this thesis.'

Signed: *J.V. Motson*

Date: *06/11/2020*

Acknowledgements:

I would like express my sincere gratitude to my supervisor Professor Terry Gourlay for his invaluable knowledge, advice and guidance over the period of my PhD.

I would also like to specially thank Dr Craig Robertson, Dr Craig Simpson and Dr Paul Davis for their input, technical guidance and for their assistance at every stage of the project.

Finally, I am grateful to the EPSRC for providing my studentship which enabled me to undertake this PhD.

Table of Contents:

Abstract:.....	I
Declaration of Authenticity and Author’s Rights:	III
Acknowledgements:.....	IV
Table of Contents:.....	V
List of Figures:	XI
List of Tables:	XVIII
Chapter 1. Combat Injury Overview:	1
1.1. Combat Injury Characteristics:.....	1
1.2. Mechanism of injury:	4
1.3. Combat Casualty Care:.....	9
1.3.1. Considerations for Air Evacuation:	18
1.4. Amputation vs Limb Salvage:.....	21
1.4.1. Post Amputation Complications:	21
1.4.2. Predicted Costs of OIF/OEF amputations:	25
1.4.3. Benefits of Limb Salvage:	26
1.4.4. Limb Salvage Techniques:	27
1.5. Future Therapies:	30
1.5.1. Haemorrhage Control:	30

1.5.2.	Resuscitation Control:.....	33
1.5.3.	Regenerative Medicine:.....	38
Chapter 2.	Thesis objectives and hypothesis:.....	39
2.1.	Proposed Technology:.....	39
2.2.	Thesis hypothesis:.....	41
Chapter 3.	Tourniquet Design:.....	42
3.1.	Overview of Tourniquets:.....	42
3.1.1.	Current Tourniquet Use:.....	42
3.1.2.	Tourniquet Considerations:.....	45
3.1.3.	Tourniquet complications:.....	48
3.2.	Design Considerations:.....	53
3.3.	Design of dual-outlet valve:.....	57
3.4.	Initial Tourniquet Design:.....	59
3.5.	Design Alterations:.....	61
3.5.1.	Second Iteration Tourniquet:.....	61
3.5.2.	Third Iteration Tourniquet:.....	62
3.5.3.	Fourth Iteration Tourniquet:.....	63
3.5.4.	Fifth Iteration Tourniquet:.....	65
3.5.5.	Sixth Iteration Tourniquet:.....	68
3.5.6.	Seventh Iteration Tourniquet:.....	71
3.6.	Future developments:.....	73

Chapter 4.	Cooling sock design:.....	75
4.1.	Benefits of therapeutic hypothermia:	75
4.2.	Design considerations:	82
4.3.	Feasibility maths:	84
4.4.	Initial design:.....	88
4.4.1	Preliminary temperature testing:	90
4.5.	Second iteration:.....	91
4.5.1.	Design alterations:	91
4.5.2.	Temperature testing:	94
4.6.	Third iteration:	96
4.6.1.	Design alterations:	96
4.6.2.	Temperature testing:	98
4.7.	Fourth iteration:.....	101
4.7.1.	Design alterations:	101
4.7.2.	Temperature testing:	102
4.8.	Fifth iteration:	103
4.8.1.	Design alterations:	103
4.8.2.	Temperature testing:	105
4.9.	Sixth iteration:.....	108
4.9.1.	Design Alterations:.....	108
4.9.2.	Temperature Testing:.....	110

4.10.	Iteration 6.2:	113
4.10.1.	Protocol development:	113
4.10.2.	Design of iteration 6.2:.....	116
4.11.	Seventh Iteration:	119
4.12.	Eighth iteration:	122
Chapter 5.	Small-scale tissue testing:	125
5.1.	Justification for testing:	125
5.2.	Testing protocol:	127
5.3.	Results:.....	131
5.3.1.	2 initial bottles of CO ₂ :	131
5.3.2.	3 initial bottles of CO ₂ :	134
5.3.3.	Ice:.....	138
5.3.4.	No cooling:	142
5.3.5.	Comparison of cooling methods:.....	146
5.4.	Discussion of results:.....	154
Chapter 6.	Testing of technology in simulated combat setting – porcine tissue:	160
6.1.	Testing protocol:	160
6.2.	Justification of methods of analysis:.....	168
6.3.	Results:.....	172
6.3.1.	Temperature changes:	172
6.3.2.	LDI and thermal camera images:	177

6.3.1.1.	<i>Porcine limb Test 4:</i>	178
6.3.1.2.	<i>Porcine limb Test 5:</i>	180
6.3.1.3.	<i>Porcine limb Test 6:</i>	186
6.3.2.	Neural Stimulation:	192
6.4.	Results analysis:	194
6.4.1.	Temperature changes:	194
6.4.2.	LDI and thermal camera data:	198
6.4.3.	Neural Stimulation:	200
6.5.	Future considerations:	202
6.5.1.	Limb cooling:	202
6.5.2.	Perfusion:	203
6.5.3.	Methods of analysis:	203
6.5.4.	Experimental design:	204
Chapter 7.	Testing of technology in simulated combat setting – Ovine tissue:	206
7.1.	Justification of methods of analysis:	206
7.2.	Testing protocol:	212
7.2.1.	Cooling protocol:	212
7.2.2.	Perfusion protocol:	214
7.2.3.	Data collection protocol:	215
7.3.	Results:	219
7.3.1.	Cooled – perfused limbs:	219

7.3.2.	Non-cooled – perfused limbs:.....	236
7.3.3.	Cooled – non-perfused limbs:.....	253
7.3.4.	Non-cooled – non-perfused limbs:	257
7.3.5.	Cooling data:	260
7.4.	Results analysis:	264
7.5.	Future considerations:	278
Chapter 8.	Conclusions:	280
References:	XIII
Appendix 1	XXXI

List of Figures:

Figure 1-1: Loading a casualty into a Blackhawk Medivac helicopter, Helmand Province, Afghanistan, 2009. Defenceimagery.mod.uk, Crown copyright.....	18
Figure 1-2: Loading a casualty onto C-17, Bagram Air Field, Afghanistan, 2002. National Public Radio	18
Figure 3-1: CAD drawing and 3D printed dual way valve with inflation mechanism demonstrated	58
Figure 3-2: Dimensions of initial tourniquet.....	59
Figure 3-3: Individual parts and assembled connector.....	60
Figure 3-4: Initial tourniquet.....	60
Figure 3-5: Second iteration tourniquet	61
Figure 3-6: Dimensions of one tourniquet bladder	62
Figure 3-7: Third iteration of tourniquet	63
Figure 3-8: Dimensions of one bladder for fourth iteration tourniquet.....	64
Figure 3-9: 4 th iteration of tourniquet with two different colour bladders and Velcro holding them together.....	64
Figure 3-10: Dimensions of the fifth iteration of tourniquet.....	65
Figure 3-11: Completed fifth iteration of tourniquet	66
Figure 3-12: Dimensions of sixth iteration of tourniquet	68
Figure 3-13: Testing of tourniquet iteration 6 on the HapMed and a close-up of the results screen.....	70
Figure 3-14: Dimensions of the seventh iteration tourniquet.....	71
Figure 4-1: Experimental set up for testing 1 st iteration of cooling sock.....	89

Figure 4-2: Testing the porosity of the ePTFE tubing by flushing gas through submerged tubing	89
Figure 4-3: Temperature profile over 500 seconds using CO ₂ in 1 st iteration of cooling sock	90
Figure 4-4: Manifold used with 2 nd iteration of cooling sock.....	92
Figure 4-5: Arrangement of tubes in 2 nd iteration of cooling sock	93
Figure 4-6: 2 nd iteration of cooling sock both open and closed around the mannequin leg.	94
Figure 4-7: Location of the defined thermocouple positions on the mannequin limb	95
Figure 4-8: Temperature profile using iteration 2 over 500 seconds	95
Figure 4-9: Arrangement of tubes on 3 rd iteration	97
Figure 4-10: 3 graphs placed in chronological order showing the temperature profile over 20 minutes for the 3 rd iteration of cooling sock	100
Figure 4-11: New design of manifold and tube arrangement of 4 th iteration of cooling sock	101
Figure 4-12: Completed 4 th iteration cooling sock.....	102
Figure 4-13: Temperature profile over 20 minutes when using 4 th iteration of cooling sock on mannequin limb	103
Figure 4-14: 5 th iteration both open and zipped up.....	105
Figure 4-15: Temperature profile produced with 5 th iteration over 8 minutes.....	105
Figure 4-16: Temperature profile of 5th iteration over 20 minutes.....	107
Figure 4-17: Arrangement of non-porous tubing for 6 th iteration.....	109
Figure 4-18: Experimental set up using 6 th iteration cooling sock.....	109
Figure 4-19: Temperature profile produced over 20 minutes with 6th iteration	110

Figure 4-20: Temperature profile produced over 20 minutes using 6 th iteration with holes made in tubing	112
Figure 4-21: New positions for 4 thermocouple placements for testing 6 th iteration.....	113
Figure 4-22: Temperature profile over 45 minutes. One bottle of CO ₂ released at beginning of experiment.....	114
Figure 4-23: Temperature profile produced with 6 th iteration when releasing 10 seconds of CO ₂ every 5 minutes.....	115
Figure 4-24: Temperature profile for 6 th iteration when full bottle of CO ₂ released at beginning of experiment followed by 10 seconds every 5 minutes	116
Figure 4-25: Layout of non-porous tubing for smaller version of 6 th iteration.....	117
Figure 4-26: Location of thermocouples on mannequin arm	118
Figure 4-27: Temperature profile produced over 1 hour using shorter 6 th iteration cooling sock	118
Figure 4-28: Gas and coolant distribution mechanism	120
Figure 4-29: Arrangement of tubes and outlets in the seventh iteration of cooling sock ..	121
Figure 4-30: Completed seventh iteration of the cooling sock.....	121
Figure 4-31: Eighth iteration of cooling sock. Both open and closed as well as close ups of foot covering mechanism	123
Figure 5-1: Small-scale tissue test rig.....	127
Figure 5-2: Temperature change at each depth of tissue for 2 bottles of CO ₂ during the initial cooling period	131
Figure 5-3: Temperature change from 37°C temperature using 3 initial bottles of CO ₂ during initial cooling period	134

Figure 5-4: Temperature change at each tissue depth for 3 initial bottles of CO ₂ with a starting tissue temperature of 25°C.....	136
Figure 5-5: Temperature change at each tissue depth using ice with starting tissue temperature 37°C	138
Figure 5-6: Temperature change at each tissue depth from 25°C using ice.....	140
Figure 5-7: Temperature change at each tissue depth from 37°C with no active cooling mechanism.....	142
Figure 5-8: Temperature change at each tissue depth rom 25°C with no active cooling applied	144
Figure 5-9: Mean temperature change at each tissue level using the 3 different topical cooling methods starting at 37°C	146
Figure 5-10: Mean temperature change at each tissue level using the 4 different topical cooling methods starting at 25°C.....	149
Figure 5-11: Temperature difference between the mean starting temperature and mean end temperature of the deep tissue in all cooling experiments.....	153
Figure 6-1: Cooling sock iteration 7.2 for use with CO ₂ and coolant fluid	162
Figure 6-2: Moor LDI imager taking an LDI scan and FLIR One Pro thermal camera used for thermal imaging. Images taken every 15 minutes during perfusion.....	164
Figure 6-3: Disarticulated porcine limb being perfused in the LSS with mean arterial pressure and flow rate displayed on screen. Red dot is the LDI scan being performed. Cannula is filled with primer fluid	165
Figure 6-4: Flow chart of the protocol for porcine limb tests.....	166
Figure 6-5: Temperature change in the deep tissue for the first 30 minutes of transportation for the 6 isolated porcine limb tests.....	174

Figure 6-6: Temperature change in the superficial tissue for first 30 minutes of transportation in the 6 isolated porcine limb tests.....	175
Figure 6-7: Temperature in the trotter injury for the first 30 minutes of transportation for the 6 isolated porcine limb tests.....	176
Figure 6-8: Change in mean flux in each ROI for porcine limb test 4	178
Figure 6-9: LDI images from porcine limb test 4.....	179
Figure 6-10: Pre-perfusion LDI scan for porcine limb test 5	180
Figure 6-11: Figure showing LDI scans for porcine limb test 5	181
Figure 6-12: Mean change in Flux in each ROI for porcine limb test 5.....	182
Figure 6-13: Pre-perfusion thermal camera photograph for porcine limb Test 5	183
Figure 6-14: Thermal camera images for porcine limb Test 5	184
Figure 6-15: Thermal camera spot data for the fifth porcine limb test.....	185
Figure 6-16: Porcine limb Test 6 pre-perfusion LDI scan.	186
Figure 6-17: Mean change in Flux for porcine limb Test 6	187
Figure 6-18: LDI images for porcine limb test 6.....	188
Figure 6-19: Pre-perfusion thermal photograph for porcine limb Test 6.....	189
Figure 6-20: Thermal camera images during perfusion for porcine limb Test 6	190
Figure 6-21: Thermal camera temperature data for porcine limb Test 6.....	191
Figure 7-1: Difference between porcine and ovine limb anatomy. Illustration by Dr Vanda Morton.....	207
Figure 7-2: Perfusion set up of the ovine limb.....	215
Figure 7-3: Left - Thermocouples placed in the muscle and the location of the electrode pads. Right upper – TrainFES neurostimulation equipment. Right lower – neurostimulation equipment in use	216

Figure 7-4: Flow chart of protocol for ovine limb tests	218
Figure 7-5: Mean flowrate and pressure for C-P limbs.....	224
Figure 7-6: Mean arterial blood gas data for C-P limbs	226
Figure 7-7: Mean venous blood gas data for C-P limbs	228
Figure 7-8: Example thermal camera spot point data for C-P 3 test	229
Figure 7-9: Example thermal camera images from C-P 3 0-75 minutes	230
Figure 7-10: Example thermal camera images from C-P 3 continued (90-120 minutes)	231
Figure 7-11: Example LDI data for C-P 3 (15-90 minutes).....	232
Figure 7-12: Example LDI data for C-P 3 continued (105 and 120 minutes).....	233
Figure 7-13: Example histology data for C-P 1. Images a, b and c are 3 slices of the tissue samples taken at each depth.	234
Figure 7-14: Mean pressure and flowrate over time for NC-P limb	241
Figure 7-15: Mean arterial blood gas data for C-P limbs	243
Figure 7-16: Mean venous blood gas data for C-P limbs	245
Figure 7-17: Example thermal camera spot point data for NC-P 4 test.....	246
Figure 7-18: Example thermal camera images from NC-P 4 test (0-75 minutes)	247
Figure 7-19: Example thermal images from NC-P 4 test continued (90-120 minutes).....	248
Figure 7-20: Example LDI data for NC-P 4 (15-90 minutes)	249
Figure 7-21: Example LDI data for NC-P 4 continued (105 and 120 minutes).....	250
Figure 7-22: Example histology for NC-P 1	251
Figure 7-23: Example thermal camera data for C-NP 3 test	255
Figure 7-24: Example thermal camera spot point data for C-NP 3 test.....	256
Figure 7-25: Anatomical picture of NC-NP 5 limb.....	257
Figure 7-26: Example thermal camera data for NC-NP 5 test.....	258

Figure 7-27: Example thermal camera spot point data for NC-NP 5 test	259
Figure 7-28: Start and end temperatures in the superficial tissue for all cooled tests	260
Figure 7-29: Start and end temperatures in the mid tissue for all cooled tests.....	261
Figure 7-30: Start and end temperatures in the deep tissue for all cooled tests.....	262
Figure 7-31: Mean temperature change in deep tissue for C and NC limbs.....	264
Figure 7-32: Demonstration of thermocouple location compared to muscle tissue depth. (Image not to scale)	267
Figure 7-33: Mean potassium concentration for C-P and NC-P tests.....	268
Figure 7-34: Mean arterial base excess for C-P and NC-P limbs.....	270
Figure 7-35: Mean arterial lactate concentration for C-P and NC-P limbs	270
Figure 7-36: Mean baseline and end of test amplitude needed to initiate twitch for each experimental condition.....	274

List of Tables:

Table 3-1: Recommended tourniquet inflation pressures based on limb occlusion pressure (Van der Spuy, 2012, Deloughry and Griffiths, 2009)	47
Table 3-2: Critical ischaemic time of various tissue types (Gillani et al., 2012, Perkins et al., 2012)	49
Table 3-3: Tourniquet pressure settings and when they should be used (Checketts, 2013, Jafarian et al., 2016, AnaesthesiaUK, 2005).....	54
Table 3-4: Pressure required to halt haemorrhage in tourniquet iteration 5	67
Table 3-5: Pressure required to halt haemorrhage in tourniquet iteration 6	69
Table 3-6: Pressure required to halt haemorrhage in tourniquet iteration 7	72
Table 4-1: Maximum temperature change at each location for 3 tests using third iteration with mean and SD	98
Table 4-2: Greatest initial temperature change at all limb locations for two tests using 5 th iteration sock	107
Table 5-1: Summary of the tests for each cooling mechanism.....	130
Table 5-2: Temperature change at the end of the cooling period for 2 initial bottles of CO ₂	133
Table 5-3: Tissue temperature change from 37°C at the end of secondary cooling period for 3 initial bottles of CO ₂	135
Table 5-4: Temperature change at end of cooling for three initial bottles at 25°C.....	137
Table 5-5: Temperature change at 46 minutes for each tissue depth using Ice at 37°C starting tissue temperature	139
Table 5-6: Temperature change at 46 minutes for each tissue depth using ice with 25°C starting tissue temperature	141

Table 5-7: Temperature change at 46 minutes for each tissue depth with no cooling and 37°C starting tissue temperature	143
Table 5-8: Temperature change at 46 minutes for each tissue depth with no cooling and 25°C starting tissue temperature	145
Table 5-9: Mean room temperature and both the starting and end temperature of the 3 tissue depths for all small-scale tissue tests	152
Table 6-1: Summary of porcine limbs collected and the conditions they were kept under	167
Table 6-2: Temperature change in porcine limbs over the duration of the total journey time from collection to the university	173
Table 6-3: Porcine limb test conditions and the outcome of neural stimulation	192
Table 7-1: Mean and standard deviation for weight, temperature and nerve stimulation data for cooled - perfused limbs	219
Table 7-2: Mean and standard deviation of perfusion data for cooled - perfused limbs....	221
Table 7-3: Mean and standard deviation of perfusion parameters for the C-P limbs.....	222
Table 7-4: Mean and standard deviation for perfusion parameters at each time point for C-P limbs.....	224
Table 7-5: Mean and standard deviation of arterial perfusion data at each time point for cooled perfused limbs.....	225
Table 7-6: Mean and standard deviation for venous perfusion data at each time point for cooled perfused limbs.....	227
Table 7-7: Histologist's notes for C-P 1	235
Table 7-8: Mean and standard deviation for weight, temperature and nerve stimulation data for non-cooled - perfused limbs	236

Table 7-9: Mean and standard deviation for perfusion data for non-cooled - perfused limbs	238
Table 7-10: Mean and standard deviation of perfusion parameters for the NC-P limbs	239
Table 7-11: Mean and standard deviation of perfusion parameters at each time point for NC-P limbs.....	240
Table 7-12: Mean and standard deviation of arterial perfusion data at each time point for non-cooled - perfused limbs	242
Table 7-13: Mean and standard deviation of venous perfusion data at each time point for non-cooled - perfused limbs	244
Table 7-14: Histologist's notes for NC-P 1.....	252
Table 7-15: Mean and standard deviation of weight, temperature and nerve stimulation data for cooled - non-perfused limbs	253
Table 7-16: Mean and standard deviation of weight, temperature and nerve stimulation data for non-cooled - non-perfused limbs	257
Table 7-17: Mean temperature change for cooled and non-cooled tests.....	263

Chapter 1. Combat Injury Overview:

1.1. Combat Injury Characteristics:

Traumatic lower extremity amputations caused by improvised explosive devices (IEDs) and traumatic brain injuries (TBIs) became the signature wounds of the recent wars in Afghanistan and Iraq (Morrison *et al.*, 2012, Perkins *et al.*, 2012, Wallace, 2012, Wojcik *et al.*, 2010, Lehman, 2008). In 2007 it was predicted that 17-22% of soldiers returning back to the United States could have a TBI, the majority of which were type 1 TBIs (the mildest form) received in battle (Wojcik *et al.*, 2010). A TBI can significantly hinder the rehabilitation of soldiers with other co-morbidities such as major tissue damage to the extremities as a decrease in mental capacity can make it harder to adapt to the rehabilitation needs of the other injuries. Throughout the conflicts in Iraq and Afghanistan, damage to the extremities was extremely frequent with 77% of all British casualties sustaining an extremity injury of some description (Chandler, MacLeod and Penn-Barwell, 2017). The most common injuries affecting the extremities were open wounds (42-63.7%), fractures (16.3-19.1%), burns (6.3%) and contusions (9.2%) (Amber L. Dougherty *et al.*, 2009, Zouris *et al.*, 2006, Ramasamy *et al.*, 2009). Fractures are often open which complicates the healing process and can lead to infection (Belmont, Schoenfeld and Goodman, 2010). When undertaking the different operations in Iraq during Operations Iraqi Freedom and New Dawn (referred to collectively from here as OIF) and in Afghanistan during Operation Enduring Freedom (OEF), 20-60% of US military casualties sustained multiple limb loss (Pasquina *et al.*, 2014). Over a 4-year period in Camp Bastion, Afghanistan, 169 casualties sustained 278 traumatic amputations (Morrison *et al.*, 2012). Lower extremity injuries were more likely to be coded serious to fatal when compared to upper extremity injuries (Amber L. Dougherty *et al.*, 2009). Whilst those soldiers with extremity injuries

surviving the incident were more likely to be evacuated to higher levels of care than those with injuries to other areas of the body, extremity injuries were less likely to prove fatal at the time of wounding (Amber L. Dougherty *et al.*, 2009). This shows that with prompt and effective care many extremity injuries are survivable.

Statistics show that more allied personnel wounded in combat are surviving their injuries than ever before. Whilst the percentage of soldiers killed in action during OIF and OEF has stayed roughly comparable to previous combat operations at 21%, the ratio of wounded to killed has increased dramatically (Morrison *et al.*, 2012). During World War I this ratio for US servicemen was 1.8:1, by Vietnam it had risen to 2.6:1. In 2007 during OIF this ratio was 16:1 (Lehman, 2008). This is because fewer soldiers are succumbing to their wounds once they have reached hospital. This increased survival rate is due to a multitude of factors.

The first is the introduction of Kevlar combat body armour in the 1970s (Ramasamy *et al.*, 2009). Kevlar body armour has proven to be very effective at reducing the number of injuries to the torso (Gawande, 2004, Ramasamy *et al.*, 2009, Robbins *et al.*, 2009). Secondly, the time taken for the injured soldier to reach medical care has decreased. During the conflict in Vietnam it could take between 4 and 6 hours for an injured soldier to reach a level III medical facility (Manring *et al.*, 2009). A level III medical facility is the most sophisticated medical facility in the warzone. The level III medical facility has specialist diagnostic technology e.g. CT scanners and is where more complex emergency surgery can be undertaken. In OIF/ OEF a casualty could reach a level III medical facility in as little as 30-90 minutes if the battle conditions were favourable i.e. not in the middle of a firefight (Manring *et al.*, 2009). The decrease in evacuation time enables the casualty to

undergo life-saving surgery much closer to the time of injury. Improved resuscitative strategies such as resuscitation with whole blood and increased use of tourniquets have also contributed to an increase in survival (Dharm-Datta *et al.*, 2011).

The use of whole blood as opposed to crystalloid fluids to replace fluid volume lost through major haemorrhage has been shown to improve casualty outcomes (David Brown, 2012). Since more soldiers are surviving their injuries, medical facilities are now faced with treating large numbers of patients with complex wound profiles. Indeed, from the start of operations in Afghanistan and Iraq (2001 and 2003 respectively) until September 2009, the Royal Centre for Defence Medicine in Birmingham received 44 unexpected survivors, defined as casualties with an injury severity score (ISS) of 60 or more (Evriviades *et al.*, 2010). The ISS is a numerical method of classifying the overall severity of injuries to multiple regions of the body (Baker *et al.*, 1974). It is calculated by assigning each injury a score of 1 to 5 with 5 being the most severe injury. The highest score of each of the three most severely injured regions is squared and then these 3 numbers are added together (Baker *et al.*, 1974).

Wounds resulting from explosive blasts have a high infection rate (Pasquina and Fitzpatrick, 2006). During the explosion debris and bacteria are forced deep into the wound bed and so can be difficult to remove, 23% of the injured US soldiers presenting at Landstuhl Regional Medical Centre, Germany, between 2009 and 2012 had an infection at their wound site (Stewart *et al.*, 2016). Whilst 39% of these infections were monomicrobial, consisting mainly of bacterial infections, 61% were polymicrobial infections (Stewart *et al.*, 2016). Patients with a higher ISS or who required admission to intensive care at Landstuhl were significantly more likely to have a polymicrobial

infection (Stewart *et al.*, 2016). Invasive fungal infections were particularly common in patients returning from injury in the Green Zone, Helmand Province, and could lead to the loss of large volumes of muscle tissue in response to the extensive debridement needed to remove all tissues contaminated by the fungus (Gordon *et al.*, 2015, Tribble and Rodriguez, 2014). This creates further challenges in their care. As well as complex open wounds to the extremities blast injuries present with many co-morbidities. These include fractures, traumatic brain injury, damage to the spinal cord, visual impairment and psychological issues (Pasquina and Fitzpatrick, 2006). The combination of these means that blast injuries lead to high levels of disability and impairment.

1.2. Mechanism of injury:

The two main causes of US combat injury in OIF and OEF were gunshot wounds and explosions, accounting for 19% and 79% respectively (Owens *et al.*, 2008). The proportion of casualties injured by gunshot compared to explosive mechanisms has switched between World War I and OEF/ OIF. In World War I 65% of all recorded combat casualties received their injuries by gunshot and in OIF and OEF this number varied between 16% and 23% (Belmont, Schoenfeld and Goodman, 2010). Explosive mechanisms encompass blasts, IEDs, mortar rounds, grenades, landmines, bombs and rocket propelled grenades (RPGs) (Owens *et al.*, 2008). Suicide bombers can also cause severe injuries to serving personnel (Manring *et al.*, 2009).

Injuries caused by IEDs accounted for 50.6% of all hostile action casualties received by a single British Iraqi field hospital between January and October 2006 (Ramasamy *et al.*, 2009). Data from the US Joint Theater Trauma Registry showed that between October 2001 to January 2005 IEDs

were responsible for 38% of combat casualties (Belmont, Schoenfeld and Goodman, 2010). IEDs are homemade explosive devices where the explosive material is utilised differently to conventional military means (Belmont, Schoenfeld and Goodman, 2010). The explosive material is either homemade or obtained from captured military explosives. IEDs are used to inflict maximum damage to the opposing military force with minimum damage to own fighters. Such devices can include buried artillery rounds, mines and vehicles packed with high explosives (Belmont, Schoenfeld and Goodman, 2010). Casualties exposed to an IED blast tend to receive multiple injuries, usually to more than one body segment. British IED casualties to an Iraqi field hospital in 2006 presented with a mean of 2.61 body regions affected compared to 2.05 body regions affected in gunshot wounds. Moreover, 67.8% of all injuries were to the extremities which suggests improved treatments are needed for extremity injuries (Ramasamy *et al.*, 2009).

Blast injuries present with a high proportion of severe limb injuries. These so called 'mangled limbs' have severe soft tissue damage often coupled with bone and vascular injuries (Gawande, 2004). A mangled limb is defined as a limb with damage to at least 3 systems, out of soft tissue, bone, nerves and vessels, which threatens limb viability and functionality (Patel, Richter and Shafi, 2015, Prasarn, Helfet and Kloen, 2012). Blast injuries occurring when the soldier is dismounted on foot patrol have been shown to lead to a higher number of amputations per casualty (Godfrey *et al.*, 2017, Cannon *et al.*, 2016). Fractures of the non-dominant arm are also common due to the position that the rifle is held during foot patrols (Cannon *et al.*, 2016). The severity of blast injuries relates to their ability cause injury in four ways linked to the different stages of the explosion.

Primary blast injuries are principally found in the gas-filled organs of the body. These injuries occur when the wave of overpressure caused by the blast reaches a person (Sayer *et al.*, 2008, Wolf *et al.*). Injury to the tympanic membrane can occur at pressures as low as 35kPa and so are the most common primary blast injury seen (Wolf *et al.*). However primary blast injuries can also cause significant damage to the lungs and the GI tract (Sayer *et al.*, 2008). Secondary blast injuries are caused by the propulsion of debris by the blast winds (Sayer *et al.*, 2008, Wolf *et al.*). Injury to the extremities are the most commonly seen secondary blast injuries (Evriviades *et al.*, 2010). Tertiary blast injuries are also caused by the blast winds. However, unlike in secondary blast injuries, it is the person being displaced or thrown by the blast wind (Sayer *et al.*, 2008, Wolf *et al.*). Quaternary blast injuries are injuries that result from the blast but without being caused by the blast winds or overpressure wave (Wolf *et al.*). These injuries include burns, crush injuries and exposure to toxic substances (Sayer *et al.*, 2008). Due to the many mechanisms of injury pertaining to a blast, casualties are often polytraumatic presenting with penetrating, blunt and burn injuries (Gawande, 2004, Sayer *et al.*, 2008).

Of the potentially survivable deaths in US Special Operations Forces (SOF), which occurred between October 2001 and November 2004, 82% were the result of haemorrhage (J. Holcomb *et al.*, 2007). Severe haemorrhage has many contributing factors to the death of a patient. Loss of blood volume can lead to haemorrhagic shock (Carr Jr, 2004). Haemorrhagic shock is a pathological state resulting in low blood pressure and decreased oxygen delivery (Bouglé, Harrois and Duranteau, 2013, National Trauma Institute). Inadequate perfusion can lead to tissue hypoxia, inflammation and ultimately organ failure (Bouglé, Harrois and Duranteau, 2013, National Trauma Institute). Arterial pressure is the factor which has the biggest role in altering tissue perfusion (Bouglé, Harrois and Duranteau, 2013). Haemorrhage can also lead to coagulopathy (National Trauma Institute). Coagulopathy is the disruption

of the blood coagulation process, likely to be due to the loss of platelets and other clotting factors as a result of haemorrhage (Bouglé, Harrois and Duranteau, 2013, National Trauma Institute). Coagulopathy has been associated with hypothermia and an increased mortality (Spinella and Holcomb, 2009). Hypothermia occurs when heat is not adequately transferred efficiently around the body because of the drop in blood volume (Spinella and Holcomb, 2009).

Techniques to decrease the number of deaths from exsanguination (defined by the Collins Dictionary of Medicine as 'the loss of a substantial portion, or almost the whole volume of the blood. The result of severe haemorrhage' (Youngson, 2004, 2005)) include tourniquets and haemostatic dressings which contain blood clotting factors to help stem the bleeding (J. Holcomb *et al.*, 2007, David Brown, 2012). 50% of the potentially survivable deaths experienced by the US SOF were from non-compressible truncal haemorrhage which is not easily stopped without surgical intervention (J. Holcomb *et al.*, 2007). However, 13% of the deaths were from haemorrhage amenable to tourniquet, i.e. haemorrhage from the extremities which is far enough down the limb to enable the tourniquet to be placed, suggesting they could have been prevented if prompt tourniquet application occurred (J. Holcomb *et al.*, 2007). The tourniquet is an efficient method at preventing exsanguination from the extremities. Multiple tourniquets are issued to allied troops fighting in OEF and OIF. Multiple tourniquets are provided as a single tourniquet may not be able to produce enough pressure for the haemorrhage to be halted in more muscular areas such as the thigh. Furthermore, provision of multiple tourniquets means that mechanical failure or breakage of one tourniquet will still allow haemorrhage to be controlled. As the conflict progressed these tourniquets were developed to be applied with just one hand to enable them to be easily used when injured or under fire (Wallace, 2012).

The severity of a combat wound to the extremities depends on a multitude of factors, firstly a gunshot wound is less likely to produce the major tissue damage seen in blast injuries. Secondly, proximity to explosion generally determines the severity of the injury with the extent of injury increasing the closer the casualty is to the explosion origin (Ibrahim and Oneisi, 2017). The initial blast overpressure cannot travel very far. On the other hand, the blast winds can propel fragments over a large area meaning those standing a substantial distance from the blast can still receive penetrating wounds (Wolf *et al.*). The composition of the explosive, thereby the intensity of the blast will affect the severity of the wounds (Ibrahim and Oneisi, 2017).

Explosives can be sorted into 2 categories, low-order explosives e.g. gun powder and high-order explosives such as C4 plastic explosive (Wolf *et al.*, 2009). Unlike low-order explosives, high-order explosives detonate with a large shock wave which will cause more primary blast injuries (Wolf *et al.*). Moreover, the method construction of the IED will also change the injuries observed (Sayer *et al.*, 2008). For example, bombs laden with nails will cause far more widely dispersed penetrating injuries. Furthermore, the mass, shape and velocity of the projectiles formed in the explosion or contained in the IED will change the type of injuries seen (Ibrahim and Oneisi, 2017). Altering the construction of the IED will change the type of projectile that it produces. The location of the IED will also affect the injuries seen, an IED buried in the road will cause far more lower extremity injuries. On the contrary, IEDs mounted in trees will cause far more damage to the upper extremities and the face.

1.3. Combat Casualty Care:

Blast injuries to the extremities present with complex wounds that often require intervention from multiple surgical specialties, especially orthopaedic teams (Ramasamy *et al.*, 2009). Throughout the stages of care the overlying consideration is always “life before limb” (Rigal, 2012). Level I care, also called buddy care, occurs at the point of injury and abides by the principles of Tactical Combat Casualty Care (TCCC). When following TCCC the traditional trauma checklist of Airway, Breathing, Circulation is succeeded by MARCH. MARCH stands for Massive haemorrhage, Airway, Respiration, Circulation, Hypothermia/ Head injury (Davis, Martin and Schreiber, 2017). This shows that the new priority is to stop the casualty bleeding out before resuscitation can occur. TCCC takes into account the changing situation on the battlefield i.e. the different priorities when exchanging fire with the hostile force compared to organising casualty evacuation.

When injury first occurs, the casualty is treated using the “care under fire” principles. Here the priority is to return fire and suppress the hostile force, even the casualty is expected to perform self-care and then return fire where possible (Davis, Martin and Schreiber, 2017). The only treatment that occurs at this point is extinguishing flames and the control of massive haemorrhage by use of tourniquets and dressings. If it is safe to do so, the casualty may also be dragged out of the line of fire (Davis, Martin and Schreiber, 2017). The basic medical training received by troops and the distribution of tourniquets means that even if the combat medic is overwhelmed or incapacitated then others on patrol can provide this care (Manning *et al.*, 2009, Davis,

Martin and Schreiber, 2017). The care provided when under fire should be rapid as every second that is spent providing aid is a second that the person providing aid is a vulnerable target.

Once the hostile force has been subdued “tactical field care” begins. Tactical field care allows for further life saving measures of airway stabilisation and needle decompression of tension pneumothorax (allowing air trapped in the pleural cavity to escape thereby reducing pressure on the lungs and heart) to be carried out (Davis, Martin and Schreiber, 2017). If the patient displays a decreased mental status or absent or weak pulse they are assumed to be in shock and small boluses of IV fluid are given (Davis, Martin and Schreiber, 2017). The casualty must be kept warm to prevent the onset of hypothermia. An air evacuation is called for during this stage to evacuate the casualty to a level II care centre.

The role of the level II medical centre or forward surgical team (FST) is to provide life-saving procedures to stabilise the casualty before further transfer (Davis, Martin and Schreiber, 2017). The type of procedures that occur in an FST involve endotracheal intubation, tube and resuscitative thoracotomies, cricothyroidotomies and damage control surgery to prevent the casualty bleeding out. External fixation of long bone and pelvic fractures is also done here to help stabilise the casualty and provide haemorrhage control (Manring *et al.*, 2009, Evriviades *et al.*, 2010, Balazs *et al.*, 2015, Davis, Martin and Schreiber, 2017). Surgery at a FST is limited to less than 2 hours, if possible, before the casualty is moved onwards (Gawande, 2004). From an FST the casualty is transferred to a level III Combat Support Hospital (CSH).

A CSH provides the highest level of medical care given while still in the combat zone. Here wound exploration, emergency amputations and the first debridement are done. Emergency amputations are left open and performed at the lowest level possible to preserve length (Balazs *et al.*, 2015). The aim of debridement is to remove all necrotic tissue and contamination (Evrivades *et al.*, 2010). Wound debridement should be thorough whilst retaining all injured but potentially viable tissue (Evrivades *et al.*, 2010). Debridement should be done with the deployment of a tourniquet; this prevents blood obscuring the pits seen in the non-uniform surface of a blast injury (Taylor and Jeffery, 2009). To provide the best chance of saving both life and limb, multiple surgical procedures may be performed simultaneously (Rattan, Jones and Namias, 2015). Decisions on whether or not to amputate the limb might have to be made during life-saving procedures (Fox *et al.*, 2010). This may mean that limbs that could potentially be salvaged are being removed under high-pressure decisions. Surgical wounds in level III medical centres are left open and will be closed once no further signs of infection or necrosis can be seen (Manring *et al.*, 2009). Re-debridement is done every 48-72 hours throughout the casualty's evacuation (Evrivades *et al.*, 2010). After a maximum of 3 days the casualty is moved up the chain of casualty care (Manring *et al.*, 2009).

For British casualties, this is the Royal Centre for Defence Medicine in Birmingham, usually within 48 hours of injury (Evrivades *et al.*, 2010). US casualties are moved to a level IV hospital, usually Landstuhl Regional Medical Centre, Germany, before being transferred back to the United States in as little as 36 hours post injury (Manring *et al.*, 2009). Definitive amputation, limb salvage and reconstructive surgeries are not undertaken until the casualty has reached their home country (Manring *et al.*, 2009). When deciding on the level of amputation it is the degree of soft tissue injury that is taken into account as opposed to the fracture level (Manring *et al.*, 2009). The benefit of this is to retain as much residual limb length as possible whilst still maintaining an

adequate soft tissue covering (Perkins *et al.*, 2012, Rigal, 2012). A higher level of amputation or inadequate soft tissue will increase the physical disability in the casualty when they have recovered (Perkins *et al.*, 2012). In those soldiers who underwent emergency amputations, the final amputation level will be decided when the patient is on home soil (Rigal, 2012).

When British forces first entered Afghanistan in 2001 and Iraq in 2003 the clinical doctrine for emergency care by the UK medical forces followed the 1-2-4 hour timeline (Bricknell, 2003). This stated that emergency trauma resuscitation and initial evacuation should be done within 1 hour of wounding (Bricknell, 2003, Tien *et al.*, 2015). Damage control surgery, such as haemorrhage control, should be completed within 2 hours of injury. Finally, the initial surgical repair of the injury should be undertaken within 4 hours (Bricknell, 2003, Tien *et al.*, 2015). The importance of getting the casualty to a medical facility in the first hour post-injury was deemed to be such that it was named the golden hour. The term golden hour was promoted by a former US military surgeon to emphasise the urgency of getting the critically injured to a medical care facility (Kotwal *et al.*, 2016). It is thought that prompt medical intervention within this hour improved mortality rates among trauma patients (Harmsen *et al.*, 2015).

However, in 2011 a NATO meeting of the Committee of the Chiefs of Military Medical Services created a new timeline within which emergency care should be provided on the battlefield (Tien *et al.*, 2015, Hooper *et al.*, 2014). This timeline is called the life and limb saving timeline and works on a 10-1-2 basis. Initial emergency care including haemorrhage control and airway stabilisation should be achieved within 10 minutes of wounding (Tien *et al.*, 2015). In the first hour after injury damage control resuscitation strategies should be implemented (Tien *et*

et al., 2015). By 2 hours post-injury the patient should have undergone damage control surgery (*Tien et al., 2015*). It is thought that abiding by this timeline will provide the patient with the best chance of survival.

Negative pressure wound therapy (NPWT) is often used to treat combat trauma injuries (*Jeffery, 2009*). NPWT is used prior to definitive closure in soft tissue wounds (*Krug et al., 2011*). During NPWT the wound bed is filled with either foam or gauze. A dressing is then applied over the top to achieve an airtight seal. This seal can be difficult to achieve in settings with external fixator pins or on non-uniform wound locations such as the groin or round the digits (*Gordon et al., 2015*). A pump is connected to the dressing to create an isolated environment with sub-atmospheric pressure (*Evriviades et al., 2010*). Combat injuries produce large amounts of exudate, and NPWT enables this exudate to be removed meaning patient's wounds are at a lesser risk of infection caused by contact with soiled dressings (*Jowan G Penn-Barwell et al., 2011*). Reports suggest that use of NPWT significantly reduces infection rates (*Jowan G Penn-Barwell et al., 2011*).

Moreover, NPWT dressings can be left in place for longer than conventional dressings (*Jowan G Penn-Barwell et al., 2011*). Most dressing changes are done in surgery thereby reducing the number of dressing changes, which means that surgical interventions on other parts of the body can be undertaken or the patient can be given longer to stabilise between surgeries (*Jowan G Penn-Barwell et al., 2011*). It is thought NPWT helps to ready the wound bed for definitive late closure by preventing the wound drying out, reducing oedema and helping the wound drain (*Krug et al., 2011, Balazs et al., 2015*). Furthermore, it is thought that application of NPWT helps to stabilise the wound, provoke contraction of the wound bed and stimulate the formation of granulation

tissue deep in the wound which forms a covering over tendons or bones which may have been exposed by the injury (Krug *et al.*, 2011, Ibrahim and Oneisi, 2017). Additionally, NPWT helps to simplify casualty care and isolate the wound from the environment during air medical evacuations

(Mathieu *et al.*, 2014).

The recent conflicts have led to the development of a resuscitation concept called damage control resuscitation (DCR). DCR promotes the rapid control of bleeding, reducing haemodilution by decreasing the amount of crystalloid fluid used and limiting coagulopathy by preventing acidosis, hypocalcaemia and hypothermia (Spinella and Holcomb, 2009). One major factor in DCR is allowing the patient to be slightly hypotensive, with a systolic blood pressure of around 90mmHg, to encourage the formation of thrombi whilst still having enough blood flow to support major organs (Spinella and Holcomb, 2009, Bogert, Harvin and Cotton, 2014). High blood flow and pressures brought about by aggressive resuscitation can cause blood clots that have already formed to become dislodged leading to an increase in bleeding (Bogert, Harvin and Cotton, 2014, Chauhan, Copeland and Murray, 2018). Keeping the patient hypotensive helps to prevent this. Moreover, the dilution of coagulation factors brought about by aggressive fluid replacement resuscitation can also increase bleeding as the blood is not able to clot as efficiently (Chauhan, Copeland and Murray, 2018). Other acute medical conditions linked to aggressive resuscitation are transfusion-related acute lung injury, acute respiratory distress syndrome and transfusion-associated circulatory overload caused by the large increase in fluid volume (Chauhan, Copeland and Murray, 2018).

The transfusion of fresh whole blood in major trauma is encouraged where possible, otherwise it is suggested to transfuse red blood cells, platelets and plasma in a 1:1:1 ratio

(Spinella and Holcomb, 2009). Studies show that reducing the time taken for plasma to be transfused significantly increases the survival chances (Pohlman *et al.*, 2015). Administration of cryoprecipitate can help to improve the fibrinogen deficit seen in major trauma when volume replacement is no longer necessary (Pohlman *et al.*, 2015). Orthopaedic injuries have their own damage control protocol. This involves rapid early stabilisation of the fracture to prevent further blood loss before general resuscitation protocols are followed (John B. Holcomb and Mitchell, 2017).

Two serious conditions can develop in a patient with severe limb trauma. The first is compartment syndrome which develops within the injured limb. Compartment syndrome is defined as “a condition in which increased pressure within a limited space compromises the circulation and function of the tissues within that space” (Köstler, Strohm and Südkamp, 2004). Compartment syndrome occurs when there is swelling in the muscle or when the blood perfusion pressure gets too low due to low blood volume (Köstler, Strohm and Südkamp, 2004). Swelling of the muscle causes the lymphatic vessels and small venules to close which in turn leads to hypertension in the capillaries. The lack of blood flow can lead to ischaemia leading to further inflammation continuing the cycle (Köstler, Strohm and Südkamp, 2004). If unchecked compartment syndrome can lead to nerve damage and tissue necrosis (Köstler, Strohm and Südkamp, 2004). Compartment syndrome is associated with trauma, particularly explosions, but can also be triggered after a period of ischaemia and during reperfusion (Köstler, Strohm and Südkamp, 2004, Pohlman *et al.*, 2015). Compartment syndrome is treated via a fasciotomy. A fasciotomy uses a single or double incision to cut through the fascia surrounding the tissues in all compartments in the limb to release the pressure and allowing the tissues to swell (Köstler, Strohm and Südkamp, 2004). The limbs should not be raised to allow for adequate perfusion of the tissues (Köstler, Strohm and Südkamp, 2004).

The other life-threatening condition that is frequently seen in injured soldiers is systemic inflammatory response syndrome (SIRS). SIRS results in a hyperinflammatory state, triggered by an unchecked response to the activation of the complement cascade by the initial inflammatory response (Adams-Chapman and Stoll, 2001, Robertson and Coopersmith, 2006). Every aspect of normal body function can be altered by SIRS. An increase in vascular permeability results in capillary leak into the tissues and alveoli. This pulmonary oedema leads to altered gas exchange resulting in acute respiratory distress syndrome (Adams-Chapman and Stoll, 2001). The excessive activation of the complement cascade leads to disseminated intravascular coagulation (DIC). DIC causes damage to endothelial tissues and can lead to organ damage and ultimately organ failure (Adams-Chapman and Stoll, 2001). If SIRS isn't controlled, the disruption of normal homeostasis causes huge tissue damage leading to multiple organ failure and death (Adams-Chapman and Stoll, 2001, Lord *et al.*, 2014). Therapy for SIRS is supportive (for example fluid resuscitation), as opposed to curative (Robertson and Coopersmith, 2006). Furthermore, the injury causing the SIRS must be treated (Robertson and Coopersmith, 2006).

One issue in severely injured troops in field hospitals is that life-saving surgery to stabilise the patient can be enough to tip the patient into multiple organ failure due to the secondary insult of the immune system (Evriviades *et al.*, 2010). The secondary insult is caused by the further inflammatory response and activation of the complement cascade in response to the action of the surgery itself. The additional complement activation can cause a controlled complement cascade to become unchecked leading to SIRS. For this reason, it is not uncommon for the patient to be transferred to the ICU during surgery for resuscitation and stabilisation (Gordon *et al.*, 2015). In addition, patients may not be able to tolerate limb

reconstruction after the initial injury (Evriviades *et al.*, 2010). To prevent this fatal 'second hit' the timing of limb salvage must be carefully considered (Evriviades *et al.*, 2010). The time taken for the patient to stabilise may mean that the limb tissue is no longer viable leading to amputation of a once potentially salvageable limb.

1.3.1. Considerations for Air Evacuation:

Air evacuation from the battlefield is generally performed using a helicopter and transfer out of theatre is usually done using a fixed wing aircraft such as a Boeing C17-A Globemaster.

Figure 1-1 (Cpl Dan Bardsley RLC, 2009) and Figure 1-2 (Wally Santana, 2002) show the difference between the evacuation from the battlefield compared to the evacuation out of theatre with more sophisticated medical equipment being carried with the casualty onto the C-17



Figure 1-1: Loading a casualty into a Blackhawk Medivac helicopter, Helmand Province, Afghanistan, 2009. Defenceimagery.mod.uk, Crown copyright



Figure 1-2: Loading a casualty onto C-17, Bagram Air Field, Afghanistan, 2002. National Public Radio

It should be noted that air evacuation from the front line is only possible when there is control of the airspace. In a war against a similarly equipped force, control of the air space may not be guaranteed. Whilst air evacuation is able to rapidly get the patient to lifesaving surgery there can be issues associated with it. A change in altitude will change the air pressure and will also alter the partial pressure of oxygen (Lehman, 2008). However, considering most air evacuations from the battle field are done at low altitude this will not be a significant issue in the care of the patient (Wayne, 2004). When evacuating the patient out of the combat zone the aircraft is typically pressurised to around 8,000ft. At 8,000ft gas will have increased in volume by around 35% when compared to sea level (Ewington, 2016, Teichman, Donchin and Kot, 2007). This can cause problems with both air-filled equipment such as pneumatic tourniquets and in injuries where air has become trapped in a cavity.

There are some factors of air evacuation which can give rise to issues with patient care. The vibration of the aircraft can cause issues with poorly placed IV lines and improperly secured equipment as they may become dislodged (Lehman, 2008). Similarly, the vibrations can affect the readings on monitoring devices leading to false results (Teichman, Donchin and Kot, 2007). The loud noise of the aircrafts engines can mean that alarms indicating issues with the patient cannot be heard so visual clues are often needed as well (Schrager, Branson and Johannigman, 2012, Wayne, 2004). Flying out of the combat zone requires a black out of the plane with the nurses often working under red lamps or the glow of green chemsticks (Schrager, Branson and Johannigman, 2012, Wayne, 2004). This means that the equipment must be able to be used or monitored in near darkness.

In addition, flying out of a combat zone requires a tactical take off. This entails a very steep take off and consequent steep banking (Wayne, 2004). Furthermore, a horizontal gravitational force will be produced from the acceleration needed for take-off. The combination of these forces will cause changes in fluid distribution in the patient which will need to be taken into consideration, such as pooling of blood in the lower limbs when the patient is loaded head first (Ewington, 2016). Moreover, the nose of the C-17 is angled upwards during flight, this could alter how fluids are administered as the plane will not be completely level (Ewington, 2016). The medical equipment must be well secured during flight to prevent movement during take-off, landing, turbulence or any emergencies such as rapid decompression or an emergency landing (Ewington, 2016).

There is very little space to manoeuvre in a medical evacuation aircraft so equipment should be kept as small as possible. In addition, equipment should be checked to see it does not interfere with the plane avionics and vice versa (Ewington, 2016). Finally, one vital factor during a medical evacuation flight is the battery life of the equipment (Wayne, 2004). Running out of battery on the flight could lead to the death of the patient if they are relying on the equipment to live, i.e. ventilators. For this reason, the battery should be able to last at least 1.5 times as long as the anticipated flight time (Wayne, 2004). The average flight time from Iraq and Afghanistan to the US hospital Landstuhl in Germany is 6.3 hours \pm 1.8 hours with pre- and post- flight times of 30 minutes each (Bridges and Evers, 2009). Using these numbers, the battery life of a bit of equipment should be at least 16.35 hours. This figure is calculated by adding the pre- and post- flight times to the flight time, plus 2 standard deviations of the mean and multiplying it by 1.5: $((6.3 + (2 \times 1.8) + 1) \times 1.5)$.

1.4. Amputation vs Limb Salvage:

Limb salvage can be defined as ‘the returning of a limb to a state of reasonable functionality after severe trauma which might otherwise result in amputation’ (*‘limb salvage’, 2002*). Limb salvage should aim not just to ‘save’ the limb but to produce a painless extremity that is functional and has some sensation in it (*Korompilias et al., 2009*).

1.4.1. Post Amputation Complications:

Combat injuries produce wounds with complex scar lines, and this can make fitting a comfortable prosthesis exceedingly difficult. Another issue facing prosthetists when the amputation has resulted from combat is the short residual limbs. Short stumps can make it difficult to get stability and can increase the level of disability in the returning soldier (*Perkins et al., 2012*). Moreover, amputations have been shown to cause an increase in other long-term health issues which can affect all areas of the veteran’s life.

When studying blood flow in amputees, haemodynamic changes and abnormalities in arterial blood flow have been demonstrated which have been linked to development of cardiovascular problems (*Perkins et al., 2012*). A 2 year study of US traumatic amputees from Iraq and Afghanistan found that traumatic amputees, particularly those with a transfemoral amputation, had a higher risk of developing a pulmonary embolism or deep vein thrombosis (*Hannon et al., 2016*). However, up to 70% of these venous thromboembolisms occurred within the first 10 days after injury so they are less likely to be a long-term problem (*Hannon et al., 2016*). A 30 year follow up of 3,890 World War II proximal limb amputees showed the relative risk of

coronary vascular disease was 4 times greater than those personnel who were disfigured but obtained no amputation during the same conflict (Robbins *et al.*, 2009). Lower limb amputees have been shown to have a greater risk of ischaemic heart disease (IHD) (Robbins *et al.*, 2009, Perkins *et al.*, 2012). Evidence suggests the relative risk for a cardiac related death is much higher in traumatic amputee veterans than it is for healthy controls (Perkins *et al.*, 2012). This could be due to increased insulin resistance and increased blood coagulation seen in amputees (Perkins *et al.*, 2012, Robbins *et al.*, 2009).

Chronic pain is another recurring issue for military trauma amputees (Perkins *et al.*, 2012). This constant pain has been linked to lower functional outcomes for the patient (Perkins *et al.*, 2012). The pain experienced by amputees is found in many areas. Pain in the residual limb can affect the ability of the patient to go about day life. This pain can be caused by a poor fitting prosthesis which is relatively easily fixable. Less easily solved are symptomatic neuromas and symptomatic scar tissue, among other soft tissue pathologies (Perkins *et al.*, 2012). Phantom limb pain is present with varying severities in 50-80% of all amputees (Flor, 2002). It is characterised by pain in the limb that is no longer present and is thought to be neuropathic (Flor, 2002). However, the severity of the pain has been shown to be affected by the magnitude and duration of pain prior to amputation (Perkins *et al.*, 2012). The pain can be exacerbated by emotional stress and many other psychological or physical factors (Flor, 2002). Treatment of phantom limb pain is often ineffective but is usually based on methods to treat neuropathic pain such as anti-depressants, calcium-channel blockers and opioids (Flor, 2002). Although the studies examining the effect of prompt analgesic administration at time of injury on phantom limb pain are inconclusive, minimising pain on the battlefield is recommended in an attempt to reduce the severity of possible phantom limb pain (Flor, 2002, Perkins *et al.*, 2012).

Secondary overuse musculoskeletal injuries are often seen in long-term lower limb prosthetic users. Lower back pain is reported in the majority of lower limb amputees, with a more proximal amputation resulting in a higher incidence (Perkins *et al.*, 2012, Robbins *et al.*, 2009, Farrokhi *et al.*, 2018). A retrospective study of the Expeditionary Medical Encounter Database (data about injury recorded in the combat zone) combined with the Military Health System Medical Data Repository (data on corresponding musculoskeletal injury) compared the incidence of overuse musculoskeletal injuries in the first-year post-injury of soldiers who had received an immediate combat injury related lower limb amputation (an amputation within the first 24 hours post-injury) with those who had mild combat related lower limb injury that did not require extensive medical care (Farrokhi *et al.*, 2018). This study excluded musculoskeletal injuries that were diagnosed pre-combat injury. It was found that the incidence of musculoskeletal injuries was consistently higher in the amputation groups (Farrokhi *et al.*, 2018). Lumbar spine and upper limb injuries were most common in bilateral amputees whilst lower limb overuse injuries were most common in unilateral amputees (Farrokhi *et al.*, 2018). This study did not include limb salvage patients so it is not possible to know if limb salvage would reduce the incidence of overuse injuries. Furthermore, the study only went up to 1-year post-injury which may not be long enough to pick up chronic overuse injuries.

On top of musculoskeletal injuries, lower limb amputees experience higher rates of joint pain than the general population (Robbins *et al.*, 2009). 50-65% of transfemoral amputees and 36-41% of transtibial amputees are affected by knee pain, in either the residual or sound limb (Perkins *et al.*, 2012). This is likely to be due to the increased load going through the knee. Osteoarthritis in the hip is far more common in an amputee than in the general population. In the general

population, around 9% experience hip osteoarthritis. In World War II unilateral lower limb amputees this figure was 23% on the sound side and up to 61% on the side with the amputation (Robbins *et al.*, 2009). Residual limb bone density is also significantly lower; this can result in a higher incidence of fractures and complications in later life (Robbins *et al.*, 2009). This study involves World War II veterans as they are in a similar age group to those who have hip osteoarthritis in the general population. Therefore, data from recent conflicts cannot be compared to age matched uninjured counterparts.

Heterotopic ossification has been a problematic factor in many combat amputees in the recent conflicts in Afghanistan and Iraq. A US retrospective study looking at the radiographs of 213 military amputees more than two months after injury, found that heterotopic ossification was seen in 63% of stumps (Evriviades *et al.*, 2010). Heterotopic ossification is the formation of lamellar bone in soft tissues, this can create bony spurs possibly leading to residual limb pain and a poorly fitting prosthesis (Potter *et al.*, 2007). Treatment of heterotopic ossification may require surgery and can result in additional associated complications (Potter *et al.*, 2007). Risk factors for heterotopic ossification include amputation within the zone of injury and injury due to a blast (Potter *et al.*, 2007). Due to the many complications that can result from an amputation and the costs involved in treating them attempting limb salvage is still preferable

(Dismounted Complex Blast Injury Task Force, 2011).

1.4.2. Predicted Costs of OIF/OEF amputations:

Providing limbs and lifetime care to the veterans of the conflicts in Afghanistan and Iraq will come at a substantial cost. Between 2003 and 2014, 265 British soldiers sustained 416 amputations (Bilmes, 2007). Wounded British personnel mainly undertook rehabilitation at DMRC Headley Court, here amputees received on average 5 prosthetic limbs (Royal College of Physicians, 2011, All Wales Military Prosthetics Working Group, 2013). A study in 2014 examining the prosthesis use of bilateral US amputees returning from OEF and OIF, with a transfemoral and transtibial amputation found that on average they currently used 6.1 ± 4.5 prostheses (Paul J. Dougherty *et al.*, 2014). The Murrison Review estimated that the care for British combat amputees' costs around £20,000 per person per year. With advances in prosthetics this figure could rise to £30,000-£40,000 (All Wales Military Prosthetics Working Group, 2013). The cost of prosthetic limbs is predicted to rise due to developments in technology, such as neuronally-controlled prosthetic limbs. Prosthetics for upper limbs are likely to experience the biggest advances in technology as currently the hand function of these limbs is rudimentary. The more technologically advanced prostheses will bring higher repair and maintenance costs. The predicted 40-year cost of care for the British lower limb amputees returning from Afghanistan is £288 million, assuming that a prosthetic limb will be replaced on a 2.3-year cycle (Edwards *et al.*, 2015). This figure does not include care for secondary conditions (Edwards *et al.*, 2015). Increased success in limb salvage may have helped reduce these predicted costs.

1.4.3. Benefits of Limb Salvage:

Surgery in the combat zone aims to save as much of the mangled limb as possible. Once the injured serviceman has been repatriated further assessment of the limb can be undertaken and a plan for feasible limb salvage formulated (Bevevino *et al.*, 2014). Not all limbs are able to be salvaged successfully. Unfortunately, no test or score can accurately predict if the limb should be amputated or if salvage should be attempted. The only absolute indicators for amputation are irreparable damage to bone, an extremity where most soft tissue has been stripped off or a warm ischaemia time of more than 6 hours where substantial soft tissue necrosis is present (K. V. Brown *et al.*, 2012).

In patients with lower limb amputations and a mangled upper extremity, all efforts should be made to preserve function in the upper limb for the greatest chance of successful rehabilitation and provide some independence to the injured soldier (Mathieu *et al.*, 2014, Dismounted Complex Blast Injury Task Force, 2011). In addition, salvage of a lower limb when accompanied by an amputation on the contralateral limb can provide stability and balance when mobility is regained (Pasquina *et al.*, 2014). Other than life saving surgery, attempts at limb salvage should not be undertaken until such time as the patient is stable and no longer at risk of developing SIRS (Prasarn, Helfet and Kloen, 2012).

1.4.4. Limb Salvage Techniques:

To have the greatest chance of successful limb salvage the aim is to restore blood flow to the limb within 6 hours (Alam and DiMusto, 2015). The time of tourniquet application should be written on the casualty with permanent marker so medical personnel can easily tell the warm ischaemia time (Patel, Richter and Shafi, 2015). In the early stages of trauma care blood flow can be restored by the insertion of temporary intravascular shunts (Alam and DiMusto, 2015). Arterial shunts enable the restoration of distal flow whilst venous shunts enable the blood to be drained from the limb (Alam and DiMusto, 2015). These temporary shunts are replaced by permanent ones at higher levels of care. Temporary shunting has been shown to decrease the need for amputation by 50% (J. G. Penn-Barwell *et al.*, 2014). Trauma to the popliteal vessels carries the greatest risk of amputation than injury to any other extremity vessels (Mullenix *et al.*, 2006). A preventative fasciotomy is performed in the combat zone to prevent the development of compartment syndrome during the air evacuation. A preventative fasciotomy can reduce the probability of complications including amputation, 4-fold (Rattan, Jones and Namias, 2015).

Fracture fixation can be done internally or through external mechanisms. Emergency external fixation is done in the early stages of combat casualty orthopaedic care (Balazs *et al.*, 2015, Mathieu *et al.*, 2011). During emergency fixation few pins are used and are placed as far from the fracture site as possible to reduce the chance of infection if the fixation is changed to internal (Mathieu *et al.*, 2011). Even though a small number of pins are used, they should be of sufficient stiffness to provide adequate traction and stability during evacuation (Mathieu *et al.*, 2011). Analysis of 16 French combat casualties injured between 2004-2009 showed that early conversion to internal fixation gave rise to better healing outcomes (Mathieu *et al.*, 2011). On the other hand,

conversion to internal fixation can lead to relatively high rates of infection especially if a late conversion is performed (Mathieu *et al.*, 2011). Internal fixation using plates, screws and nails provides adequate fixation for most fracture types (Hoyt *et al.*, 2015). Internally fixed bones will usually require non-weight bearing of 6-12 weeks to allow for adequate healing (Hoyt *et al.*, 2015). Internal fixation failures include malunion or non-union due to interfragmentary instability and high axial strain (Hoyt *et al.*, 2015).

When converting from emergency external fixation to long term external fixation more pins should be added to increase stiffness and to manage bone defects (Mathieu *et al.*, 2011). External fixation can be useful for traumatic injuries due to the low level of tissue disruption required to place it. External fixation can also be more easily removed if osteomyelitis (infection of the bone) occurs (Hoyt *et al.*, 2015). The benefit of external fixation is that it can apply forces to the bones in all directions meaning that it can be used to treat a wide range of fractures (Hoyt *et al.*, 2015). When treating a fracture, the timing of weight bearing should be considered. Whilst premature weight bearing and excessive movement can lead to failure of fracture fixation and/ or soft tissue repair, immobility can lead to deconditioning, arthrofibrosis and possible venous thrombotic events (Hoyt *et al.*, 2015, Gordon *et al.*, 2015). Furthermore, prolonged immobility can give rise to joint stiffness, atrophy of the muscles and pressure ulcers creating further challenges to treatment (Hoyt *et al.*, 2015). Maintaining the full range of motion in joints in blast injury patients is very difficult due to lack a movement of the joint, particularly if large amounts of time is spent in the ICU (Gordon *et al.*, 2015). Joint stiffness, particularly in the lower limbs, can lead to functional limitations which may inhibit the later rehabilitation (Hoyt *et al.*, 2015).

One problem with a mangled extremity is where to harvest tissue from. With major tissue damage, there is often no spare tissue on the limb to use. For this reason, free flap transfer is a technique commonly used during limb salvage as it allows for the movement of undamaged tissue to the injured extremity. Tissue can be harvested from the undamaged areas of the body which were protected from the blast by body armour (Ian L. Valerio *et al.*, 2013). However, where possible, tissue should not be harvested from areas which may compromise strength for future rehabilitation such as the rectus abdominis (Pasquina *et al.*, 2014).

Complications with limb salvage are more likely to occur than complications after amputation. This can lead to some limb salvage patients wanting to have an elective amputation when they see those that received amputations at a similar time progressing much faster through rehabilitation. Major complications include flap failure, haematoma, fracture non-union, chronic pain, osteomyelitis, post-traumatic arthrosis and wound infection and break-down (Connolly, Ibrahim and Johnson, 2016, Prasarn, Helfet and Kloen, 2012). These major complications can lead to late amputation. Calcaneal fractures are particularly prone to complications and often lead to elective amputations (Gordon *et al.*, 2015). Patients who underwent late amputation have been shown to have significantly higher rates of physical and psychological problems (Connolly, Ibrahim and Johnson, 2016).

Other complaints from limb salvage patients include oedema, and ambulation difficulties as well as pain and decreased sensation (Prasarn, Helfet and Kloen, 2012). Studies have found that while patients with amputations progress with rehabilitation relatively quickly, after 2 years the physical and functional ability of the amputee and limb salvage cohorts is very similar (Patel,

Richter and Shafi, 2015). Limb salvage is thought to fail more often when there is extensive damage to the limb or coinciding injuries to other major organs. This is usually due to a combination of major blood loss, ischaemia and sepsis (Gawande, 2004). On the other hand, advances in surgical methods means limbs that would previously have been amputated are now able to be salvaged (Bevino *et al.*, 2014).

1.5. Future Therapies:

1.5.1. Haemorrhage Control:

Increased research into methods to improve survival rates of the wounded began in response to the high numbers of soldiers being injured in the wars in Iraq and Afghanistan. This research has continued even after the wars have ended. Exsanguination due to haemorrhage not amenable to tourniquet was one of the biggest factors in potentially preventable deaths in OIF and OEF (Rappold and Bochicchio, 2016). For this reason, research into haemorrhage control, particularly in the trunk, has been undertaken. Many new technologies have been developed, including Retrograde Endovascular Balloon Occlusion of the Aorta (REBOA) (Rappold and Bochicchio, 2016). In REBOA, a catheter with a balloon is introduced to the femoral artery. When in the correct position the balloon can be inflated which can stop bleeding in the pelvic or abdominal regions by occluding the injured artery (Rappold and Bochicchio, 2016). REBOA improved survival rates when compared to a resuscitative thoracotomy in two major US level 1 trauma centres (Rappold and Bochicchio, 2016). 9.7% of the 24 patients who underwent REBOA died compared to 37.5% of the 72 patients who received a resuscitative thoracotomy ($p=0.003$) (Laura J. Moore *et al.*, 2015).

The use of nanotechnology to control haemorrhage has been investigated. Haemostatic nanoparticles have been shown to reduce haemorrhage and improve survival when introduced intravenously in rat models by interacting with the platelets stimulating clot formation (Margaret Lashof-Sullivan *et al.*, 2016, Shoffstall *et al.*, 2012). In addition, nanotechnology has been utilised in creating synthetic platelets which have been shown to reduce bleeding by 50% in rodent models (Rappold and Bochicchio, 2016). Hubbard *et al* produced haemostatic nanoparticles capable of binding to the glycoprotein IIb/IIIa receptor on activated platelets (Hubbard *et al.*, 2015). The use of these haemostatic nanoparticles in rodent polytrauma blast models showed reduced amounts of apoptosis and a smaller percentage area of TNF- α fluorescence in lung tissue 7 days after injury compared to other treatment methods, leading to less severe lung injury and increased survival rates (Hubbard *et al.*, 2015). Lashof-Sullivan *et al* investigated the ability of haemostatic nanoparticles at a dose of 40mg/kg to halt internal bleeding in mice after exposure to a blast of 20psi (Margaret M. Lashof-Sullivan *et al.*, 2014). This study found a significantly increased survival rate when compared to no treatment. However, when compared to other fluid replacement therapies, use of haemostatic nanoparticles did not produce a statistically significant survival benefit (Margaret M. Lashof-Sullivan *et al.*, 2014). No survival benefit could be seen at 25psi implying there is a limit to the severity of injury that haemostatic nanoparticles can be a useful therapy for (Margaret M. Lashof-Sullivan *et al.*, 2014). When comparing histological analysis of lung injury, a trend was demonstrated towards reduced levels of lung injury in those treated with haemostatic nanoparticles compared to controls (Margaret M. Lashof-Sullivan *et al.*, 2014). This study also looked at the long term effect of using haemostatic nanoparticles, no complications such as stroke were observed after 1 or 3 weeks (Margaret M. Lashof-Sullivan *et al.*, 2014). Whilst this suggests that haemostatic nanoparticles would be safe to use in therapy without compromising patient safety, this study only included a small number of mice so further observations would be

necessary. In future, the use of nanoparticles could provide a method for controlling haemorrhage on the battlefield. However, it is unlikely that the administration of haemostatic nanoparticles will be able to prevent catastrophic bleeding without other haemorrhage control methods.

Multiple different self-expanding foam-based materials have been developed to control haemorrhage. The first is polyurethane foam. When introduced into the abdominal cavity this foam expands to compress the bleeding (Rappold and Bochicchio, 2016). Whilst polyurethane foam does result in increased survival, it can be difficult to introduce it into the abdominal cavity without creating additional injury (Rappold and Bochicchio, 2016). Furthermore, once at the hospital this foam needs to be surgically removed which can often result in an immediate resuming of haemorrhage (Rappold and Bochicchio, 2016).

To counteract this need for removal, a fibrin-based haemostatic foam is in the process of being developed. 'ClotFoam' consists of a fibrin-based sealant contained in a biomimetic complex polymer (Rappold and Bochicchio, 2016). This combination provides a stable structure upon which a fibrin clot can develop, in other words it helps to support the body's natural clot forming ability (Rappold and Bochicchio, 2016). Supporting the formation of a blood clot means that haemorrhage can be controlled without having to provide pressure or surgical intervention (Rappold and Bochicchio, 2016). ClotFoam is a biocompatible foam and can be kept in place after use meaning surgical removal is not necessary (Rappold and Bochicchio, 2016).

Self-expanding materials can also be used in extremity or junctional injuries. XStat is a haemostatic device licenced for use by the FDA developed for bullet or shrapnel injuries (FDA, 2015). When the XStat is introduced into the wound, small sponges expand rapidly and fill the wound cavity causing compression and blocking the flow of blood (Rappold and Bochicchio, 2016).

1.5.2. Resuscitation Control:

Resuscitation strategies are also being investigated. The use of arginine vasopressin (AVP) in models of uncontrolled haemorrhage has also been investigated. AVP binds to vasopressinergic receptors which stimulates the vasoconstriction of all vessels not associated with cerebral, coronary or pulmonary circulation (Wenzel, Raab and Dünser, 2008). This causes blood flow to be diverted away from the site of bleeding which can increase the aortic blood pressure and maintain the blood supply to the heart lungs and brain (Wenzel, Raab and Dünser, 2008). Vasopressin is released naturally in response to major fluid loss by the detection of low fluid levels by the arterial baroreceptors (Anand and Skinner, 2012). However, the stores of vasopressin in the body are insufficient to maintain perfusion pressure when shock is prolonged (Wenzel, Raab and Dünser, 2008, Anand and Skinner, 2012).

Studies have shown that in the administration of AVP in anaesthetised swine, the total blood loss was lower than that of swine treated with standard fluid replacement protocols or saline placebos. These studies also demonstrated a vastly improved survival rate with all pigs treated with fluid resuscitation or saline dying within 20 minutes of therapy whereas 8 of 9 AVP treated pigs survived longer than 7 days (Wenzel, Raab and Dünser, 2008). Conversely, metabolic acidosis in the quadriceps muscle was shown to increase in dogs treated with an AVP infusion

(Wenzel, Raab and Dünser, 2008). This suggests that the use of large amounts of AVP can increase the risk of ischaemic injury in other tissues.

Valproic acid (VPA) is a histone deacetylase inhibitor (HDACI). Treatment with a HDACI is thought to improve early survival rates in haemorrhage and reduce organ damage by enhancing transcription of protective genes (Alam *et al.*, 2009). Fukudome *et al.* studied the effect of VPA on survival rates of rats in lethal haemorrhagic shock. They found VPA provided a survival advantage at 24 hours with 80% of rats treated with VPA surviving compared to 17% of control rats (Fukudome *et al.*, 2010). However, group sizes were small (n=5 and 6 respectively) and as such further research is necessary. Alam *et al.* studied the effect of VPA in a swine poly-trauma model. The study compared the effect of VPA, a saline control and fresh whole blood (FWB). Survival rates when treated with FWB or VPA were found to be significantly higher than in those animals treated with saline. However, there was no significant difference in the survival rates of those animals treated with FWB or VPA (Alam *et al.*, 2009). VPA did not correct the acidosis seen after poly-trauma, this may imply that VPA improves the ability of tissues to survive in ischaemic conditions (Alam *et al.*, 2009). Considering the survival rates between treatment with VPA or FWB were not significantly different, VPA may be a viable option for immediate administration to injured soldiers in the field to prolong survival before proper resuscitation can occur.

Suspended animation is a novel technique that is being researched to try and elongate the so called “golden hour”. Suspended animation aims to place the injured party into a low metabolic state similar to hibernation. Studies are still in the animal testing stage and involve

the use of profound hypothermia or the use of hydrogen sulphide (H₂S) (Rappold and Bochicchio, 2016, Mooyaart *et al.*, 2016). In 2004, the US military was in its 7th year of study of suspended animation using profound hypothermia. The focus of their research was to enable delayed resuscitation to be performed in casualties who had undergone cardiac arrest after rapid internal exsanguination (Kochanek, 2004). The initiation of suspended animation was achieved by a rapid aortic flush of ice cold saline to a tympanic temperature of 10°C (Kochanek, 2004). These studies found that 2 hours of suspended animation followed by resuscitation enabled dogs to be resuscitated with no brain damage evident (Kochanek, 2004). The study was then adapted to see the effect of suspended animation after exsanguinating cardiac arrest when haemorrhagic shock was present beforehand. Once cardiac arrest had occurred, after an average of 124 ± 16 minutes, those dogs in the suspended animation categories were given a 20L flush of ice cold saline (Kochanek, 2004). Cardiopulmonary bypass (CPB) was started 60 minutes after cardiac arrest in all groups. The dogs in the two suspended animation groups were rewarmed to 34°C with successful defibrillation occurring at 32°C (Kochanek, 2004). All dogs who had undergone CPR died in a median time of 14.7 hours (Kochanek, 2004). However, of the dogs who underwent suspended animation with 12 hours of mild hypothermia (34°C) followed by rewarming at 1°C/h to 37°C, all but 1 dog survived to 72h. However, only 1 dog survived without neurological injury (Kochanek, 2004). The other suspended animation group remained mildly hypothermic for 36h before being rewarmed at a rate of 0.3°C/h. No dogs in this second group had seizures and only 1 displayed signs of neurological damage at 96h (Kochanek, 2004). These results show that the success of suspended animation depends on a multitude of factors. The problem with producing suspended animation using ice-cold saline on the battlefield is the difficulty in having a supply of ice-cold saline to hand. For this reason, other methods of inducing suspended animation may be preferable.

H₂S is naturally present in the cell in very low concentrations during normal conditions (Kolluru *et al.*, 2016). H₂S binds to the haemoglobin creating sulfhaemoglobin which has a much lower affinity for O₂ meaning less O₂ is transported (Kolluru *et al.*, 2016). When high levels of H₂S are combined with hypoxic conditions, the O₂ transportation capacity of the blood is greatly reduced causing a state of hypometabolism (Kolluru *et al.*, 2016). H₂S has been linked to the regulation of cellular oxygen consumption by inhibiting the action of cytochrome oxidase C (Szabo, 2007). In addition, H₂S is thought to cause the upregulation of anti-inflammatory or cytoprotective genes and anti-oxidant processes as well as suppressing inflammatory pathways such as the iNOS/NOS pathway (Szabo, 2007, Ning *et al.*, 2013). It is thought this is where the protective effect of H₂S stems from. However, if the concentrations of H₂S and O₂ are not carefully controlled, H₂S can cause chemical suffocation (Mooyaart *et al.*, 2016). A retrospective review of all patients involved in manure storage accidents with H₂S poisoning in the Netherlands between 1980-2013 was undertaken. When observing the survival rates of the 8 patients in the study who had received CPR, the survival rate without neurological complications was 75%. This number is far higher than the survival rate without neurological complications of patients who experience an out of hospital cardiac arrest (5-8%) (Mooyaart *et al.*, 2016). Whilst 8 is not a very large number of patients to draw conclusions from, the high survival rate without neurological complications does suggest that H₂S does provide some sort of protection against hypoxia.

Animal studies have shown that mice exposed to a combination of both H₂S and O₂ entered a state of hibernation which they could be aroused from by removing the presence of H₂S and increasing the concentration of inhaled O₂ (Mooyaart *et al.*, 2016). This state of hibernation was

characterised by a decreased metabolic rate, stemming from a reduced heart rate and breathing frequency, as well as a lower body temperature (Mooyaart *et al.*, 2016). Mice revived from this state of hibernation showed no negative effects from the H₂S (Mooyaart *et al.*, 2016). A study in pigs also demonstrated this decrease in heart rate upon receiving H₂S (Causey *et al.*, 2015). Furthermore, H₂S showed a protective effect allowing mice to survive with no complications when breathing air with only 3% O₂ for 6.5 hours (Causey *et al.*, 2015). However, these results could not be reproduced in larger animals (Mooyaart *et al.*, 2016, Satterly *et al.*, 2015). Studies have found that there is a significant reduction in histologic damage seen in the liver and kidneys in response to ischaemia or traumatic shock when H₂S is administered early (Mooyaart *et al.*, 2016, Satterly *et al.*, 2015). Ning *et al.* studied the effect of the H₂S donor, NaHS, on lung injury after blast limb trauma in rats (Ning *et al.*, 2013). This study found that treatment with NaHS suppressed the activation of neutrophils and reduced the inflammatory reaction both locally and systemically when compared with controls (Ning *et al.*, 2013). Ganster *et al.* found that NaHS reduced ischaemia-reperfusion oxidative stress and haemodynamic dysfunction during rat resuscitated haemorrhage models (Ganster *et al.*, 2010). However, the mean arterial pressure was maintained at 40 ± 2mmHg with the reinfusion or withdrawal of blood in the period before the administration of the therapy occurred (Ganster *et al.*, 2010). This could have affected the formation of ischaemia-reperfusion injury. The aforementioned studies show that H₂S may be able to provide a method to place injured patients into a state of suspended animation to prolong the therapy time before ischaemic injury occurs. However, due to its toxicity many further studies will need to be done before the therapeutic use of H₂S becomes a viable option.

1.5.3. Regenerative Medicine:

Regenerative medicine is beginning to play a large part in the therapy of injured soldiers particularly in the treatment of full thickness wounds (Ian L. Valerio *et al.*, 2016). One such therapy is the application of extracellular matrices to convert a full thickness wound into a partial thickness one (Ian L. Valerio *et al.*, 2016). The extracellular matrices create a 'neodermis' which allows for easier engraftment of autologous skin grafts (Ian L. Valerio *et al.*, 2016). Urinary Bladder Matrix (UBM) is an example of this. In general, it was found that treatment with UBM stimulated the formation of granulation tissue and helped prepare the wound bed for successful placement of secondary dermal regeneration templates, flap coverage or skin grafts (I. L. Valerio *et al.*, 2015). Of the 51 uses of UBM at Walter Reed National Military Medical Center between 2010-14, failure occurred in 7 cases (I. L. Valerio *et al.*, 2015). This failure was most often found to be due to shearing forces, wound infection or inadequate neovascularisation (I. L. Valerio *et al.*, 2015). Another method allows a small section of skin to be used to cover a much larger graft area (Ian L. Valerio *et al.*, 2016). This so-called spray skin technique has been utilised in burns patients with promising early results but has now been used in a military casualty for the first time. The spray skin is a suspension of keratinocytes, Langerhans cells, melanocytes and fibroblasts (Ian L. Valerio *et al.*, 2016). Initially a dermal regenerate template was used to cover the abdominal wound. Then a thin 6:1 meshed split thickness skin graft was applied to the abdomen followed by spray skin application to both the abdominal wound and the skin graft donor sites (Ian L. Valerio *et al.*, 2016). One benefit of the spray skin technology is that it enabled surgeons to cover a 600cm² wound using a donor skin graft for only 140cm² (Ian L. Valerio *et al.*, 2016). On top of reducing healing time, being able to cover a much larger area than the skin graft size will help surgeons treating those military patients where extensive trauma means that donation sites are limited.

Chapter 2. Thesis objectives and hypothesis:

The objective of this thesis is to develop technology to support the care of critically limb injured casualties from the battlefield through to hospital care. The technology will be focussed on 3 aspects of advanced casualty care, these are:

1. Improved haemorrhage control to reduce the number of potentially survivable deaths
2. Intervention to protect and preserve damaged tissue during transport from the battlefield to hospital
3. A perfusion system, totally isolated from the systemic circulation, to allow for limb support and a staged reconstruction process once in the hospital setting

2.1. Proposed Technology:

In this work we will develop three technologies, directed at the various stages of the casualty journey and subsequent recovery. These technologies will be utilised in combination to achieve the best possible outcome for the casualty.

1. The first of these devices is an automated dual-bladder pneumatic tourniquet that will be applied as soon as the casualty is injured to halt haemorrhage. The tourniquet will be strapped around the injured limb and, once activated, one bladder of the tourniquet will inflate to eliminate arterial flow. After a fixed time has passed, the

second bladder will inflate leading to a shift in the location of pressure with the aim of reducing compression related tissue damage. This alternating tourniquet approach is new to the clinical sector and is directed at eliminating haemorrhage, reducing compression injury and through very brief periods of reperfusion during the changeover cycle, reducing ischaemic injury.

2. Immediately after tourniquet placement, whilst the casualty is still in the field, the second device will be deployed. This device is designed to be a cooling sock which will fully enclose the injured limb and will be used to topically cool the limb. The objective is to pass compressed gas through the cooling sock to maintain a state of controlled hypothermia. It is the intention to cool the limb tissue by 10°C to reduce metabolism and prolong tissue viability. Topically cooling the limb throughout the evacuation to a medical centre will, it is anticipated, preserve the tissues and reduce the need for amputation due to ischaemic injury.

3. Once the casualty arrives in a medical centre the cooling sock will be removed whilst the tourniquet is kept in place. When the casualty is undergoing damage control surgery the limb will be cannulated and connected to the limb support system. The limb support system is proposed as a sterile environment in which the limb can heal. The limb itself will be kept isolated from the systemic circulation by the tourniquet and will be perfused by blood in a small self-contained extracorporeal membrane oxygenation circuit. The system is intended to support the limb for up to 100 days.

2.2. Thesis hypothesis:

The hypothesis for the work included in this thesis is:

It is possible to develop dual bladder tourniquet, limb cooling and tissue perfusion technologies that will enhance the preservation of tissues subsequent to battlefield injury and that the impact of this approach can be demonstrated under laboratory conditions.

Chapter 3. Tourniquet Design:

3.1. Overview of Tourniquets:

3.1.1. Current Tourniquet Use:

Tourniquet design has changed very little since the 1600's where tourniquet design consisted of a belt tied around the limb with a windlass tightened to increase the pressure and to stop blood flow (Kragh Jr *et al.*, 2012). When applied correctly, early tourniquet use has been shown to improve casualty survival rates significantly and is seen as an effective method at reducing mortality in the fighting force (Perkins *et al.*, 2012). The sooner an emergency tourniquet is applied the greater the survival rates (Dunn *et al.*, 2016). The ideal time to place an emergency tourniquet is before haemorrhagic shock can develop because, whilst able to stop the development of shock, a tourniquet will not reverse the effects (Kragh Jr *et al.*, 2011). A prospective study compared survival rates of patients with tourniquets applied to those who presented at hospital with no tourniquet but were perceived to have potentially benefited from tourniquet application (Kragh Jr *et al.*, 2009). The patients were matched by ISS and AIS score and had obtained only limb injuries. This study found a 92% improvement in survival rate when tourniquets were applied and an 80% increase in survival rate if the tourniquet was applied before the onset of shock (Kragh Jr *et al.*, 2009). A further study by Kragh *et al* found similar results with a 90% survival rate if the tourniquet was applied pre-shock onset compared to an 18% survival rate when the tourniquet was placed post-shock (Kragh Jr *et al.*, 2011).

The tourniquet is also routinely used in surgery on the extremities, particularly during total knee arthroplasty (TKA) operations. When combined with proper exsanguination of the limb, a bloodless surgical field can be created improving visualisation of the operative site (Zhang *et*

et al., 2014, Tarwala *et al.*, 2014, Harsten *et al.*, 2015). It should be noted that blood may still enter the surgical field through the intramedullary vessels of the long bones (Van der Spuy, 2012). Many surgeons are of the opinion that tourniquet use helps to decrease blood loss, enables better cementation and also reduces the operative time (Zhang *et al.*, 2014, Tarwala *et al.*, 2014, Harsten *et al.*, 2015). On the other hand, some surgeons think that tourniquet use leads to increased limb pain post-operatively and can lead to a delayed recovery.

Possible complications associated with operative tourniquet use include thigh pain, soft tissue damage, post-operative stiffness, limb swelling, nerve palsy, thromboembolic complications, rhabdomyolysis and post-tourniquet syndrome (Zhang *et al.*, 2014, Wang *et al.*, 2016, Ejaz *et al.*, 2014, Tarwala *et al.*, 2014, Harsten *et al.*, 2015, Van der Spuy, 2012). Post-tourniquet syndrome is characterised by pain, swelling, weakness and stiffness in the affected limb which is thought to be caused by oedema, vascular congestion and ischaemic reperfusion injury (Harsten *et al.*, 2015, Van der Spuy, 2012, Nishikant Kumar *et al.*, 2015). Post-tourniquet syndrome should resolve in 1 to 6 weeks but the increased pain coupled with reduced muscle strength and a smaller range of motion in the knee could lead to delayed recovery (Van der Spuy, 2012, Ejaz *et al.*, 2014). Many studies have been undertaken to try and determine if patient recovery after TKA is affected by the presence and duration of tourniquet use.

Dual bladder tourniquets do exist but currently are only used during intravenous regional anaesthesia (IVRA). IVRA is a technique used to provide localised anaesthesia to an extremity to enable operations to be carried out on an awake patient (Rawal, 2000, AnaesthesiaUK, 2005). In IVRA the extremity is isolated using a tourniquet and injected with local anaesthetic, the effects of the local anaesthetic rapidly disappear once the tourniquet has been released (Rawal, 2000). To

prevent leakage of local anaesthetic the tourniquet should be inflated to a high pressure and the local anaesthetic injected slowly (Rawal, 2000, AnaesthesiaUK, 2005).

When a dual bladder tourniquet is used the proximal cuff is inflated first. If the patient starts complaining of tourniquet pain the distal cuff, positioned on the anaesthetised area, should be inflated. Once the distal cuff is inflated the proximal cuff should be deflated (Rawal, 2000, Jafarian *et al.*, 2016, Checketts, 2013, Cave and Finegan, 2007). Care should be taken when switching between bladders to ensure both bladders are not deflated at the same time as this could lead to toxic levels of local anaesthetic entering the systemic circulation (Rawal, 2000, Cave and Finegan, 2007). The anaesthetist should consider switching between bladders after 30 minutes even if no tourniquet pain is felt to reduce the chance of nerve injury (Cave and Finegan, 2007).

Tourniquet pain is a phenomenon that develops 30-60 minutes after tourniquet inflation. It presents as a dull aching pain which cannot be relieved by anaesthesia or administration of intravenous opiates (Van der Spuy, 2012, Wong and Irwin, 2015). Clinical signs are seen in patients under general, local or regional anaesthesia and include hypertension and a faster heart rate. The current thought is that tourniquet pain is due to the conduction of pain signals from the slow acting unmyelinated C fibres (Van der Spuy, 2012). In addition to swapping bladders on a dual tourniquet, tourniquet pain may be relieved by deflating the tourniquet for 15 minutes (Wong and Irwin, 2015).

3.1.2. Tourniquet Considerations:

When applying a tourniquet in a combat scenario, it is recommended to apply the tourniquet as proximally as possible. High placement ensures that any hidden injuries are also included under the tourniquet to prevent possible increased bleeding at these sites (Shackelford *et al.*, 2014). The tourniquet should be applied with sufficient compression to restrict blood loss. If the tourniquet is not tight enough it will not occlude arterial flow leading to increased venous bleeding (Shackelford *et al.*, 2014). Analysis of tourniquets applied in the field showed that tourniquets were often relatively loose when checked by physicians at a medical centre (Kragh Jr and Dubick, 2016).

One reason for tourniquet looseness is the presence of clothing or filled pockets under the tourniquet belt (Kragh Jr *et al.*, 2011). However, there are many reasons why the tourniquet may become loose after being applied sufficiently tightly. The first of these is the relaxation of the limb muscles. When applying a tourniquet, particularly when self-applying, the muscles are likely to be tensed. When the muscles relax the size of the limb reduces, thereby decreasing the effectiveness of the tourniquet (Kragh Jr and Dubick, 2016). Compression of the limb by tourniquet will force fluid from both the blood vessels and the lymphatic system. This will alter the volume of the limb resulting in a less effective tourniquet as the pressure on the limb has been reduced (Kragh Jr and Dubick, 2016). Furthermore, movement of the limb can cause tourniquet looseness. Moving the limb, especially by elevation of the leg by hip extension will cause the muscles to relax and contract in response (Kragh Jr *et al.*, 2008). This change will alter the location of pressure on the limb and can lead to looseness and increased bleeding. Therefore, continuous monitoring of tourniquet pressure is an essential part of this therapy.

Tourniquet failure can also cause a huge problem in the field as exsanguination can occur resulting in patient death. Tourniquets can fail for a number of reasons. It is possible that one tourniquet will not produce enough pressure to stop blood flow in limbs with a wide girth, e.g. the thigh. In these situations, multiple tourniquets should be used to achieve sufficient pressure. A retrospective study of tourniquet applications over 7 months in Iraq found that only 53% of tourniquets were effective first time (Kragh Jr et al., 2008). Applying one or more additional tourniquets next to this original one increased the effectiveness by 34% (Kragh Jr et al., 2008). The narrowness of the tourniquet when compared to limb girth was the most common reason for tourniquets to fail (Kragh Jr et al., 2008, Schreckengaust, Littlejohn and Zarow, 2014).

Additional reasons for tourniquet failure included device breakage such as bursting of pneumatic tourniquets or strap breakage, incorrect use such as placing the tourniquet upside down or incorrect placement such as placing the tourniquet distally to the wound (Kragh Jr et al., 2008). When a tourniquet has been applied, it should be checked initially to see if complete occlusion of blood flow is achieved. Complete effectiveness of the tourniquet should halt the distal pulse (Kragh Jr et al., 2008). The suitability of continued use of the tourniquet should be assessed after, at most, 2 hours to see if another method of haemorrhage control can be used (Shackelford et al., 2014).

The operative tourniquet pressure is usually decided by one of three methods. The first is a fixed inflation pressure. These fixed inflation pressures are normally 250mmHg for the upper arm and 300mmHg for the thigh (Sharma and Salhotra, 2012, Deloughry and Griffiths, 2009). The second method is to inflate the tourniquet to a fixed amount above the systolic arterial pressure (Deloughry and Griffiths, 2009, Sharma and Salhotra, 2012). When positioning the tourniquet on the upper arm it should be

inflated to 100mmHg above the systolic arterial pressure. When positioned on the thigh the pressure should 100-150mmHg higher than systolic arterial pressure (Sharma and Salhotra, 2012, Deloughry and Griffiths, 2009). Alternatively the tourniquet can be inflated to a pressure based on the limb occlusion pressure (Van der Spuy, 2012, Deloughry and Griffiths, 2009).

<i>Table 3-1: Recommended tourniquet inflation pressures based on limb occlusion pressure (Van der Spuy, 2012, Deloughry and Griffiths, 2009)</i>	
Limb occlusion pressure	Additional pressure
<130mmHg	40mmHg
131-190mmHg	60mmHg
>190mmHg	80mmHg

Reducing the tourniquet pressure may help to reduce post-operative pain, therefore, the pressure of the operative tourniquet should be kept to a minimum (Nishikant Kumar *et al.*, 2015). Setting the tourniquet inflation pressure based on the limb occlusion pressure is likely to result in the lowest effective tourniquet pressures. However, these pressures may be too low to prevent leakage when trying to isolate and perfuse the limb as has been found in IVRA (AnaesthesiaUK, 2005).

The operative tourniquet cuff should be selected to ensure it is the right size for the limb. The cuff should overlap by at least 75mm to ensure an even pressure is applied to the limb (Kamal Kumar, Railton and Tawfic, 2016). The cuff should not overlap by more than 150mm to prevent overly high pressures occurring (Kamal Kumar, Railton and Tawfic, 2016). Padding is recommended to protect the skin under the band. However, the padding shouldn't be too thick as to prevent

adequate pressure being transferred to the limb (Wong and Irwin, 2015). The padding should also be kept smooth as creases under the tourniquet can create blisters and lesions on the skin (Van der Spuy, 2012, Wong and Irwin, 2015). It is important to keep alcohol-based solutions used in skin preparation from seeping under the tourniquet band as they can cause chemical burns when held against the skin under pressure (Van der Spuy, 2012). Trying to re-position a fully inflated tourniquet can create friction burns on the skin and should be avoided (Van der Spuy, 2012).

3.1.3. Tourniquet complications:

Tourniquet use was controversial and considered as a method of last resort all the way up to 2005 (Shackelford *et al.*, 2014). This was due to the association of nerve damage and cellular morbidity. Cellular morbidity is uncommon when tourniquet use is brief. One study showed that nerve paralysis occurred in between 1.5-1.7% of patients whilst major limb shortening occurred in 0.4% (Kragh Jr *et al.*, 2011). It has been shown that incorrect or prolonged usage of a tourniquet can lead to iatrogenic morbidity particularly in skeletal muscle (Perkins *et al.*, 2012). The two most commonly affected cell types are nerves and skeletal muscle, damage to these cells is caused by ischaemia and/ or mechanical action (Wong and Irwin, 2015). During ischaemic conditions, there is a build-up of reactive oxygen species (ROS) and activated neutrophils (Gillani *et al.*, 2012). The ROS are potent reducing agents which cause damage to the lipids in the cell membrane which can lead to necrosis (Gillani *et al.*, 2012). The activated neutrophils can also cause necrosis which in turn leads to further inflammation and tissue damage. Once the tourniquet is removed these neutrophils and ROS can enter the systemic circulation and cause ischaemic reperfusion injury. Crush injury is the systemic presentation of ischaemic reperfusion injury due to direct pressure (Gillani *et al.*, 2012).

The critical ischaemic time is defined as ‘the maximum time interval that a tissue can tolerate ischaemia and still remain viable’ (Gillani *et al.*, 2012). Skeletal muscle is the tissue that is most vulnerable to ischaemia, its critical ischaemic time is around 3 hours of warm ischaemia, as seen in Table 3-2 (Perkins *et al.*, 2012). The next most susceptible tissue is peripheral nervous tissue which can tolerate 8 hours of warm ischaemia (Gillani *et al.*, 2012). Loss of viable muscle tissue causes issues with limb salvage and limb function. Fast twitch type II myosin fibres are more susceptible to ischaemic damage than slow twitch fibres (Gillani *et al.*, 2012). The extent of muscle injury increases when higher tourniquet inflation pressures are used and for a longer time (Van der Spuy, 2012).

*Table 3-2: Critical ischaemic time of various tissue types (Gillani *et al.*, 2012, Perkins *et al.*, 2012)*

Tissue type	Critical warm ischaemic time
Muscle	3 hours
Peripheral nerves	8 hours
Fat	13 hours
Skin	24 hours
Bone	4 days

Whilst ischaemic injury is the bigger cause of damage to muscle cells, mechanical pressure has a bigger influence in nerve injury (Van der Spuy, 2012, Checketts, 2013). Most nerve damage occurs at the edge of the tourniquet cuff where the pressure is greatest (Van der Spuy, 2012, Wong and Irwin, 2015). Compression of the nerve causes the Node of Ranvier to be displaced from its normal placement at the Schwann cell junction leading to signal disruption (Van der Spuy, 2012, Wong and Irwin, 2015). Furthermore, mechanical pressure disrupts the myelin lamellae and can lead to

shrinkage of the axon (Wong and Irwin, 2015). This damage is irreversible. Nerve injury occurs in between 0.1-7.7% of cases (Van der Spuy, 2012). Other possible complications due to tourniquet use are the increased risk of pulmonary embolism and deep vein thrombosis and the risk of circulatory overload (Van der Spuy, 2012). The risk of thromboembolic complications is increased due to cessation of venous blood flow leading to clot formation (Harsten *et al.*, 2015, Zan *et al.*, 2015). Circulatory overload can be induced by the combination of an increase in the vascular resistance and central venous pressure caused by exsanguination and the consequent inflation of a tourniquet (Van der Spuy, 2012). Compartment syndrome can be triggered when the tourniquet is released. Once the tourniquet is released there is an immediate inflow of blood into the vessels of the limb, observable by swelling of the limb (Estebe, Davies and Richebe, 2011). The inflow of blood also causes a rapid increase in the intercompartmental pressure of the limb which, if unchecked, can lead to compartment syndrome (Estebe, Davies and Richebe, 2011).

Harsten *et al* studied the effect of tourniquet use on knee extension strength after TKA. They found that at 48 hours after surgery there was no significant difference between knee extension strength, pain, nausea or periarticular swelling between patients operated on with or without the presence of a tourniquet (Harsten *et al.*, 2015). Similarly, Liu *et al* found that the range of motion in the knee was not significantly different when TKA was performed using a tourniquet compared to no tourniquet application (Liu *et al.*, 2014). In addition, Tai *et al* found that there was no significant difference in the severity of limb swelling post-operatively between tourniquet use or no tourniquet use (Tai *et al.*, 2012). Whilst these studies suggest tourniquet use does not affect recovery, it is possible that due to the number of patients used in these studies, the sample size was not big enough to demonstrate significance.

Results from other studies contradict the above results and suggest that tourniquet use is related to a delayed recovery and higher pain levels post-surgery. Ejaz et al found that post-operatively patients who had undergone TKA without a tourniquet had improved range of motion in the knee with the difference still detectable at 8 weeks. The range of motion in the knee in the tourniquet group was similar to the no tourniquet group by the 6 month follow up (Ejaz et al., 2014). Furthermore, Ejaz et al found that those patients in the tourniquet group had greater analgesic consumption and pain in the thigh for up to 3 weeks after discharge (Ejaz et al., 2014). Studies by Tai et al, Guler et al and Liu et al also found that pain was lower in the no tourniquet groups, however, this difference was only significant on sporadic days after the surgery (Tai et al., 2012, Guler et al., 2016, Liu et al., 2014). One problem with comparing pain scores is that pain is subjective, therefore patients with a lower pain tolerance would perceive the post-operative pain to be much higher.

Guler et al used MRI to observe the thigh volumes of patients who underwent TKA with or without a tourniquet and compared them to the contralateral control leg. This study found that no difference in the thigh volume at one month of patients who were in the non-tourniquet group but saw a 20% volume decrease at one month in those patients who were in the tourniquet group (Guler et al., 2016). The volume difference had resolved by 12 months post-surgery (Guler et al., 2016). The use of a tourniquet in this study was not randomised but was down to surgeon preference, this may mean that differences seen may have been due in part to surgical technique rather than the use of a tourniquet. Liu et al also looked at the effect of a tourniquet on the quadriceps muscle. They found that the quadriceps muscles of the tourniquet group had significantly less activity than the quadriceps of those in the no tourniquet group, this difference had resolved by 6 months (Liu et al., 2014).

Considering the fact the extent of injury underneath the tourniquet is related in part to the duration of tourniquet inflation (Nishikant Kumar *et al.*, 2015), it would be logical that reducing the amount of time the tourniquet is inflated would result in better outcomes for the patient. For this reason, studies have compared the outcomes of patients who have a tourniquet inflated for the whole TKA procedure (operative tourniquet) to inflation of the tourniquet for only the cementation portion of the operation (cementation tourniquet). Tarwala *et al.* did not find any significant difference in the mean pain scores, knee range of motion or quadriceps strength when comparing the operative tourniquet to the cementation tourniquet (Tarwala *et al.*, 2014).

On the other hand, Wang *et al.* found that patients in the cementation tourniquet group had significant reductions in thigh and knee pain, thigh and knee circumference and knee range of motion at days 1 and 2 and 1 week post-operation (Wang *et al.*, 2016). The patients in this trial underwent TKA operations with both tourniquet application methods. Each knee was operated on separately with 3 months between operations. The benefit of this method is that the patients can be compared to themselves. However, it is possible that the patients had not fully recovered from their first operation at 3 months so the comparison between legs may be skewed by this.

Olivecrona *et al.* also found that patients who underwent TKA with a shorter tourniquet time displayed better knee flexion compared to longer tourniquet times (Olivecrona *et al.*, 2013). The local effects seen when using a tourniquet may be due to direct pressure of the tourniquet or from ischaemia (Harsten *et al.*, 2015). If the inflation time of the tourniquet is reduced the injury to the

local tissue may well be reduced. One way it may be possible to decrease the tissue injury produced during a TKA would be to have a dual bladder tourniquet where the bladder that is inflated alternately at set intervals. Alternating the location of the pressure would give the tissues time to recover and would hopefully reduce tissue damage during the surgery.

3.2. Design Considerations:

To determine the length of the tourniquet the National Statistics Report on Anthropometric Reference Data for Children and Adults in the United States between 2003-2006 was consulted. This report stated that the average adult mid-arm circumference was 341mm and the mid-thigh circumference was 529mm (McDowell *et al.*, 2008). To ensure at least a 75mm overlap, as suggested in the tourniquet considerations above, a thigh tourniquet length of at least 604mm should be created (Kamal Kumar, Railton and Tawfic, 2016). A separate arm tourniquet should be designed with a length of at least 416mm. The same length tourniquet should not be used for both limbs as a tourniquet of 625mm would create an overlap greater than the 150mm stated by Kumar *et al* leading to extreme pressures on the tissue (Kamal Kumar, Railton and Tawfic, 2016). The length of the thigh is a natural restriction to the width of the tourniquet. The tourniquet needs to be relatively narrow to still be able to be used on injuries further up the thigh. However, this means that both bladders also need to be narrow. The disadvantage of narrower bladders is that increased pressures are then necessary to occlude blood flow, increasing the risk of tissue damage. The tourniquet has been designed with each bladder to have a width of 60mm after accounting for glue lines as a compromise between width and pressure.

The tourniquet must be effective at stopping blood flow through the limb. The maximum proposed inflation pressure is 350mmHg which is the highest pressure commonly used during intravenous regional anaesthesia (IVRA) (Jafarian *et al.*, 2016, Checketts, 2013, AnaesthesiaUK, 2005). Using the highest pressure should halt haemorrhage. The lower pressure settings can be used whilst the limb is isolated on the limb support system.

<i>Table 3-3: Tourniquet pressure settings and when they should be used (Checketts, 2013, Jafarian et al., 2016, AnaesthesiaUK, 2005)</i>	
Pressure	Use
250mmHg	Upper limb
300mmHg	Standard lower limb
350mmHg	High pressure – use if 300mmHg is not able to sufficiently isolate the limb or halt bleeding

Due to the need to keep the limb isolated from the rest of the circulation when on limb support it may not be possible to drop the tourniquet pressure any further to reduce the chance of tissue damage over an extended period of time. The tourniquet should stay at a constant pressure to ensure the pressure on the limb is consistent. Furthermore, it is important to ensure the tourniquet will not release unexpectedly.

Each bladder will be inflated alternately. Bladder inflation can either be achieved manually with a sphygmomanometer or automatically using an air compressor. The tourniquet bladder should not be inflated for extended periods of time to prevent tissue damage. The bladder should also be deflated for long enough to allow for the tissue underneath to recover and

get sufficiently re-perfused. Considering the fact tourniquet pain can be relieved by deflation of the tourniquet for 15 minutes, this is likely to be a suitable time for bladder change intervals (Wong and Irwin, 2015). However, this timing will need to be tested to determine if it is the most effective in terms of protection from tissue damage. If the bladder is inflated automatically, contingency plans will need to be put in place in case of power failure. Deflation of the tourniquet upon power failure could lead to catastrophic haemorrhage or toxic levels of drugs, such as local anaesthetics, in systemic circulation due to the mixing of the blood from the limb and body, both of which could be fatal. Therefore, if the power fails it is important that the tourniquet will stay inflated

The tourniquet may need to be originally applied during a firefight. This means that the tourniquet must be able to easily be applied by either the injured soldier or one of their uninjured compatriots. The tourniquet should be able to be rapidly applied to an appropriate standard to enable the uninjured personnel to continue fighting and provide the casualty with the best chance of survival. For this reason, the tourniquet should be simple to use with no complicated or unnecessary steps involved in its application, such as assembly of different parts. An automated tourniquet would have the benefit of the medic not having to keep track of how long each bladder had been inflated for. Furthermore, the medic would not have to change which bladder is inflated at set intervals allowing them to concentrate on other tasks such as treating other casualties.

One issue with the tourniquet being battery powered is the shelf-life of the battery. The tourniquet is issued at the start of the tour, hopefully the soldier will never need to use it. However, it is important that if the tourniquet needs to be used the battery will still be

charged, be it on the first day of the tour or the last. This means that the battery should be easily changed and have some sort of indicator that the battery is fully charged. The battery also needs to be big enough to power the tourniquet for some time without going flat whilst not taking up too much space or weight. Furthermore, an automated tourniquet needs to have minimal noise (Kragh *et al.*, 2011). If the air compressor makes a lot of noise then this could represent a security risk. Additionally, the noise could prove distracting to the soldier or prevent orders from being heard. For the prior stated reasons, it may be beneficial to have the ability to manually inflate the tourniquet in times of power loss or tactical use.

Multiple tourniquets are currently issued to troops on the front line. The new tourniquet must be lightweight to not create a weight burden, e.g. less than 230g per soldier (Kragh *et al.*, 2011). Moreover, the tourniquet must be compact so it can easily be carried in kit bags or trouser pockets. Tourniquets should be easily accessible on the battlefield so it is beneficial if the tourniquet can fit in bag or trouser pockets. Additionally, the tourniquet should be highly durable. It will need to withstand being thrown into kit bags and carried on the battlefield. If the tourniquet gets punctured it is no use so the material needs to be strong enough to withstand damage. Moreover, the military is deployed to many different environments encountering varying conditions from snow and ice to rain and mud to the sand and dust of the desert (Kragh *et al.*, 2011). The tourniquet needs to be able to be effectively used in a variety of different conditions and not influenced by the operative setting.

Ideally the tourniquet should be able to be used at all stages in the casualties' care from the battlefield to the operating theatre. Having a tourniquet suitable for all situations means that the military will not have to invest in multiple styles of tourniquet for the different stages of

care of one patient. Moreover, tourniquets are reused where possible and are not seen as a single-use device. Bearing this in mind, the tourniquet should be easily cleaned, repaired and tested to be shipped back to the field to be used again (Kragh *et al.*, 2011). To help this, the tourniquet should be easily removable and not require cutting off (Kragh *et al.*, 2011). If the tourniquet is going to be used multiple times, the integrity of the tourniquet should remain. The tourniquet should not stretch or deform overtime to ensure the haemorrhage is stopped effectively every time the tourniquet is used.

3.3. Design of dual-outlet valve:

Central to the function of a pneumatic tourniquet is the pressure control apparatus. The valve apparatus was designed to enable air flow to be directed into one of the two bladders. The valve was printed using an EnvisionTEC® Perfactory® Desktop XL printer (EnvisionTEC GmbH, Gladbeck, Germany) at a resolution of 25 microns. The valve has two positions, each corresponding to the filling of a single bladder by connecting the airflow from the pump to the inlet for that bladder. When the valve is positioned to fill up one bladder, the air in the other is released through a vent in the top of the valve to ensure the pressure is relieved completely. Figure 3-1 shows both the CAD drawing and a photograph of the valve along with a diagrammatic demonstration of the inflation mechanism. A sphygmomanometer was used initially to inflate the bladders.



Figure 3-1: CAD drawing and 3D printed dual way valve with inflation mechanism demonstrated

3.4. Initial Tourniquet Design:

The tourniquet bladders were designed to be made out of a durable PVC-coated fabric to enable the bladders to be air-tight. Different methods of sealing this material were investigated. The initial idea was to heat seal the material, however, this did not prove to be suitable under laboratory conditions. Ultimately it was decided to use Polymarine PVC adhesive (Polymarine Ltd, Conwy, UK). This glue was able to produce an airtight bladder and to securely hold the sections of the tourniquet together.

The first iteration was made from 290 g/m² PVC-coated polyester (Attwools Manufacturing, Gloucester, UK). The dimensions of this tourniquet prototype were as seen below. The bladders were sealed and the parts connected together using the Polymarine adhesive mentioned previously.

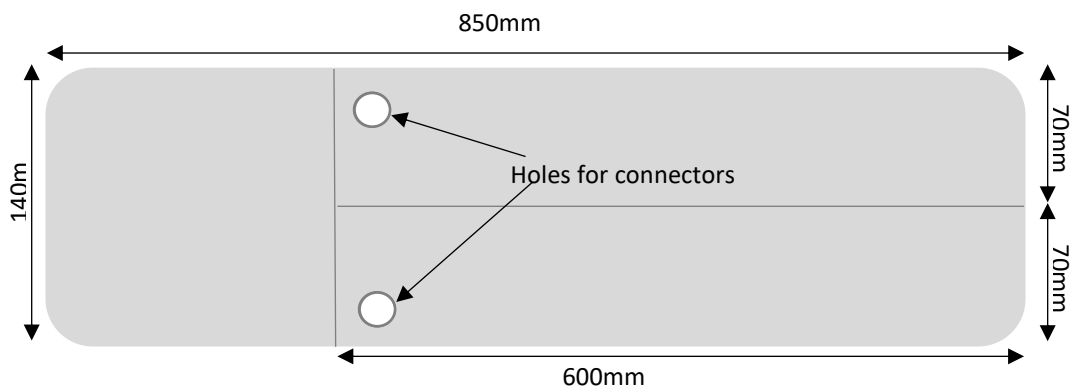


Figure 3-2: Dimensions of initial tourniquet

14mm holes were punched in the bladder material before assembly using a Harris uni-core tip (Ted Pella, Inc, CA, US). These holes provide the connection between the bladder and the pump system. A special unit was designed and 3D printed to enable a Welch Allyn Flexiport blood pressure cuff connector (ProCure Health t/a Medical Supermarket, Buckinghamshire,

UK) to be attached to the bladders. These units were printed using the same EnvisionTEC® printer as described previously. Once printed these parts were glued into the holes punched previously, before the blood pressure connector was clipped on. Welch Allyn Flexiport tubing (Medisave, Dorset, UK) was used to connect the valve and pump.



Figure 3-3: Individual parts and assembled connector

Velcro (MPD Hook and Loop, Wiltshire, UK) was glued to the top side of the bladders and the underside of the cuff to allow the tourniquet to be fastened round the limb.



Figure 3-4: Initial tourniquet

3.5. Design Alterations:

3.5.1. Second Iteration Tourniquet:

After initial trials which highlighted some technical issues with the initial configuration a second iteration of the tourniquet was made. The second iteration of the tourniquet was made using the same techniques as the first. However, this time a thicker 560 g/m² PVC-coated polyester material (Attwools Manufacturing, Gloucester, UK) was used. This thicker material means that the tourniquet will be more durable.

The tourniquet was made to the same dimensions as the first iteration.



Figure 3-5: Second iteration tourniquet

3.5.2. Third Iteration Tourniquet:

The design of the tourniquet was changed slightly for the 3rd iteration. Previously the tourniquet was made as one part. For the 3rd iteration this was changed to enable the bladders to be separated. One benefit of this is that even if there is a wound very high on the limb it is still possible to use the tourniquet even if only one bladder is utilised.

The bladders were created individually using the same method as the two previous iterations. The cuff was also created in two separate sections. The dimensions of one of the cuffs and bladders can be seen in Figure 3-6. When building this iteration of tourniquet an airtight seal was not achieved after gluing. To resolve this problem the bladders were inflated under water to identify where air was leaking from. The position of these leaks was marked and then superglue (Loctite, RS Components, Corby, UK) was applied to these areas of weakness when the bladders were dry. Air was also found to leak around the housing units for the blood pressure cuff connectors. Superglue was applied to resolve this issue. In addition, the blood pressure cuff connectors were superglued to their housing units to prevent air leaking here.

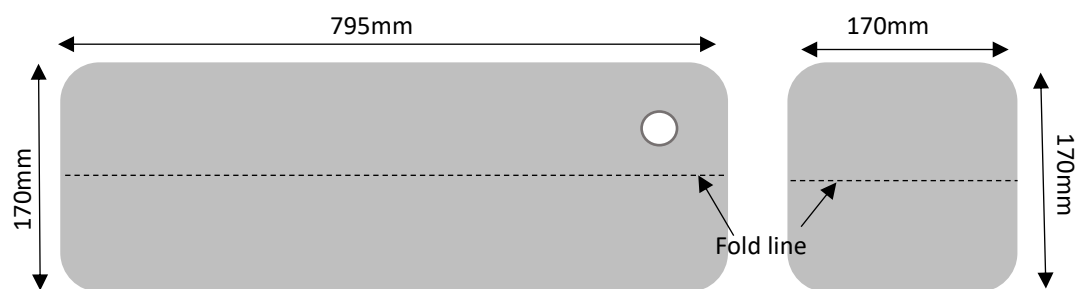


Figure 3-6: Dimensions of one tourniquet bladder

To connect the two sides together Velcro was applied down the glued long edge of each bladder and cuff. To allow for easy identification of which bladder would inflate in that valve

position coloured tape was applied to the long edges of the bladders and on the tubes leading to the valve. The bladder will inflate when the colours are matched up. The completed 3rd iteration of tourniquet is shown in Figure 3-7.



Figure 3-7: Third iteration of tourniquet

3.5.3. Fourth Iteration Tourniquet:

The design had another slight change when creating the 4th iteration. Firstly, the material the tourniquet is made out of was altered to a slightly thinner PVC-coated polyester (Attwools Manufacturing, Gloucester, UK). An airtight seal was easier to achieve with this material.

Furthermore, 2 different coloured materials were used to create the bladders. This is because having the whole bladder in a different colour makes it easier to tell which bladder will be inflated with the valve position. The two colours used were green and blue. It may ultimately be necessary to change these colours depending on how well the two colours can be distinguished by colour blind personnel.

An additional change in the design was to make each side of the tourniquet from just one section, i.e. the bladder and cuff are made out of one continuous piece of material. The glue

join is an area where failure of the device could occur so removing this reduces the chance of failure. The dimensions for the new design can be seen in Figure 3-8.

Velcro was placed both along the glued long edges of each side of the tourniquet and in the same place as the other iterations to provide the fastener.

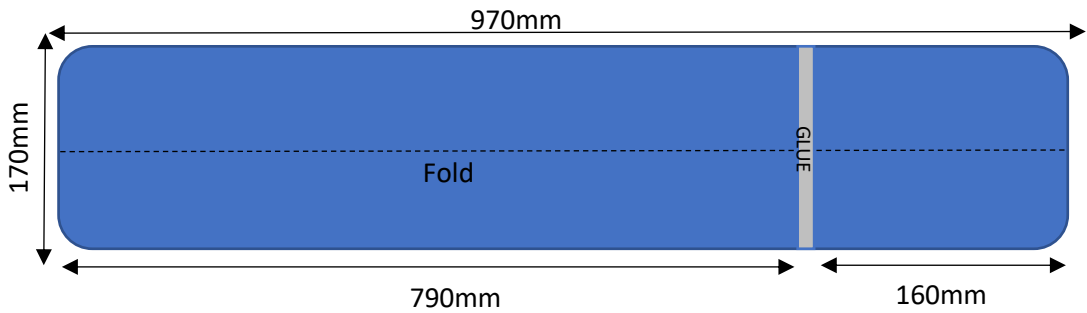


Figure 3-8: Dimensions of one bladder for fourth iteration tourniquet



Figure 3-9: 4th iteration of tourniquet with two different colour bladders and Velcro holding them together

When inflating this tourniquet, it was found that the Velcro did not hold the tourniquet in position very well. This is likely to be due to the fact that the thinner material was more flexible and therefore would bend out of place when the air bladders were inflated. The 3rd iteration of tourniquet was also better at holding the pressure in the bladders, probably because the bladders wouldn't move out of position when inflated.

3.5.4. Fifth Iteration Tourniquet:

This tourniquet was made of the same material as the third iteration. However, the difference in this tourniquet was the dimensions were changed to make it longer as shown in Figure 3-10. The technique of making the tourniquet was also to create the bladder and end tab as two separate parts due to the difficulties in achieving a seal in the join on the middle glue line.

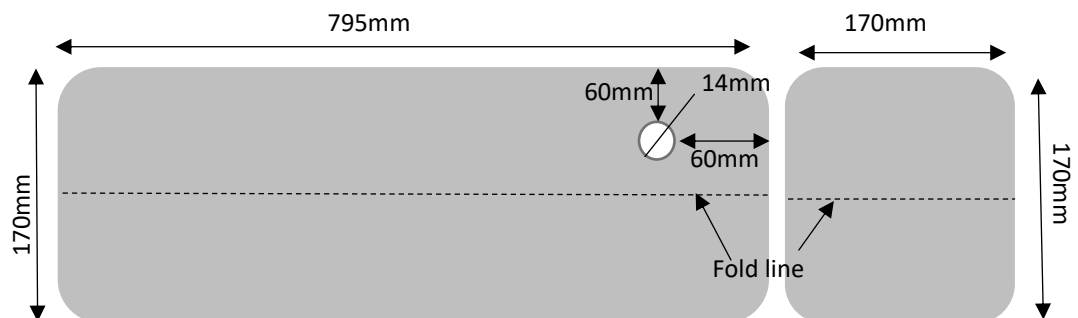


Figure 3-10: Dimensions of the fifth iteration of tourniquet

Coloured tape was not used to mark the bladders in this iteration. The inflation of this tourniquet is controlled using an automated system. For this reason, it was not necessary for the bladders to be labelled for easy identification. Additionally, the two-way valve was not needed to switch between the inflation of the two bladders. Figure 3-11 shows the completed tourniquet.



Figure 3-11: Completed fifth iteration of tourniquet

3.5.4.1. Testing of fifth iteration of tourniquet

To test the effectiveness of this tourniquet at stopping the bleeding in a casualty, the tourniquet was tested on the CHI Systems HapMed tourniquet trainer (CHI Systems Inc, Pennsylvania, USA). The HapMed is a mannequin which simulates an above knee amputation. The HapMed is the accepted test for tourniquets within industry (Glick *et al.*, 2018, Kragh Jr *et al.*, 2014). The HapMed has lights which go out as bleeding is successfully controlled. There is also a distal pulse which will stop if the tourniquet is correctly applied. There is a feedback screen which provides feedback on the tourniquet position and application. The HapMed has 7 different training scenarios which have increasing levels of difficulty (CHI Systems Inc, 2019). The scenario used in the following testing was scenario 1.

To test the tourniquet, the bladder was wrapped around the HapMed. The HapMed was turned on and scenario 1 was started. The bladder inflated using a sphygmomanometer to determine if the bladder was in the correct position. The bladder was then deflated and the scenario restarted. The tourniquet bladder was then inflated 10 times and the pressure required to stop the blood flow according to the feedback on the HapMed was recorded. The pressure required can be seen in the table below

<i>Table 3-4: Pressure required to halt haemorrhage in tourniquet iteration 5</i>	
Test	Pressure required to halt haemorrhage (mmHg)
1	220
2	220
3	210
4	220
5	220
6	230
7	220
8	220
9	220
10	220

As Table 3-4 shows, the original width tourniquet was able to stop the bleeding on all 10 occasions with a mean of 220 ± 4.71 mmHg. The HapMed is designed for the bleeding to stop at 200mmHg so this tourniquet seems to work well. It was difficult to wrap the tourniquet tightly round the limb which may be responsible for the 20mmHg more pressure needed to stop the bleeding. This shows that the tourniquet will be able to stop the bleeding in most cases.

3.5.5. Sixth Iteration Tourniquet:

The previous iterations of tourniquet have a considerable width (150mm). This width will take up a large portion of the thigh, if the wound is located high on the thigh then the tourniquet will be too wide to be used. Consequently, the tourniquet was redesigned to have thinner bladders with a total width of 70mm as seen in Figure 3-12.

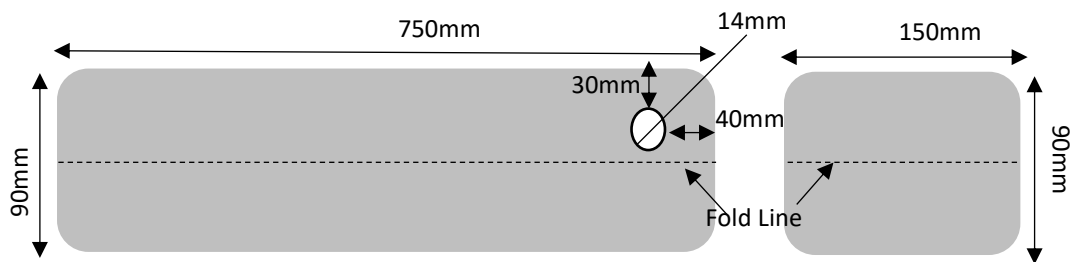


Figure 3-12: Dimensions of sixth iteration of tourniquet

Whilst thinner bladders would allow for use with proximal wounds, it is possible that the tourniquet will not produce enough pressure to adequately halt haemorrhage. Thus, testing of the tourniquet was required to establish if the tourniquet is able to stop the bleeding.

3.5.5.1. Testing of tourniquet iteration six:

The protocol to test the sixth iteration tourniquet was the same as the one used to test iteration 5. The ability of the tourniquet to stop the bleeding can be seen in Table 3-5.

Table 3-5: Pressure required to halt haemorrhage in tourniquet iteration 6

Test number	Pressure required to halt haemorrhage (mmHg)
1	Haemorrhage not controlled
2	Haemorrhage not controlled
3	Haemorrhage not controlled
4	Haemorrhage not controlled
5	Haemorrhage not controlled
6	Haemorrhage not controlled
7	Haemorrhage not controlled
8	Haemorrhage not controlled
9	Haemorrhage not controlled
10	Haemorrhage not controlled

As these results show, the thinner sixth iteration of tourniquet was not able to stop the bleeding in any of the 10 tests. This is not too surprising. It was difficult to get the tourniquet tightly round the limb so pressure would not be able to be applied uniformly round the limb. The tourniquet is only 6mm wider than the CAT and SOFTT tourniquets in current use by the

military which also struggle to gain control of bleeding in the thigh (Wall, Sahr and Busing, 2015). This tourniquet may be suitable for use on the arm but the HapMed doesn't have the capability to test for this.

The photographs in Figure 3-13 show the testing of the tourniquet and the results screen seen on the HapMed. This screen shows that although the tourniquet is in a good position the bleeding is not controlled. The tourniquet on the left is iteration 6 with the thinner bladder. The tourniquet on the right is iteration 5, the adjacent placement of the two tourniquet iterations shows the difference in width.



Figure 3-13: Testing of tourniquet iteration 6 on the HapMed and a close-up of the results screen

3.5.6. Seventh Iteration Tourniquet:

To create a thinner tourniquet that could be used for high injuries on the thigh the seventh iteration of tourniquet was redesigned to have a width which was between iterations 5 and 6. The dimensions of the tourniquet are shown in Figure 3-14. This tourniquet has a combined width of 115mm. The glue line along the long edge was 15mm and the glue line on the short edge was 20mm.

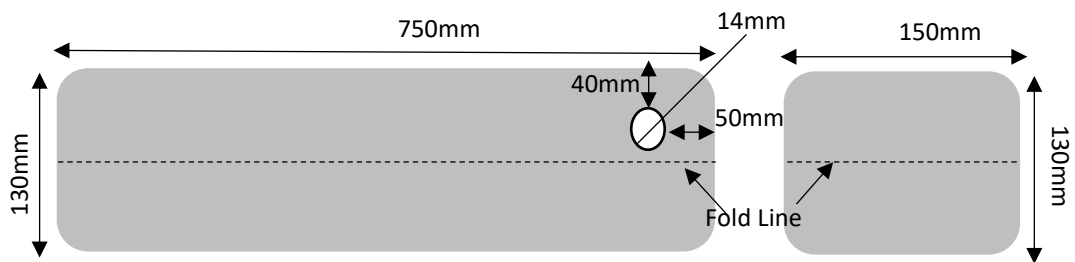


Figure 3-14: Dimensions of the seventh iteration tourniquet

3.5.6.1. Seventh iteration tourniquet testing:

The same protocol used for testing the 5th and 6th iterations was used to test this iteration of tourniquet. Table 3-6 shows the pressure required to halt the haemorrhage with this iteration of tourniquet.

Table 3-6: Pressure required to halt haemorrhage in tourniquet iteration 7

Test number	Pressure required to halt haemorrhage (mmHg)
1	300
2	300
3	300
4	300
5	300
6	300
7	300
8	280
9	280
10	280

The medium thickness tourniquet is able to stop the bleeding at a mean pressure of 294 ± 9.66 mmHg. This high pressure would not be suitable to use for a long time. However, again

it was difficult to get the tourniquet wrapped tightly around the limb which could have increased the pressure required. Similar to iteration 6, the tourniquet may be suitable to be used on an arm.

3.6. Future developments:

The final tourniquet design for the lower limb is iteration 5. This iteration had a length that was suitable for wrapping around a variety of limb sizes, guided by the National Statistics Report on Anthropometric Reference Data for Children and Adults in the United States between 2003-2006 and input from UK Military medical personnel. The different iterations of the tourniquet involved changes to the material that the tourniquet was constructed from, to examine the effect of different weights of PVC-coated polyester. It was found that the 560g/m² PVC-coated polyester was most effective in holding pressure and maintaining structure when compared to the lighter materials used in iterations 1 and 4. In summary, the tourniquet was designed to be a compromise between pressure application and width with the heavier material selected to ensure a more constant pressure in the bladders. However, further development of the tourniquet is planned.

The data from the testing of the fifth iteration tourniquet shows that the individual bladders of the tourniquet are able to halt haemorrhage in an amputated limb meeting the objective of haemorrhage control. The seventh iteration of tourniquet is also able to meet this objective, albeit at a higher pressure than desired. The tourniquet is much too long to be suitable for use on the arm as there will be a lot of overlap of the bladder, creating a higher

pressure on the skin. A shorter tourniquet should be developed for this purpose. Furthermore, the tourniquet cannot be wrapped around the limb very tightly even when using two hands. Therefore, it would not be suitable for self-application.

The problem with wrapping the tourniquet round the limb could be reduced in two ways. The first is by changing the material that the tourniquet is made from. The PVC-coated polyester used to make the tourniquets is not very flexible, therefore, it doesn't conform to the shape of the limb very well. Changing this material to something similar to the nylon used in blood pressure cuffs will make the tourniquet conform to the limb better which should also reduce the pressure needed to halt haemorrhage. Additionally, the tourniquet could be made with a conical shape. If the tourniquet had a narrower diameter at the bottom compared to the top it would be able to wrap more tightly around the limb. Again, this should reduce the pressure needed to halt the haemorrhage.

Chapter 4. Cooling sock design:

4.1. Benefits of therapeutic hypothermia:

Hypothermia has been used for centuries as a therapy for all kinds of conditions. Deliberate therapeutic hypothermia has many benefits and is often used in cardiac surgery, neurosurgery and some major vascular procedures (Polderman, 2004a). Therapeutic hypothermia is used frequently in the hospital to reduce the neurological damage induced by a cardiac arrest (de Waard *et al.*, 2013). The aim of therapeutic hypothermia is to increase the time window a procedure can be undertaken in before cell damage occurs (Polderman, 2004a). Therapeutic hypothermia has many useful mechanisms of action, the first is the effect of hypothermia on metabolism. Studies have shown that the metabolic rate decreases by 5% with each degree of temperature lost whilst enzyme activity shows a two-fold decrease with every 10°C decrease in tissue temperature (Gonzalez-Ibarra, Varon and Lopez-Meza, 2011, Hildebrand *et al.*, 2004). In vitro studies have shown that this decreased metabolism only occurs when the temperature drops below 35°C (Kohlhauer *et al.*, 2016). A decreased metabolic rate means that the consumption of O₂ and glucose is reduced which allows the cells to cope better with lower O₂ concentrations resulting from ischaemic conditions thereby providing some protection against tissue injury (Elizabeth M. Moore *et al.*, 2011).

Experiments in rabbits showed that topical hypothermia reduced the amount of cardiac ATP and glycogen used during 20 minutes of regional ischaemia (Simkhovich, Hale and Kloner, 2004). Seiyama *et al.* observed an increase in O₂ binding to myoglobin in rat skeletal muscle as temperature decreased (Seiyama *et al.*, 1996). This suggested that the myoglobin oxygen affinity increased and more O₂ was available to bind due to a decreased consumption (Seiyama *et al.*, 1996). Further studies

by Seiyama et al suggested that lowering the temperature reduced the rate of mitochondrial respiration (Seiyama *et al.*, 1996). The conclusion that can be gathered from this is that oxidative phosphorylation is suppressed more than glycolysis under hypothermia, leading to the theory that in hypothermia the process of glycolysis is important for producing ATP to allow for the preservation of the sodium-potassium ion concentration gradient across the cell membrane (Seiyama *et al.*, 1996).

Hypothermia is also thought to reduce the inflammatory response by inhibiting the release of pro-inflammatory cytokines such as Nuclear Factor κ B (NF- κ B) and suppressing the migration of leukocytes (Polderman, 2004b, Hassoun *et al.*, 2002). NF- κ B controls a number of transcription factors which regulate various genes involved in the production of the inflammatory response such as chemokines and cytokines (Lawrence, 2009). Additionally, it has been shown that hypothermia prevents the production and build-up of reactive oxygen species (ROS) such as superoxide ($\cdot\text{O}_2^-$) and other free radicals (Polderman, 2004a). Hassoun et al showed that hypothermia prevented the formation of nitrous oxide synthase meaning increased amounts of nitrous oxide (a potent free radical) was not produced (Hassoun *et al.*, 2002). A lower concentration of ROS being produced during ischaemia means that the cells anti-oxidative mechanisms are not overwhelmed and therefore, oxidative damage to the cell is reduced (Elizabeth M. Moore *et al.*, 2011, Polderman, 2004a). Reduced oxidative damage means that the cell is less likely to be triggered to undergo apoptosis.

The process of apoptosis in the cell is also prevented by several other methods during hypothermia. These mechanisms include the inhibition of the caspase pathway and decreasing the concentration of apoptotic gene transcription factors (Gonzalez-Ibarra, Varon and Lopez-

Meza, 2011). Moreover, hypothermia is thought to prevent excessive flow of Ca^{2+} into the cell (Polderman, 2004b). High levels of Ca^{2+} can cause mitochondrial dysfunction and trigger enzymatic pathways which lead to cell death (Polderman, 2004b). Furthermore, hypothermia induces the production of cold shock proteins which help prevent cell damage in the presence of ischaemia or trauma (Elizabeth M. Moore *et al.*, 2011).

Following cardiac stress of laboratory-induced cardiac arrest, hypothermia has been shown to help maintain blood pressure and the oxygen saturation in the brain (Ostadal *et al.*, 2013). Maintaining blood pressure will also contribute to protecting the organs from damage as it allows for adequate perfusion. Hypothermia has also been linked to decreased vascular permeability in ischaemia helping to prevent the formation of oedema (Polderman, 2004a). However, many undesirable effects can be seen in the blood stream when the patient is hypothermic. The first of these is the inhibition of the enzymatic reactions of the coagulation cascade (Hildebrand *et al.*, 2004). Significantly increased blood loss has been reported to occur in operations conducted where the core body temperature is 35°C than at normothermia (Hildebrand *et al.*, 2004). It has been observed that cooling the skin of the forearm from 32°C to 30°C leads to a significantly prolonged bleeding time (Forsyth *et al.*, 2012). In addition, patients can end up with a fibrinogen deficit as hypothermia causes fibrinogen synthesis to decrease by up to 50% whilst causing no change in the rate of breakdown (Martini, 2007). Reducing the temperature of the blood dramatically reduces platelet aggregation, after 8 minutes at 6°C minimal platelet aggregation could be observed (Forsyth *et al.*, 2012). This effect was reversed when the blood temperature was increased back to 37°C (Forsyth *et al.*, 2012). Whilst, this suggests that cooling the body to prevent ischaemia will cause problems with platelet aggregation, it is unlikely the patient will be deliberately cooled to 6°C . However, platelet adhesion was seen

to decrease by 33% at 33°C (Forsyth *et al.*, 2012). This is more likely to cause an observable effect in patients who are bleeding profusely. Whilst the effect of hypothermia on blood has the potential to cause major problems, few bleeding complications have been reported during clinical trials (Polderman, 2004b).

Ning *et al.* studied the effect of different durations of mild whole body hypothermia on local limb damage as well as distant lung, liver and kidney injury in rats with blast limb trauma (Ning *et al.*, 2016). It was found that 6 hours of whole body hypothermia significantly increased blood loss compared to rats with no intervention (Ning *et al.*, 2016). All rats were euthanised at 6 hours so the increase in blood loss suggests hypothermia increases bleeding rate. Rats treated with whole body hypothermia for 3 or 6 hours showed a decrease in muscle swelling, lung morphologic changes and liver and water content (Ning *et al.*, 2016). This is likely to be due to reductions seen in the levels of TNF- α , IL-6 and hydrogen peroxide in the plasma at 3 and 6 hours of hypothermia compared to normothermic rats (Ning *et al.*, 2016). A decrease in TNF- α and IL-6 suggests that hypothermia is playing a role in suppressing the inflammatory response. In addition, Ning *et al.* found an increase in the activity of superoxide dismutase (SOD) in the muscles, lungs and liver after prolonged hypothermia compared to normothermic rats (Ning *et al.*, 2016). SOD is an anti-oxidant, a higher concentration of SOD after prolonged hypothermia suggests that the hypothermia is able to limit the oxidative damage seen in these tissues. These results suggest that whole body hypothermia is able to provide a protective effect after blast limb trauma. However, this study was terminated after 6 hours, therefore the long-term effects of the blast limb trauma and hypothermia could not be studied. In addition, no other therapeutic intervention, such as haemorrhage control or volume replacement, was

undertaken which could have affected results. Furthermore, only 12 rats were used in each group which would not give a strong statistical significance to the results.

Therapeutic hypothermia has the potential to be used in many aspects of healthcare not just during surgery to reduce the chance of ischaemia. Hypothermia has been used when transporting donated organs. Studies have found that those organs transported at colder temperatures show delayed graft function less often as well as allowing more successful donations from expanded-criteria donors (Niemann *et al.*, 2015). When using therapeutic hypothermia, the target temperature should be achieved as quickly as possible (Elizabeth M. Moore *et al.*, 2011). However, re-warming should be done slowly (Elizabeth M. Moore *et al.*, 2011). Sedatives or anaesthetics are administered to prevent shivering to enhance heat loss (Elizabeth M. Moore *et al.*, 2011). Hypothermia decreases insulin sensitivity and secretion so careful monitoring should be done to prevent the patient becoming hypo- or hyperglycaemic (Elizabeth M. Moore *et al.*, 2011). Some studies have reported higher risks of wound infection whilst the patient is in therapeutic hypothermia, thought to be related to decreased immune function and vasoconstriction induced by the hypothermia (Polderman, 2004b). Patient wound site should be checked regularly for signs of infection.

Multiple techniques are used by hospitals to assist with cooling the patient. These methods fall under two categories, topical cooling or core cooling. The benefit of topical cooling is that it is less invasive and can be implemented quickly and easily (Oh *et al.*, 2015) whilst topical cooling can restrict access to the patient due to the required coverage of the cooling device. Ensuring the cooling devices are still sufficiently cold can be very labour intensive for the nurses (Oh *et al.*, 2015). Topical cooling mechanisms include water circulating blankets, hydrogel pads, cooling

caps, cooling mattresses and ice packs (Oh *et al.*, 2015, Forsyth *et al.*, 2012, Gillies *et al.*, 2010). Clothing is removed from the patient to enhance the amount of heat lost by radiation. Ice packs are positioned on both sides of the neck, axillae, groin and under the knees (Gillies *et al.*, 2010). It has been observed that when ice is placed on the anterior of the knee, the intra-articular (IA) space also decreases in temperature (Forsyth *et al.*, 2012). However, like other deep tissues the minimum temperature of the IA space actually occurs after the ice pack is removed (Forsyth *et al.*, 2012). This is important when considering the response of the deep tissues to surface cooling and could mean that the internal temperature could drop more than intended.

Core cooling methods usually incorporate a cold intravenous infusion by either endovascular catheters or by the use of extracorporeal membrane oxygenation (ECMO) (Oh *et al.*, 2015). One study using a veno-venous extracorporeal circuit found a cooling rate of 12.2°C/hour could be achieved suggesting that core cooling methods are able to safely achieve a rapid rate of cooling (Testori *et al.*, 2013). The safety of core cooling is defined to be the incidence of both serious adverse events e.g. heart failure, major haemorrhage or stroke, or the occurrence of minor adverse events including minor bleeding or pneumonia (Testori *et al.*, 2013). The study by Testori *et al.* found no incidence of serious or minor adverse events and the mean arterial blood pressure did not drop (Testori *et al.*, 2013). For this reason, the study was defined as safe. However, the aforementioned study only consisted of 8 patients so wider studies would be needed to confirm the rate of cooling that is achievable with endovascular cooling. The rapidity of cooling is a benefit of using core cooling in mild therapeutic hypothermia. Endovascular cooling was found to have a longer rewarming time which could prove therapeutically beneficial (Oh *et al.*, 2015). In addition, core cooling has a lower incidence of overcooling (considered to be a body temperature of less than 32°C) and is more often able to attain the

target temperature (Oh *et al.*, 2015, Gillies *et al.*, 2010). Core cooling is also able to maintain the temperature at the target for longer and reduce temperature variation (Gillies *et al.*, 2010, de Waard *et al.*, 2013).

Other techniques of core cooling are being investigated. The RhinoChill Device (RCD) uses a nasal catheter inserted into the nasopharynx (Abou-Chebl *et al.*, 2011). A combination of a perfluorocarbon and oxygen is sprayed onto the upper surface of the nasal cavity, evaporation of this mixture creates a cooling effect on the tissues of the head (Abou-Chebl *et al.*, 2011). It is thought that the RCD will be useful in reducing the temperature of the brain, especially in obese patients who do not respond as well to surface cooling (Abou-Chebl *et al.*, 2011). All patients in the RCD trial had achieved a core temperature reduction within 30 minutes. The mean core temperature reduction after 60 minutes was $1.1 \pm 0.6^{\circ}\text{C}$ with a range of 0.3 to 2.1°C (Abou-Chebl *et al.*, 2011). Due to the small number of patients in this study (n=15) it is not possible to draw any conclusions about the effectiveness of the RCD in cooling core body temperatures. Another study of 16 patients has used automatically controlled peritoneal lavage to reduce the core body temperature. Lactated Ringer's solution at different temperatures was used to induce, maintain and reverse mild hypothermia by continuous peritoneal lavage (de Waard *et al.*, 2013). Patients undergoing peritoneal lavage reached the target oesophageal temperature of 32.5°C in a significantly shorter time than those patients who were treated with the standard mild therapeutic hypothermia protocol of that centre (de Waard *et al.*, 2013). However, the time from the patient arriving in hospital to the commencement of peritoneal lavage was significantly longer than to implement the usual mild therapeutic hypothermia protocol which could reduce this benefit (de Waard *et al.*, 2013).

4.2. Design considerations:

To provide the highest chance of limb salvage the limb will need to be cooled immediately after injury. Therefore, the cooling sock will need to be portable. This means that the cooling sock must easily be carried by medics on the battlefield. The cooling sock must be lightweight to keep the additional weight to the medic's kit to a minimum. Furthermore, the cooling sock must be compact to enable it to easily fit inside a kit bag. Durability is also very important to ensure the cooling sock is not damaged when it is carried around. For the device to be truly portable, the cooling sock should be able to cool the leg without a power supply. For this reason, the use of compressed gas is warranted.

The cooling sock must be easy to apply so time is not wasted trying to get the sock on and would not potentially cause further injury. Ideally, the cooling sock would be able to be applied when abiding by the care under fire protocol. The cooling sock must also be able to fit a wide variety of limb sizes and still cool them effectively. There is a big difference in the size and depth of a leg compared to an arm which could lead to a decrease in core cooling capability. This difference should be minimised as much as possible. The cooling sock will come into direct contact with injured tissues, thereby, the materials need to be fully biocompatible.

Certain factors need to be taken into consideration to select the right gas. The first of these is that the gas must be non-toxic and biocompatible, the act of cooling the limb should not induce further injury. The gas should have a long shelf-life as it will not be efficient use of resources if the bottles have to be constantly replaced without being used. To prolong the shelf-life of the gas, the gas should be inert and not temperature sensitive to prevent

breakdown during storage. There are many sources of ignition on the battlefield. Therefore, the gas should be non-flammable to prevent fires or explosions when the cooling sock is in use. The release of the gas should also result in a large drop in temperature which will in turn reduce the temperature of the limb tissue. Taking all these factors into consideration the gas selected for testing is compressed CO₂.

4.3. Feasibility maths:

Assume male leg is 16.68% of total body weight (Plagenhoef, Evans and Abdelnour, 1983).

It is acknowledged that this percentage will change with both gender (female leg is 18.43% of total body weight (Plagenhoef, Evans and Abdelnour, 1983)) and changes in body morphology caused by exercise or diet.

Assume body weight = 80kg

$$\begin{aligned}\text{Weight of leg} &= 80 \times 16.68\% \\ &= 13.34\text{kg}\end{aligned}$$

CO₂ used was 60L SodaStream gas cylinder (SodaStream, Airport City, Israel)

$$\begin{aligned}\text{CO}_2 \text{ vapour pressure at } 20^\circ\text{C} &= 57.3 \text{ bar} \\ &= 5.73 \text{ MPa}\end{aligned}$$

Bottle states 0.425g CO₂ in bottle

Average specific heat capacity of human body = 3470J/kg/°C (Engineering ToolBox, 2003a)

Energy (Q) = mass (m) x specific heat capacity (v) x ΔT

To change leg temperature by 10°C

$$\begin{aligned}Q &= 13.34 \times 3470 \times -10 \\ &= -462898\text{J} \\ &= \underline{-462.9\text{kJ}}\end{aligned}$$

Need to remove 462.9kJ of energy to reduce leg temperature from 37°C to 27°C

Theoretical temperature change:

To calculate temperature change of gas leaving bottle:

Assuming that the gas leaving bottle is an adiabatic system. Work done when leaving bottle

= 0 because gas is expanding too quickly for work to be done.

Ideal gas law (Tatum, 2008a) $PV = nRT$

Equation for reversible adiabatic expansion of ideal gas (change of energy at constant pressure) (Tatum, 2008b)

$$dU = -PdV$$

Ideal gas heat capacity (change of energy, depends on temperature but independent of volume) (Tatum, 2008b)

$$dU = C_v dT$$

Able to eliminate dU

$$C_v dT = -PdU$$

Integrate

$$\int_{T_i}^{T_f} C_v \frac{dT}{T} = \int_{V_i}^{V_f} -P \frac{dV}{V}$$

$$= C_v (T_i - T_f) = -P_{ext} (V_i - V_f)$$

Don't know V_f so substitute V for ideal gas law

$$C_v (T_i - T_f) = -P_{ext} \left(\frac{nRT_i}{P_i} - \frac{nRT_f}{P_f} \right)$$

$$C_v T_i - C_v T_f = \frac{-P_{ext} nRT_i}{P_i} + \frac{P_{ext} nRT_f}{P_f}$$

$$C_v T_i + \frac{P_{ext} nRT_i}{P_i} = C_v T_f + \frac{P_{ext} nRT_f}{P_f}$$

Make $n=1$ (1 mole of substance)

$$C_v T_i + \frac{P_{ext} RT_i}{P_i} = C_v T_f + \frac{P_{ext} RT_f}{P_f}$$

Take T_i and T_f out of brackets so can solve to find T_f

$$\left(C_v + \frac{RP_{ext}}{P_f} \right) T_f = \left(C_v + \frac{RP_{ext}}{P_i} \right) T_i$$

Where

C_v = molar heat capacity at constant volume

R = gas constant

P_{ext} = external pressure

P_f = final pressure (in this case assume the same as external)

T_f = final temperature

P_i = initial pressure

T_i = initial temperature

$$T_f = \frac{\left(C_{v1}m + \frac{RP_{ext}}{P_i} \right)}{\left(C_{v1}m + \frac{RP_{ext}}{P_f} \right)} \times T_i$$
$$= \frac{131.99 + \frac{188.9 \times 101325}{5.73 \times 10^6}}{131.99 + \frac{188.9 \times 101325}{101325}} \times 293$$
$$= \frac{131.99 + 3.34}{131.99 + 188.9} \times 293$$
$$= -123.57K$$
$$= -149.58^\circ C$$

$$\Delta T = -149.58 - 20$$

$$= -169.58^\circ C$$

Specific heat capacity of CO_2 at constant pressure at $20^\circ C$ and $1atm = 0.844kJ/kg/K$ (Engineering

ToolBox, 2003b)

Energy taken in by CO_2 (Q) = $mv\Delta T$

$$Q = 0.425 \times 844 \times -169.58$$

$$= -60828.35J$$

$$= -60.83kJ$$

Change in leg temperature available with $-60.83kJ$

$$Q = mv\Delta T$$

$$-60.83 \times 10^3 = 13.34 \times 3470 \times \Delta T$$

$$\Delta T = \frac{-60.83 \times 10^3}{13.34 \times 3470}$$
$$= \underline{-1.31^\circ\text{C}}$$

Leg would decrease in temperature from 37°C to 35.87°C

Amount of CO₂ required to achieve 10°C drop in leg temperature

$$-462.9 \times 10^3 = m \times 844 \times -169.58$$

$$m = \frac{-462.9 \times 10^3}{844 \times -169.58}$$
$$= 3.23g$$

$$\text{Number of bottles of CO}_2 = \frac{3.23}{0.425}$$

$$= \underline{7.6 \text{ bottles}}$$

The CO₂ was released through a manually controlled screw valve (CO₂ Supermarket, South Milford, UK). The flowrate of the CO₂ was therefore difficult to control as it was not quantifiable. The varying flow rate will alter how quickly the gas expands and thereby the speed at which the tissue can be cooled. Moreover, the temperature of the tissue will also affect the temperature change, a steeper temperature gradient will lead to greater heat loss. In addition, the ambient temperature will affect the speed of temperature change due to the temperature gradient between the CO₂ and the surrounding air leading to heat loss here. These inconsistencies will cause variations in the efficacy of tissue cooling by CO₂.

4.4. Initial design:

The skin contacting material in the first iteration of the cooling sock was made from UnderArmour CoolSwitch compression leggings (UnderArmour Inc, Baltimore, Maryland, USA). These were made from a 130g polyester/ elastane material that was designed to conduct heat from the skin to the atmosphere. Imbedded into the UnderArmour are sections of Mesh HeatGear fabric which has been specially designed to aid ventilation which will help with the contact of the gas with the skin. The elasticity of the UnderArmour material will enable it to stretch round different sized limbs.

Polyester mesh with a hole diameter of 8mm (UK Fabrics Online, Stockport, UK) was sewn onto the outside of the UnderArmour material as a support material for the tubing. Velcro was sewn onto the edge of the UnderArmour material to enable the cooling sock to be fastened round the leg. 12m of flexible expanded polytetrafluoroethylene (ePTFE) (Wuxi Mayshee Developing Company, Wuxi, China) tubing was then fed through this mesh as it was considered the maximum material that could be accommodated in this setting as seen in Figure 4-1. The tubing had an inner diameter of 6mm and an outside diameter of 7.75mm. ePTFE tubing was picked due to the porosity of the enabling easy gas release. The porosity of the ePTFE tubing was tested by flushing gas through the tubing when it was submerged in water to see how much gas escaped as depicted in Figure 4-2. Additionally, ePTFE is a class VI approved, biocompatible, chemically inert and chemically resistant material making it suitable for use in a wound environment.



Figure 4-1: Experimental set up for testing 1st iteration of cooling sock

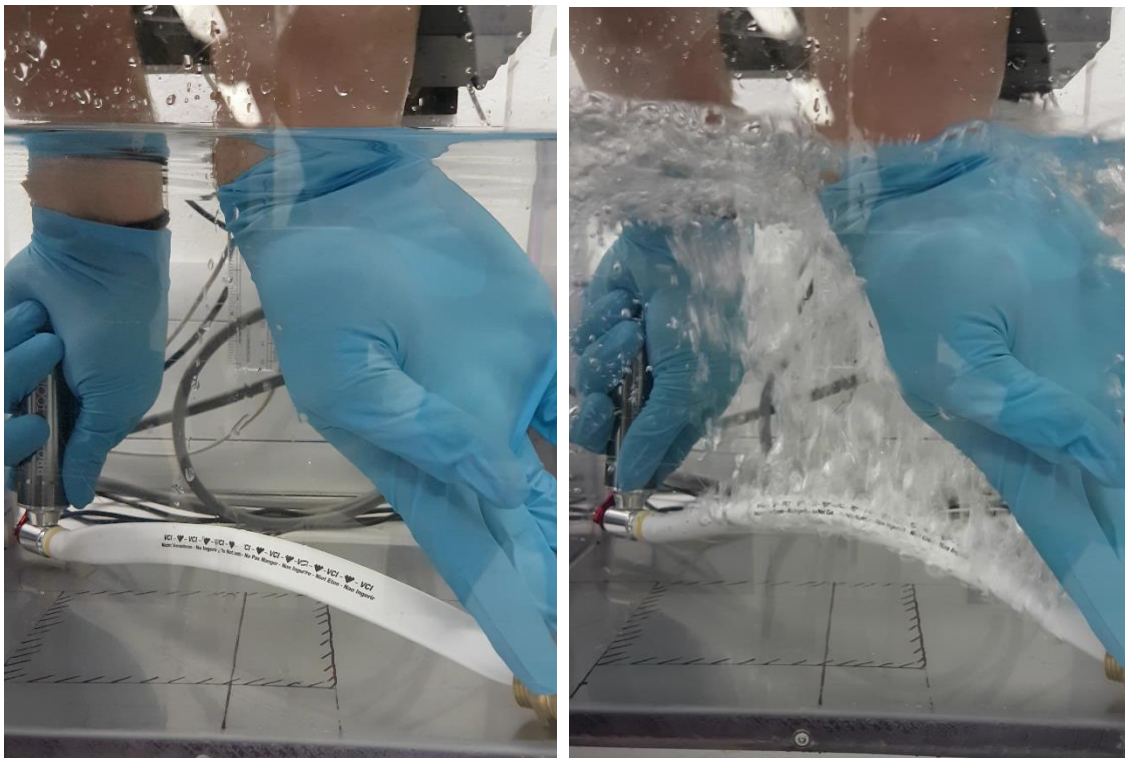


Figure 4-2: Testing the porosity of the ePTFE tubing by flushing gas through submerged tubing

4.4.1 Preliminary temperature testing:

A thermocouple (RS Components, Corby, Northamptonshire, UK) was placed at the CO₂ source and at the end of the ePTFE tubing. As stated in section 4.3 the CO₂ was released by way of a manually controlled valve activated with a screw system. This adaptor was then connected the cooling sock via a series of connectors (Fisher Scientific, Leicestershire, UK). The temperatures were then recorded by a Pico USB TC-08 Thermocouple Data Logger (Pico Technology, Cambridgeshire, UK) for 500 seconds. As can be seen in Figure 4-3, whilst a large drop in temperature was seen at the source (-36.08°C at 21 seconds, the lowest temperature achieved) the temperature drop at the distal end of the tubing was less substantial (12.49°C at 21 seconds).

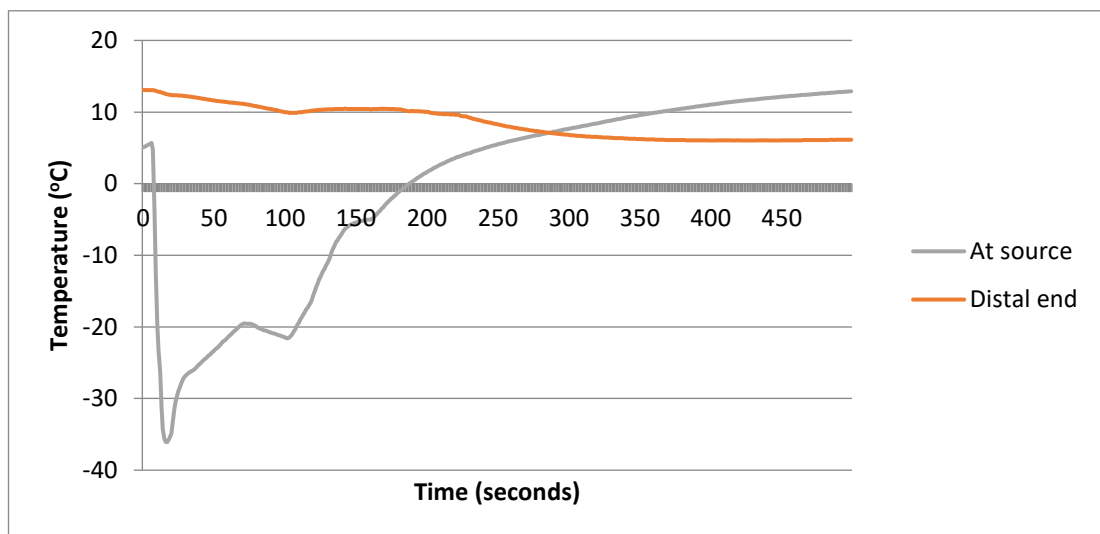


Figure 4-3: Temperature profile over 500 seconds using CO₂ in 1st iteration of cooling sock

The far smaller drop in temperature as the distal end is most likely due to a few different reasons. Firstly, the CO₂ had to travel 12m down porous tubing to reach the end thermocouple. This means that the CO₂ will have gained a lot of heat from the atmosphere

whilst travelling along the tube to the distal end. Additionally, the porosity of the tube means that most of the CO₂ will have left the tube by the time it has travelled to the distal end. A smaller volume of CO₂ means a reduced cooling effect. Furthermore, no material was placed over the polyester netting as an outer layer to create an enclosed environment around the ePTFE tubing when constructing the cooling sock. This means that any CO₂ lost from the tube will disperse into the environment rather than being contained in the area immediately around the limb. Finally, it is possible that a heat reflective outer layer may have prevented the heat from the environment passing to the CO₂.

4.5. Second iteration:

4.5.1. Design alterations:

To achieve a more even distribution of CO₂ over the leg, and therefore a better cooling effect, the design of the cooling sock was changed. Instead of one long 12m length of ePTFE tubing the sock was covered by 16 1m lengths of ePTFE tube positioned equal distances apart. This means that the CO₂ covered the leg with a more even distribution. The distal ends of the ePTFE tubes were sealed with superglue. It is thought that by sealing the ends of the tubes the CO₂ will vent into the sock rather than escaping out the bottom.

A manifold was designed and fabricated to enable CO₂ to be passed through 16 tubes from one bottle of gas. The manifold was designed using CAD and then printed using an EnvisionTEC® Perfactory® Desktop XL printer (EnvisionTEC GmbH, Gladbeck, Germany) with Magics® software (Materialise, Sheffield, UK). The resolution selected for printing was 25 microns and parts were printed using HTM140 material, a methacrylic-/acrylic- resin manufactured by EnvisionTEC®, with ABS-like material properties. At the gas inlet, a polymer

male fitting for a 16mm tubing diameter (Valves Online, Devon, UK) was screwed onto the manifold. Flexible nylon tubing (16 mm OD, 13 mm ID) (Advanced Fluid Solutions, Chelmsford, UK) was used to connect the gas bottle to this fitting. At the manifold outlet, 4 polymer male thread Y stud push fittings (10 mm tube diameter, 3/8") (Valves Online, Devon, UK) were screwed on and connected to flexible nylon tubing (10 mm OD, 8 mm ID) (Advanced Fluid Solutions, Chelmsford, UK). At the ends of these 8 lengths of tubing were 6mm Y-piece hose connectors (Automotive Silicone Hoses, Mirfield, UK) which connected to the 16 ePTFE tubes. Figure 4-4 shows the manifold configuration.

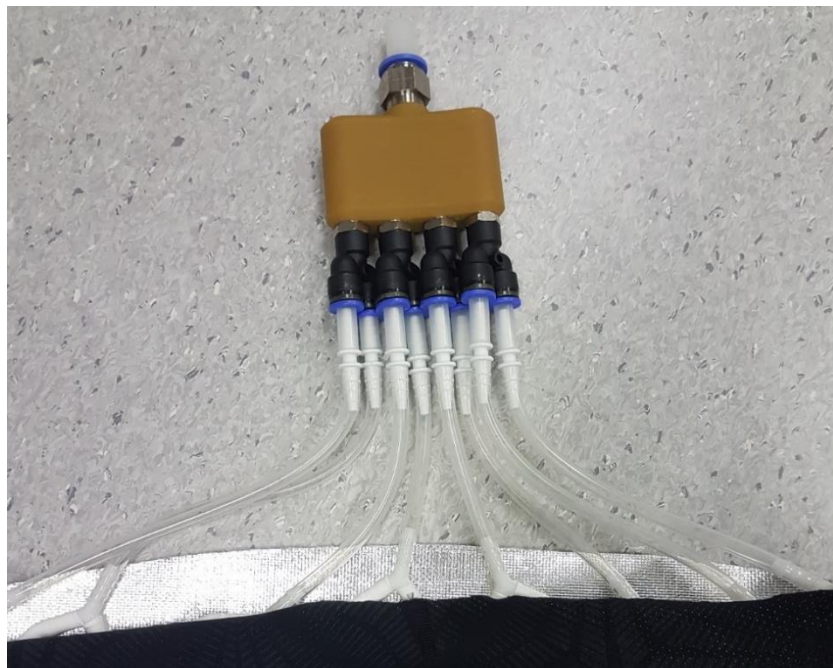


Figure 4-4: Manifold used with 2nd iteration of cooling sock

To reduce the amount of CO₂ escaping to the environment a backing material was used. The backing material selected was Shieldtex/780 heat shield fabric (Textile Technologies Europe Ltd, Hyde, Cheshire, UK). This material consists of a 20-micron aluminium sheet which is impregnated with a black flame-resistant polyurethane coating. The material should contain the CO₂ within the cooling sock. In addition, the aluminium sheet should prevent a rapid

increase in the temperature of the CO₂. Keeping the temperature increase low will prolong the cooling effect of the gas. The 16 ePTFE tubes were attached to the backing material using Velcro. Under Armour was again used as the skin contacting material, this was attached to the backing material by stitching down two sides as seen in Figure 4-5

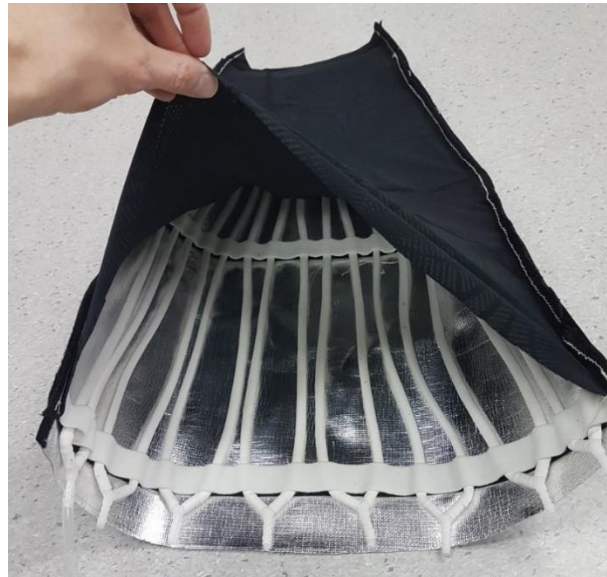


Figure 4-5: Arrangement of tubes in 2nd iteration of cooling sock

Velcro straps were used to close the cooling sock around the mannequin leg used for testing. Figure 4-6 shows the completed cooling sock in an open position as well as closed around the mannequin leg.



Figure 4-6: 2nd iteration of cooling sock both open and closed around the mannequin leg.

4.5.2. Temperature testing:

To test the efficiency of the 2nd iteration of the cooling sock the temperature was recorded using thermocouples placed at 5 defined positions on the mannequin limb. These positions were the thigh, upper calf, mid-calf, lower calf and the ankle. The thermocouple locations alternated between the lateral and medial side of the leg. The positions of the markers were marked with tape so the thermocouples could be placed in the same places each test. These defined positions were chosen as they allowed for the maximum amount of coverage of the limb. Figure 4-7 shows the chosen location of these thermocouples. The mannequin limb was made of a clear plastic material. This material may have an effect on the cooling profile recorded as the plastic is likely to be cooled by the gas and then retain this temperature. This

effect is mitigated between the tests because the same mannequin limb is used for all tests. However, the effect may be noticeable when transferring the cooling sock from the mannequin to tissue.



Figure 4-7: Location of the defined thermocouple positions on the mannequin limb

One full bottle of CO₂ was flushed through the cooling sock. The temperatures were recorded once a second over 500 seconds. Figure 4-8 shows the graph of these results.

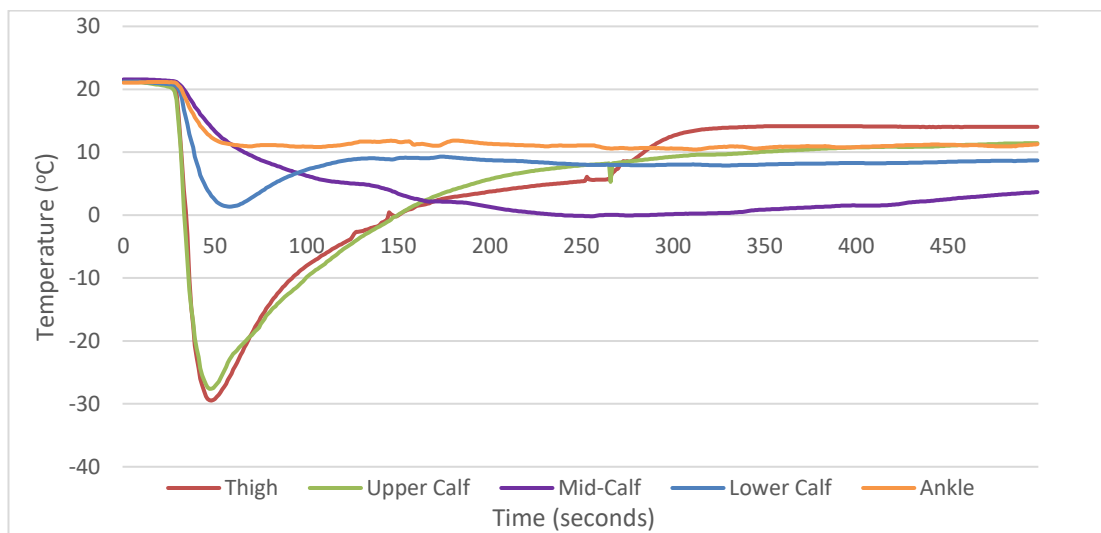


Figure 4-8: Temperature profile using iteration 2 over 500 seconds

As can be seen from this graph a sharp temperature decrease was seen at the thigh and upper calf markers (-29.39°C and -27.49°C respectively). The temperature change at the other locations was far more moderate (12.17°C, 13.61°C and 2.72°C at the same time point). This may be due to the longer distance for the CO₂ to travel. However, comparing the results to those seen in Figure 4-3 it can be seen that the temperature stays low for longer in this second iteration. Using iteration 2 of the cooling sock the temperatures after 500 seconds

range between 3.66°C – 14.02°C (with 4 of the 5 values below 11.5°C) whereas using iteration 1 the temperatures are 6.14°C and 12.89°C. The likely explanation for this is that the backing material prevented the CO₂ dissipating into the environment. The thigh rewarmed the most rapidly, this may be due to the fact the top of the mannequin leg was open and therefore the external air increased the temperature at the thermocouple. Considering the temperature at all the thermocouples was below 15°C at 500 seconds it may be that these temperatures are sufficient to reduce the temperature of the limb. One factor that should be examined in future is whether the rapid initial drop in temperature to almost -30°C is able to cause flash freezing of the tissue. Flash freezing of the tissue would be detrimental to the recovery of the patient and the risk of it should be negated as much as possible.

4.6. Third iteration:

4.6.1. Design alterations:

The 3rd iteration of the cooling sock was very similar to the second. However, there were a few small changes. Firstly, the skin contacting material was changed. Rather than using Under Armour, material with a similar composition of 190g polyester/ elastane (Fabric Land, Bournemouth, UK) was used. When creating the cooling sock, the skin contacting material was not stretched over the ShieldTex backing material but laid over it and cut to size. Secondly, the ePTFE tubes were superglued to the backing material rather than using Velcro to attach them (Figure 4-9). The size of the sock was also increased slightly to increase the variety of limbs this cooling sock could be used on. The backing material and the skin contacting material were stitched together down three sides. Velcro was sewn along the long

edges to close the sock and double-sided Velcro straps were used to increase the security of fastening.



Figure 4-9: Arrangement of tubes on 3rd iteration

4.6.2. Temperature testing:

Three tests were run over 20 minutes using the 3rd iteration of cooling sock on the mannequin leg. Thermocouples were placed at the same 5 defined points on the mannequin leg. Figure 4-10 shows the temperature profile of the three tests in chronological order.

Table 4-1: Maximum temperature change at each location for 3 tests using third iteration with mean and SD

Test	Thigh	Upper calf	Mid-calf	Lower calf	Ankle
Test 1	10.94	8.46	8.80	10.16	14.05
Test 2	22.24	10.57	4.92	12.78	12.19
Test 3	9.02	10.66	10.81	8.71	15.35
Mean	14.07	9.90	8.18	10.55	13.86
SD	7.14	1.25	2.99	2.06	1.59

As can be seen in Figure 4-10, the tests did not produce consistent cooling profiles. Table 4-1 shows that the thermocouple location with the greatest temperature change varied with each test and that the temperature change at each location was not reproduced between the tests. The thigh produced the most variable results with the lowest temperatures recorded ranging from 13.23°C to 1.18°C. One possible explanation for this is that the thermocouple may not have been covered fully by the cooling sock each time. Furthermore, as the flow of CO₂ was manually controlled the CO₂ may have been flushed through the sock at an inconsistent speed which will affect the cooling effect produced. In addition, the CO₂ flow may have been halted when there was still some CO₂ left in the bottle so the full cooling capability would not have been utilised. The ankle produced consistently low temperatures; this may be because the thermocouple was positioned near the tubes that were straight below the manifold. Therefore, the CO₂ had the shortest distance to travel outside the

cooling sock meaning the amount of heat gained from the environment would be reduced. The temperature did not return to baseline over 20 minutes in any of the tests which suggests the backing material did prevent rapid rewarming. However, it is unlikely the temperatures produced would be low enough to sufficiently cool a limb. The reason for this is that the end temperatures for all tests ranged between 14.08°C and 19.58°C, standing outside when the ambient temperature is in this range will not result in the rapid reduction of the core temperature of the limbs. It is possible that with extra flushes of CO₂ the temperature within the cooling sock could be maintained at a lower temperature which could result in the reduction of the core limb temperature.

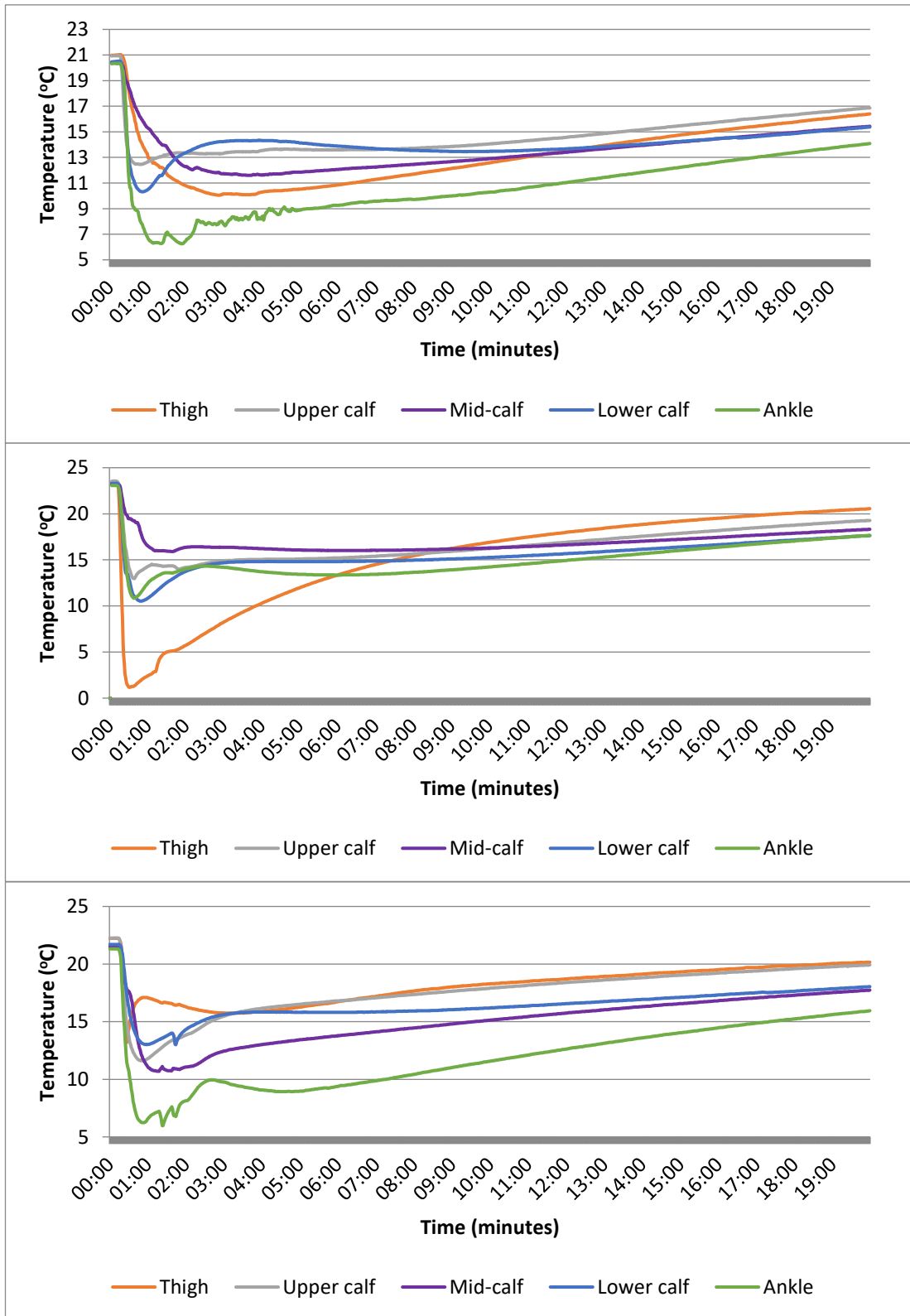


Figure 4-10: 3 graphs placed in chronological order showing the temperature profile over 20 minutes for the 3rd iteration of cooling sock

4.7. Fourth iteration:

4.7.1. Design alterations:

In an attempt to counteract the lower temperatures being experienced higher up the limb due to them being closer to the CO₂ source, the arrangement of ePTFE tubes was altered for the 4th iteration. Rather than running down the cooling sock, the tubes in the new design stemmed from the middle of the sock. This meant that the manifold needed to be redesigned and 3D printed with the printing specifications as described in section 4.5.1 (pages 91 to 92). The new manifold was circular with 10 male push fittings (10 mm tube diameter, 3/8") screwed into the manifold at evenly spaced distances. 10 1m lengths of ePTFE tubing were connected to these fittings. The ePTFE tubes were arranged in a wavy pattern (Figure 4-11) to cover the largest possible surface area. The ePTFE tubes were sealed at one end with superglue and held onto the ShieldTex backing material using medical tape (3M United Kingdom PLC, Bracknell, UK).

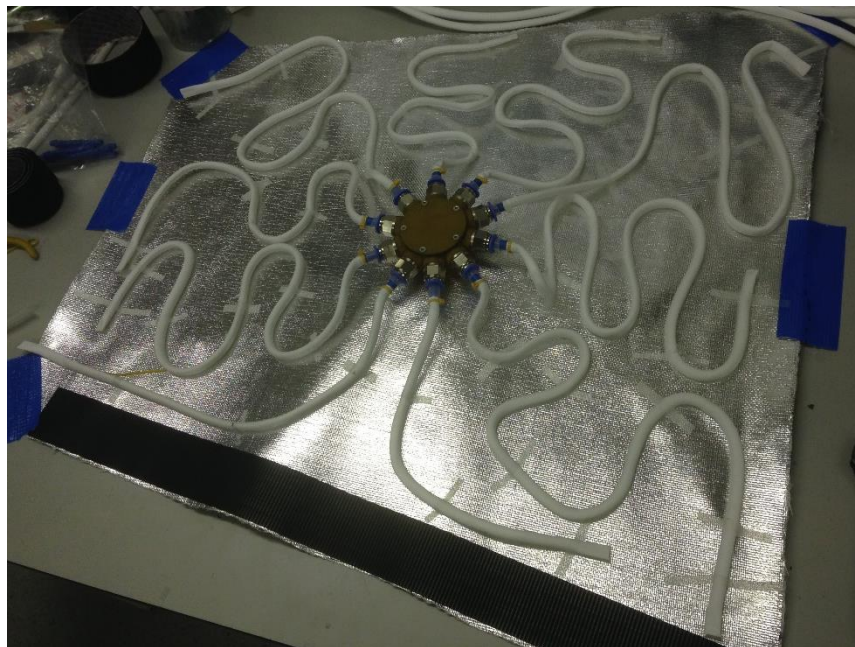


Figure 4-11: New design of manifold and tube arrangement of 4th iteration of cooling sock

Velcro provided a fastening for the cooling sock along two edges. Additionally, thin strips of Velcro were placed along all 4 edges of the backing material to enable a polyester mesh, as used in iteration 1 (described on page 88), to be positioned over the tubes. The skin contacting material was changed from the polyester/ elastane material to polyester netting. The reason for this was to reduce the number of layers that the CO₂ had to pass through to reach the limb. The mesh did not impede the flow of CO₂ whilst at the same time provided some protection of the tubes to prevent them becoming dislodged. Figure 4-12 shows the finished 4th iteration of the cooling sock.



Figure 4-12: Completed 4th iteration cooling sock

4.7.2. Temperature testing:

To test the efficiency of this iteration of cooling sock it was applied to the mannequin limb and the temperature profile recorded (Figure 4-13). The test ran for 20 minutes with sampling occurring once a second.

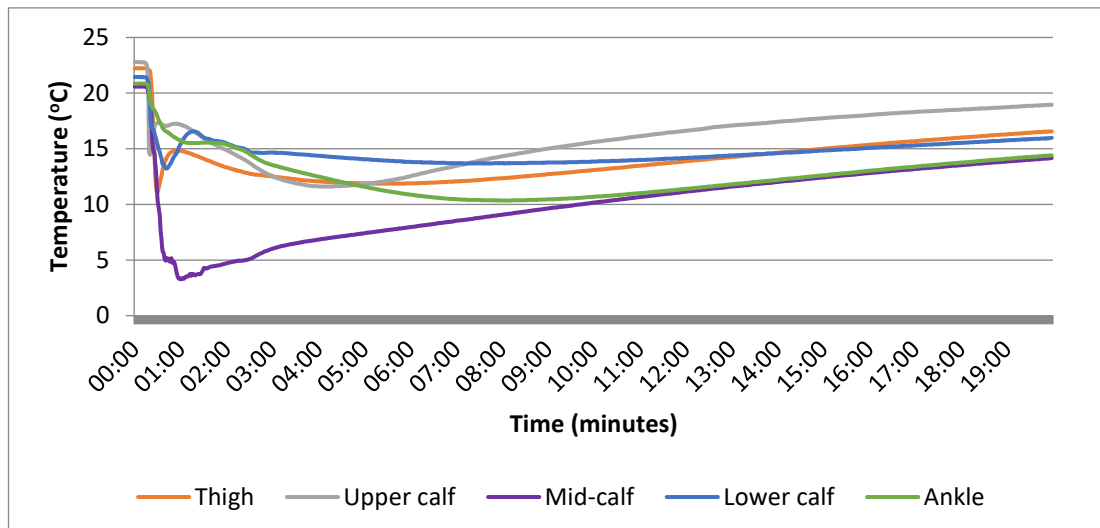


Figure 4-13: Temperature profile over 20 minutes when using 4th iteration of cooling sock on mannequin limb

When the cooling sock was removed it transpired that the thermocouple positioned at the mid-calf was placed close to the manifold which explains the much larger decrease in temperature. This test did not show a great decrease in temperature when compared to the previous tests as the temperature only dropped by 10°C in one location. However, after 20 minutes the temperature still had not returned to baseline.

4.8. Fifth iteration:

4.8.1. Design alterations:

The ShieldTex backing material used in the previous 3 iterations was not a very flexible material, this meant that the cooling sock did not conform to the contours of the leg very well. A greater distance between the ePTFE tubes and the limb will reduce the cooling capability of the CO₂ as it is not in direct contact with the skin. The cooling sock did not fit tightly around the ankle and the top of the thigh. This meant that a large amount of CO₂ was lost to the atmosphere and therefore was not able to cool the limb. In addition, the ShieldTex

was not appropriately elastic so the cooling sock was not able to fit a wide variety of limbs. For the aforementioned reasons the backing material of the cooling sock was changed.

The new design was constructed using a 1.5mm neoprene-insulated water sport material (Gill, Nottingham, UK). This neoprene-based material conformed to the limb much better than the ShieldTex material. It is also elastic so should be able to fit various limb sizes. Due to the cross-linking process of making neoprene the material is not easily permeable to gas so the CO₂ should be contained within the cooling sock. Both legs of the surf trousers were removed and cut down the middle of the front of the leg to enable them to be opened up. A 76cm open-ended 10mm chain zip (ProFabrics, Chester, Cheshire, UK) was sewn down the long edges to enable the sock to be zipped shut. This should prevent CO₂ from being lost through the fastening and provides stronger fastening mechanism.

The manifold design was changed back to the manifold configuration used in iterations 2 and 3 (described previously on pages 91 to 92). 16 1m lengths of ePTFE tubing were separated by 40mm at the proximal end of the sock with the sealed end of the tube at the distal end of the cooling sock and stitched on as seen in Figure 4-14.



Figure 4-14: 5th iteration both open and zipped up

4.8.2. Temperature testing:

Figure 4-15 shows the temperature profile of the thermocouples when CO₂ was flushed through the 5th iteration of the cooling sock. Temperatures were recorded twice a second for 8 minutes.

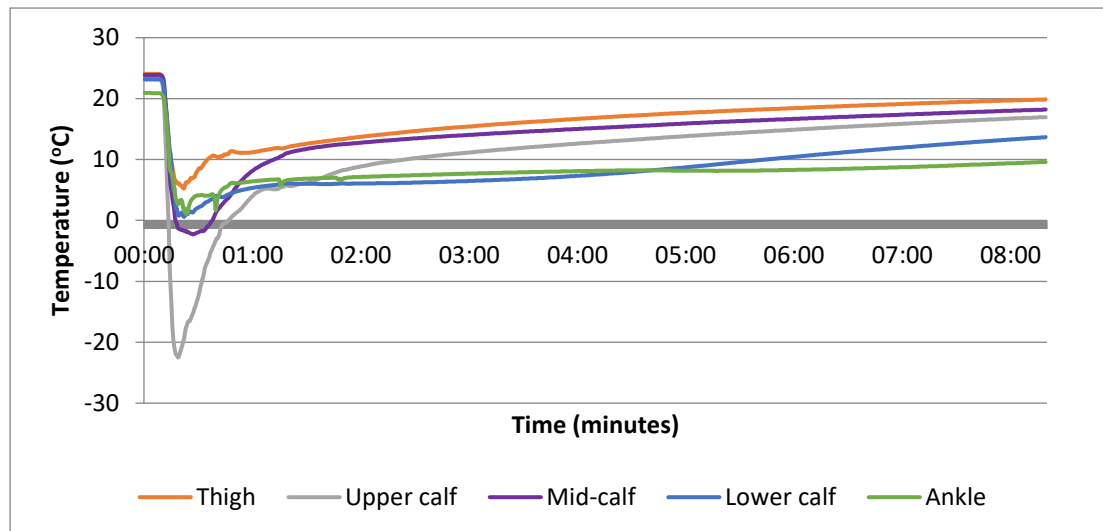


Figure 4-15: Temperature profile produced with 5th iteration over 8 minutes.

All thermocouples experienced a large decrease in temperature (temperature decreases as follows: thigh 18.8°C, upper calf, 45.62°C, mid-calf 26.18°C, lower calf 22.61°C, ankle 19.86°C). This iteration was the first one to produce an initial decrease in temperature of more than 15°C across all 5 thermocouples. This indicates that a tighter cooling sock may produce a better cooling effect. Furthermore, the increased cooling effecting of this iteration of the cooling sock could have been caused by the insulating ability of the neoprene material compared to the ShieldTex material. Having a material with greater insulating properties will mean that the heat from the environment will not pass into the CO₂ so more heat will therefore be removed from the limb. Whilst all thermocouples were still showing temperatures below 20°C at 8 minutes, only 2 thermocouples (lower calf and ankle) were still below 15°C. This rate of rewarming is unlikely to sufficiently cool the limb. A warmer baseline temperature i.e. 37°C (normal body temperature) will result in a greater initial temperature decrease due to the larger temperature change gradient, it is possible that a greater temperature reduction will lead to slower rewarming of the limb and therefore a better cooling capability.

The 5th iteration of the cooling sock was tested again with CO₂ being flushed through it. The CO₂ valve was opened to around 90% with the full 60L bottle being emptied in less than 30 seconds. Temperature values were recorded once a second for 20 minutes. Figure 4-16 shows the temperature profile produced from this test.

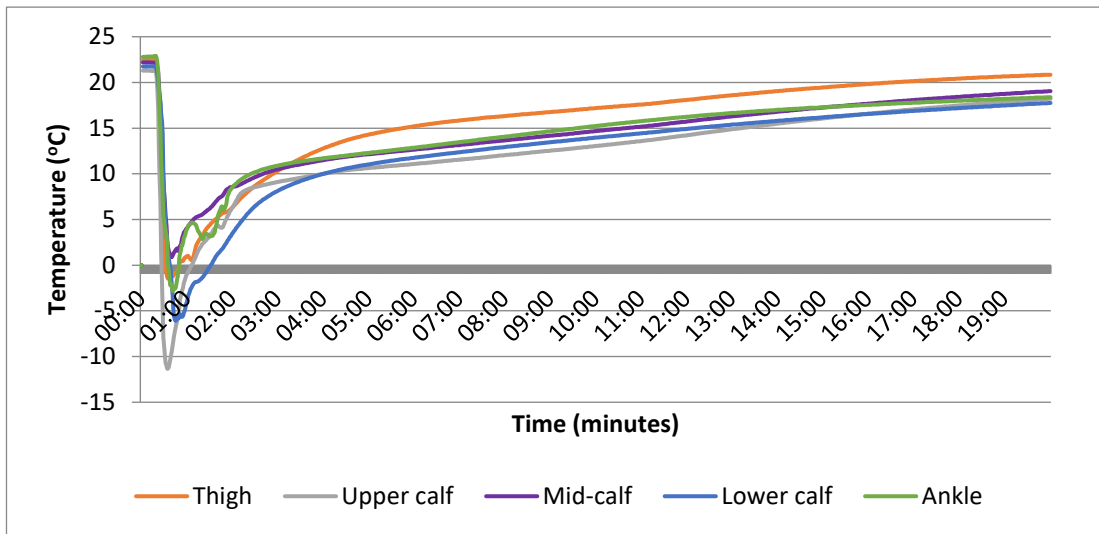


Figure 4-16: Temperature profile of 5th iteration over 20 minutes

From this graph it can be seen that a much sharper temperature decrease was produced when the CO₂ started flowing (temperature decreases as follows: thigh 23.96°C, upper calf 32.64°C, mid-calf 21.31°C, lower calf 27.83°C, ankle 25.63°C). The mid-calf thermocouple consistently showed the highest temperatures however, a temperature of 1°C was still achieved when the CO₂ started flowing. Nevertheless, this may offer a degree of safety for the long-term use of the cooling sock. If the temperature remains above freezing then the risk of accidentally freezing the superficial tissue is negligible. By 20 minutes the temperatures had recovered to almost baseline, a slower rewarming rate will be needed to efficiently cool the limb with one flush.

Test	Thigh	Upper calf	Mid-calf	Lower calf	Ankle
1	18.81	45.62	26.18	22.61	19.86
2	23.96	32.64	21.31	27.83	25.63

When comparing Figure 4-15 and Figure 4-16 the initial temperature change when the gas was flowing differs between the two tests as shown in Table 4-2. The greatest initial temperature change is shown in Table 4-2 because the time that the location takes to reach its lowest temperature varied by 9 seconds in test 1 (18-27 seconds) and by 10 seconds in test 2 (33-43 seconds). This suggests that the cooling profile was affected by how the gas is released from the canister. At 8 minutes the temperatures of all thermocouples were lower in the second test with all but the one at the thigh still below 15°C, suggesting a faster cooling rate when the gas is first released increases the rewarming time.

4.9. Sixth iteration:

4.9.1. Design Alterations:

The 6th iteration was made in a very similar way to the 5th iteration. 1.5mm neoprene-insulated water sport material was used for the cooling sock outer material and a 76cm open-ended 10mm chain zip was stitched to the long edges to hold the cooling sock closed. However, non-porous silicone tubing (10 mm OD, 8 mm ID) was used to carry the CO₂. A non-porous material was used on this occasion to prevent the CO₂ being lost out of the tubing before it could reach the end of the tubing. Furthermore, the cooling of the tubing by the CO₂ may cause a secondary cooling effect on the limb. The manifold was at the distal end of the cooling sock. The non-porous tubes start here and pass along the length of the sock. The tubes were then folded back on themselves and end at different distances down the sock. This will enable the CO₂ to be released at different distances along the leg. Figure 4-17 shows the new arrangement of non-porous tubing.

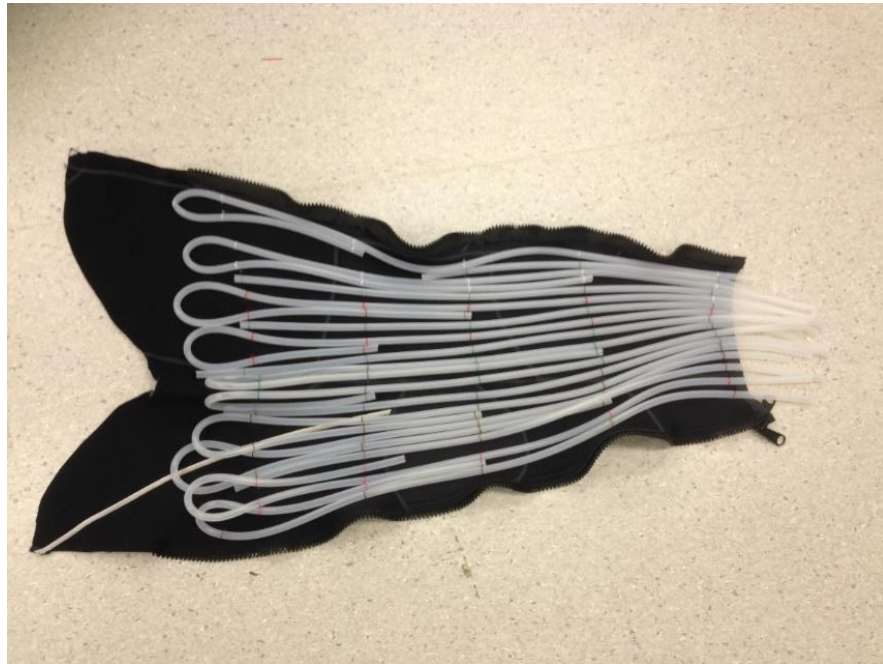


Figure 4-17: Arrangement of non-porous tubing for 6th iteration

To prevent the tubes leading from the manifold from kinking new lengths of tubing were cut.

Figure 4-18 shows the experimental set up for testing iteration 6 with CO₂.



Figure 4-18: Experimental set up using 6th iteration cooling sock

4.9.2. Temperature Testing:

Iteration 6 was tested using CO₂ for 20 minutes. Figure 4-19 shows the temperature profile recorded.

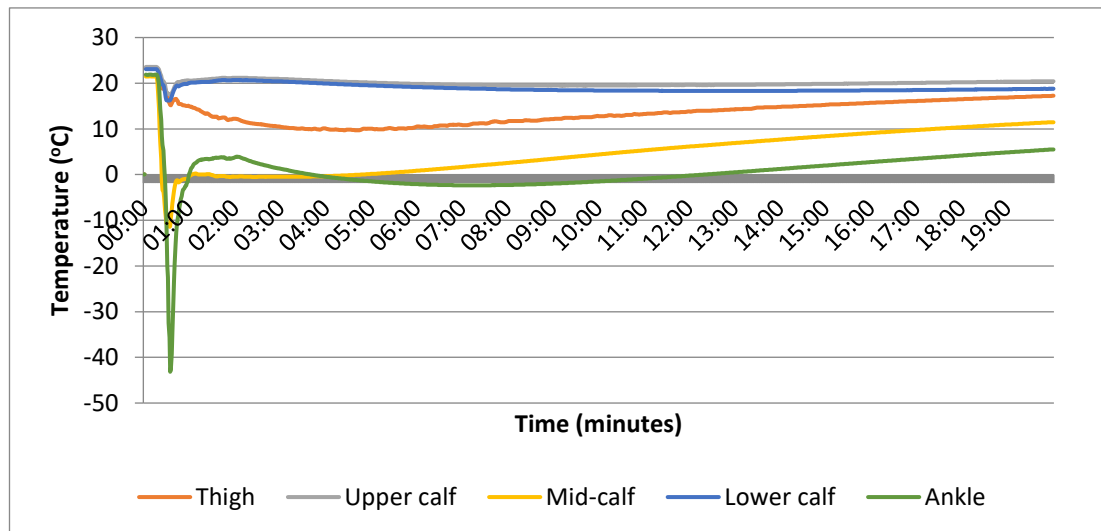


Figure 4-19: Temperature profile produced over 20 minutes with 6th iteration

The thermocouples showed dramatically different temperatures during this test. The results for the thermocouples located at the ankle and mid-calf were promising. The lowest temperature achieved at the ankle was -43.16°C. It is likely that this was due to how tight the tubes were held around the ankle allowing for efficient heat exchange. In addition, the tubes were close together at the ankle meaning that a greater surface area was covered which would have increased the amount of heat that can be removed. At 20 minutes the thermocouple at the ankle was reading 5.52°C, this suggests that the non-porous tubing produced a much slower rewarming time than the porous tubing. This slower rewarming time may have been due to the non-porous tubing holding the cold and thereby producing a cooling effect once the CO₂ was no longer flowing. The thermocouple at the mid-calf also experienced a sharp decline in temperature when the CO₂ started flowing reaching a

temperature of -11.43°C . After 20 minutes this value had only risen to 11.47°C which again suggests that the non-porous tubing increased the rewarming time.

However, the temperatures produced at the thigh, upper calf and lower calf were not as promising. The thigh thermocouple did not show a temperature below 9.5°C . This may have been because the thermocouple was not positioned right next to a tube. At the proximal end of the leg the tubes are far more spaced out and therefore there was a smaller surface area of the limb covered. Whilst the thigh thermocouple demonstrated a relatively slow rewarming rate, much lower temperatures will be needed to cool the mass of the thigh. The thermocouples placed at the lower calf and upper calf did not display much cooling at all. This may have been due to a number of reasons. Firstly, once the cooling sock was opened it was seen that the thermocouples were not placed under a tube but were instead relatively close to the zip. This means that there was no CO_2 directly cooling these thermocouples. In addition, there were no open tube ends near the thermocouples which again means that the CO_2 was not able to cool the thermocouple directly. This suggests that whilst the non-porous tubing may have been able to slow down the rewarming process it was not able to distribute the CO_2 throughout the cooling sock meaning some sections of the limb were not cooled. However, the temperature at the lower and upper calf did begin to decrease over the 20 minutes. This may mean that the chilled non-porous tubes produced a secondary cooling effect. This secondary cooling effect was caused by the tubing being cooled down as the CO_2 flowed through it. The tubing then held this reduced temperature for a prolonged period which will help to cool the limb tissue.

To help with the distribution of CO₂ over the limb from the non-porous tubing 1mm holes were made in a line at 10cm intervals along the top of the tubing. These holes started 1cm further along each tube to ensure the CO₂ would be able to cool sections of the limb not directly covered by a tube. Another test was undertaken to see if the addition of the holes resulted in lower temperatures at the thigh, upper and lower calf. Temperatures were recorded once a second for 20 minutes. Figure 4-20 shows the temperature profile recorded.

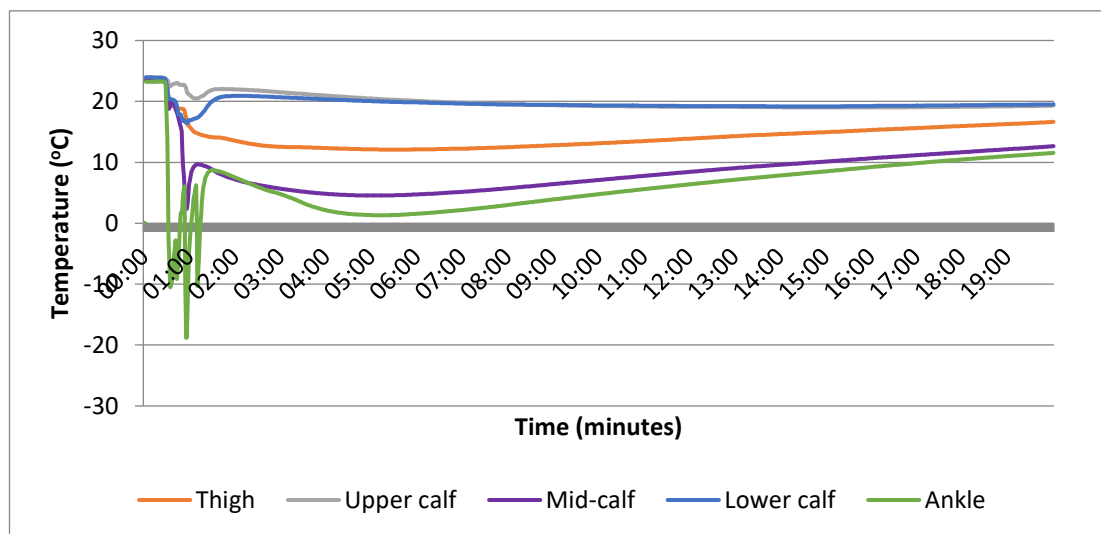


Figure 4-20: Temperature profile produced over 20 minutes using 6th iteration with holes made in tubing

Figure 4-20 shows that despite holes being made in the tubing the temperature at the upper and lower calf did not reduce significantly. Although the temperature at these thermocouples continued to decrease over the 20 minutes this would not be sufficient to cool the limb in any way. On the other hand, the ankle was the only thermocouple to record a temperature below 0°C at any point. This suggests that the addition of holes to the tubes caused the release of enough CO₂ to prevent efficient cooling further down the limb away from the manifold.

4.10. Iteration 6.2:

4.10.1. Protocol development:

After consideration of the data the decision was made to examine the use of non-porous tubing again. It was thought that the prolonged re-warming time may have more of a cooling effect than the initial low temperatures. The 6th iteration of the cooling sock was tested again using three different protocols to determine the best method to use when cooling the next animal limb. Before the limb tests took place a modification to the cooling sock was done. This involved polyester/ elastane material being stretched over the tubes to protect them. Covering the tubes had the additional benefit of stopping the tubing getting stuck to the plastic mannequin limb and therefore enabled the better positioning of the cooling sock.

For these tests the position of the thermocouples was changed slightly. The thermocouples were positioned at the same height on the mannequin leg. However rather than being positioned on the sides of the limb, the thermocouples were placed on the front and back, as shown in Figure 4-21.

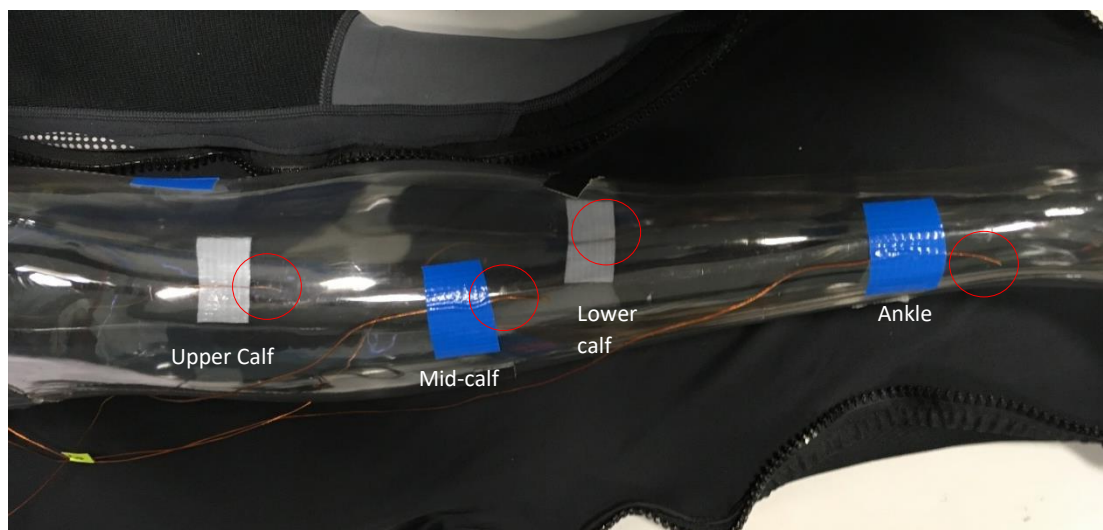


Figure 4-21: New positions for 4 thermocouple placements for testing 6th iteration

The first protocol followed the same method of the previous tests with the whole CO₂ bottle being flushed through the cooling sock at the beginning of the experiment. Figure 4-22 shows the results for this test (lowest temperature achieved: Thigh 17.15°C, Upper calf 15.53°C, mid-calf 18.07°C, lower calf, 11.76°C, ankle 15.24°C).

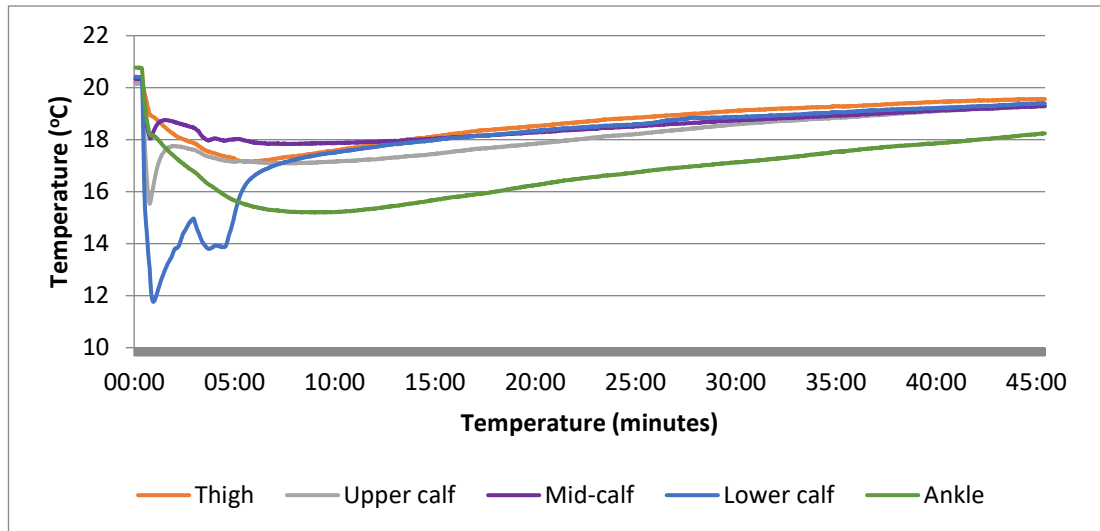


Figure 4-22: Temperature profile over 45 minutes. One bottle of CO₂ released at beginning of experiment

This graph shows that although there wasn't a huge decrease in temperature when the CO₂ started flowing, by 45 minutes the temperatures had not returned to baseline.

4.10.1.1. Refinement of cooling protocol:

The rationale for changing the protocol was to observe if the releasing one bottle of CO₂ in a number of flushes over a protracted period could prevent rewarming at the limb surface and thereby creating a prolonged cooling effect. The second protocol was to release CO₂ for 10 seconds every 5 minutes. At 25 minutes the CO₂ was released for 20 seconds as this was the end of the bottle. When the bottle was running out the pressure of the CO₂ in the bottle has decreased, this means that the energy taken in when the CO₂ expands when leaving the

bottle is reduced. Therefore, the cooling effect of the CO₂ is lessened. Figure 4-23 is a graph showing the temperature recorded at the thermocouples during this experiment.

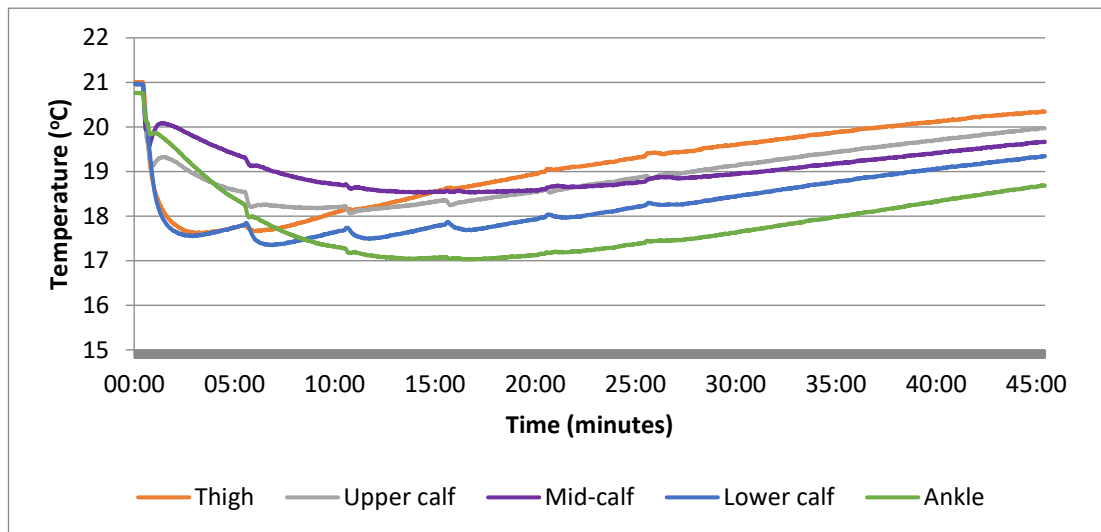


Figure 4-23: Temperature profile produced with 6th iteration when releasing 10 seconds of CO₂ every 5 minutes

The release of CO₂ every 5 minutes can be distinguished on this graph. It can also be seen how the decrease in temperature was reduced as the bottle empties. However, releasing the CO₂ in small bursts did not enable the limb to be cooled as much initially.

4.10.1.2. New cooling protocol:

Releasing one full bottle of CO₂ resulted in an initial rapid decrease in temperature at the mannequin limb surface. This temperature then rose steadily due to no further application of cooling. Releasing 10 second flushes of CO₂ caused smaller reductions in temperature at each time point. To achieve prolonged cooling these two methods were combined so initial cooling was rapid and the rewarming could be slowed due to smaller bursts of cooling every 5 minutes. This will also enable the tubing to remain cold and provide a more effective secondary cooling effect. Therefore, the new protocol involved the initial release of one full

bottle of CO₂ followed by 10 second flushes every 5 minutes from a fresh bottle. At 30 minutes the CO₂ was released for 45 seconds, again due to the fact the bottle was running out. Figure 4-24 shows the temperature at the thermocouples for this test.

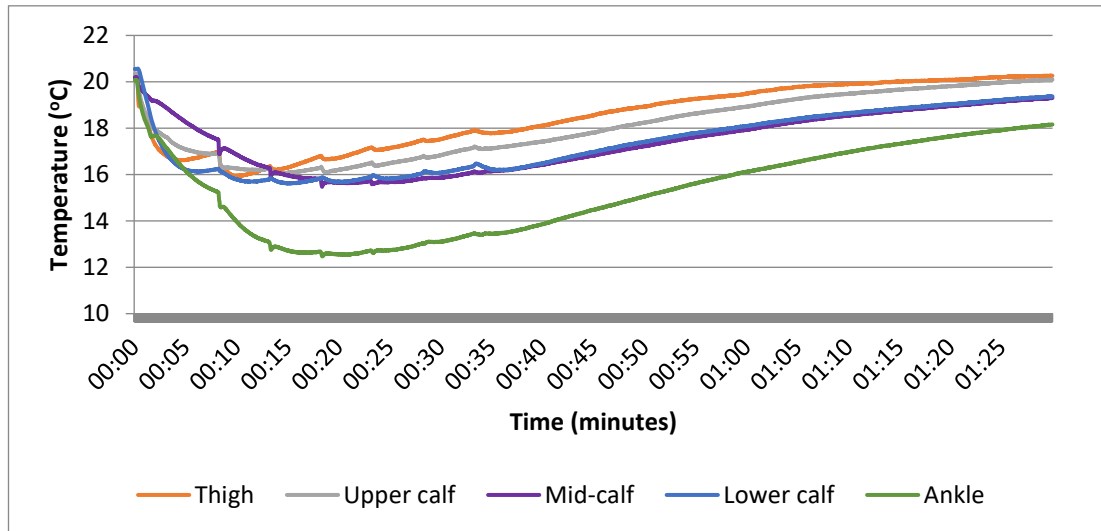


Figure 4-24: Temperature profile for 6th iteration when full bottle of CO₂ released at beginning of experiment followed by 10 seconds every 5 minutes

From this graph it can be seen that combining the two protocols produced a much slower rewarming time. Even after 1.5 hours the temperature at the thermocouples had not yet recovered to baseline. It is hoped that a prolonged rewarming time of the tubes will increase the cooling of the limb.

4.10.2. Design of iteration 6.2:

The dimensions of the sixth iteration cooling sock were too large for the porcine limb (limb size defined in Chapter 6 page 160). This meant that the CO₂ was being flushed through far more tubing than it needed to be which could be reducing the cooling effect due to the resistance in the tubes and the distance travelled. Thereby, a shorter cooling sock was made. This cooling sock was also made from 1.5mm neoprene-insulated water sport material. The

leg was cut off around the knee and cut open along one side. The original manifold described in section 4.5.1 will be used for this cooling sock. 16 lengths of non-porous AVECOR 7/64 1/16 class VI silicon (AVECOR Cardiovascular Inc, Minneapolis, Minnesota, USA) tubing were cut. The tubing was cut to different lengths to enable the CO₂ to be distributed around the limb. The tubes were stitched on and polyester/ elastane material stretched over the tubing. Figure 4-25 shows the arrangement of tubes in the cooling sock.



Figure 4-25: Layout of non-porous tubing for smaller version of 6th iteration

The mannequin leg used previously was too big to test this cooling sock so therefore an arm from the same mannequin was used to test what temperatures could be produced at the surface of the limb. Thermocouples were placed at similar positions to those located on the mannequin leg as seen in Figure 4-26.

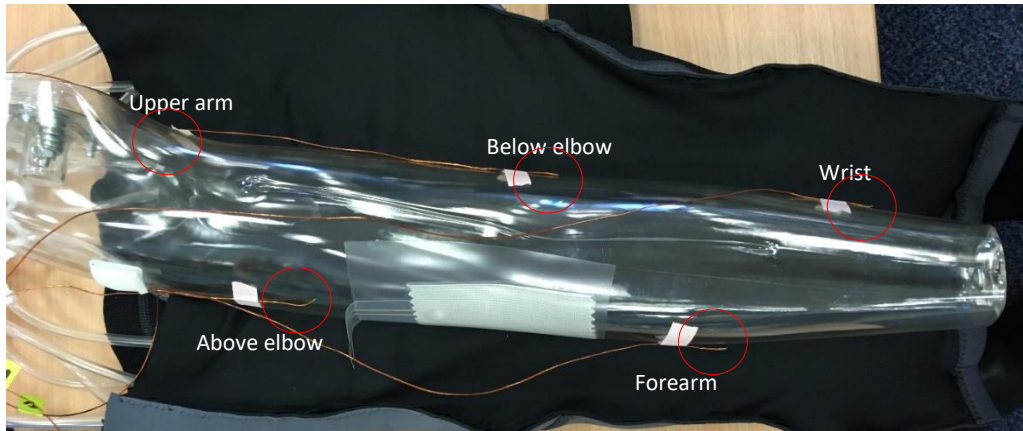


Figure 4-26: Location of thermocouples on mannequin arm

The graph in Figure 4-27 shows the temperatures produced at these thermocouples over 1 hour after the release of one bottle of CO₂.

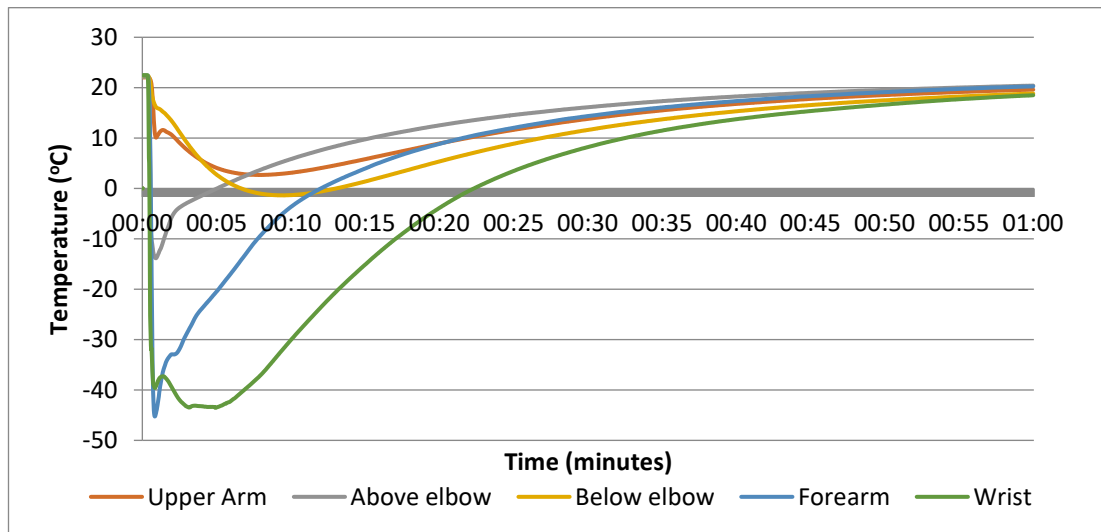


Figure 4-27: Temperature profile produced over 1 hour using shorter 6th iteration cooling sock

This graph shows that there was a large decrease in temperature at the wrist, forearm and above the elbow when the CO₂ started flowing. The upper arm and below the elbow also showed a substantial drop in temperature though not as dramatic as the other 3 thermocouples. There was also a slow rewarming time at all thermocouples with the baseline temperatures still not being reached after an hour. There seemed to be a build-up of dry ice

crystals (CO₂ snow) in the cooling sock at the wrist. Dry ice is produced by deposition, the change of gas to solid particles without forming liquid, due to the rapid expansion of compressed CO₂. CO₂ exists in a solid form at temperatures of -78.5°C and below (Engineering Toolbox, 2018). The dry ice then sublimates straight from solid to gas and evaporates. The presence of this very cold material in the sock will have caused a cooling effect until such time as the dry ice crystals had evaporated and disappeared. The presence of dry ice crystals was presumably why the thermocouple at the wrist took such a long time to reach 0°C. It is possible that the low temperatures produced at the wrist and forearm could cause tissue damage, especially if the temperature stays below 0°C for a prolonged period. However, the results produced in this test do show that the use of CO₂ can produce low temperatures and the use of non-porous tubing can prolong them.

4.11. Seventh Iteration:

Iteration 6.2 of the cooling sock was used during tests of the technology in a simulated combat setting using isolated porcine limbs as described in Chapter 6. Looking at the data of these studies it was decided that a change in the design of the cooling sock was needed to enhance cooling. A second topical cooling method was introduced by using the flow of gas to disperse FLUTEC PP80, a Perfluoro-2-methyl-3-ethylpentane coolant fluid, over the limb (specification sheet included in Appendix 1). This fluid works by removing heat due to evaporation of the fluid from the skin surface. As the CO₂ stream passes over the top of the coolant bottle the force draws the coolant up to the gas flow and it is then carried onto the limb. Figure 4-28 shows the arrangement of the gas and coolant distribution mechanism.



Figure 4-28: Gas and coolant distribution mechanism

FLUTEC PP80 was used for a number of reasons. The first is that it considered biologically inert thereby should not cause any ill effects when being used within the wound environment (see Appendix 1). However, it should be noted that this fluid has not been defined as biocompatible so further testing will be needed before it can be used in patient trials. Furthermore, FLUTEC PP80 is chemically inert, non-flammable and is not temperature sensitive (see Appendix 1). This means it is suitable for use in the field and will not degrade when stored for long periods.

To make the seventh iteration of the cooling sock a pair of 1.5mm neoprene surf trousers were cut up the inside seam. Open-ended chain zips were then stitched on to enable secure closure of the sock. To make the CO₂ and coolant dispersal system AVECOR 7/64 x 1/16 class VI silicone tubing was used in conjunction with Y connectors and female Luer to barb connectors (Nordson Medical, Westlake, Ohio, USA). Figure 4-29 shows the arrangement of these tubes and outlet points.



Figure 4-29: Arrangement of tubes and outlets in the seventh iteration of cooling sock

The tubes were then covered with a polyester/elastane material which was stitched along the seams to hold it in place. Holes were cut in this material and the Luer connectors were poked through to enable to FLUTEC PP80 fluid to come into direct contact with the limb. Figure 4-30 shows a photograph of the inside of the completed seventh iteration.



Figure 4-30: Completed seventh iteration of the cooling sock

4.12. Eighth iteration:

The seventh iteration of the cooling sock does not cover the foot, it only goes as far as covering the ankle. Evidently this will not allow for the cooling of the soft tissue of the foot, nor will it protect the foot from environmental contamination such as dust. For this reason the cooling sock was redesigned with a section suitable for cooling and covering the foot.

The main body of the cooling sock was made with the same specifications as the seventh iteration. However, more 1.5mm neoprene was cut from the disused waistband of the surf trousers which was large enough for the sole of the foot of the mannequin limb to fit in. 1.5mm neoprene was then used to create flaps which will fold over the sides and top of the foot. Velcro was stitched onto this foot covering to hold it closed. The coolant nozzles were extended further so that CO₂ and the FLUTEC PP80 would flow over the foot. Figure 4-31 shows the completed eighth iteration of the cooling sock. It shows both the locations of the coolant distribution nozzles as well as the cooling sock closed around the mannequin limb. In addition, Figure 4-31 shows the a close up of the mannequin foot in the foot section of the cooling sock as well as the complete encapsulation of the foot.



Figure 4-31: Eight iteration of cooling sock. Both open and closed as well as close ups of foot covering mechanism

The cooling sock went through many design changes during the development process. The data obtained in cooling tests of each iteration were taken into consideration when designing the next one. The aim of the changes was to maximise temperature reduction and maintenance at all 5 thermocouples. The first of these was to change the backing material from ShieldTex to a neoprene-based water sports material. The reason for this was to allow a more intimate sock fit around the limb with the aim of preventing the loss of CO₂ into the atmosphere. The arrangement of the tubes and the tube openings was intended to ensure maximum exposure to cooling over the surface area of the limb.

The change from porous tubing to non-porous tubing was to identify if the non-porous tubing would also be cooled by the CO₂ and act as a secondary cooling mechanism. The cooling data recorded for iteration 6 does indicate this when compared to iteration 5 confirming the choice of non-porous tubing going forward. Altering the CO₂ release protocol was done to develop a protocol which would result in prolonged low temperatures at each of the 5 thermocouples. The use of PP80 coolant fluid was introduced to examine if this would result in continued cooling during the periods between CO₂ flushes. The data suggested that this was the case so the cooling sock was redesigned with nozzles protruding through the lining material to allow for even distribution of coolant fluid over the limb. In summary, the design changes of the cooling sock were in response to perceived shortcomings in the previous approaches with the end objective of maximising controlled cooling over the largest surface area possible.

Chapter 5. Small-scale tissue testing:

5.1. Justification for testing:

The aim of these small-scale tissue tests is to see how the temperature propagates through different tissue types by measuring the temperature change at 3 different depths in slices of porcine tissue with the skin and fatty layer still present. The design of the following experiments was based on work on the effect of scalding on tissues previously carried out by Professor Gourlay as part of an MSc project at Imperial College London, investigating heat propagation through tissue associated with topical scalding agents. The main reason porcine tissue will be used was due to its similarities to human tissue. Porcine tissue is already an accepted model for human skin studies (Jacobi *et al.*, 2007, Swindle *et al.*, 2011). The structure of porcine skin is very similar with the same ratio of dermal to epidermal thickness and hair covering (Swindle *et al.*, 2011, Summerfield, Meurens and Ricklin, 2015, Jacobi *et al.*, 2007). However, the porcine tissue does generally have a thicker subcutaneous fat layer which will provide extra insulation when cooling (Swindle *et al.*, 2011).

Using smaller sections of tissue enables the tissue to be seen side on with each tissue type and layer displayed. Having each tissue type present will mean that the difference in cold propagation at each point from topical cooling can be observed. Smaller tissue samples also mean that the tissue can be more easily obtained. Furthermore, the tissue samples will be dead tissue so can be re-used for multiple tests of the same topical cooling mechanism. The benefit of this is that it minimises tissue variation, presenting a more standard testing scenario. Using tissue samples with the skin and fatty tissue present means that the tissue

sample will more closely resemble that environment in which the cooling technology will be deployed.

Three different cooling mechanisms were used during the small-scale tissue tests. The conditions were as follows:

- (a) CO₂
- (b) Ice
- (c) No cooling

The tests with no topical cooling application will be used as a control to investigate how the tissue cools without any intervention. Ice is the standard method of topical cryotherapy used during sports injuries. For this reason, it was decided to compare the ability of CO₂ to cool compared with the results produced using ice. If the results for using CO₂ are similar to the results with ice then it would suggest that the CO₂ will be an effective coolant and more appropriate for austere settings. Two different protocols for CO₂ release will be used to discover which method is more effective at cooling the tissue. These protocols differ in the number of CO₂ bottles utilised during the initial cooling period. The first tests will use 2 bottles while the second will employ 3 bottles. Moreover, all three methods of cooling will be repeated at two different tissue starting temperatures. The first of these is 37°C, reflecting the normal human tissue temperature. The second is a starting tissue temperature of 25°C to demonstrate the impact of initial tissue hypothermia on the cooling profile.

5.2. Testing protocol:

The tissue sample used in these experiments was skin-on pork obtained from a local butcher. The tissue sample was prepared by being cut into a rectangle of 100mm x 60mm. The tissue sample was then placed into a sealed plastic bag and submerged in a water bath to warm to the desired starting tissue temperature (37°C or 25°C). Whilst the tissue sample was warming up the test rig was set up. A FLIR One Pro thermal camera (Flir Systems Inc, Wilsonville, Oregon, USA) was attached to an iPhone SE and placed in a clamp 100mm from the test rig. A G clamp was then used to secure the test rig in position. Three markers were positioned on the thermal camera screen at the top, middle and bottom of the test window to allow the temperature of the superficial, mid and deep tissue to be measured. Once the tissue sample was at the desired temperature it was removed from the water bath and placed into the test rig. Figure 5-1 shows the empty test rig used in this series of experiments



Figure 5-1: Small-scale tissue test rig

For the experiments using CO₂ a length of silicone tubing was threaded through the top of the rig and taped to the table to retain it when the gas was flowing. Tissue paper was placed between the tubing and the lid to ensure contact of the tubing with the tissue sample. The lid was secured using rubber bands. Just prior to the start of cooling, the room temperature and starting temperatures of each tissue depth were recorded. A thermal photograph was taken every 30 seconds for the duration of the experiment.

The cooling protocol for each method of cooling was as follows:

- *2 initial bottles of CO₂*: 2 full bottles of CO₂ were emptied consecutively during the initial 6-minute cooling period. From 7 minutes, 10 seconds of CO₂ was flushed through the system every 3 minutes until 55 minutes has passed. Each bottle of CO₂ could produce 4 flushes of gas and 4 bottles of CO₂ were used in the secondary cooling period. Once the 55 minutes had passed, the temperature of the tissue was recorded for the next 5 minutes to see how the tissue re-warmed. This experiment was repeated 3 times.
- *3 initial bottles of CO₂*: 3 bottles were emptied consecutively in the initial 10-minute cooling period. During the secondary cooling period, 10 seconds of CO₂ were flushed through the test rig every 3 minutes until 46 minutes had passed. Again, one bottle of CO₂ was used for 4 flushes. However, to keep the total amount of CO₂ used equal, only 3 CO₂ bottles were used during the secondary cooling period. Thermal photographs were taken until 60 minutes had passed so the re-warming of the tissues could be studied. This test was repeated 3 times at each of the starting temperatures.

- *Ice*: the lid was not placed on the test rig during the ice tests. A Gio' style 200g Ice Olè classic ice pack (Gio'Style Spa, Urganano, Bergamo, Italy) was placed on the top of the rig. The ice pack was removed at 46 minutes to replicate the total cooling time during the 3 initial bottles of CO₂ tests. Thermal camera photos continued to be taken till 60 minutes. This experiment was repeated 6 times at each of the starting temperatures.
- *No cooling*: during these tests the lid was placed on the rig. Thermal camera photographs were taken for 60 minutes. The experiment was repeated 6 times at both temperatures.

Table 5-1 shows a summary of the experiments conducted according to this principle

Table 5-1: Summary of the tests for each cooling mechanism

Cooling method	Starting tissue temperature (°C)	Time for initial cooling (minutes)	Total cooling time (minutes)	Rewarming time (minutes)	Total experimental time (minutes)	Number of repeats
2 initial bottles of CO ₂	25	6	55	5	60	3
3 initial bottles of CO ₂	37	12	48	12	60	3
	25	10	46	14	60	3
Ice	37	N/A	46	14	60	6
	25	N /A	46	14	60	6
No cooling	37	N/A	60	N/A	60	3
	25	N/A	60	N/A	60	5

5.3. Results:

5.3.1. 2 initial bottles of CO₂:

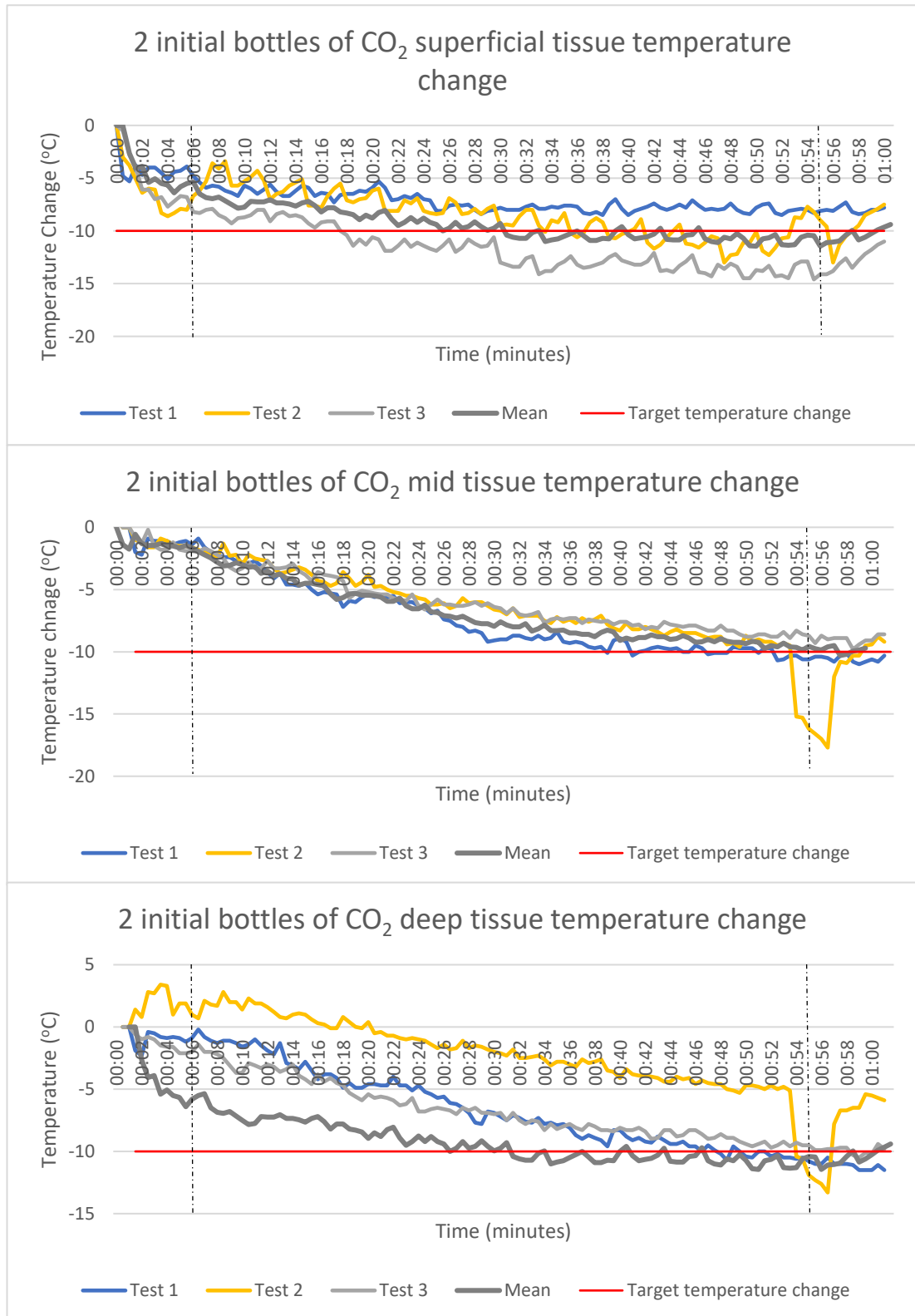


Figure 5-2: Temperature change at each depth of tissue for 2 bottles of CO₂ during the initial cooling period

As Figure 5-2 shows the temperature decreased at each tissue depth during both the initial and secondary cooling periods, shown by the grey dotted lines on the graph. The exception to this is the temperature recorded in the deep tissue during test 2. In this test there is a large change in temperature (-2.4°C in the superficial tissue and -8.2°C in the mid and deep tissue) at around 54 minutes which is after cooling had stopped and the tissue was rewarming. No logical reason could be found for this brief temperature alteration from the numerical data provided so the data for test 2 was not included in the calculation of the mean for 2 initial bottles of CO₂. If the data for test 2 is included in the mean it causes the line of the mean to mirror that of test 2 with a drop in temperature of -0.56°C in the superficial tissue, -2.83°C in the mid tissue and -2.80°C in the deep tissue during the rewarming period.

Furthermore, the temperature in the deep tissue in test 2 increases in temperature throughout the initial cooling period by a maximum of 3.4°C at 2.5 minutes. The temperature of the deep tissue does not drop below the starting temperature until 16 minutes. This effect is not seen across any of the other tests using an active cooling mechanism. Therefore, it is likely that there was a fault with the technology or the recording of data meaning the data for this test should not be used in the mean.

As the data in Table 5-2 shows, the mean temperature change in the superficial and deep tissue was more than the target 10°C. In the mid tissue the mean temperature change was just under this target at -9.55°C.

Table 5-2: Temperature change at the end of the cooling period for 2 initial bottles of CO₂

Tissue depth	Test 1 (°C)	Test 2 (°C)	Test 3 (°C)	Mean ± SD (°C)
Superficial tissue	-8.1	-9.0	-14.1	-11.10 ± 4.24
Mid tissue	-10.4	-17.0	-8.7	-9.55 ± 1.20
Deep tissue	-11.0	-12.6	-9.9	-10.45 ± 0.78

5.3.2. 3 initial bottles of CO₂:

5.3.2.1. 37°C starting tissue temperature:

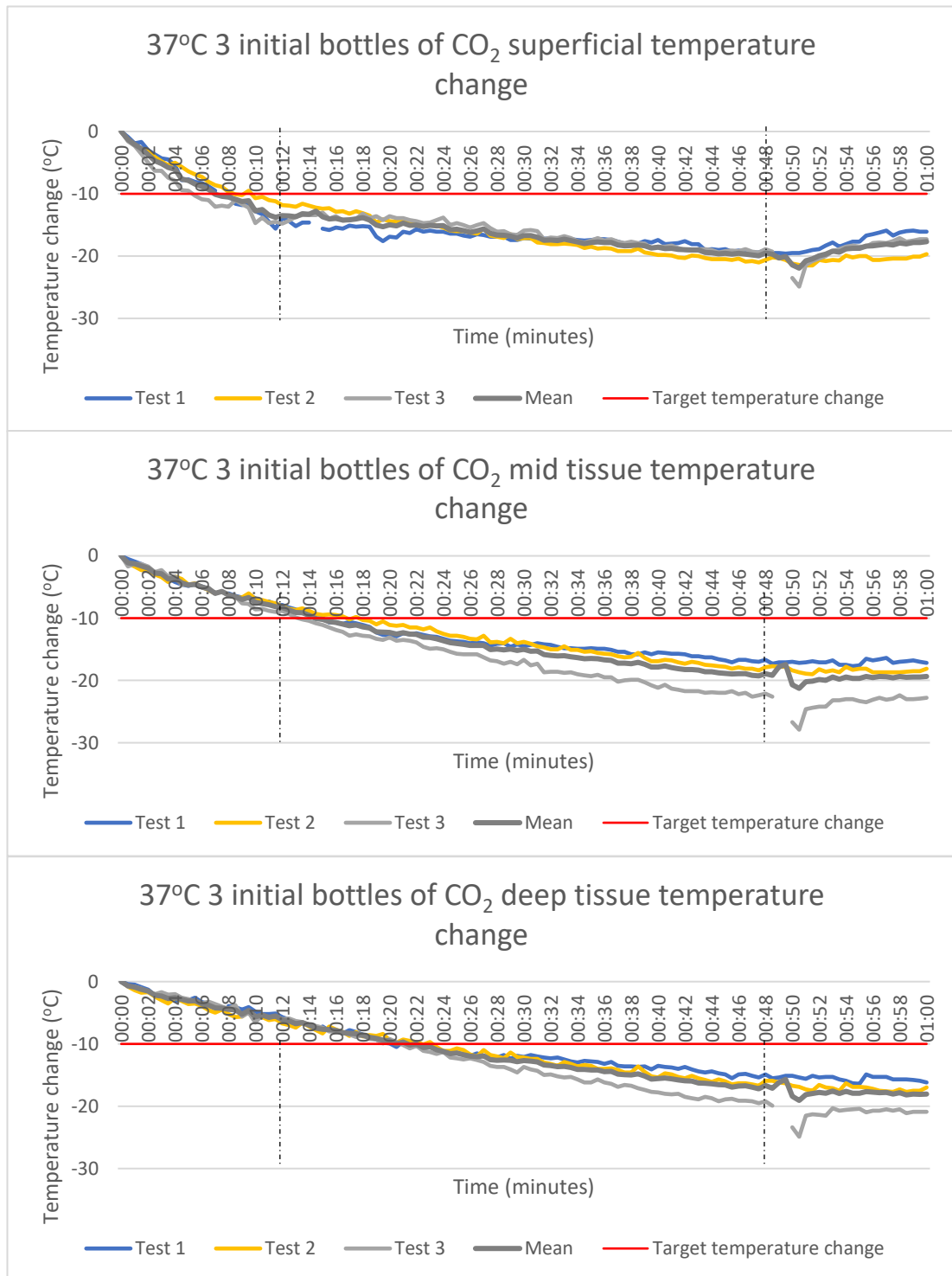


Figure 5-3: Temperature change from 37°C temperature using 3 initial bottles of CO₂ during initial cooling period

<i>Table 5-3: Tissue temperature change from 37°C at the end of secondary cooling period for 3 initial bottles of CO₂</i>				
Tissue depth	Test 1 (°C)	Test 2 (°C)	Test 3 (°C)	Mean ± SD (°C)
Superficial	-19.5	-20.2	-19.3	-19.67 ± 0.47
Mid	-17.3	-17.7	-22.6	-19.20 ± 2.95
Deep	-15.5	-15.9	-19.9	-17.10 ± 2.43

As the graphs in Figure 5-3 show, the tissue temperature decreases for the duration of both cooling periods. The temperature decreased at a faster rate during the initial cooling period (to the left of the first grey dashed line) than during the secondary cooling period between the two grey dashed lines. The tissue temperature had decreased by 10°C at all depths within 22 minutes in all tests. Table 5-3 shows that at the end of the secondary cooling period (48.5 minutes) the temperature in the deep tissue was at least 15.5°C below the starting temperature whilst the superficial tissue was up to 22.6°C below the initial temperature. There is a much greater variation in the tissue temperature at the end of cooling in the deep and mid tissue than there is in the superficial tissue. As Table 5-3 shows, there is 4.4°C difference between the deep tissue temperatures, 5.3°C difference in the mid tissue and only 0.9°C difference in the superficial tissue temperature change.

5.3.2.2. 25°C starting tissue temperature:

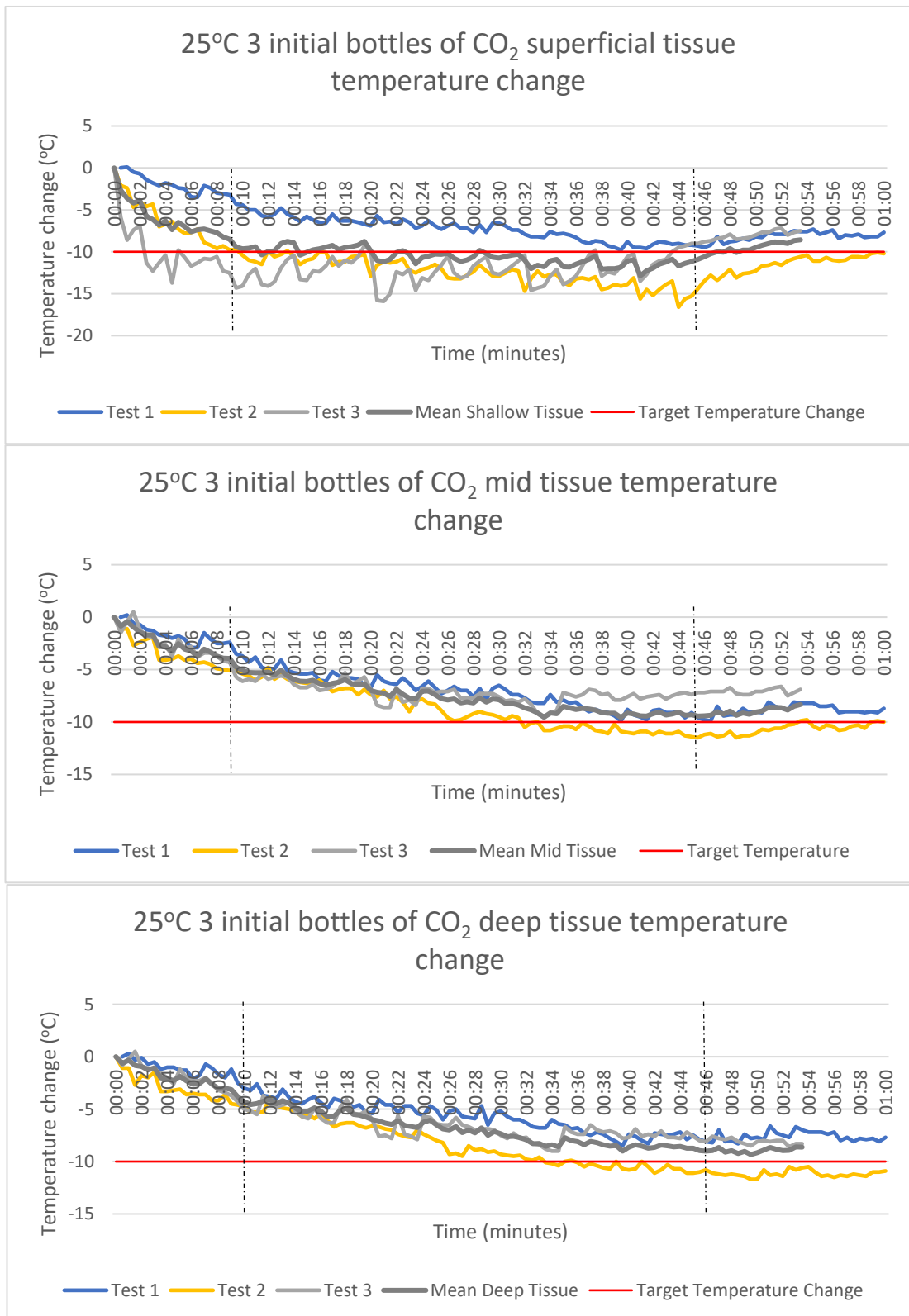


Figure 5-4: Temperature change at each tissue depth for 3 initial bottles of CO₂ with a starting tissue temperature of 25°C

<i>Table 5-4: Temperature change at end of cooling for three initial bottles at 25°C</i>				
<i>Tissue depth</i>	<i>Test 1 (°C)</i>	<i>Test 2 (°C)</i>	<i>Test 3 (°C)</i>	<i>Mean ± SD (°C)</i>
Superficial	-9.5	-13.5	-8.8	-10.6 ± 2.54
Mid	-9.8	-11.2	-7.2	-9.4 ± 2.03
Deep	-8.1	-10.8	-8.1	-9.0 ± 1.56

As the graphs in Figure 5-4 show, the temperature at all 3 tissue depths decreased over the course of the experiment. The only tissue depth where the mean tissue temperature decreased by 10°C was in the superficial tissue as demonstrated in Table 5-4. The graphs in Figure 5-4 show that the temperature decrease was not consistent between tests. The temperature during the secondary cooling period (marked by the grey dashed line) indicates that the cooling rate in the mid and deep tissue was similar to the cooling rate in the initial cooling period. The temperature in the deep tissue decreased slightly after the secondary cooling period is over. The temperature in the mid and superficial tissue increased during this same period.

5.3.3. Ice:

5.3.3.1. 37°C starting tissue temperature:

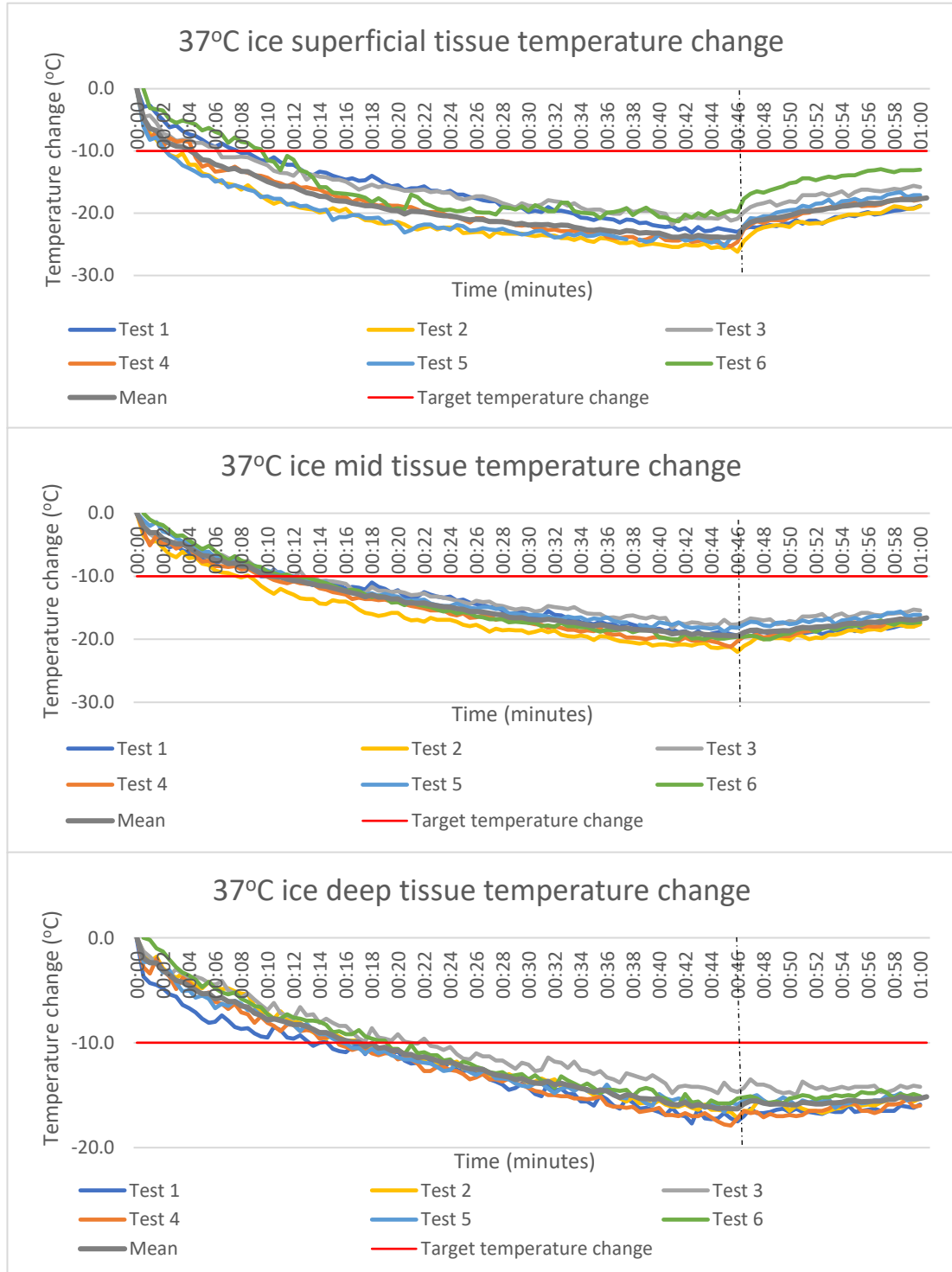


Figure 5-5: Temperature change at each tissue depth using ice with starting tissue temperature 37°C

<i>Table 5-5: Temperature change at 46 minutes for each tissue depth using ice at 37°C starting tissue temperature</i>							
Tissue depth	Test 1 (°C)	Test 2 (°C)	Test 3 (°C)	Test 4 (°C)	Test 5 (°C)	Test 6 (°C)	Mean ± SD (°C)
Superficial	-23.0	-26.2	-20.9	-24.6	-23.9	-19.8	-23.8 ± 2.38
Mid	-19.4	-22.0	-17.6	-20.3	-18.2	-19.6	-19.4 ± 1.56
Deep	-17.5	-17.2	-14.7	-17.2	-15.9	-15.3	-16.3 ± 1.16

The graphs in Figure 5-5 show the temperature at each tissue depth decreased steadily throughout the whole cooling period. The initial temperature change in the first 2 minutes was much more rapid before the rate of change slows down. As Table 5-5 shows, by 46 minutes the tissue temperature had decreased by much more than the target 10°C, reducing by a mean of 23.8°C in the superficial tissue and 16.3°C in the deep tissue. When the ice was removed, as shown by the grey dashed line, the temperature in the superficial tissue rebounded at a much faster rate than the deep tissue.

5.3.3.2. 25°C starting tissue temperature:

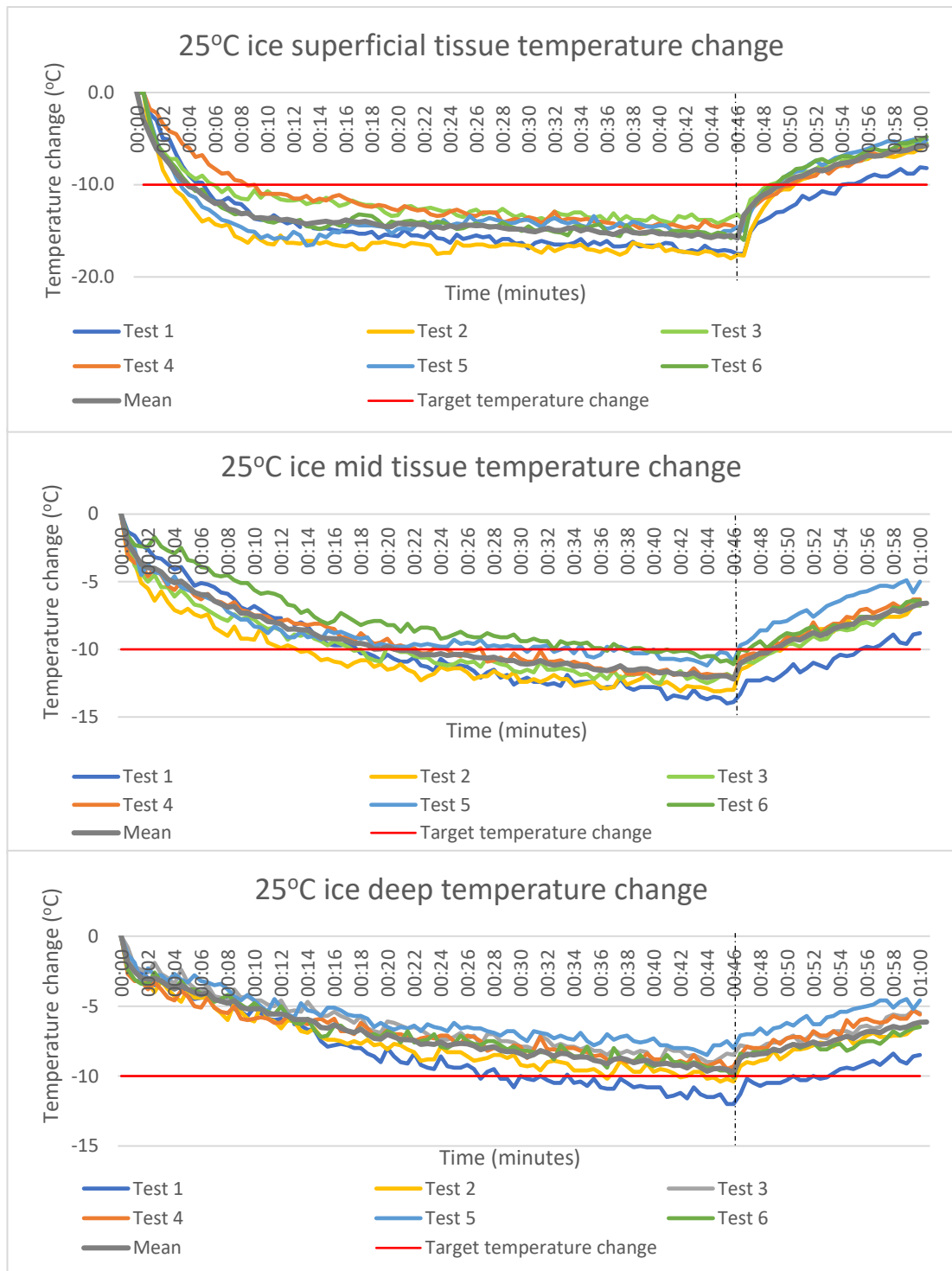


Figure 5-6: Temperature change at each tissue depth from 25°C using ice

<i>Table 5-6: Temperature change at 46 minutes for each tissue depth using ice with 25°C starting tissue temperature</i>							
Tissue depth	Test 1 (°C)	Test 2 (°C)	Test 3 (°C)	Test 4 (°C)	Test 5 (°C)	Test 6 (°C)	Mean ± SD (°C)
Superficial	-17.5	-17.7	-13.8	-14.8	-15.0	-16.0	-15.8 ± 1.56
Mid	-13.9	-13.0	-12.1	-12.2	-10.9	-11.1	-12.2 ± 1.13
Deep	-12.0	-10.4	-8.5	-9.3	-8.0	-10.1	-9.7 ± 1.44

Similar to the test at 37°C, at 25°C the temperature at all tissue depths decreased more rapidly over the first 2 minutes as seen in Figure 5-6. However, unlike at 37°C, at 25°C the tissue temperature rebounded quickly at all 3 tissue depths once the ice was removed. The cooling profile produced during each test is very similar. The mean temperature decrease in the deep tissue was not able to decrease by the target of 10°C as seen in Table 5-6. This table also shows that in the deep tissue the target 10°C decrease in temperature was only achieved at 46 minutes in 50% of the 6 tests.

5.3.4. No cooling:

5.3.4.1. 37°C starting tissue temperature:

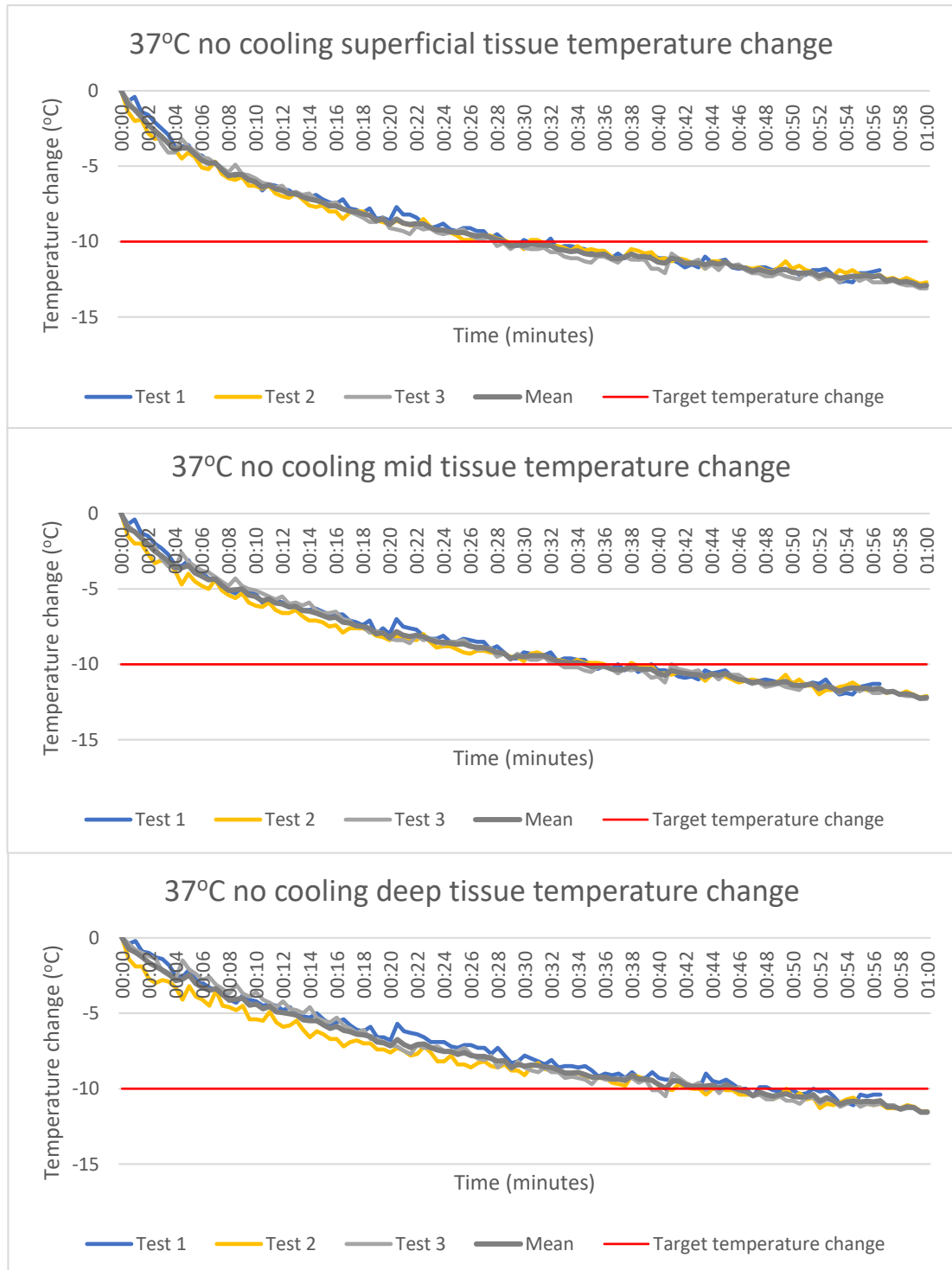


Figure 5-7: Temperature change at each tissue depth from 37°C with no active cooling mechanism

<i>Table 5-7: Temperature change at 46 minutes for each tissue depth with no cooling and 37°C starting tissue temperature</i>				
<i>Tissue depth</i>	<i>Test 1 (°C)</i>	<i>Test 2 (°C)</i>	<i>Test 3 (°C)</i>	<i>Mean ± SD (°C)</i>
Superficial	-11.8	-11.7	-11.5	-11.7 ± 0.15
Mid	-11.1	-11.2	-10.7	-11.0 ± 0.26
Deep	-10.0	-10.4	-9.9	-10.1 ± 0.26

As the graphs in Figure 5-7 show, the temperature at each tissue depth decreased over the entire test period with the deep tissue taking the longest to decrease by the target 10°C. However, as Table 5-7 shows, by 46 minutes the temperature in all but 1 test had dropped by 10°C. The rate of temperature change decreased as time increased. However, the graphs show that the temperature change was very consistent between the tests with the lines being very close together at each tissue depth as demonstrated by the small standard deviations seen in Table 5-7.

5.3.4.2. 25°C starting tissue temperature:

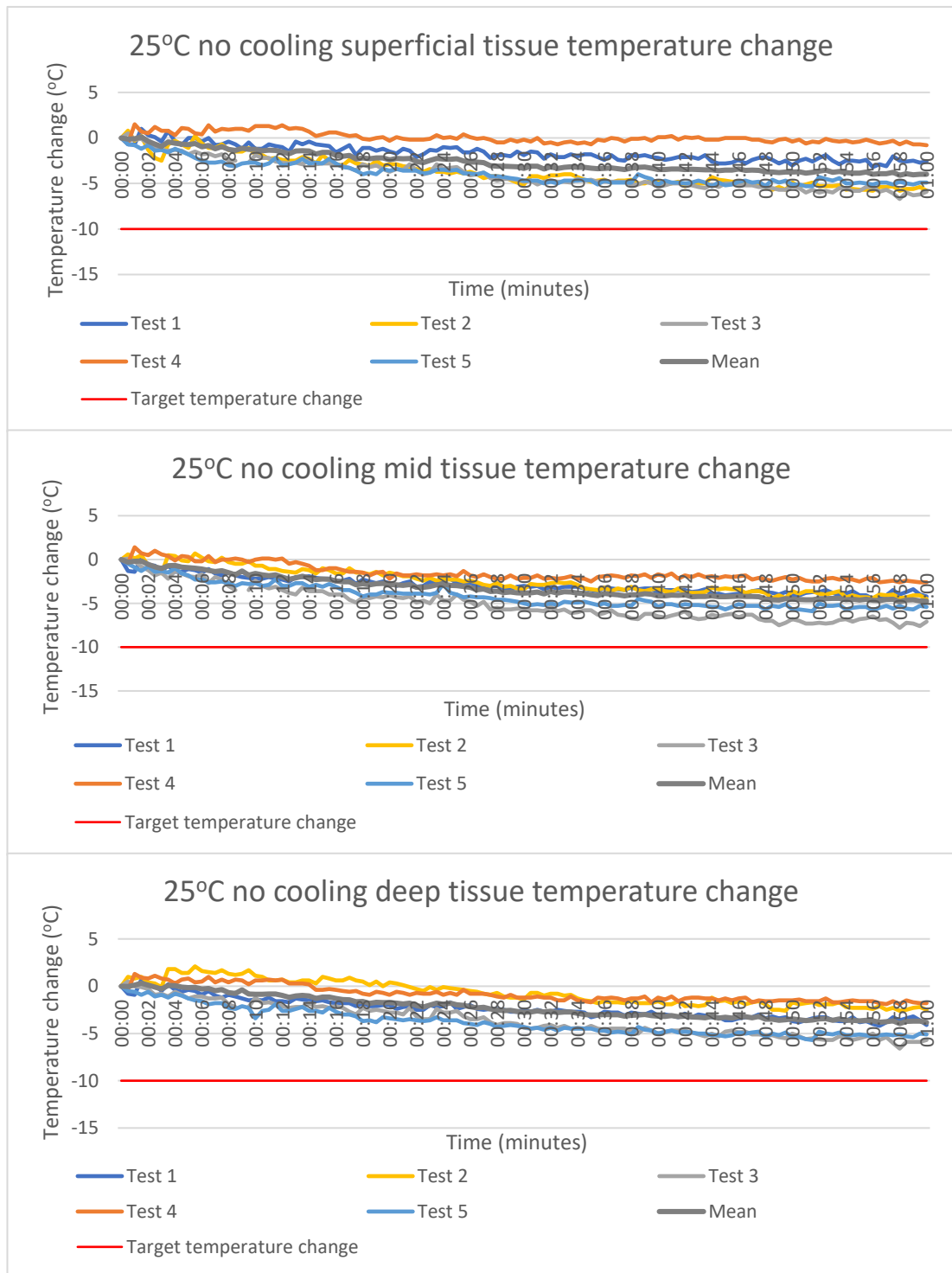


Figure 5-8: Temperature change at each tissue depth rom 25°C with no active cooling applied

Table 5-8: Temperature change at 46 minutes for each tissue depth with no cooling and 25°C starting tissue temperature

<i>Tissue depth</i>	<i>Test 1 (°C)</i>	<i>Test 2 (°C)</i>	<i>Test 3 (°C)</i>	<i>Test 4 (°C)</i>	<i>Test 5 (°C)</i>	<i>Mean ± SD (°C)</i>
Superficial	-2.4	-4.8	-5.1	0.0	-4.8	-3.4 ± 2.20
Mid	-3.9	-3.4	-6.6	-1.9	-5.1	-4.2 ± 1.77
Deep	-3.4	-1.6	-4.9	-1.3	-4.9	-3.2 ± 1.73

As the graphs in Figure 5-8 show, the temperature at each tissue depth did not decrease very rapidly. In fact, the temperature even increased slightly at the beginning of the experiment before starting to fall. By 46 minutes none of the tissue temperatures had decreased by more than 6.6°C with the temperature of the superficial tissue in Test 4 being the same as the initial temperature, as demonstrated in Table 5-8. There was also a wider range of rate of tissue temperature change when the tissue started at 25°C than at 37°C.

5.3.5. Comparison of cooling methods:

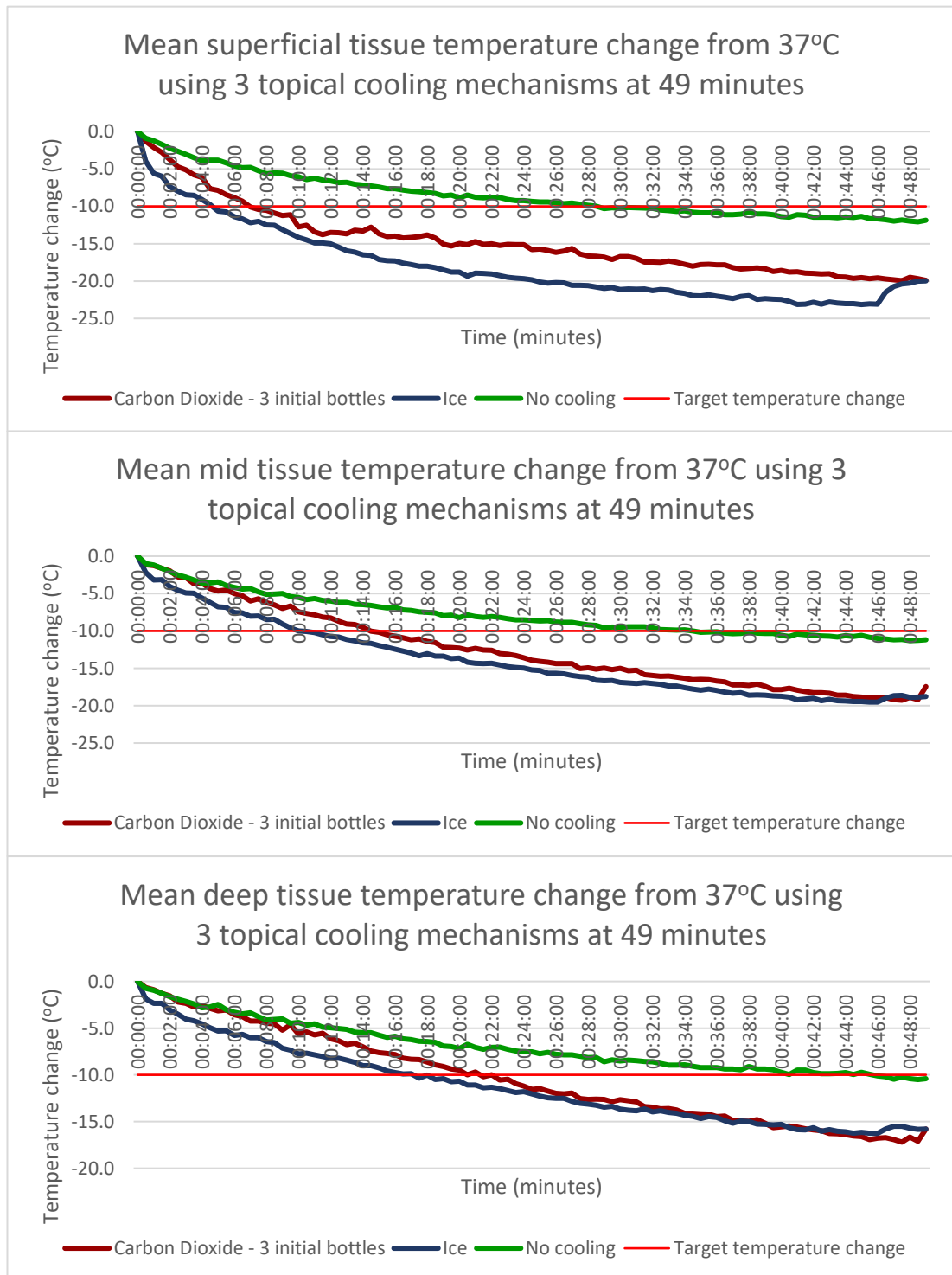


Figure 5-9: Mean temperature change at each tissue level using the 3 different topical cooling methods starting at 37°C

The graphs in Figure 5-9 show that the tissue samples that started at 37°C were all cooled to more than the 10°C target under all conditions. The end temperature at each tissue level was statistically different ($p < 0.05$) from its starting temperature for all 3 experimental conditions, shown in Table 5-9. The graphs also show that the ice consistently cooled the tissue sample fastest at all tissue depths. However, in the deep tissue, the rate of cooling using CO₂ ended up equalled that of ice assisted cooling after approximately 31 minutes. The superficial tissue temperature decreased very rapidly when both ice and CO₂ was used. When ice was used the superficial temperature had dropped by 10°C in around 4.5 minutes with the CO₂ cooled tissue taking only 3 minutes longer. Therefore, the superficial tissue temperature had dropped by 10°C before the 3 CO₂ bottles in the initial cooling period were emptied. Conversely to the experiments where the tissue temperature started at 25°C, a starting tissue temperature of 37°C did lead to a 10°C drop in the superficial tissue when no topical cooling mechanism was applied. The rate of cooling in the superficial tissue was faster during the initial cooling period when using CO₂ as shown by a steeper curve. The ice cooling curves start to rebound at 46 minutes as this is when the ice was removed.

The gap between the cooling profiles in the mid tissue of the CO₂ and ice were much closer together. Again, there was about 5 minutes between the time it took the tissue temperature to drop by 10°C when using ice (around 10.5 minutes) and CO₂ (around 15 minutes). The mid tissue temperature had also dropped by 10°C by 36 minutes when no cooling was used. The end temperature in the mid tissue was not statistically different ($p > 0.05$) between the ice and the CO₂ as shown in Table 5-9. However, the end tissue temperatures in both these active cooling tests were significantly colder than the no cooling tests.

In the deep tissue the CO₂ cooled the tissue at a relatively steady rate. This is in contrast to the ice whereby the cooling rate decreased slightly as the experiment progressed. Indeed, by the time the ice was removed (46 minutes), the CO₂ had reduced the temperature in the deep tissue by slightly more than the ice. When no cooling was applied, the tissue temperature took almost the entire cooling period to reduce by 10°C, however, this target temperature reduction was achieved.

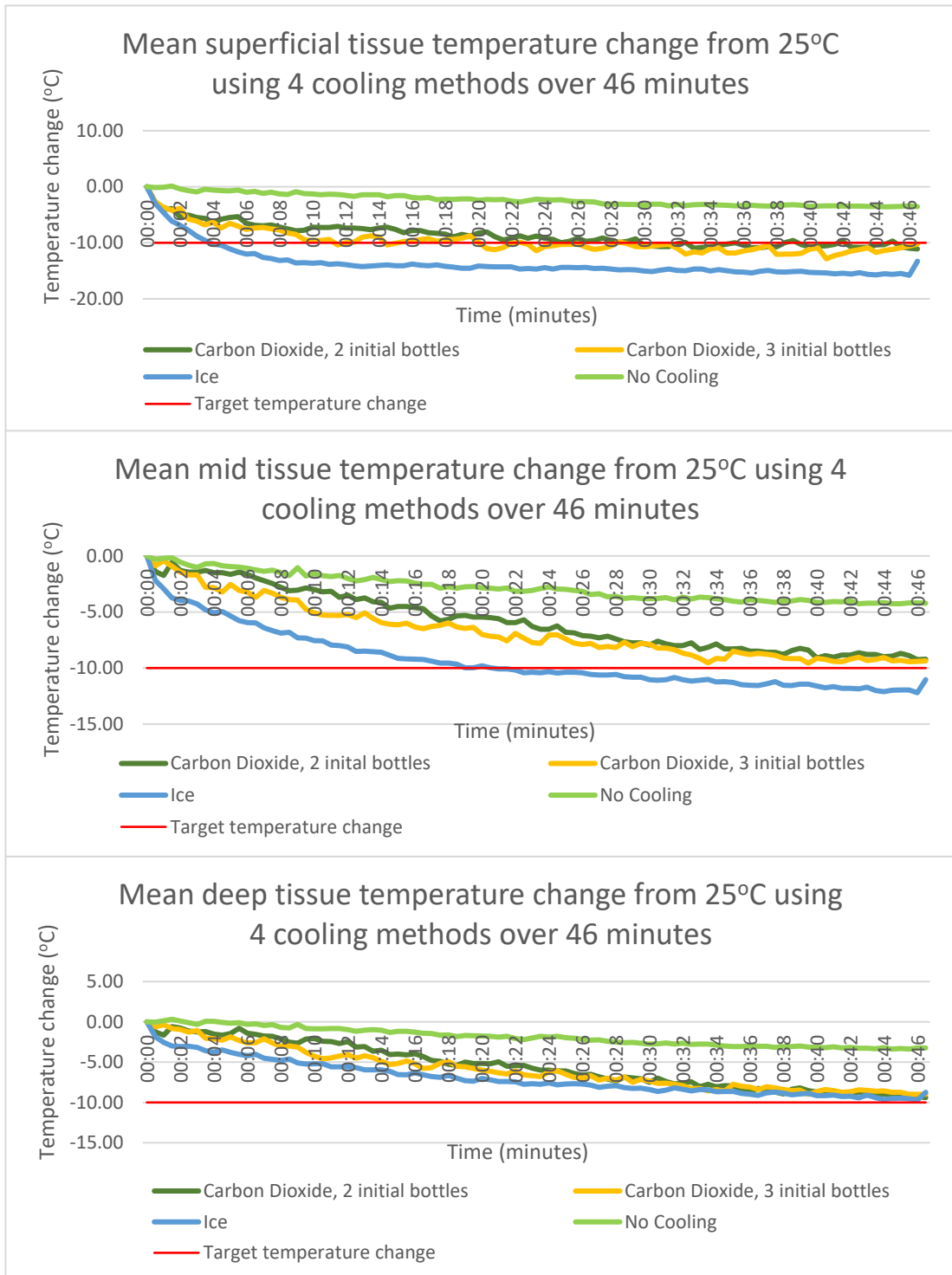


Figure 5-10: Mean temperature change at each tissue level using the 4 different topical cooling methods starting at 25°C

As the graphs in Figure 5-10 show, the 4 cooling methods cooled differently at 25°C. In the superficial tissue there was a distinct difference between the cooling profile of the ice, compared to the carbon dioxide, compared to no cooling. The ice was able to create a much larger temperature decrease, with the target temperature being achieved at 4 minutes. The carbon dioxide was able to cool the superficial tissue by 10°C but this was not achieved until closer to 15 minutes when 3 initial bottles were used and 25 minutes when 2 initial bottles were used. When no topical cooling mechanism was used, the superficial tissue temperature barely decreased.

When comparing the mid tissue temperatures using the 4 cooling methods it can be seen that ice was the only method that reduced the temperature by more than the target 10°C, at around 21 minutes. As at the superficial tissue level, the mid tissue cooled at a similar rate when either 2 or 3 bottles were used during the initial cooling period. Again, using no cooling mechanism meant that the tissue did not decrease by more than 5°C.

Interestingly, in the deep tissue it can be seen that the temperature decrease was similar when using both 2 and 3 initial bottles of CO₂ and when using ice. This is contrary to expected. However, when the starting tissue temperature was 25°C, none of the cooling methods were able to decrease the deep tissue temperature by 10°C. The deep tissue temperature decrease in the no cooling test was similar to the decrease at the other 3 tissue depths with a decrease of less than 5°C observed.

Table 5-9 shows that the end temperatures for the no cooling test were statistically higher ($p < 0.05$) than the other 2 experimental conditions. The temperature in the deep tissue at the

end of cooling was not statistically different ($p>0.05$) between the ice and both CO₂ tests when the starting temperature was 25°C. However, the temperature of the superficial tissue at the end of cooling from 25°C when using ice was statistically colder ($p<0.05$) than when using CO₂.

Table 5-9: Mean room temperature and both the starting and end temperature of the 3 tissue depths for all small-scale tissue tests

Test conditions	Mean ± SD room temperature (°C)	Mean ± SD tissue starting temperature (°C)			Mean ± SD tissue temperature at end of secondary cooling period (°C)		
		<i>Superficial</i>	<i>Mid</i>	<i>Deep</i>	<i>Superficial</i>	<i>Mid</i>	<i>Deep</i>
3 initial bottles of CO ₂ 37°C	19.9 ± 1.5	31.3 ± 2.80* ^D	33.8 ± 0.09* ^{C,D}	33.8 ± 1.27* ^{B,C,D}	11.7 ± 2.4* ^I	14.6 ± 3.15* ^{G,H}	16.7 ± 3.08* ^G
Ice 37°C	24.5 ± 0.5* [*]	36.5 ± 0.78* ^{A,B,C}	36.2 ± 0.64* ^A	36.1 ± 0.66* ^{A,B,C}	12.7 ± 1.82* ^H	16.8 ± 1.70* ^G	19.8 ± 1.32* ^F
No cooling 37°C	21.3 ± 1.6	37.1 ± 1.39* ^A	36.4 ± 1.30* ^{A,B,C}	36.1 ± 1.44* ^{A,B,C}	25.3 ± 1.51* ^E	25.4 ± 1.42* ^E	26.0 ± 1.30* ^E
2 initial bottles of CO ₂ 25°C	N/A	25.1 ± 0.71* ^{A,B,C,D,E}	24.7 ± 0.28* ^{B,C,D,E}	28.1 ± 0.71* ^A	13.8 ± 3.54* ^G	15.1 ± 1.48* ^{F,G}	18.1 ± 0.07* ^F
3 initial bottles of CO ₂ 25°C	16.5 ± 1.4	24.2 ± 1.44* ^{C,D,E}	25.1 ± 2.55* ^{B,C,D}	26.2 ± 0.98* ^{A,B,C}	13.6 ± 3.04* ^G	15.7 ± 2.66* ^{F,G}	17.2 ± 2.22* ^F
Ice 25°C	27.1 ± 1.5* [*]	27.1 ± 1.04* ^{B,C}	25.4 ± 1.16* ^{A,B,C}	26.0 ± 1.18* ^{A,B,C}	9.5 ± 1.30* ^H	13.8 ± 0.71* ^G	16.7 ± 0.90* ^F
No cooling 25°C	22.6 ± 0.7** ^{**}	26.3 ± 2.36* ^{A,B,C}	26.8 ± 2.19* ^{A,B}	26.4 ± 2.02* ^{A,B,C}	22.9 ± 1.06* ^{D,E}	22.6 ± 1.22* ^E	23.2 ± 1.24* ^{D,E}

Values that do not share a letter are statistically different ($p < 0.05$). The data for 25°C and 37°C starting temperatures have been separately analysed.

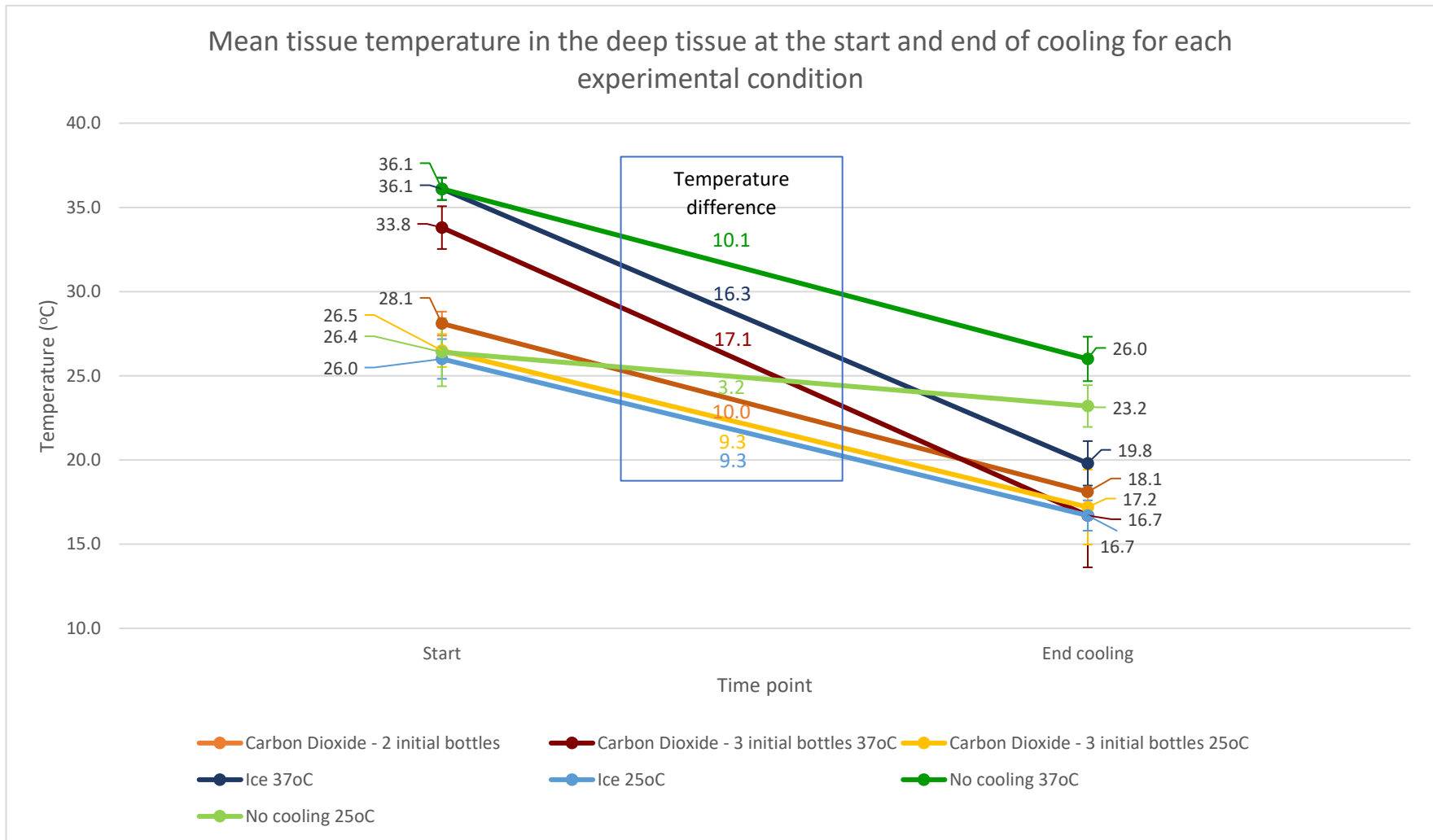


Figure 5-11: Temperature difference between the mean starting temperature and mean end temperature of the deep tissue in all cooling experiments

Table 5-9 shows the mean and standard deviation for the start temperature and the temperature at the end of the secondary cooling period for each of the experimental conditions undertaken in these tests, which demonstrates the differences in the end temperatures achieved in each experiment. The table also shows the room temperature. This is included as the ambient temperature varied by over 10°C which would have affected how the tissue cooled. The graph in Figure 5-11 shows the temperature data from Table 5-9 in a graphical form. The effect of starting temperature on the temperature change is visible in this graph with much sharper gradients in the darker lines corresponding to the start temperature of 37°C. This graph clearly shows that the mean starting temperatures of the ice and no cooling tests at 37°C were higher than that of the CO₂ test but that the temperature change between the ice and CO₂ tests was not too different. The slope of the line between the start and end temperature of the no cooling test starting at 37°C was less steep than that of the ice and CO₂ showing that the temperature was not reduced as efficiently. The gradient of the line for both CO₂ tests and the ice test for the experiments starting at 25°C were very similar. This is in contrast to the line showing the temperature change when no cooling was applied starting at 25°C which is much flatter.

5.4. Discussion of results:

The results of the CO₂ and ice tests show that, on a small scale, topically applied CO₂ could cool the deep tissue as effectively as ice. The implication of this is that the cooling sock in the proposed technology should be able to provide cooling to the injured limb. When considering the graphs in Figure 5-9 and Figure 5-10 it can be seen that the cooling profile for using CO₂ is very similar to the cooling profile when ice was used and different to the no active cooling

profile. Indeed, as Table 5-9 confirms, the end temperature of the deep tissue which started at 25°C was statistically similar ($p>0.05$) when using CO₂ and ice. The end temperature of the deep tissue which started at 37°C was statistically colder ($p<0.05$) when using CO₂ compared to ice. However, this could be misleading since the deep tissue for the CO₂ test started off at a lower temperature. The effect of the starting temperature on the statistical significance can clearly be seen in the superficial tissue where the end temperature in the test using CO₂ starting at 37°C is significantly colder ($p<0.05$) but the graph in Figure 5-9 shows that the ice test produced a greater tissue temperature change. On the other hand, when looking at the graph in Figure 5-11, the mean temperature change in the deep tissue from 37°C was 0.8°C bigger when CO₂ was used compared to ice. To ensure the cooling effect of topical application of CO₂ can be reproduced on a larger scale, this size of the tissue sample will need to be increased.

One important thing that these results show is the difference in the temperature change for the no cooling tests at the different starting temperatures. As Table 5-9 shows, the room temperature for both of these experimental conditions was similar (21.3°C for the 37°C tests and 22.6°C for the 25°C tests). However, the change in the deep tissue temperature was very different. The tissue that started off at 25°C was only able to cool by 3.2°C whilst the tissue starting at 37°C cooled by 10.1°C. It goes without saying, the tissue will cool faster when there is a greater temperature gradient for the heat to pass down and the tissue will not cool below room temperature without intervention. Thereby, this difference in deep tissue cooling is to be expected as the tissue starting off at 25°C was only a mean of 3.7°C above room temperature. In future testing, the ambient temperature that the experiment is undertaken at should be considered as it may alter the results of how well the tissue is able to be cooled.

The effect of the starting tissue temperature on the temperature change experienced in the deep tissue can also be seen when comparing both the ice and CO₂ tests. The tests undertaken with a starting tissue temperature of 37°C resulted in a greater change in tissue temperature each time. Interestingly, this difference in the temperature change seen from 25°C and 37°C was similar for all the tests. When considering the change in the mean deep tissue temperature for no cooling, ice and 3 initial bottles of CO₂, the difference between the temperature change at 25°C and 37°C varied by less than 1°C (6.9°C, 7.0°C and 7.8°C respectively). Whilst this may be coincidental it may suggest that there is a pattern in the rate of cooling, more data would be needed to confirm this. However, seeing as the technology is designed to be used at the point of injury it is unlikely that the tissue temperature will have dropped much below 37°C anyway.

The temperature gradient of the tissue temperature to ambient temperature altering the rate of cooling in the tissue has already been established. Table 5-9 shows that the room temperature is statistically different ($p < 0.05$) in all 3 tests at 25°C and in the ice test at 37°C. Although the method of cooling will have the biggest effect on the temperature change of the tissue, heat will also be lost to the environment through radiation. The plastic of the rig will provide some insulation from heat loss to the environment but it will not stop it completely. At both 25°C and 37°C, the room temperature was much warmer for the ice tests compared to the CO₂ tests. This could have skewed the results slightly in favour of the CO₂ approach. Future experiments should be done in controlled conditions so that the ambient temperature is constant to assess this.

Another factor which effected the starting temperature of the tissues was the time it took to assemble the rig for the CO₂ experiments. This was more of a factor for the experiments with a starting tissue temperature of 37°C because, as previously mentioned, the tissue cooled faster. Although the tissue sample was taken out of the water bath when it was at 37°C, by the time the tissue had been placed in the rig, the tube positioned correctly and the flow of gas started the tissue temperature had decreased. As previously mentioned, this meant that the superficial tissue temperature in the 37°C was statistically colder ($p < 0.05$) than the other tests at 37°C from the start which could have altered the results.

One problem in the execution of the experiment was the fact that a video could not be used and instead a photo was taken every 30 seconds. This meant that if a problem occurred, or something else required attention such as switching over CO₂ bottles, a photograph could be missed. Although missing one data point will not affect the overall results of the experiment, if the missed data point was not noted down then it was difficult to know which data point was missed which could lead to temperatures at different points being compared.

The speed of changing over the bottles varied between tests, faster changing of bottles means a more constant flow of gas to cool the tissue. However, if the bottles are changed over too quickly then there is a period of no cooling before the secondary cooling period starts which will allow the tissue to warm up slightly if it is below ambient temperature. Another way the CO₂ affected the experiment was the speed of gas release. The valve used on the CO₂ bottle was manually controlled, that means that the CO₂ was released at different speeds every time. Consequently, 10 seconds of CO₂ release may not equate to the same volume of CO₂ used for cooling. The CO₂ was released as similarly as possible between tests

and it is likely that over the course of the test the amount of CO₂ used each time would even out. However, since the release of CO₂ was not measured this cannot be confirmed.

The FLIR app enables you to place markers on the thermal camera screen which stay in place until they are deleted. The position of the markers was set in the first small scale tissue test that was undertaken and then they were kept in position for the duration of the testing. This means that the distance between the superficial, mid and deep tissue markers was kept the same throughout testing. The use of a clamp stand meant that the thermal camera was held in position and each photo taken during 1 test was taken from exactly the same place. However, there was no way on ensuring that the camera was at the same height during each test. It was endeavoured to position the makers in the middle of the test window on the rig for each experiment, nevertheless, the markers would have been in a slightly different position each time. Thereby, the depth of the deep tissue in one test would not be quite the same as the deep tissue in another test. This could affect the results as the deep tissue in one test could be the depth of the mid tissue in another. Furthermore, the markers could be positioned on the fatty tissue which would alter the cooling profile seen. This variation was controlled for as much as possible but a fixed position camera should be used in future if these tests are repeated.

Overall, the small-scale tissue tests show that CO₂ used in the protocol described is able to reduce the temperature of the tissue sample down at the three tissue depths measured as effectively as ice. This confirms that is may be suitable as aa method for cooling tissues under battlefield conditions. However, further testing needs to be done using a more mimetic model. Therefore, in future testing larger tissue samples e.g. animal limbs will be used to see

how effective the CO₂ is when spread over a larger area. Moreover, the cooling sock divides the gas flow into 16 different tubes and has a layer of elastane material in between the tubing and the limb. This will reduce the ability of the CO₂ to cool and this will also be examined.

Chapter 6. Testing of technology in simulated combat setting –

porcine tissue:

6.1. Testing protocol:

Experiments were designed to test the efficiency of the newly developed technology over a simulated casualty treatment pathway as it would happen from a combat incident. The simulated treatment pathway first tested the ability to cool the limb down and keep it cool from the point of injury (collection at the abattoir) and throughout the journey to the hospital (the university laboratory). Additionally, the limb was placed in the limb support system (LSS) and perfused to simulate the perfusion of the injured limb in a hospital setting. Various types of data were collected during the perfusion period to assess the performance of the new technology at preserving the viability of the limb tissue. During these experiments disarticulated porcine hind limbs were used. The disarticulated limbs had a length of around 40cm with a circumference of the top of the limb of roughly 35cm. Consequently, the ability of the tourniquet was not assessed as the limbs did not require haemorrhage control.

To maximise the possibility of tissue viability, porcine hind limbs were collected from an abattoir immediately after being freshly harvested. Immediately after collection thermocouples were inserted into the tissue. One thermocouple was placed into the deep tissue and one was inserted into the superficial tissue just beneath the skin. A third thermocouple was placed at the site of injury in the trotter sustained as a result of suspension

hook placement in the abattoir. Finally, one thermocouple was placed on the skin surface. The porcine limb was then zipped into the cooling sock and cooling commenced.

The cooling protocol (n=5) was as follows: when the cooling sock was closed one full 60L bottle of CO₂ was released through the sock using a manually controlled valve as described in Chapter 4 page 87. Following this, a 10 second flush of CO₂ was released every 5 minutes for the duration of the car journey back to the university lab. The CO₂ bottle was changed after every 4th flush. Upon arrival at the university the final partially emptied CO₂ bottle was flushed through the cooling sock. The mean journey time was 41.8 ± 7.29 minutes with 4 CO₂ bottles emptied over this time.

During the first 3 porcine limb tests a second freshly harvested limb was also collected as a control limb. This limb was placed in the car and was not actively cooled during the journey back to the university. It was then taken up to the lab and left on the side whilst the cooled limb was cannulated and perfused. At the end of the perfusion period neural stimulation was attempted on both limbs to see if toe twitch could be achieved. This was to identify if there was any difference of twitch between the control limbs and the cooled and perfused limbs. Control limbs were collected to identify if the intervention of the new technology could preserve tissue viability over the treatment time. The electrical signal started off at a low amplitude (10mA), this amplitude was gradually increased to 100mA, if no twitch was seen by this point it was determined that it was unlikely that a twitch could be achieved. Control limbs were not collected for tests 4, 5 and 6 because the first 3 tests showed the control limbs to be completely inactive at the end of the perfusion period.

The cooling protocol for a sixth test with porcine tissue was slightly different. The protocol for this test was changed to assess how the combined use of CO₂ and coolant fluid affected the cooling of the limb to inform the protocol for future tests. The new protocol was as follows. Firstly, the thermocouples were inserted with the aid of a needle into the deep, mid and superficial tissue as well as the injury site. The use of a needle enabled the thermocouples to be placed deeper within the tissue. Furthermore, the cooling sock had been redesigned to allow for an additional coolant fluid to be dispersed over the limb in combination with the CO₂, a description of the coolant fluid can be found in Chapter 4 pages 119 to 120. The redesigned cooling sock can be seen in Figure 6-1. The coolant fluid used was FLUTEC PP80. The CO₂ was released very slowly (at 25% of normal experimental capacity) to allow the coolant to be siphoned into the gas stream by the action of the fast-moving gas passing the opening of the FLUTEC PP80 feeder tube.



Figure 6-1: Cooling sock iteration 7.2 for use with CO₂ and coolant fluid

The sixth test had 2 periods of active cooling. The reason for this was to enable the effect of the coolant fluid on the rewarming process to be examined. Furthermore, the prolonged cooling effect of the coolant fluid could also be assessed to see if the limb continues cooling after the CO₂ stops flowing via evaporation of the coolant fluid. The temperatures of the tissue were monitored throughout the journey so cooling was restarted to see if the limb temperature could be reduced by 10°C.

In the first period of active cooling, 3 bottles of CO₂ were released consecutively. The coolant phial was replenished every time the CO₂ bottle was changed. The first 2 phials contained 40ml coolant fluid; the 3rd phial contained 20ml as we only had 100ml of coolant available to us for this experiment. The first active cooling period lasted for 9 minutes. For the next 9 minutes the limb tissue was not actively cooled but instead was monitored to see how the temperature of the deep tissue changed. At 18 minutes another CO₂ bottle was emptied. The empty CO₂ bottles were kept away from the cooling sock to prevent them acting as an additional cooling mechanism. The journey back to the university took 30 minutes with 4 bottles of CO₂ used during this time. Figure 6-4 is a visual depiction of the protocol and details the steps taken for each part of the experiment.

The protocol for limb support was the same for all 6 tests carried out on porcine tissue. Upon arrival at the university the thermocouples were removed from the limb and the limb was carried up to the laboratory. As soon as the limb was in the lab cannulation of the femoral artery was initiated. The arteries in the porcine tissue were small and so were difficult to cannulate with a large catheter. The largest cannula possible was used to minimise the

resistance to flow and to reduce pressure in the circuit. An 8 French Portex cannula (Smiths Medical International Ltd, Ashford, Kent, UK) was used in these experiments. Once cannulation had been achieved the limb was placed in the hammock of the limb support system (LSS). The arterial line of the pre-primed circuit was connected to the catheter. The circuit was primed with a combination of ringers and gelofusine. Before perfusion began a Laser doppler image (LDI) scan and a thermal camera photograph were taken using a Moor LDI Laser Doppler imager (Moor instruments, Axminster, Devon, UK) and a FLIR One Pro (Flir Systems Inc, Wilsonville, Oregon, USA) respectively.



Figure 6-2: Moor LDI imager taking an LDI scan and FLIR One Pro thermal camera used for thermal imaging. Images taken every 15 minutes during perfusion.

Once both baseline data samples had been taken the isolated limb was then perfused with warm bovine whole blood. The target perfusion flowrate was 110ml/kg to mimic physiological tissue flowrate. LDI scans and thermal photographs were taken every 15 minutes for the duration of the 90-minute perfusion time. Figure 6-3 shows the disarticulated limb in the LSS whilst being perfused. When data was not being collected the limb was covered with silver foil to reduce heat loss due to the fact the top covers of the LSS could not

be positioned because the LDI scanner was in the way. The peroneal nerve was stimulated to promote a twitch in the extensor digitorum brevis at 90 minutes using a Digitimer DS7A (Cephalon, Nørresundby, Denmark).



Figure 6-3: Disarticulated porcine limb being perfused in the LSS with mean arterial pressure and flow rate displayed on screen. Red dot is the LDI scan being performed. Cannula is filled with primer fluid

0 minutes: Collection of limbs

Limbs designated for cooling placed in cooling sock
 Thermocouples inserted into tissue at end of limb and site of injury
 Cooling sock zipped up

Porcine limb test 1-5:

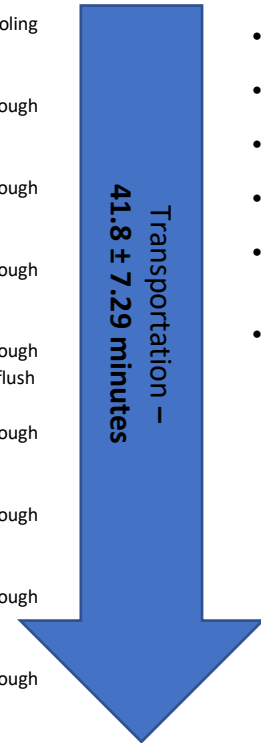
- 0 minutes:
 - 1 full bottle of CO₂ released through cooling sock
- 5 minutes:
 - 10 second flush of CO₂ released through cooling sock
- 10 minutes:
 - 10 second flush of CO₂ released through cooling sock
- 15 minutes:
 - 10 second flush of CO₂ released through cooling sock
- 20 minutes:
 - 10 second flush of CO₂ released through cooling sock. CO₂ bottle changed post-flush
- 25 minutes:
 - 10 second flush of CO₂ released through cooling sock
- 30 minutes:
 - 10 second flush of CO₂ released through cooling sock
- 35 minutes:
 - 10 second flush of CO₂ released through cooling sock
- 40 minutes:
 - 10 second flush of CO₂ released through cooling sock
- 45 minutes:
 - 10 second flush of CO₂ released through cooling sock
- 10 second flush of CO₂ released through cooling sock

Non-cooled limb control limb collected

Porcine limb test 6:

- 0-9 minutes:
 - 1 full bottle of CO₂ released through cooling sock with 40ml FLUTEC PP80
 - FLUTEC PP80 phial replenished and CO₂ bottle changed
 - 1 full bottle of CO₂ released through cooling sock with 40ml FLUTEC PP80
 - FLUTEC PP80 phial replenished and CO₂ bottle changed
- 9-18 minutes:
 - 1 full bottle of CO₂ released through cooling sock with 20ml FLUTEC PP80
- 18 minutes:
 - No active cooling applied
 - 1 full bottle of CO₂ released through cooling sock

Transportation –
41.8 ± 7.29 minutes



End of transportation period.

Final CO₂ bottle emptied through sock
 Thermocouples removed

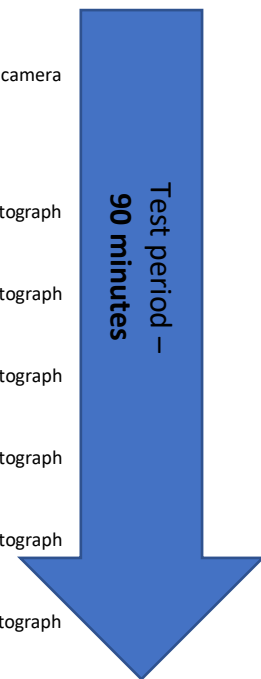
Perfused limbs (n=6)

- 0 minutes:
 - Limb cannulated
 - Baseline LDI scan and thermal camera image obtained
 - Circuit primed
 - Perfusion begins
- 15 minutes:
 - LDI Scan and thermal camera photograph obtained
- 30 minutes:
 - LDI Scan and thermal camera photograph obtained
- 45 minutes:
 - LDI Scan and thermal camera photograph obtained
- 60 minutes:
 - LDI Scan and thermal camera photograph obtained
- 75 minutes:
 - LDI Scan and thermal camera photograph obtained
- 90 minutes:
 - LDI Scan and thermal camera photograph obtained

Non-Perfused limbs

- Limb left on the side in the laboratory

Test period –
90 minutes



90 minutes: End of test.

End of test nerve stimulation performed

Figure 6-4: Flow chart of the protocol for porcine limb tests

Table 6-1: Summary of porcine limbs collected and the conditions they were kept under

Test number	Number of limbs collected	Conditions limbs held under
Test 1	2	Cooled, perfused Non-cooled, non-perfused
Test 2	2	Cooled, perfused Non-cooled, non-perfused
Test 3	2	Cooled, perfused Non-cooled, non-perfused
Test 4	1	Cooled, perfused
Test 5	1	Cooled, perfused
Test 6	1	Cooled, perfused

6.2. Justification of methods of analysis:

Similar to the small-scale tissue testing describe in Chapter 5, porcine tissue was used due to the parallels of tissue structure to human tissues. During the first 3 tests an un-cooled, un-perfused limb was also collected. This was done to determine that the technology and interventions were solely responsible for sustaining viability with regards to muscle nerve activity and gives an indication for the potential of salvage. The control limb demonstrates that the limb salvage is not possible without interventions and supports the need and efficacy for this treatment. Due to the fact the control limbs were kept in exactly the same environmental conditions as the cooled and perfused limbs it is highly likely that any differences in the response were due to the intervention applied.

The temperature of the limb tissue was recorded in the deep tissue to provide an insight into how the novel cooling technique was able to reduce the core temperature in the limb and that the mechanism of action occurs beyond the superficial tissue. As mentioned previously, the muscle is the tissue most sensitive to warm ischaemic damage. Being able to rapidly reduce the temperature in the deep tissue is vital in prevention ischaemic necrosis of the muscles. A thermocouple was inserted into the superficial tissue to ensure that the temperatures produced here are not so low that the tissue is at risk of cold burns or other cold complications. The thermocouple was not placed on the surface to stop it being directly exposed to the gas allowing it to provide a closer representation of the actual tissue temperature. The thermocouple was placed in the trotter injury to show if the cooling mechanism acted differently when the skin was not intact.

The temperature was only recorded on the journey from the abattoir when the cooling was being applied. This was for a number of reasons. The first was that the limb was now in the equivalent of the hospital. It is likely that the injured soldier would be rushed straight to surgery and thereby put on the LSS. The speed at which the tissue re-warms naturally is therefore unlikely to be necessary to consider. Another factor to consider is that the thermocouples had to be taken out when the limb was being transported to the lab. Trying to put the thermocouples back into the same positions once the limb was in the lab would not be possible so the two temperature data sets could not be compared anyway. Furthermore, the porcine limbs had small arteries which were difficult to cannulate. It was decided that the thermocouples should not be replaced to allow for quicker cannulation and thus faster commencement of perfusion.

Due to the limbs being freshly harvested the starting temperature of the deep tissue was not consistent ranging from 23.87°C – 35.0°C with a mean of 28.84±3.73°C. The deep tissue temperature at the end of cooling ranged between 12.21°C – 22.45°C, the mean was 16.48±3.78°C. Therefore, the temperature change achieved in the deep tissue was -7.26°C – -15.88°C with a mean temperature change of 12.36±3.07°C.

Although the thermocouples were not used during the LSS section of the protocol, the temperature of the limb tissue was still of interest. As perfusion continues the blood vessels in the limb begin to open up again, the tissue will begin to warm-up due to the radiation and conduction of the thermal energy being carried in the warm blood. This change in

temperature of the tissues will show up on the thermal camera images and indicates which tissues are being perfused. Thermal cameras are able to detect temperature by measuring the infrared waves that are radiated by objects (FLIR Systems). The processor in the thermal camera converts the signals from the thermal sensor into false colours which are then displayed as an image (FLIR Systems). The thermal camera is a non-invasive method of testing the superficial temperature change of the tissues and it provides data which can be compared at a later date. The thermal camera data will also show if the tissue warms up evenly and can provide evidence of the quality of tissue perfusion.

Another method used to measure perfusion was the LDI scans. LDI works by projecting a laser onto the skin surface. Some of this light will penetrate down through the skin to the tissue beneath. The wavelength of any light reflected from static cells remains unchanged. However, when moving cells are encountered, typically red blood cells, the wavelength of the returning light is altered slightly by the doppler effect. The size of the wavelength change is determined by the concentration and velocity of the red blood cells. The change in wavelength produces a signal for each location that is measured (Murray, Herrick and King, 2004, Wardell, Jakobsson and Nilsson, 1993). When combined all these signals are used to create a colour image of the scanned area. The LDI scan provides a better picture of perfusion as the presence of blood flow is numerically (all be it with arbitrary perfusion units) depicted rather than making assumptions on the temperature of the tissue.

When looking at the pre-perfusion LDI images naturally occurring movement of blood cells can be seen. This is due to random Brownian motion of macromolecules in the interstitial

space which is known as the biological zero (Millet *et al.*, 2011, Cracowski *et al.*, 2006). To see the increase in perfusion from the biological zero the pre-perfusion scan is subtracted from the scan at each time point. Regions of interest (ROIs) were retrospectively highlighted. The first ROI was always the whole perfusion area to obtain an idea of the total superficial perfusion change during the test. The other ROIs were selected to cover both areas with obvious increases of perfusion and areas with very little visible perfusion increase to compare the difference.

The final test done in the protocol is the use of neural stimulation. This test is being carried out to ascertain whether the limb muscle is viable. If the muscle fibres contract on stimulation then the muscle tissue may be considered viable. Conversely, if there is no response upon stimulation then it is safe to assume that the muscle tissue is not viable. Therefore, presence of contraction in the muscle suggests that the muscle tissue is still viable. In the context of the present study the magnitude of the muscle twitch was only evaluated visually and the individual tests could only be compared using video evidence and individual judgement. Whilst this test is not able to provide any quantifiable data it does provide an indication on whether or not the limb tissue is still viable which is why it is being used in this assessment protocol.

6.3. Results:

6.3.1. Temperature changes:

Table 6-2 shows that the temperature change at each tissue depth over each of the 6 tests varied dramatically with the temperature change in the deep tissue ranging from -7.26°C to -15.88°C . The table also shows that generally the temperature in the superficial tissue did not decrease by the same amount as the temperature in the deep tissue. The exception to this is Test 4 where the superficial tissue showed a greater temperature decrease. The journey time for the first 5 tests ranged from 33-49 minutes but due to the testing protocol for these tests requiring a new bottle of CO_2 every 4 flushes and the final partially emptied CO_2 bottle to be released upon arrival at the university this only leads to fewer CO_2 bottles used in one test. The protocol for test 6 also required the release of 4 bottles of gas through the cooling sock.

Table 6-2: Temperature change in porcine limbs over the duration of the total journey time from collection to the university

Test number	Starting temperature (°C)			End temperature (°C)			Temperature change over duration of total length of journey from collection to university (°C)			Journey time (minutes)	Number of CO ₂ bottles used			
	Superficial Tissue	Deep Tissue	Trotter injury	Superficial Tissue	Deep Tissue	Trotter injury	Superficial Tissue	Deep Tissue	Trotter injury					
Test 1	25.22	27.48	25.91	14.24	14.34	13.67	13.13	8.76	-10.88	-13.81	-12.78	-5.48	47	4
Test 2	31.20	35.00		25.42	16.83	19.95		6.77	-14.37	-15.05		-18.65	49	4
Test 3	16.45	28.09		-2.09	3.91	12.21		-10.16	-12.54	-15.88		-8.07	45	4
Test 4	29.48	29.65		26.74	4.45	17.34		-30.01	-25.03	-12.31		-56.75	35	4
Test 5	28.07	31.88		22.45	23.90	22.45		11.15	-4.17	-9.43		-11.30	33	3
Test 6	21.14	23.87		15.11	16.01	16.61		8.99	-5.13	-7.26		-6.12	30	4

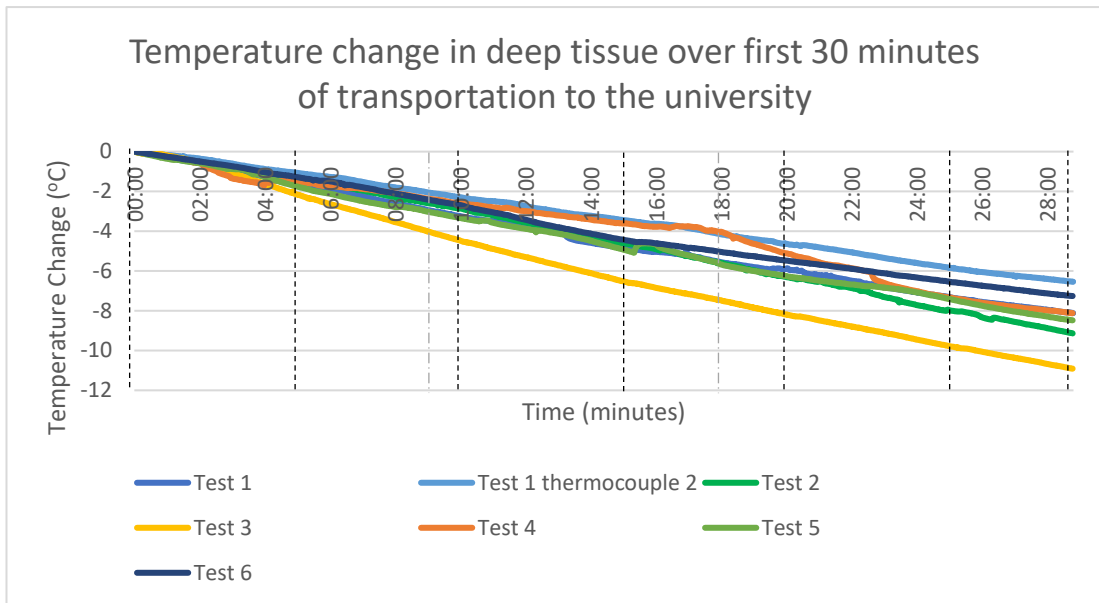


Figure 6-5: Temperature change in the deep tissue for the first 30 minutes of transportation for the 6 isolated porcine limb tests

From the graph in Figure 6-5 it can be seen that at 30 minutes there was less variation in the temperature change in each of the 6 tests with only 4.36°C between the warmest and coldest values. Test 3 cooled at a much faster rate than the other 5 tests. On the other hand, test 6 cooled at a similar rate despite the change in cooling protocol. The black dotted line shows the timing of the CO₂ release during tests 1-5. The grey dashed line shows the 3 different stages of cooling in the protocol of Test 6.

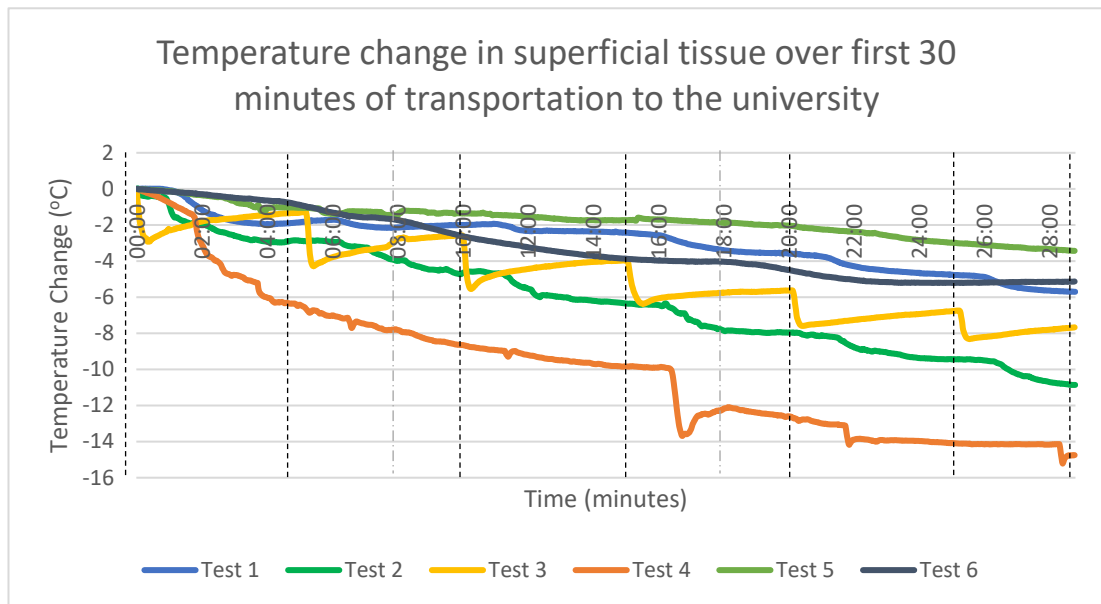


Figure 6-6: Temperature change in the superficial tissue for first 30 minutes of transportation in the 6 isolated porcine limb tests

There was a much greater variation (11.31°C) in the temperature of the superficial tissue after 30 minutes as seen in Figure 6-6. The line for Test 3 clearly shows drops in the temperature which coincide with the gas release. These drops can also be seen to an extent in the temperature graph for tests 2. Conversely, the lines for tests 1, 5 and 6 had a much smoother profile. Again, the black dotted line shows the timing of the CO₂ release during tests 1-5 whilst the grey dashed line shows the 3 different stages of cooling in the protocol of Test 6. The line for test 6 shows that tissue temperature started increasing by the end of the second active cooling period (start of the second active cooling period is indicated by the second grey dashed line).

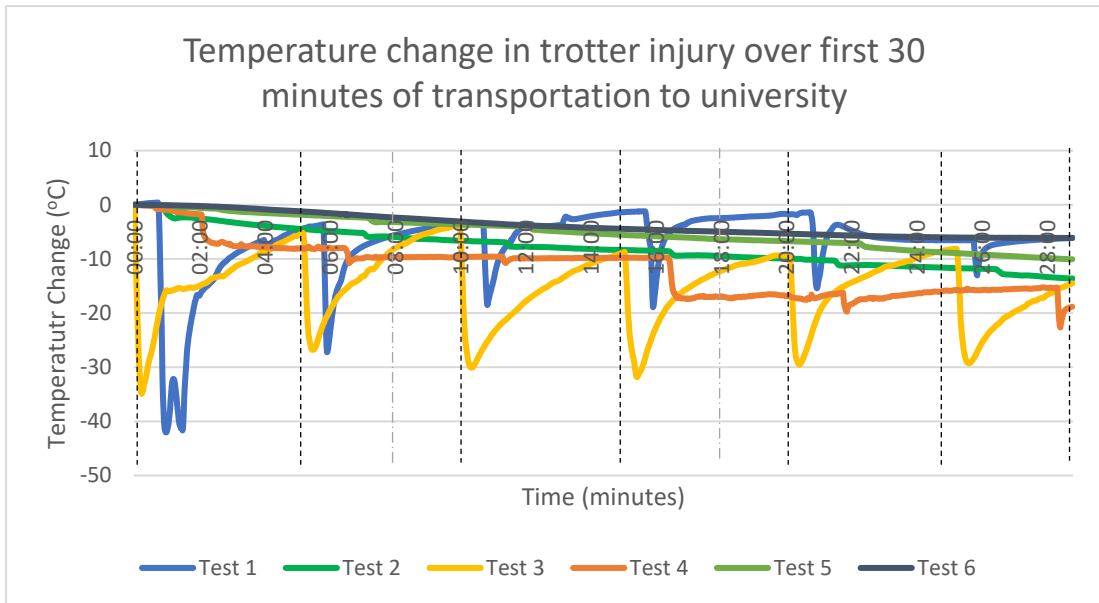


Figure 6-7: Temperature in the trotter injury for the first 30 minutes of transportation for the 6 isolated porcine limb tests

Figure 6-7 shows extreme differences in the temperature recorded in the trotter injury. The temperature profiles for tests 1 and 3 show huge drop in temperature coinciding with when the gas was released with drops of up to 42°C. Tests 2, 5 and 6 show a much more gradual decrease in temperature. Interestingly, although test 1 had massive temperature variation over the course of the 30 minutes, it had one of the smallest temperature changes after 30 minutes of the 6 tests, equalled only by the result for test 6 itself. The black dotted line shows the timing of the CO₂ release during tests 1-5. The grey dashed line shows the 3 different stages of cooling in the protocol of Test 6.

6.3.2. LDI and thermal camera images:

All the following LDI scan images have the pre-perfusion image subtracted from them to show the increase in perfusion from the biological zero. The exception to this is the pre-perfusion image which is provided as a visual reference. The ROIs were retrospectively selected and placed on all subsequent LDI images from that experiment to allow for analysis of change in perfusion in these areas.

The main analysis of the thermal camera data was to visually compare the images and to see how they changed as perfusion progressed. Spot measurement points were used to measure the temperature on the thermal camera images. Spot point measurements were part of the FLIR software and show the temperature at that specific location at that point in time. They were used to give an indication of the temperature change in the superficial tissue of the limb at each time point. The position of these spot points cannot be directly copied from one image to another but every effort was made to put them in the same spot. The temperatures from the spot points were also placed on a graph showing the temperature change.

6.3.1.1. Porcine limb Test 4:

Figure 6-9 shows there was a mean increase in perfusion over time throughout the limb with a percentage increase in ROI 1 (the whole perfusion area) of 38.7%. This increase in perfusion could particularly be seen in the two smaller highlighted sections, ROIs 2 and 3 (155.27% and 230.4% increase respectively). The graph in Figure 6-8 shows that the mean Flux increased in each of the highlighted regions of interest (ROIs) which are labelled in Figure 6-9

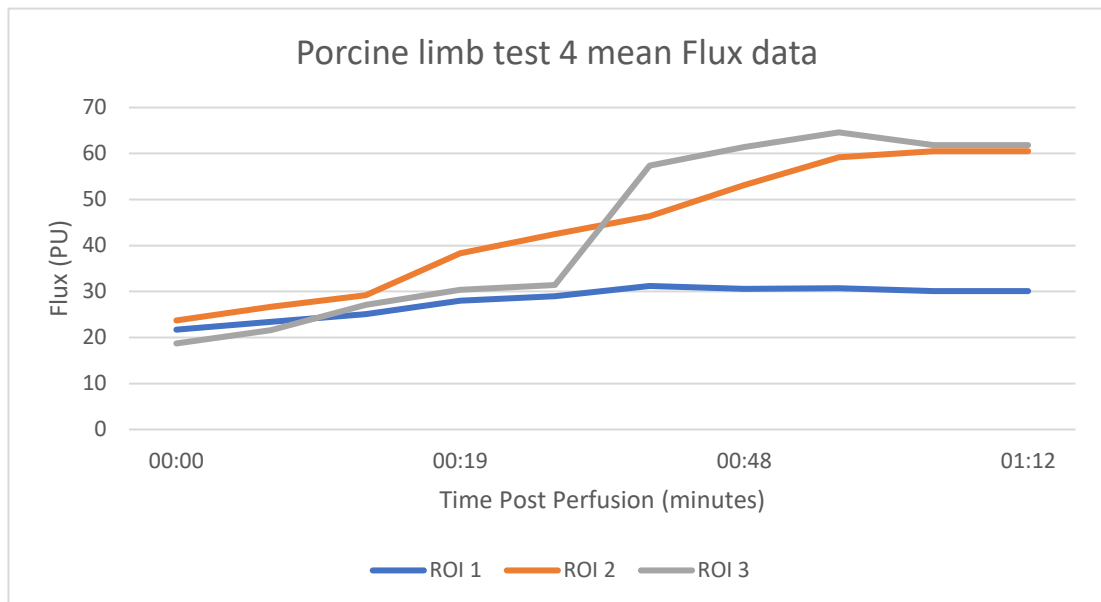


Figure 6-8: Change in mean flux in each ROI for porcine limb test 4

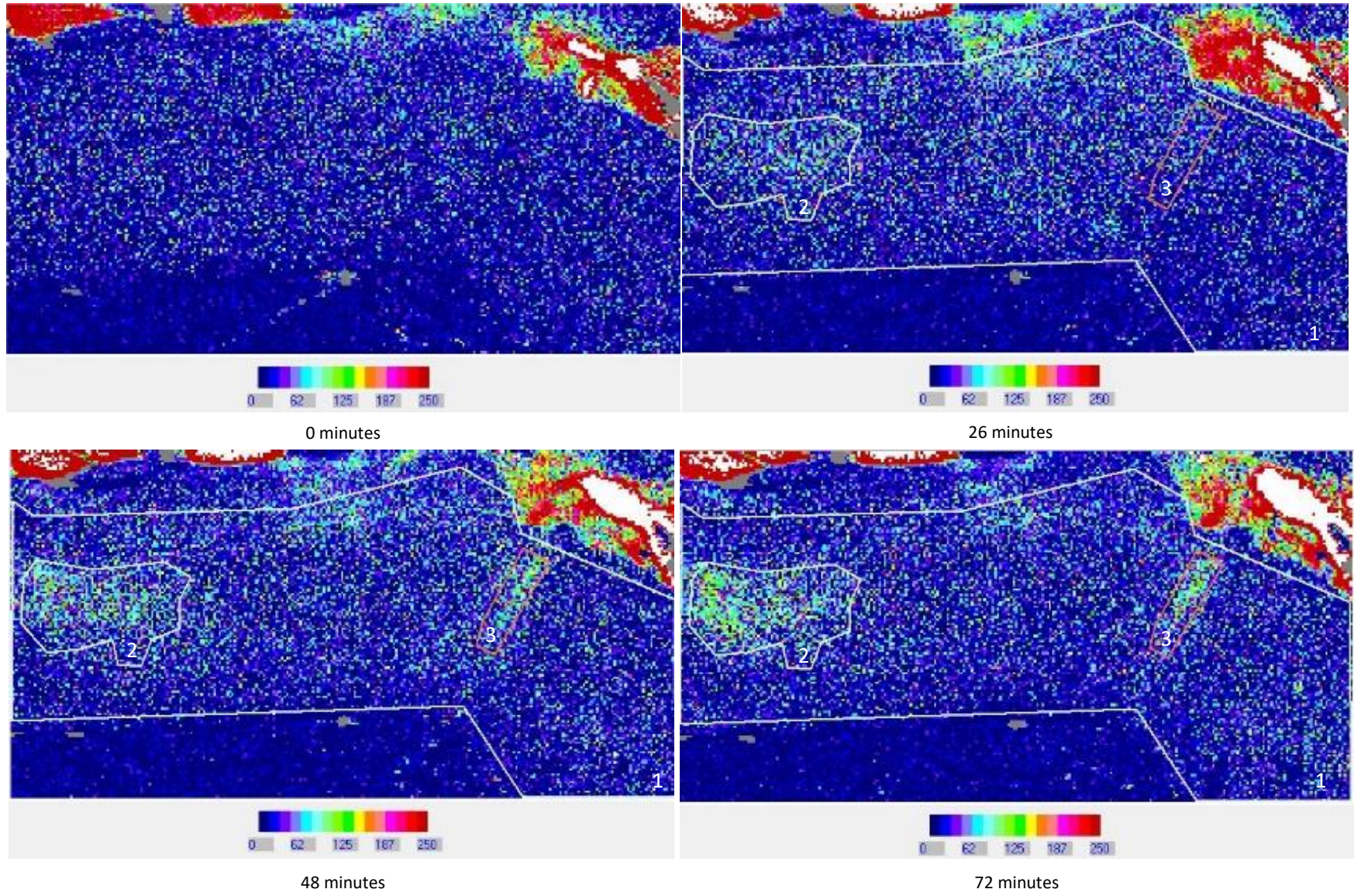


Figure 6-9: LDI images from porcine limb test 4

6.3.1.2. Porcine limb Test 5:

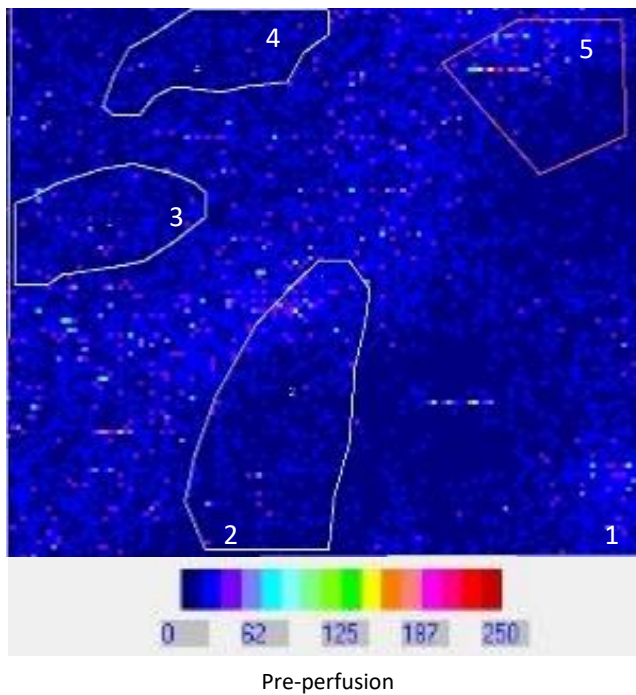


Figure 6-10: Pre-perfusion LDI scan for porcine limb test 5

From the images in Figure 6-11 it can be seen that in some areas there were large increases in perfusion which then faded away as the perfusion times continue. One example of this is ROI 2, at 15 minutes there was a large increase in surface perfusion in the ROI but by 69 minutes it had mostly disappeared before it started increasing again at 103 minutes. This may be due to an initial blockage in the capillary bed causing a blood build up before it could drain away when the blockage cleared.

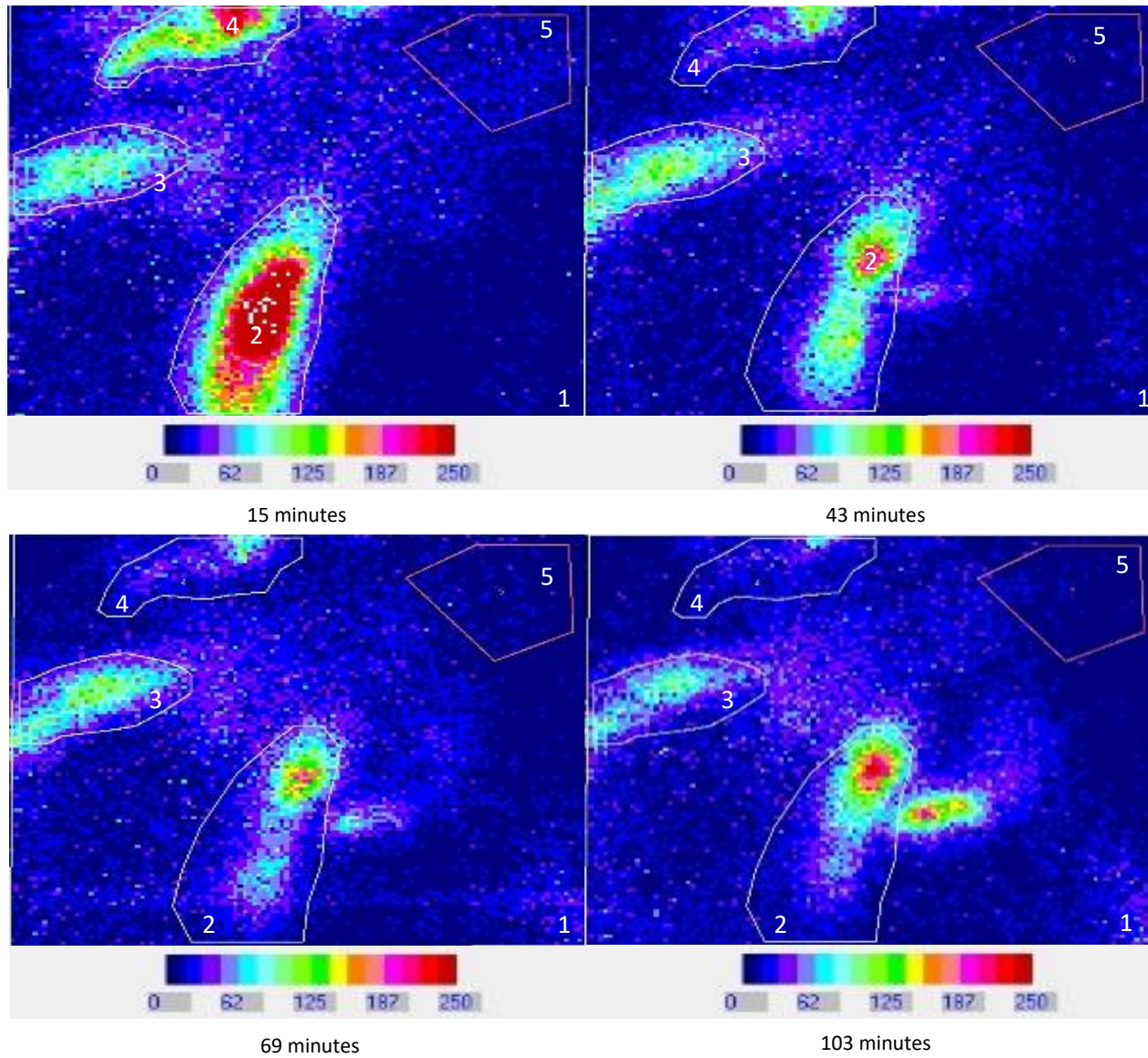


Figure 6-11: Figure showing LDI scans for porcine limb test 5

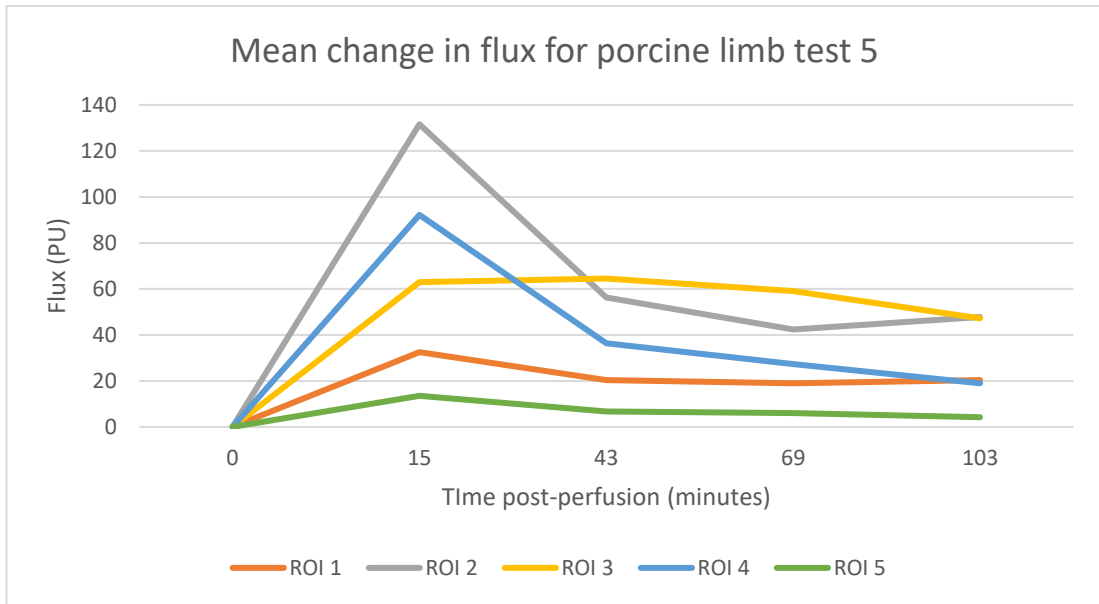


Figure 6-12: Mean change in Flux in each ROI for porcine limb test 5

The graph in Figure 6-12 shows a large increase in Flux for ROI 2 and ROI 4 which then decreased as perfusion continued. ROI 1 shows that there was a slight decrease in Flux after 15 minutes in the whole sample area. ROI 1 also encompasses all the other ROIs, therefore, the Flux will be influenced by the increase in perfusion seen in ROIs 2 and 4. However, ROI 5 does also show a very small decrease in Flux from 15 minutes. ROI 5 is an isolated section of the scanning area so it can be assumed that there was an overall decrease in Flux in the superficial tissue. This may be due to the capillaries opening up and allowing the blood to pass into further sections of the capillary bed which were out with the scanning area. Conversely, the LDI scanner only shows the superficial perfusion, the blood may also have been draining from the capillary bed into the deeper tissues of the limb thereby giving rise to a perceived decrease in perfusion.

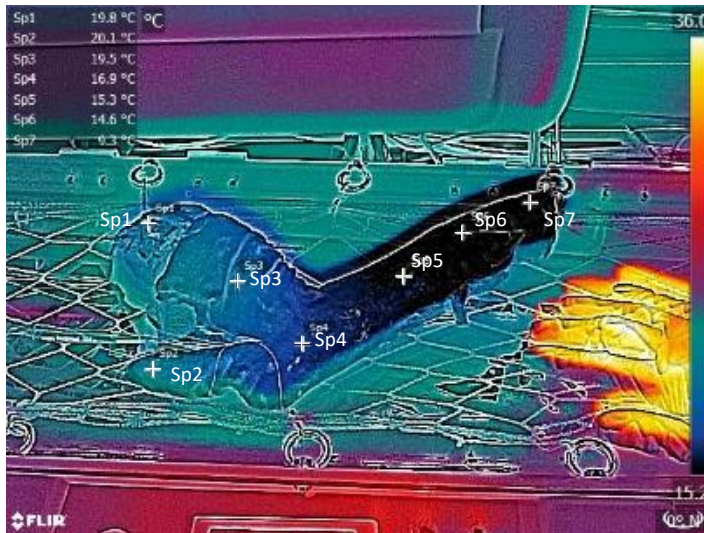


Figure 6-13: Pre-perfusion thermal camera photograph for porcine limb Test 5

The 7 spot points in the thermal camera images in Figure 6-13 and Figure 6-14 are labelled from 1 on the left to 7 on the right and are depicted by the white crosses. The scale reads from 15.2°C – 36.0°C. Figure 6-13 shows that the distal section of the limb was cooler than the other leg tissue in the pre-perfusion image. Once perfusion began the resumption of blood flow could clearly be seen as shown at all time points in Figure 6-14. This was depicted by the gradual increase in warm tissue (depicted by yellow colour), initially spreading up the leg from the cannulation point before then progressing towards the toes. At 103 minutes post perfusion most of the leg was warm with the exception of the toes.

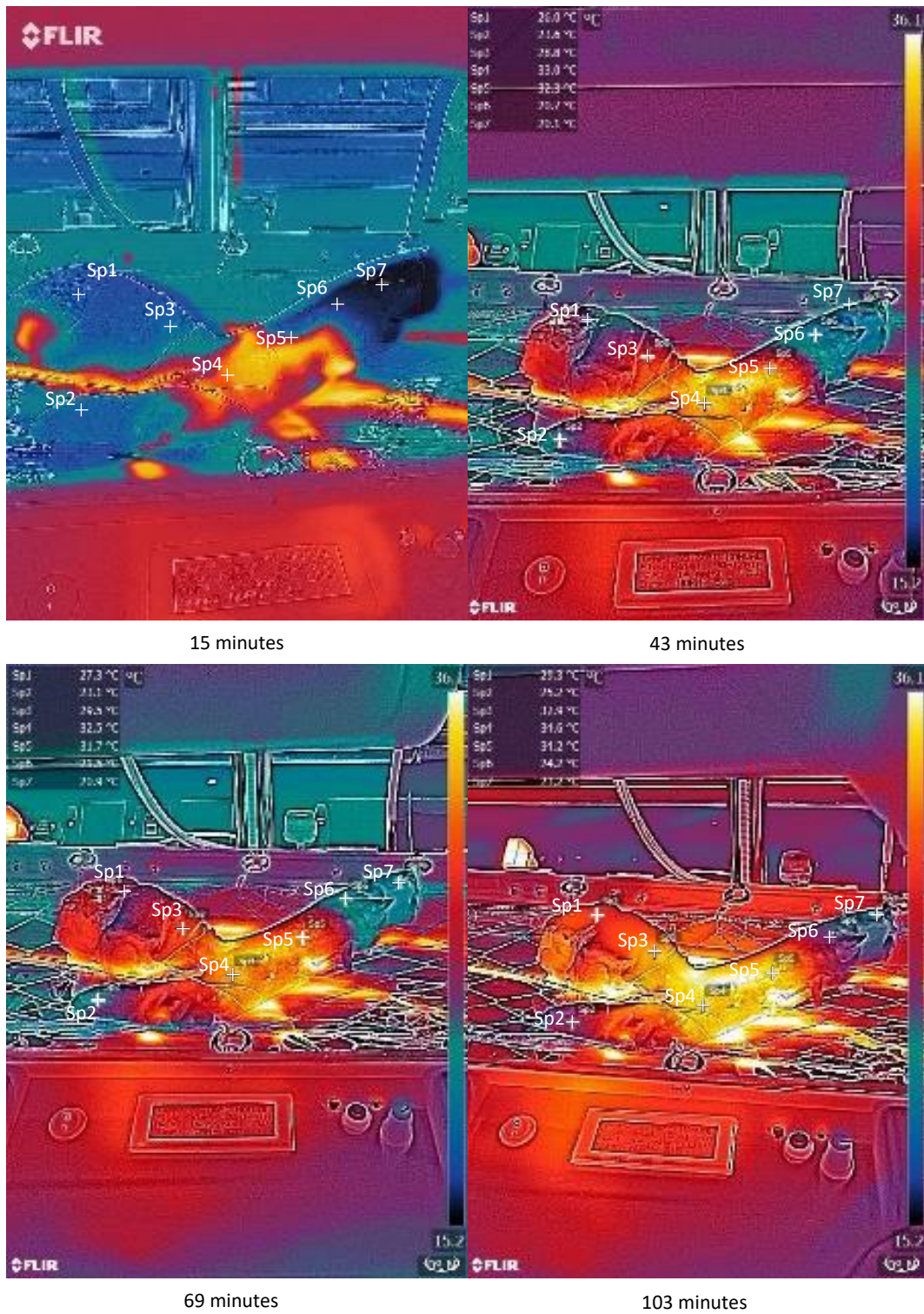


Figure 6-14: Thermal camera images for porcine limb Test 5

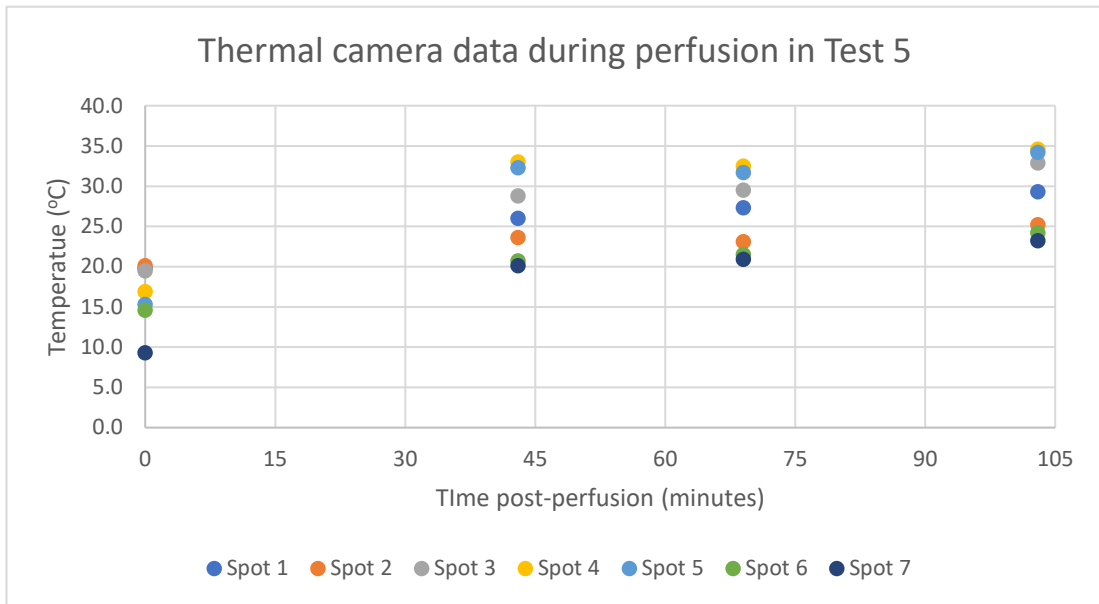


Figure 6-15: Thermal camera spot data for the fifth porcine limb test

Figure 6-15 shows a gradual increase in temperature of the tissue from 43 minutes onwards. The graph shows that regional points 2, 6 and 7 were lower than the others. These points were located below the injury (spots 6 and 7) and on the flap below the cannulation point and are labelled on Figure 6-13.

6.3.1.3. Porcine limb Test 6:

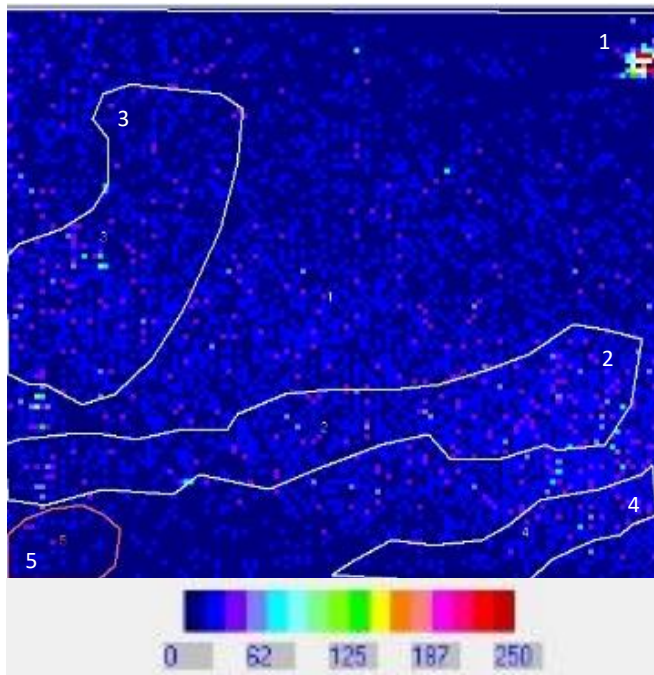


Figure 6-16: Porcine limb Test 6 pre-perfusion LDI scan.

The ROI positions were retrospectively chosen. ROI encompasses the entire scan area. ROIs 2, 3 and 4 were chosen as they show likely positions of blood vessels. ROI 5 is drawn around an area of interest where perfusion was seen at the beginning and then faded away. The LDI scans in Figure 6-18 clearly show the opening up of blood vessels in response to perfusion compared to the LDI scan seen in Figure 6-16. A 274% increase in blood flow was seen in ROI 1 depicted by the background transitioning from dark blue to lighter blue. Bright coloured patches appeared on the left-hand side of the scans at 30 and 45 minutes which had then pretty much faded away by 60 minutes. ROI 5 highlights one of these areas and this change in flux is also depicted in the graph in Figure 6-17. A patch of increased perfusion could again be seen in the gap between ROI 2 and ROI 3 at 75 minutes which had then faded away by 90 minutes. The reason for this is unknown but similarly to the bright spots seen in the LDI

images in porcine limb test 5 it was likely to be due to blockages in the capillary system causing a superficial build-up of blood which then cleared as the blockages were dislodged.

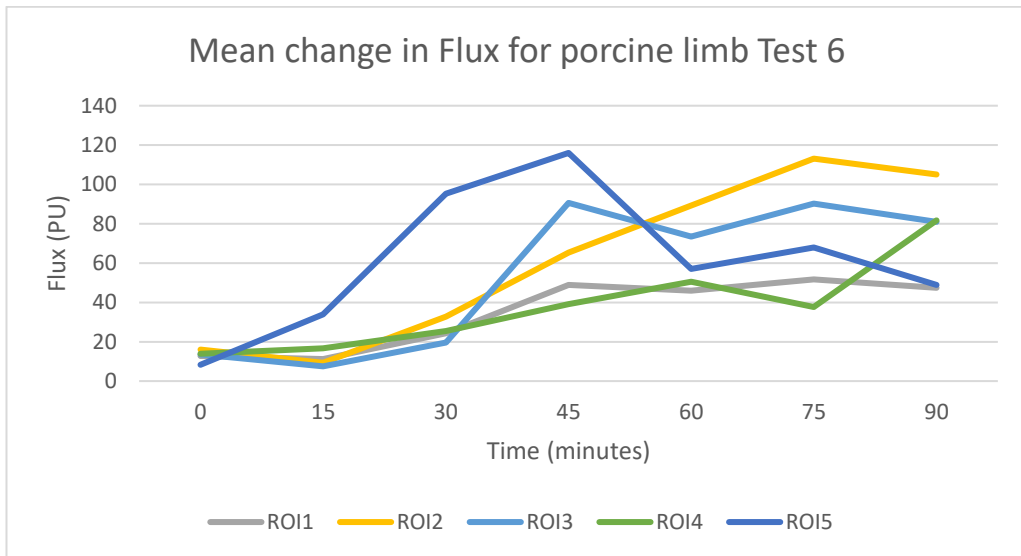


Figure 6-17: Mean change in Flux for porcine limb Test 6

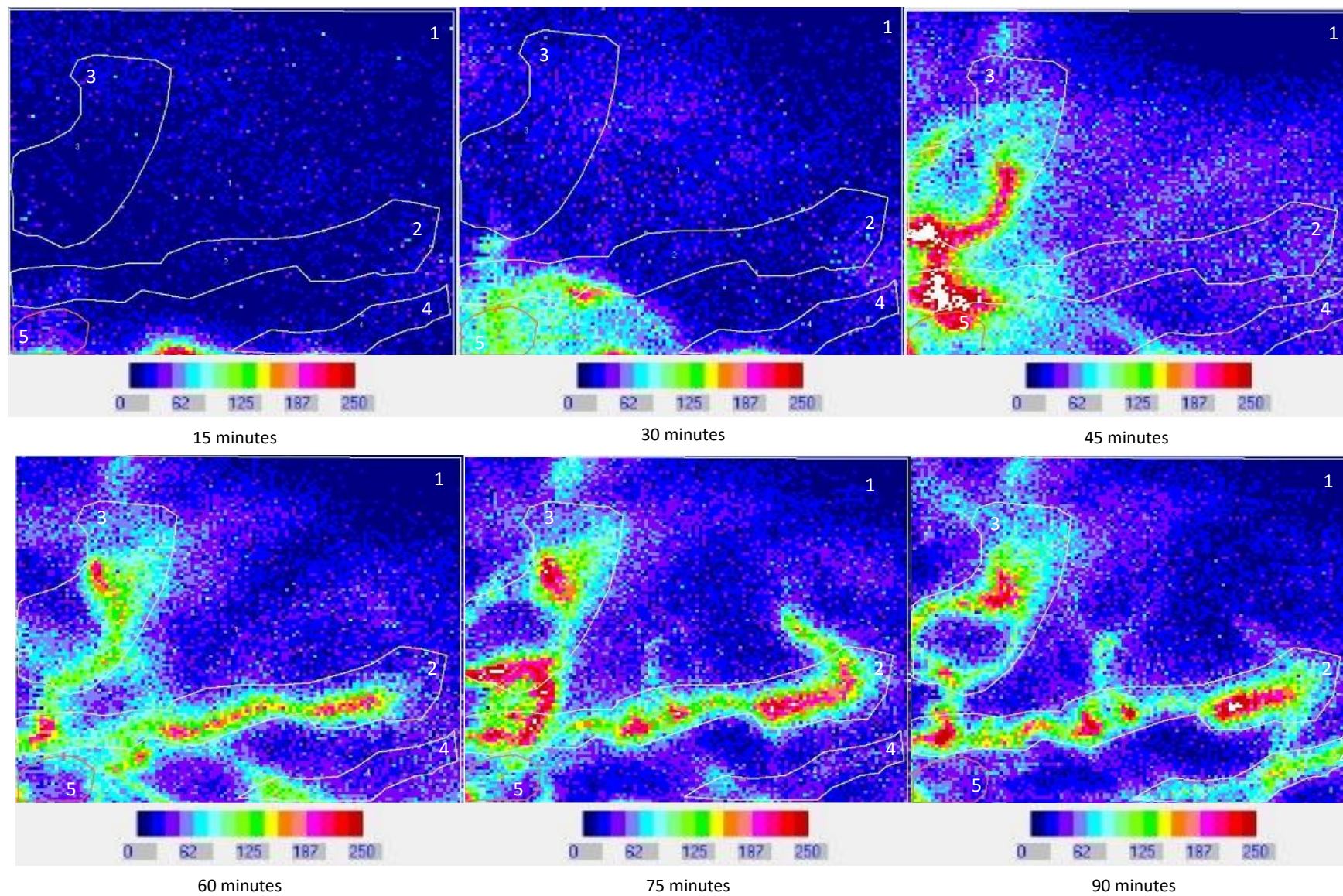


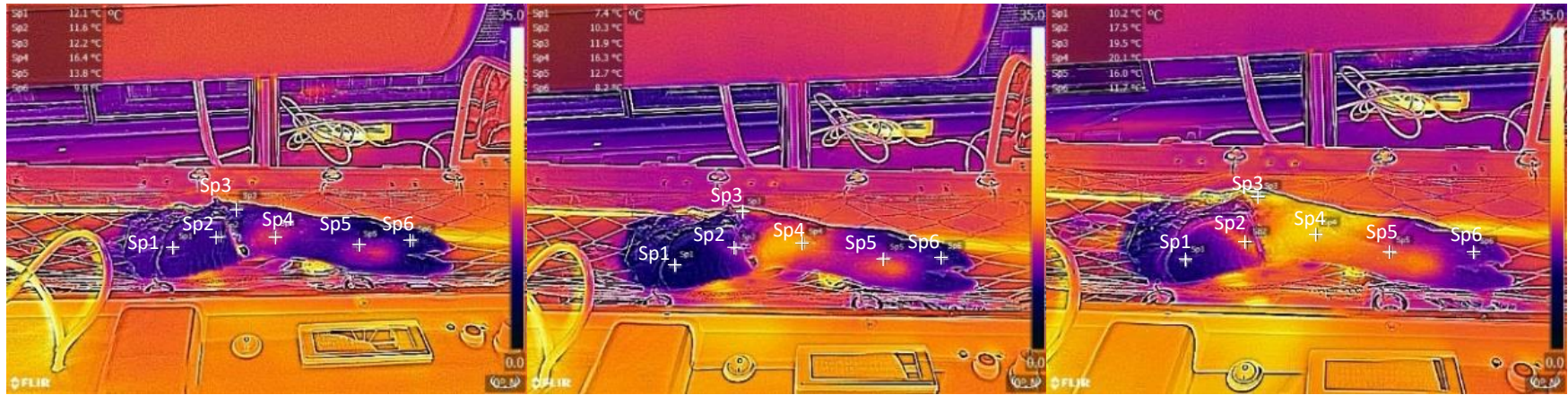
Figure 6-18: LDI images for porcine limb test 6

Figure 6-19 shows the thermal photograph taken prior to perfusion commencing.



Figure 6-19: Pre-perfusion thermal photograph for porcine limb Test 6

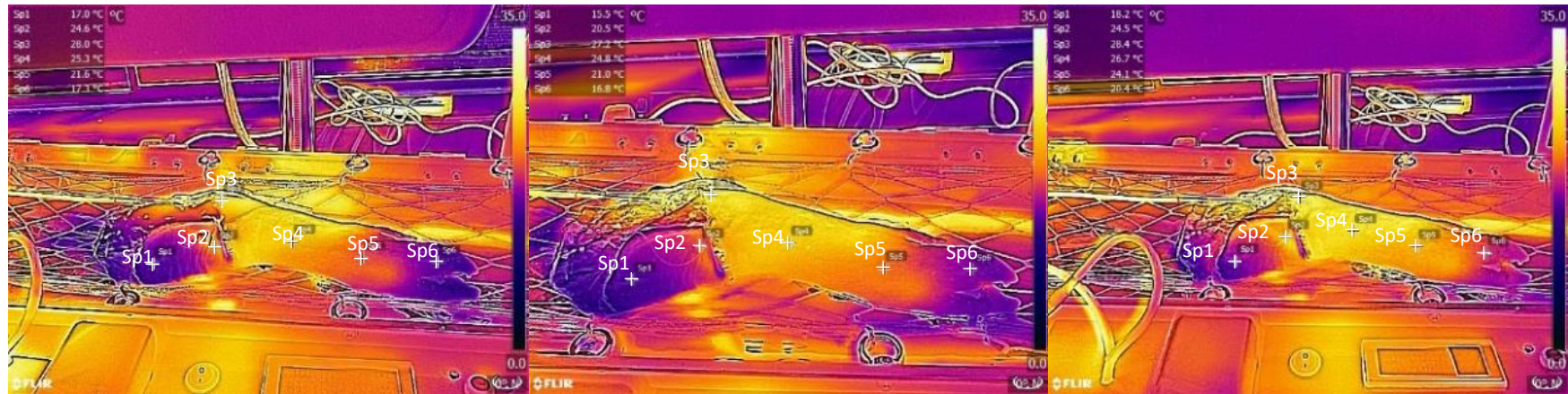
The dark colours in this Figure 6-19 show the low temperatures of the tissue surface. It shows that the toes were colder than the thicker muscle tissue above the knuckle. The warmer yellow stripe seen to the right of Sp2 (just under the Sp2 label) was the metal clip used to retract the superficial tissue. Figure 6-20 shows thermal photographs taken at equal intervals during perfusion. These photos show the heat gradually returned to the tissue. The warmth started to reach the toes by 75 minutes. The photographs at 15- and 30-minutes show bright spots developing on the leg surface before the rest of the tissue was perfused. This is likely to be due to sections of more vascularised superficial tissue warming faster due to increased blood flow. The scale in both Figure 6-19 and Figure 6-20 is from 0.0°C – 35.0°C.



15 minutes

30 minutes

45 minutes



60 minutes

75 minutes

90 minutes

Figure 6-20: Thermal camera images during perfusion for porcine limb Test 6

The graph in Figure 6-21 shows the temperature at each spot point over the perfusion time. This graph shows an increase in temperature in the tissue as could be seen in the thermal photographs. Spot 1 and 6 were at a lower temperature at all time points which corresponds to the darker colours on the photographs.

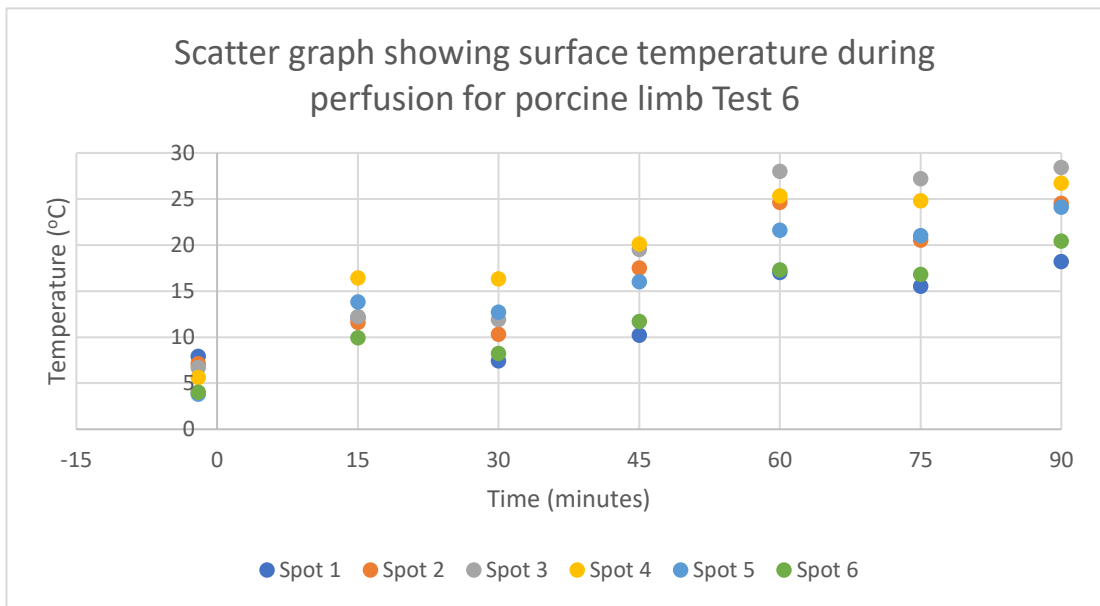


Figure 6-21: Thermal camera temperature data for porcine limb Test 6

6.3.2. Neural Stimulation:

Table 6-3: Porcine limb test conditions and the outcome of neural stimulation

Test number	Conditions limb kept in	Nerve stimulation achieved?
Test 1	Cooled, perfused	50mA 1 ms
	Non-cooled, non-perfused	No twitch achieved
Test 2	Cooled, perfused	50mA 1ms
	Non-cooled, non-perfused	No twitch achieved
Test 3	Cooled, perfused	No twitch achieved
	Non-cooled, non-perfused	No stimulation attempted
Test 4	Cooled, perfused	70mA 1ms
Test 5	Cooled, perfused	No stimulation attempted
Test 6	Cooled, perfused	No stimulation attempted

The neural stimulation intended to activate the peroneal nerve and promote a twitch in the extensor digitorum brevis creating movement in the toe. The data in Table 6-3 shows that stimulation was not evident in the tissue that was not cooled or perfused once in the lab. Twitch in the cooled and perfused leg in Test 3 could not be achieved at any amplitude. The most likely reason for this is that the limb took a very long time to cannulate (194 minutes between collection and perfusion commencing). The cannula was then dislodged again on two occasions and perfusion was halted a total of 51 minutes. Although 2 full bottles of CO₂

were used to cool the limb during the initial cannulation period it is highly likely that the tissue was under ischaemic conditions for too long and consequently the muscle tissue was no longer viable.

6.4. Results analysis:

6.4.1. Temperature changes:

The temperature changes in all of the tissue depths over the first 30 minutes of each test showed that the tissue can be cooled using both CO₂ and a combination of CO₂ and coolant. Although the temperature change in the deep tissue was less than 10°C, cooling the tissue down by 6-10°C would likely reduce the metabolism in the tissues by 30-50%. As the graph in Figure 6-5 shows the temperature decrease in the deep tissue during the first 30 minutes of each test was roughly similar for the 6 tests except for test 3. This relatively steady temperature decrease suggests that using CO₂ cooled the tissue in a consistent manner.

However, there were a few external factors which could alter how the tissue cools. During test 3 the external air temperature was around -5°C (data not shown), this would have created an additional cooling effect for the limb tissue which couldn't be controlled. This additional cooling factor may account for the bigger temperature decrease which was seen in the deep tissue in Figure 6-5. However, as stated previously, it took 194 minutes for perfusion to begin in this test and perfusion was paused for a total of 51 minutes so the ischaemic conditions meant it was very unlikely that the muscle tissue was viable. This meant that the effect of the efficient cooling could not be examined.

At 30 minutes in Test 1-5 only 3 bottles of CO₂ had been released compared to the 4 released in test 6. This suggests that the addition of the PP80 coolant to the protocol may have

reduced the effectiveness of the CO₂. The CO₂ was released at a slower rate during Test 6, thereby the energy taken in during gas expansion was decreased which in theory would result in a reduced temperature decrease. Conversely, in Test 6 the tissue did carry on cooling when the first active cooling period was over (the end of the first active period of cooling is marked by the first dark grey dotted line in Figure 6-5). This suggests that evaporation of the PP80 cooling fluid enables the continued cooling the deep tissue over the passive cooling period. If the tissue does continue cooling when the gas flow stops this would mean that potentially less gas could be used to cool each time. Conversely, there could be a danger that the tissue cooling will continue unchecked during patient transfer which could lead to unintended consequences such as cold injury.

As Figure 6-6 shows there was a variation in how the superficial tissue temperature changed over the 30 minutes. The thermocouple in test 3 was evidently close to the end of a CO₂ tube and so the timing of the release of CO₂ (indicated by the black dotted line) corresponds with temperature drops on the graph. The release cycles of CO₂ could not be seen so clearly during the other tests. The reasons for this are either that the thermocouple was not so near the end of a CO₂ tube or the thermocouple was pointed into the tissue rather than towards the outside of the limb, or a combination of the two. The rate of cooling over 30 minutes during each of the 6 tests was not consistent with decreases in temperature varying between 4-12°C. It is evidenced by this that the proximity of the tissue to the CO₂ tube is likely to alter the rate of cooling. None of the temperatures recorded at the superficial tissue thermocouples are low enough to suggest that tissue damage will occur meaning it is unlikely that the device will have a detrimental effect on the casualty.

On the other hand, when looking at Figure 6-7 it can be seen that some of the thermocouples in the trotter injury recorded temperature changes as much as -40°C . If the tissue starts off at 37°C then the temperature would decrease to -3°C , if this temperature is prolonged then it could cause tissue damage. This potential should be examined in further studies. When the cooling sock was opened after tests 1 and 3 it was observed that the end of one of the CO_2 tubes was adjacent to the injury in the trotter. It is possible that a build-up of dry ice crystals in the injury due to the release of the gas was responsible for the large drops in temperature seen in these tests. Interestingly, Table 6-2 shows that tests 1 and 3 also showed a smaller total decrease in temperature in the trotter compared to the deep tissue. The reason for this was not clear but could be due to the exposure of the thermocouple to the air so although it cooled down much faster when the gas was released it also re-warmed faster when the gas stopped flowing. In the other 4 tests, the thermocouple in the trotter demonstrated a greater decrease in temperature than the thermocouple in the deep tissue. Considering the lack of tissue around the trotter it makes sense that the limb temperature was able to decrease at a faster rate here. Furthermore, the gas was able to enter the injury so the trotter was cooled from both the inside and outside meaning a faster rate of temperature decrease.

Looking at the data in Table 6-2 it can be seen that, other than test 4, the deep tissue had a larger decrease in temperature than the superficial tissue over the total journey time. The most likely explanation for this is that the heat in the deeper tissue passed up to the superficial tissue via conduction where it could be lost to the environment. Test 4 showed a total temperature decrease of -25.03°C in the superficial tissue. This temperature decrease was almost double the temperature change seen in any of the other 5 tests. The reason for this was not clear, no incident happened during the cooling period that would suggest that

the temperature of the superficial tissue should drop by this much. Considering the fact that the deep tissue did not also show a much greater temperature decrease it is likely that the reason for the excessive temperature change is that a thermocouple became exposed to the CO₂ stream, probably due to being dislodged from the tissue. The thermocouple could have also been pushed through the insulating fat due to movement of the cooling sock.

During the porcine tissue tests the thermocouples were only pushed into the open tissue at the top of the limb. Thereby the thermocouple was not at a depth any greater than 1cm into the top of the tissue. This had two problems. The first is that, as mentioned previously, the thermocouples could easily have become dislodged in response to small readjustments of the limb/ cooling sock. This meant that in some cases complete data sets could not be recorded. Furthermore, there was an issue with the tissue that the temperature was being sampled from. The top of the limb was exposed to the environment so heat loss by radiation was affected by the outside temperature. This meant that the end of the limb where the thermocouples were placed was exposed to a secondary topical cooling mechanism which changed the rate at which the tissue temperature decreased. Additionally, the release of gas into the cooling sock meant that the top of the limb will be cooled at a faster rate than the deep tissue which will be reflected in the temperatures recorded by the thermocouples.

6.4.2. LDI and thermal camera data:

The thermal camera only showed the temperature of the outside of the limb. This meant that the temperature of the deep tissue could not be monitored during perfusion. However, the thermal camera images did show useful information. The thermal camera images seen in Figure 6-13, Figure 6-14, Figure 6-19 and Figure 6-20 show that the leg warmed up over the perfusion time starting off at the point where the cannula entered the limb. The aforementioned figures also show that the toes were much colder than the muscular tissue further up the leg. This could have been due to the fact that there was less muscle tissue below the knuckle so the leg could be cooled more efficiently by the CO₂. In addition, during cannulation a light was shone on the leg to aid the visualisation of the blood vessels. This could have contributed to the warming of the superficial tissue of the upper leg.

The jump in temperature of the toes during both tests after perfusion begins was due to the skin of the limb warming up to room temperature. Due to the fact the thermal camera only showed the superficial temperatures it was not possible to know if this change was reflected in the deeper tissue. The slow return of warmth to the toes could have been in response to a number of reasons. Firstly, it is likely that a lot of warm blood was lost out of the 'injury' as evidenced by the bright spot on the right of the leg below the knuckle in Figure 6-20. However, there is warmer tissue below the site of injury suggesting that some blood was able to get past. The cooling of the tissue would have caused the blood vessels to contract. Due to the cooler initial temperature of the toes, it is possible that the contraction of the blood vessels in response to the low temperatures took longer to reverse resulting in a slower return of blood flow.

The thermal photographs were taken from a slightly different point every time. Therefore, the temperatures could not be directly compared because the markers could not be put in exactly the same position on each picture although every effort was made to put them in as similar position as possible using visual points on the photographs. Therefore, the data points were plotted as a scatter graph not a line graph. This problem could be resolved by fixing the camera in the same point each time and using fixed marker placement on the thermal camera images when they are being taken.

The LDI data provided an insight into the resumption of perfusion into the tissue. A line of increased perfusion clearly showed the blood flow through newly opened blood vessels in Figure 6-9 and Figure 6-11. The presence of blood-filled vessels on the limb surface suggested that the deeper limb tissues were being perfused efficiently. However, the LDI scanner laser was only able to penetrate the surface tissue of the limb. For this reason, it was not possible to draw accurate conclusions about the state of perfusion of the deeper muscle. The LDI images in Figure 6-11 show bright spots appearing on the earlier scans which then faded away over time. This may have been due to damage to one of the blood vessels which led to the build-up of blood and/ or fluid under the skin. As perfusion continued this would have drained away which would account for the bright spot disappearing. As well as the shallow depth of penetration of the tissue, the LDI scanner only had a small scanning area. Therefore, it was only possible to get an indication of the perfusion in a small section of the limb. In light of this, the LDI scanner was positioned over the more muscular part of the limb where the tissue was most vulnerable to ischaemia. Whilst, the LDI scans provided a useful insight into

the limb perfusion, the images were open to interpretation and did not provide a definitive answer to what was going on within the tissue.

6.4.3. Neural Stimulation:

Stimulating the nerves to produce muscle twitch was used as an indicator of muscle viability. The theory behind it is that if the muscle tissue is dead, no twitch will be seen. However, there could be many reasons why no twitch was seen even if the muscle was still viable. The first of these is that the injury in the trotter cut through many of the tendons and nerves which run down the back of the limb. Damage to these nerves and tendons may mean that the muscle was no longer able to contract even if it was still viable. Moreover, if the muscle had been stimulated too many times then the muscle would have no longer been able to contract in response to stimulation as there would have been a shortage of Na^+ , Ca^{2+} and ATP, all of which are vital for contraction. The combination of these two factors would have resulted in a number of false negative outcomes where the muscle tissue was assessed to be non-viable when it wasn't.

Disregarding the physical factors which may have prevented muscle twitch, there were other factors which mean that nerve stimulation could not be used to determine the success of the technology. The most important of these was that the muscle twitch was not quantifiable using the current assessment methods. Although the size of the twitch was videoed and the amplitude of the impulse was recorded, each twitch could not be compared to the previous one. The size of the twitch compared to another could only be assessed using personal

judgement. Each observer would have had a different opinion on the size of the twitch and which one was bigger. The size of the twitch could have been measured if specific points in the muscle were marked and the change in distance between these markers was measured. However, this leads onto the second issue in neural stimulation. The electrodes used for stimulation may have not been placed in the best location to produce the most sizeable twitch. Building on this, even if markers were used to measure the contraction produced during stimulation, it would be difficult to place them in identical positions to enable quantifiable comparison between the size of twitch produced in the muscle. Nevertheless, although not comparable, the presence of twitch does suggest that the muscle tissue was still viable.

When taking into consideration all the data produced in this chapter, there are many positive factors which point to the potential usefulness of the novel technology in the battlefield. It has been shown that using CO₂ in the cooling sock was able to cool the deeper limb tissue, albeit less consistently and at a slower rate that is desired. The thermal camera photographs and LDI scans showed that the limb did re-warm as perfusion increased which indicated that the perfusion system within the LSS was working effectively.

6.5. Future considerations:

6.5.1. Limb cooling:

As these initial tests of the technology in a simulated combat setting move forward, the experiments can be developed to allow for more data to be collected. The first way the tests can be developed is to introduce a set cooling period. Standardising the cooling period will ensure that the tissue is cooled using the same amount of CO₂ over the same time period reducing the number of variables from test to test. Furthermore, for un-cooled limbs a defined cooling period means that any data collected will be at a comparable time. The cooling time that is decided upon should be longer than the journey back to the university to allow time for traffic and other unforeseeable situations.

Test 6 during these porcine limb studies seemed to show that the tissue could continue cooling without the flow of gas when the FLUTEK PP80 coolant was used. If the use of coolant could reduce the amount of CO₂, and thereby gas bottles, needed to cool the limb this would be beneficial for use on the battlefield. For this reason, future studies will include the use of FLUTEK PP80 coolant in combination with gas. The protocol for producing the best rate of cooling using the least amount of CO₂ and FLUTEK PP80 will be found through experimentation before being implemented for the rest of the cooling studies. It is also hoped that the use of coolant will provide a faster rate of deep tissue temperature decrease down to the maximum of 10°C below starting temperature.

6.5.2. Perfusion:

Moreover, the time that the limb is perfused whilst contained in the LSS can be increased. The intention is for this device to be used for up to 100 days. Therefore, 90 minutes of testing will not be able to demonstrate the efficiency of the device for longer periods of time. The perfusion system needs to be run for longer to establish if the limb viability can be maintained by isolated perfusion over extended periods of time. In light of this, a second stage of testing is planned to include longer perfusion times.

Whilst for most tests, the perfusion time will be 2 hours, tests with much longer perfusion times will also be undertaken. Longer perfusion times could be up to 12 hours with LDI scans and thermal photographs taken once an hour after the first 3 hours. This will adequately allow the superficial perfusion to be monitored. Furthermore, probes could be placed into the deeper tissue to enable perfusion and thereby blood flow to be monitored there. Blood gas samples will also be taken for analysis every 15 minutes and monitored to ensure that the limb is adequately perfused and that any issues with the perfusate can quickly be rectified.

6.5.3. Methods of analysis:

As was mentioned in the previous section there are a few things that can be done to improve the quality of the results in future tests. The first of these is to fix the thermal camera in position so the photographs can be directly compared between time points. Additionally, if the photos are taken from the same place then markers can be positioned on the thermal

camera which will be fixed and will show the temperature at that location at each time point. Moreover, the tests used for analysing viability should be the same for each test. Not all the tests in the porcine limb studies used both the thermal camera and LDI scanner. Standardising the testing will allow for better data analysis and more conclusions to be drawn.

None of the methods of analysis used in these studies are able to definitively assess the viability of the muscle tissue. Nor are they able to give an understanding of what is going on inside the limb. To help shed light on the status of the tissue after each study to show if the technology is helping to preserve the muscle, other methods of analysis are needed. For this reason, tissue samples from the deep, mid and superficial tissue will be taken at set time points during each limb test. These tissue samples will then be sent off for histological testing. The data returned from this analysis will provide information about the health of the muscle tissue and will be able to determine if there is unchecked necrosis within the tissue.

6.5.4. Experimental design:

The two controls used in the porcine limb studies do not distinguish which part of the technology does what when preserving tissue viability. To provide more information about how each intervention will affect the tissue viability it is proposed that four different testing conditions should be used in the next series of tests. In addition to the non-cooled non-perfused and cooled perfused tests; non-cooled perfused and cooled non-perfused tests will also be done. The cooled non-perfused tests will show what effect cooling has on the tissue

viability over the transfer time. The non-cooled perfused tests will enable the effect of perfusion on preserving muscle function to be examined. Additionally, the non-cooled perfused tests will show if the technology can still be effective even if the cooling is interrupted/ not feasible on the battlefield. 6 repeats of each test will be undertaken to enable the results to be statistically analysed.

The final proposed change for the second phase of simulated combat setting experiments is to increase the size of the limbs collected so there is more tissue. The current porcine limbs are small and are roughly a similar weight as a human male forearm (1.87kg) (Plagenhoef, Evans and Abdelnour, 1983). The diameter of the top of the porcine limb is also similar to a human forearm/ ankle. The limb collected will need to have more tissue to give an indication of how effective the technology would be on a human lower limb. However, if the porcine limb is amputated higher up there is a very large increase in the size of the limb due to the porcine anatomy. Therefore, it has been decided to change the limb from porcine to ovine for the second phase of testing.

Chapter 7. Testing of technology in simulated combat setting –

Ovine tissue:

As the previous chapter on using porcine limbs showed, using the cooling sock could successfully reduce the temperature in the deep tissue of the limb. Therefore, further experiments were designed to assess the capability of the technology to preserve the tissue over the transportation of the limb from the point of ‘injury’ and during perfusion in the ‘hospital’. These experiments will both examine the cooling capability of the technology and will investigate how the muscle tissue is affected by the experimental process.

7.1. Justification of methods of analysis:

Ovine limbs were used during the following experiments. The main reason for this is that the long bone structure of ovine limbs is more similar to human limbs than the porcine limbs were. Porcine limbs are short and the muscle depth increases very abruptly not too far past the knuckle. On the other hand, ovine limbs have a more tapered shape with a gradual increase in muscle depth as shown in Figure 7-1. Furthermore, the anatomy of the ovine limb means that more of the joints of the limb can remain when the limb is harvested before being placed in the cooling sock. This allows range of motion (ROM) of the limb to be assessed. If the ROM is undertaken at the beginning and end of the experiment then the extent that the limb has stiffened up during the experiment can be seen. The stiffening of the limb would

suggest the ATP is not being replenished to allow for muscle relaxation (Hayman and Oxenham, 2016).

Limb stiffening may also suggest severe tissue oedema.

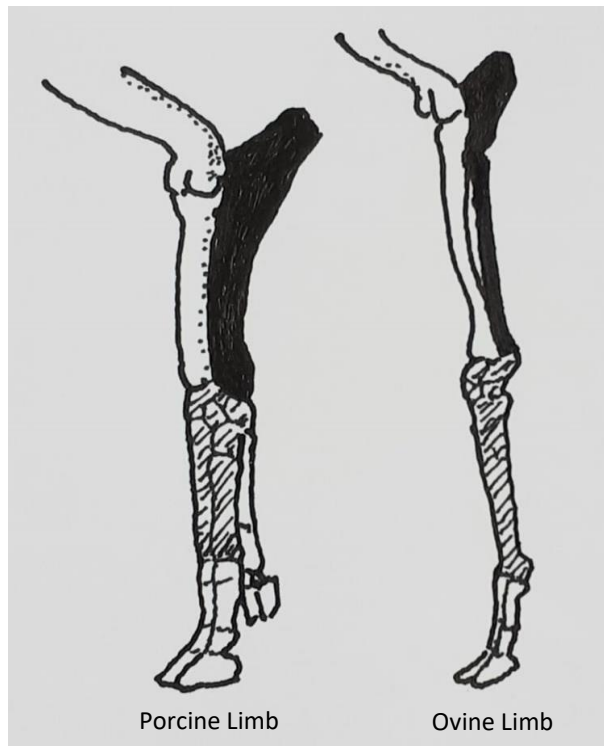


Figure 7-1: Difference between porcine and ovine limb anatomy. Illustration by Dr Vanda Morton

To test how each separate facet of the technology performs, four different experimental protocols were created. The first of these was cooled – perfused (C-P) limbs. The C-P limbs were a full test of the technology from the point of ‘injury’ to the stay in ‘hospital’. The ability of the cooling sock to cool the limb was assessed followed by how perfusing the limb was able to preserve tissue viability. The second experimental condition was non-cooled – non-perfused (NC-NP) limbs. These limbs acted as a control and showed how well the limb tissue was able to survive when no preservative actions were undertaken. The next condition was cooled – non-perfused (C-NP) limbs. This set of experiments examined what effect cooling the limb from the point of collection had on the preservation of limb tissue compared to a non-cooled limb. C-NP limb tests also gave an indication of if the combination of CO₂ and the coolant fluid will have a detrimental effect the limb tissue itself. The final condition used

during the experiments was non-cooled – perfused (NC-P) limbs. The NC-P limbs showed if the limb tissue could be preserved through perfusion alone without the immediate cooling. The C-NP and NC-P limb tests were important in determining which part of the technology, if any, has a more influential role in the preservation of the muscle fibres. C-P tests were compared to C-NP and NC-P tests to see if there is a synergistic effect of the two methods.

During the cooled tests in this set of experiments the FLUTEC PP80 coolant fluid, described in Chapter 4 pages 119 to 120, was used in combination with the CO₂. Unlike the previous porcine limb tests, a full bottle of CO₂ was used at each cooling time point. This was done for two reasons, the first was to provide maximum cooling with more gas passing over the limb, which should result in a greater cooling effect. Secondly, the full bottle of gas was needed to disperse the volume of coolant used over the limb. The coolant fluid was only used on alternate flushes to stop the cooling sock from being over-saturated in coolant fluid. This is due to the fact the coolant works through evaporation, if the coolant fluid isn't able to evaporate due to a saturated cooling sock, effective cooling won't occur.

During the porcine limb tests the duration of transportation back to the lab varied from test to test. To counteract this, the transportation time was set at 60 minutes. Having a standardised transportation time allows the direct comparison of the tissue viability at the end of transport. The limbs had a perfusion time of 2 hours. This is a long enough span of time for the effect of the perfusion on tissue viability to be observed. This perfusion time was also the time between the start and end tissue viability assessments on the non-perfused

limbs. Again, having a defined sampling time allowed the direct comparison of the perfused and non-perfused limbs.

Arterial and venous blood samples were taken from the perfusion system at set intervals during perfusion. These samples were then analysed by a Siemens RAPIDPoint 500 blood gas analyser. A number of different factors were considered to help analyse the health of the limb tissue. The first factor was the pH of the blood. This provided information on if there was a state of acidosis or alkalosis (Burns, 2014). The normal range for blood pH is between 7.35 and 7.45 (Cowley, Owen and Bion, 2013). The p_aO_2 and p_aCO_2 were also looked at. The p_aO_2 is the partial pressure of oxygen, this highlighted that there was enough O_2 in the blood (Cowley, Owen and Bion, 2013). A low p_aCO_2 value will indicate any acidosis is due to metabolic factors (Burns, 2014). The base excess will be evaluated too, the normal range of base excess is -3 to +3 (Burns, 2014). A negative base excess will also indicate that the acidosis is metabolic especially if the anion gap is large (Burns, 2014, Cowley, Owen and Bion, 2013). A large anion gap indicates the addition of acid into the blood. This is likely to be from the formation of lactic acid from anaerobic respiration in poorly perfused tissues or from the addition of toxins into the blood (Cowley, Owen and Bion, 2013). Potassium (K^+) is mainly stored within the cells in the body (Kovesdy, 2015). Therefore, hyperkalaemia, defined as a K^+ concentration of more than 5.5mmol/L, can be an indicator of the widespread release of K^+ ions into the blood stream associated with haemolysis (Rosenberry, Stone and Kalbfleisch, 2009). When taking these blood gas results into consideration it will be possible to gain an idea of whether or not the tissues are being adequately supplied with oxygen.

Histology samples were taken from the limb musculature at various points during the experiments so the success of limb preservation could be assessed on a cellular level. The first point samples were taken was at the end of the transportation period. This was so the muscle viability could be assessed before perfusion had begun. These were the baseline samples that the later samples could be compared to. At this point the non-cooled limbs had had at least 60 minutes of warm ischaemia. Taking histological samples at this point would enable the consequences of warm ischaemia compared to cooling to be assessed. This helped show if the cooling technology could help preserve limb viability. The second samples were taken after the perfusion time has elapsed.

Taking samples at the end of perfusion showed if perfusing the limbs retained tissue viability compared to the limbs that were left under ischaemic conditions. The tissue viability of the C-NP and NC-NP limbs could also be compared to show if initially cooling the limbs offered some protection to ischaemia and necrosis. Histological samples were important as they allowed a direct assessment of what was going on at a tissue and cellular level.

Laser doppler imaging scans and thermal camera photographs were taken every 15 minutes during the perfusion period. The laser doppler images and thermal camera photos were useful in the porcine limbs tests to have a visual depiction of how the blood was returning to the limb. In light of this, it was decided to carry on the collection of this data. Warmth could clearly be seen returning to the toes in the porcine limb tests, which was taken to mean the perfusion was resuming. The limitations of both thermal camera imaging and laser doppler imaging, such as their inability to measure at depth, were considered. However, on balance

it was thought that, combined with other data, they could provide a corroborative insight into the success of perfusion.

Another viability assessment of the limb that was undertaken during the porcine limb tests and was replicated in the ovine limb tests was neural stimulation. However, there were a few changes. In the previous porcine experiments, a Digitimer DS7A was used for nerve stimulation. This system had both the electrodes on one applicator which reduces the ability to stimulate across the muscle. Thus, the method of neural stimulation was changed. The stimulation system used for these experiments was the TrainFES FES6 electrostimulation system. This system was controlled by an app and used 2 electrode pads which were stuck to the belly of the muscle. These electrode pads could also be left in place for the duration of the experiment to ensure that the muscle was being stimulated in the same place. Unlike in the porcine experiments, the ovine limbs were stimulated at the end of the transportation period as well as at the end of perfusion. The initial stimulation at the end of the transportation period allowed the baseline value required for nerve twitch to be recorded. When the muscle was then stimulated at the end of the perfusion period, the amplitude that was needed to obtain a twitch can be evaluated to see if the muscle was now more or less responsive to stimuli. This provided an insight into how well the muscle tissue had been preserved. It is acknowledged that without a quantifiable measure of twitch, the increase in the twitch size can only be visually assessed. Additionally, there could be many other reasons for the lack of twitch in the limb. However, it is thought that the neural stimulation provided yet another corroborative indication of tissue viability before histological samples could be evaluated.

7.2. Testing protocol:

The testing protocol has been split into 3 separate parts. These are the cooling protocol, the perfusion protocol and the data collection protocol. The protocol used for the different tests can be created by combining these individual protocols together.

The freshly harvested limbs were collected at the abattoir and designated into one of the 4 groups. The limbs were then placed in the cooling sock and three thermocouples were inserted into the muscle tissue using a needle. The thermocouples were placed into the tissue at 3 depths, superficial tissue, mid tissue and deep tissue. The limb was then turned over so the thermocouples were on the bottom of the limb and temperature recording began. The cooling sock was then zipped up and transportation back to the laboratory commenced. The exception to this was the NC-NP limbs which were not placed within the cooling sock.

7.2.1. Cooling protocol:

The following protocol refers to the C-P and C-NP limbs.

Once the thermocouples had been inserted and the limb turned over the cooling sock was then zipped up and temperature recording began. One full bottle of CO₂ and one 100ml bottle of FLUTEC PP80 coolant fluid was flushed through the cooling sock. The CO₂ was released slowly so that the coolant fluid was properly dispersed by the flow of gas.

Every 10 minutes from 0 – 50 minutes one full bottle of CO₂ was flushed through the cooling sock to apply further topical cooling. The coolant fluid was used in combination with the CO₂ on alternate flushes i.e. 0, 20 and 40 minutes. The temperature of the deep tissue was monitored continuously and if the deep tissue was more than 10°C below the starting temperature the gas would not be flushed through the sock to prevent overcooling the tissue which could lead to damage.

During transportation any change in environmental conditions was noted incase this could be linked to a change in cooling in future analysis. Temperature recording and cooling continued until 60 minutes has elapsed. The last gas flush was at 50 minutes. At this point, a maximum of 6 bottles of CO₂ (360l of CO₂) and 300ml of coolant fluid had been used.

After the 60 minutes had passed, the temperature recording was stopped and the thermocouples were removed. The limb was then weighed in the cooling sock. The weight of the cooling sock was subsequently subtracted to calculate the weight of the limb. Finally, the limb was removed from the cooling sock and turned over to be prepared for cannulation.

7.2.2. Perfusion protocol:

The following protocol related to the C-P and NC-P limbs.

Once cannulation had been achieved the limb was transferred to the Limb support system (LSS). The LSS circuit was primed with saline. Once the circuit had been primed the baseline perfusate was introduced into the system. This baseline perfusate was made up of 500ml warmed bovine blood, 250ml gelofusine, 250ml Ringer's lactate solution and 20ml 8.4% sodium bicarbonate. The perfusion system was then connected to the cannulas in the limb and perfusion commenced.

The perfusion flowrate was determined by the circuit pressure. During perfusion arterial pressure was maintained close to 80mmHg. The gas used in the perfusion circuit was air. The flow rate of the gas was determined by the partial pressure of the O₂ and CO₂ of the arterial blood measured by a blood gas analyser. Additional perfusate was added into the perfusion circuit when the blood sump level was low. The perfusate passed through a heat exchanger to keep the limb at a temperature close to 37°C. The limb was covered by damp muslin when data analysis was not being undertaken to keep the limb surface moist. Additionally, the lid sections of the LSS were lowered when data analysis was not being done to help keep the limb warm by preventing heat being lost to the environment. The limb was perfused for a total of 2 hours.



Figure 7-2: Perfusion set up of the ovine limb

7.2.3. Data collection protocol:

The additional tests done for the perfused limbs will be described below in section 7.3.2.1. All limbs were weighed in the cooling sock at the end of the transportation period. The weight of the cooling sock was subtracted to ensure only the weight of the limb was recorded.

Immediately after the transportation period ended, the ROM of the limb was assessed. This was done by manually bending the limb and visually recording how much the joints moved and how easily this could be done. After this, neural stimulation was attempted. The electrode pads were attached to the belly of the gracilis muscle. The TrainFes app was then opened and stimulation began. The app allows for an increase in the size of the stimulation in 1mA steps. The amplitude of the stimulation was increased until a twitch was seen in the muscle. The size of the baseline amplitude was noted and the twitch video recorded. The amplitude was then increased to observe what effect this had on the size of the twitch.

Baseline histology samples were also taken. A scalpel was used to cut small pieces of the superficial, mid and deep tissue from a muscle other than the one being stimulated. The tissue samples were placed in 10% formalin and stored at 4°C. The perfusion period then began.

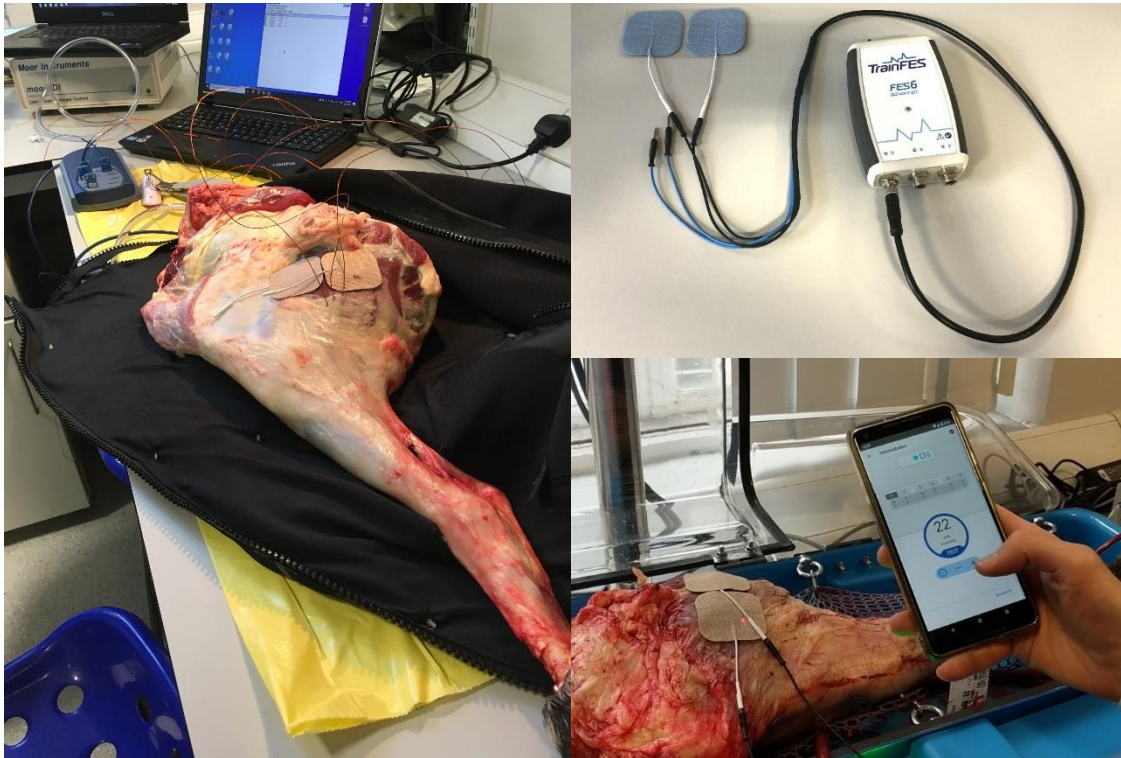


Figure 7-3: Left - Thermocouples placed in the muscle and the location of the electrode pads. Right upper – TrainFES neurostimulation equipment. Right lower – neurostimulation equipment in use

The above tests were then repeated at the end of the 2-hour perfusion period to obtain the end perfusion readings. The exact time of all the samples were recorded so the time elapsed since collection from the abattoir could be calculated.

7.2.3.1. Perfusion data collection:

Before perfusion began, a baseline LDI scan and thermal image were taken. This allowed the biological zero to be calculated for the LDI data. The biological zero is defined as the baseline movement of cells within the tissue which is then used to identify changes in velocity and blood cell density in later LDI scans. Perfusion was then started. The initial pressure, temperature, perfusion flowrate and gas flowrate were noted. Data collection during perfusion occurred every 15 minutes. An LDI scan and a thermal photograph were taken at each data collection time point. Additionally, from 15 minutes, a blood sample was taken from both an arterial and venous outlet at each sampling point. These blood samples were run through a Siemens RAPIDPoint 500 blood gas analysis machine to obtain readings of the pO_2 , pCO_2 , pH, base excess, K^+ , A-sat, V-sat, haemoglobin and haematocrit. The pressure, temperature and the perfusion and gas flowrates were also recorded every 15 minutes and the gas flowrate adjusted accordingly. At the end of perfusion, the limb was placed back in the cooling sock and weighed to allow the increase in weight of the limb during perfusion to be calculated.

0 minutes: Collection of limbs

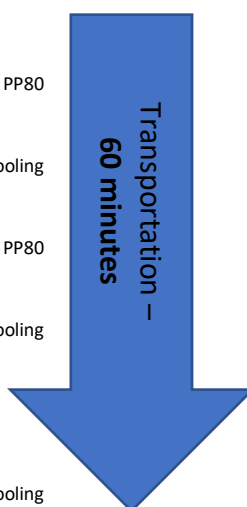
Limbs placed in cooling sock (Except NC-NP limbs)
 Thermocouples inserted into tissue using needle (Except NC-NP limbs)
 Cooling sock zipped up

Cooled limbs:

- 0 minutes:*
- 1 full bottle of CO₂ and FLUTEK PP80 released through cooling sock
- 10 minutes:*
- 1 full bottle of CO₂ released through cooling sock
- 20 minutes:*
- 1 full bottle of CO₂ and FLUTEK PP80 released through cooling sock
- 30 minutes:*
- 1 full bottle of CO₂ released through cooling sock
- 40 minutes:*
- 1 full bottle of CO₂ and FLUTEK PP80 released through cooling sock
- 50 minutes:*
- 1 full bottle of CO₂ released through cooling sock

Non-cooled limbs:

- No active cooling performed



60 minutes: End of transportation period.

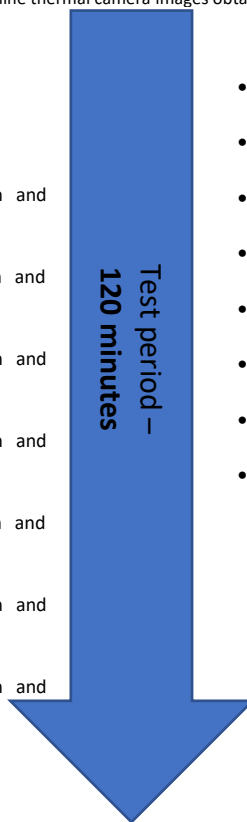
Limb weighed
 Baseline ROM performed
 Baseline nerve stimulation performed
 Baseline histology sample taken
 Baseline thermal camera images obtained

Perfused limbs

- 60 minutes:*
- Limb cannulated
 - Baseline LDI scan obtained
 - Perfusion begins
- 75 minutes:*
- Blood gas data samples, LDI Scan and thermal camera photograph obtained
- 90 minutes:*
- Blood gas data samples, LDI Scan and thermal camera photograph obtained
- 105 minutes:*
- Blood gas data samples, LDI Scan and thermal camera photograph obtained
- 120 minutes:*
- Blood gas data samples, LDI Scan and thermal camera photograph obtained
- 135 minutes:*
- Blood gas data samples, LDI Scan and thermal camera photograph obtained
- 150 minutes:*
- Blood gas data samples, LDI Scan and thermal camera photograph obtained
- 165 minutes:*
- Blood gas data samples, LDI Scan and thermal camera photograph obtained
- 180 minutes:*
- Blood gas data samples, LDI Scan and thermal camera photograph obtained
 - Limb weighed

Non-Perfused limbs

- 75 minutes*
- Thermal camera photograph taken
- 90 minutes*
- Thermal camera photograph taken
- 105 minutes*
- Thermal camera photograph taken
- 120 minutes*
- Thermal camera photograph taken
- 135 minutes*
- Thermal camera photograph taken
- 150 minutes*
- Thermal camera photograph taken
- 165 minutes*
- Thermal camera photograph taken
- 180 minutes*
- Thermal camera photograph taken



180 minutes: End of test.

End of test (EP) ROM performed
 End of test (EP) histology sample taken
 End of test (EP) nerve stimulation performed

Figure 7-4: Flow chart of protocol for ovine limb tests

7.3. Results:

7.3.1. Cooled – perfused limbs:

<i>Table 7-1: Mean and standard deviation for weight, temperature and nerve stimulation data for cooled - perfused limbs</i>	
Collection weight (kg)	4.79 ± 0.62
Temperature of deep tissue at collection (°C)	31.47 ± 8.81
Transport duration (minutes)	60 ± 0.00
Temperature of deep tissue on arrival (°C)	27.27 ± 5.95
Temperature change in deep tissue (°C)	4.53 ± 3.46
Baseline nerve stim (mA)	21 ± 20.51
Time from collection to start of perfusion (minutes)	106.33 ± 20.13
End perfusion weight (kg)	5.22 ± 0.63
Change in limb weight during perfusion (kg)	0.55 ± 0.19
Percentage change in limb weight during perfusion (%)	12.22 ± 6.23
End perfusion nerve stim (mA)	50 ± 69.31
Time since collection for EP nerve stim (minutes)	248 ± 15.89

Table 7-1 shows a range data on various parameters for the cooled – perfused tests. The first is the mean change in temperature in the deep tissue was only 4.53°C. This is less than the target 10°C temperature change. The second important thing to note from this table is the

increase in weight of the limb over the perfusion period. The limbs increased in weight by a mean of 0.55kg when perfused. Finally, the nerve stimulation data shows that a higher amplitude is needed to create twitch in the limbs at the end of perfusion. However, the amplitude needed to create a twitch at both the baseline and end of perfusion time points is very varied with the standard deviation of amplitude at the end of perfusion being greater than the mean amplitude required to obtain twitch.

Table 7-2 shows the mean values for each of the blood measurements. This table shows that the blood was acidic with a low pH and negative base excess. The K^+ values were higher than the normal range ($3.5-5.0\text{mmolL}^{-1}$) (Soar *et al.*, 2010). The arterial saturation of the blood was normal.

Table 7-3 shows the perfusion pressure was higher than intended but has a very high standard deviation. Furthermore, the standard deviation for the perfusion flowrate shows that there was a wide variation in the flowrate during the tests. On the other hand, the temperature stayed relatively steady evidenced by the small standard deviation.

Table 7-2: Mean and standard deviation of perfusion data for cooled - perfused limbs

Arterial			Venous		
	Measured value	Normal range		Measured value	Normal range
<i>pO₂</i> (mmHg)	123.9 ± 11.4	75-100	<i>pO₂</i> (mmHg)	58.8 ± 4.30	25-40
<i>pCO₂</i> (mmHg)	31.8 ± 12.77	35-45	<i>pCO₂</i> (mmHg)	51.1 ± 19.58	41-50
<i>pH</i>	7.046 ± 0.07	7.35-7.45	<i>pH</i>	6.892 ± 0.10	7.33-7.44
<i>Base Excess</i> <i>(mmol/L)</i>	-20.5 ± 4.26	-2 - +1	<i>Base Excess</i> <i>(mmol/L)</i>	-22.6 ± 4.26	-2 - +1
<i>O₂ Consumption</i> <i>(ml/min)</i>	557.71 ± 306.80	250	<i>O₂ Consumption</i> <i>(ml/min)</i>	557.71 ± 306.80	250
<i>K⁺</i> (mmol/L)	7.55 ± 1.99	3.5-5.0	<i>K⁺</i> (mmol/L)	8.3 ± 1.82	3.5-5.0
<i>Hct</i> (%)	27 ± 4.13	37-52	<i>Hct</i> (%)	28 ± 4.56	37-52
<i>tHb</i> (g/dL)	9.0 ± 1.39	12-17	<i>tHb</i> (g/dL)	9.5 ± 1.54	12-17
<i>A-Sat</i> (%)	97.6 ± 1.31	>95	<i>V-Sat</i> (%)	76.4 ± 6.63	72-75

<i>Table 7-3: Mean and standard deviation of perfusion parameters for the C-P limbs</i>	
Pressure (mmHg)	108 ± 54.92
Temperature (°C)	36.73 ± 1.10
Perfusion Flowrate (ml/min)	222 ± 104.83
Gas Flowrate (ml/min)	78 ± 11.43

Table 7-5 shows the mean arterial blood results at each time point throughout the duration of the experiment. The p_aCO_2 started off below normal range and continued decreasing throughout the perfusion period. Moreover, the arterial pH decreased through the experiment which was mirrored in the values for the base excess which started off at -15 and ended up at -24.9, a decrease of 9.9. Conversely to this, the values for the haematocrit and potassium increased steadily throughout the duration of perfusion. The arterial saturation did show a slight decrease but it stayed within normal range.

Unlike the arterial pH, Table 7-6 shows that the venous pH stayed relatively stable for the whole test. However, the base excess did decrease during perfusion showing that there was an ion imbalance in the blood. The p_vCO_2 started off above the normal range but as the experiment continued it fell into normal range and then dropped below it. Similar to the arterial blood samples, the values for K^+ and the haematocrit increased as perfusion continued.

Other than the 15-minute time point, the perfusion pressure remained within a range of 5mmHg, as seen in Table 7-4.

Conversely, the perfusion flowrate increased throughout the experiment. The temperature also increased as the blood had chance to pass through the heat exchanger in the perfusion circuit.

Table 7-4: Mean and standard deviation for perfusion parameters at each time point for C-P limbs

Time (min)	Pressure (mmHg)	Temp (°C)	Perfusion Flowrate (ml/min)	Gas Flowrate (ml/min)
0	107	34.76	159 ± 1.41	75 ± 14.14
15	118 ± 74.2	34.97 ± 0.40	220 ± 85.85	80 ± 21.21
30	109 ± 62.7	37.03 ± 1.02	221 ± 98.15	70 ± 13.23
45	104 ± 61.6	36.73 ± 1.16	219 ± 119.18	80 ± 13.23
60	106 ± 64.2	37.02 ± 0.82	192 ± 136.59	77 ± 12.58
75	106 ± 69.0	37.19 ± 0.86	231 ± 149.30	77 ± 12.58
90	105 ± 69.9	36.98 ± 0.50	231 ± 149.30	77 ± 12.58
105	109 ± 67.2	37.29 ± 0.95	252 ± 128.48	85 ± 8.66
120	107 ± 68.2	37.31 ± 0.88	252 ± 128.48	85 ± 8.66

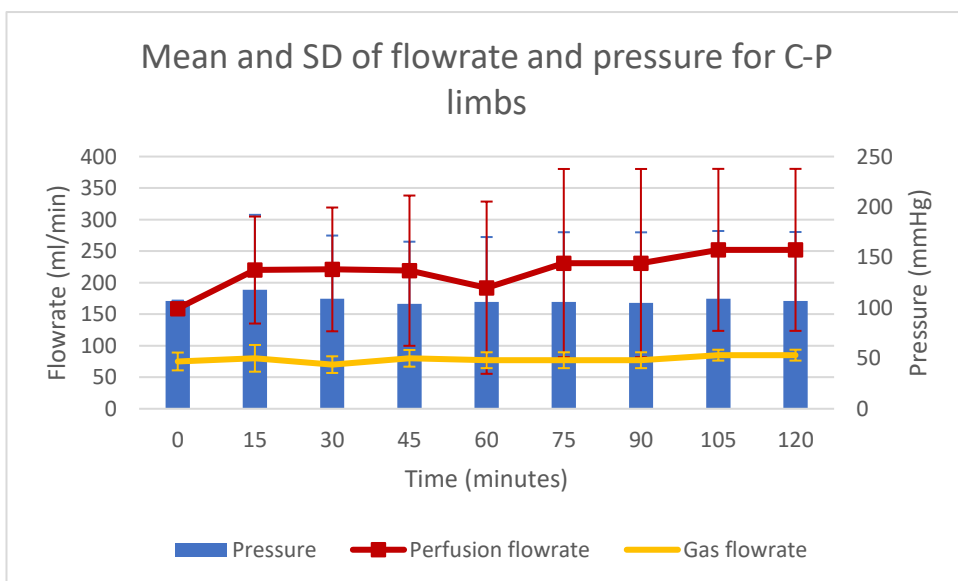


Figure 7-5: Mean flowrate and pressure for C-P limbs

Table 7-5: Mean and standard deviation of arterial perfusion data at each time point for cooled perfused limbs

Time (min)	pO₂ (mmHg)	pCO₂ (mmHg)	pH	Base Excess (mmol/L)	O₂ Consumption (ml/min)	K⁺ (mmol/L)	Hct (%)	tHb (g/dL)	A-Sat (%)
0									
15	134.9 ± 10.3	31.0 ± 3.5	7.102 ± 0.09	-15.0 ± 3.1	586.76 ± 392.08	4.98 ± 0.57	24 ± 5.2	8.2 ± 1.7	99.0 ± 0.7
30	129.9 ± 9.7	38.4 ± 6.7	7.084 ± 0.06	-17.2 ± 4.3	362.05 ± 198.88	5.70 ± 1.22	24 ± 2.1	8.2 ± 0.8	98.2 ± 0.3
45	128.1 ± 6.8	33.6 ± 7.6	7.065 ± 0.10	-19.0 ± 5.3	461.96 ± 232.33	6.73 ± 1.49	25 ± 3.8	8.6 ± 1.2	97.9 ± 0.2
60	132.0 ± 5.8	28.0 ± 3.1	7.069 ± 0.06	-20.7 ± 2.5	540.58 ± 379.74	7.16 ± 0.87	26 ± 3.8	8.9 ± 1.3	98.1 ± 0.4
75	118.8 ± 2.7	29.8 ± 3.8	7.025 ± 0.10	-21.6 ± 4.4	541.92 ± 285.22	8.07 ± 1.32	27 ± 4.0	9.2 ± 1.4	97.3 ± 0.6
90	107.8 ± 18.7	29.7 ± 2.7	7.024 ± 0.09	-21.8 ± 2.5	646.61 ± 399.15	8.31 ± 0.97	28 ± 3.5	9.3 ± 1.3	95.6 ± 2.8
105	120.1 ± 8.6	24.1 ± 2.8	7.007 ± 0.04	-23.6 ± 2.1	565.70 ± 307.81	9.30 ± 1.39	28 ± 5.1	9.7 ± 1.6	97.3 ± 0.4
120	123.0 ± 4.8	22.3 ± 1.9	6.993 ± 0.03	-24.9 ± 2.2	869.83 ± 558.83	10.19 ± 1.83	30 ± 6.1	10.2 ± 2.0	97.3 ± 0.3

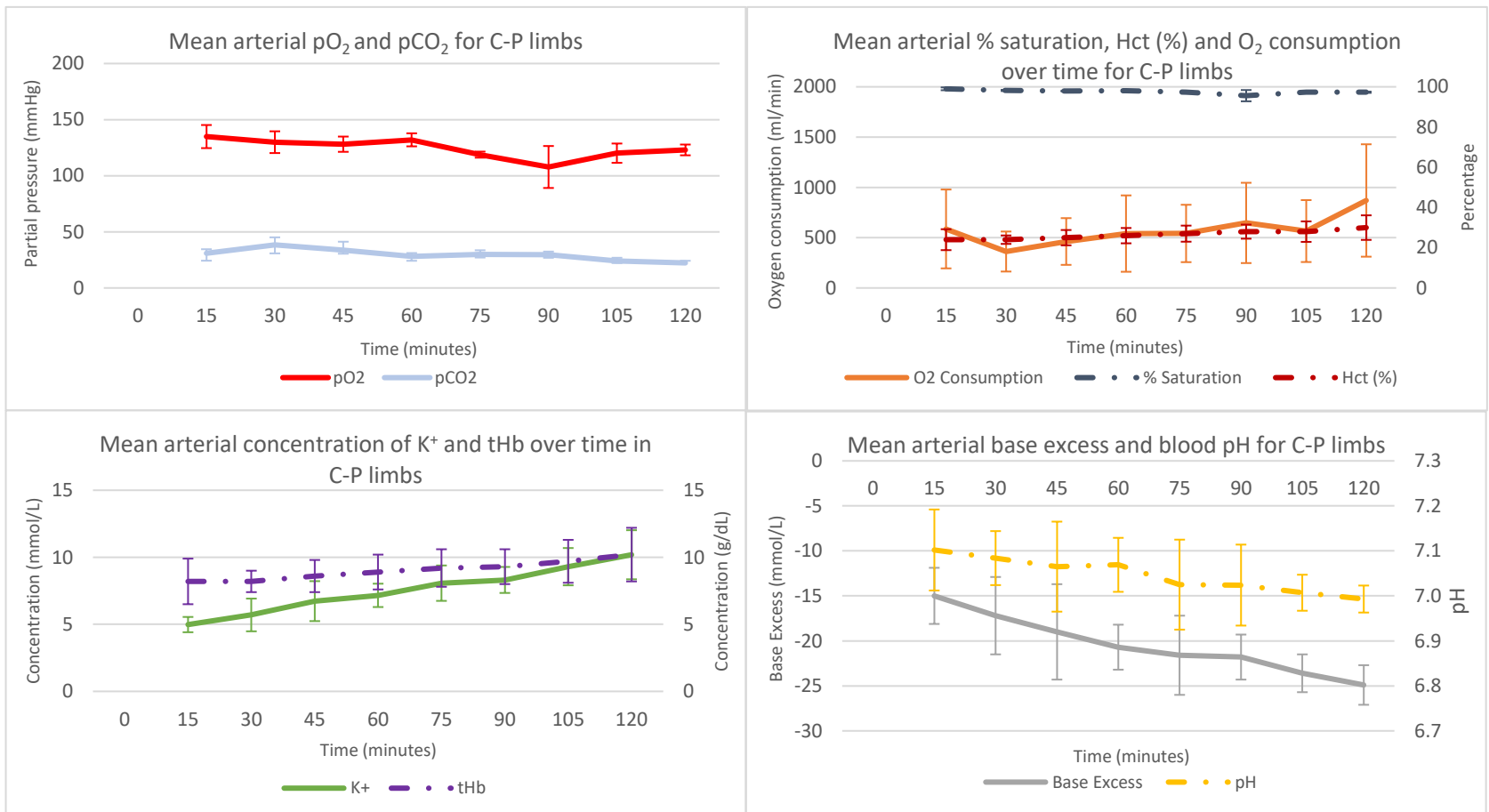


Figure 7-6: Mean arterial blood gas data for C-P limbs

Table 7-6: Mean and standard deviation for venous perfusion data at each time point for cooled perfused limbs

Time (min)	pO₂ (mmHg)	pCO₂ (mmHg)	pH	Base Excess (mmol/L)	O₂ Consumption (ml/min)	K⁺ (mmol/L)	Hct (%)	tHb (g/dL)	V-Sat (%)
0									
15	54.6 ± 0.5	70.2 ± 37.3	6.852 ± 0.21	-19.6 ± 6.3	586.76 ± 392.08	6.28 ± 1.26	26 ± 4.0	8.9 ± 1.4	75.6 ± 17.3
30	63.4 ± 5.2	62.6 ± 16.6	6.919 ± 0.14	-19.1 ± 5.8	362.05 ± 198.88	6.71 ± 1.07	26 ± 3.5	8.7 ± 1.2	81.5 ± 1.2
45	61.0 ± 4.6	52.2 ± 12.7	6.896 ± 0.15	-21.8 ± 6.0	461.96 ± 232.33	7.45 ± 1.75	26 ± 4.4	9.0 ± 1.5	78.1 ± 3.5
60	57.1 ± 4.1	52.8 ± 4.8	6.879 ± 0.10	-22.6 ± 3.4	540.58 ± 379.74	7.89 ± 1.00	27 ± 3.6	9.2 ± 1.2	73.8 ± 6.5
75	58.1 ± 5.1	46.0 ± 0.7	6.881 ± 0.09	-23.8 ± 3.7	541.92 ± 285.22	8.62 ± 1.42	28 ± 5.1	9.6 ± 1.7	75.8 ± 4.2
90	54.3 ± 0.9	41.6 ± 4.0	6.911 ± 0.08	-23.5 ± 2.5	646.61 ± 399.15	9.01 ± 1.43	29 ± 5.0	9.7 ± 1.6	71.8 ± 4.1
105	61.0 ± 2.8	37.2 ± 4.4	6.901 ± 0.05	-24.6 ± 2.2	565.70 ± 307.81	9.73 ± 1.58	30 ± 5.3	10.2 ± 1.9	78.0 ± 2.2
120	59.9 ± 1.4	33.2 ± 5.5	6.894 ± 0.07	-25.9 ± 2.4	869.83 ± 558.83	10.39 ± 1.69	34 ± 7.8	11.3 ± 2.7	76.3 ± 0.5

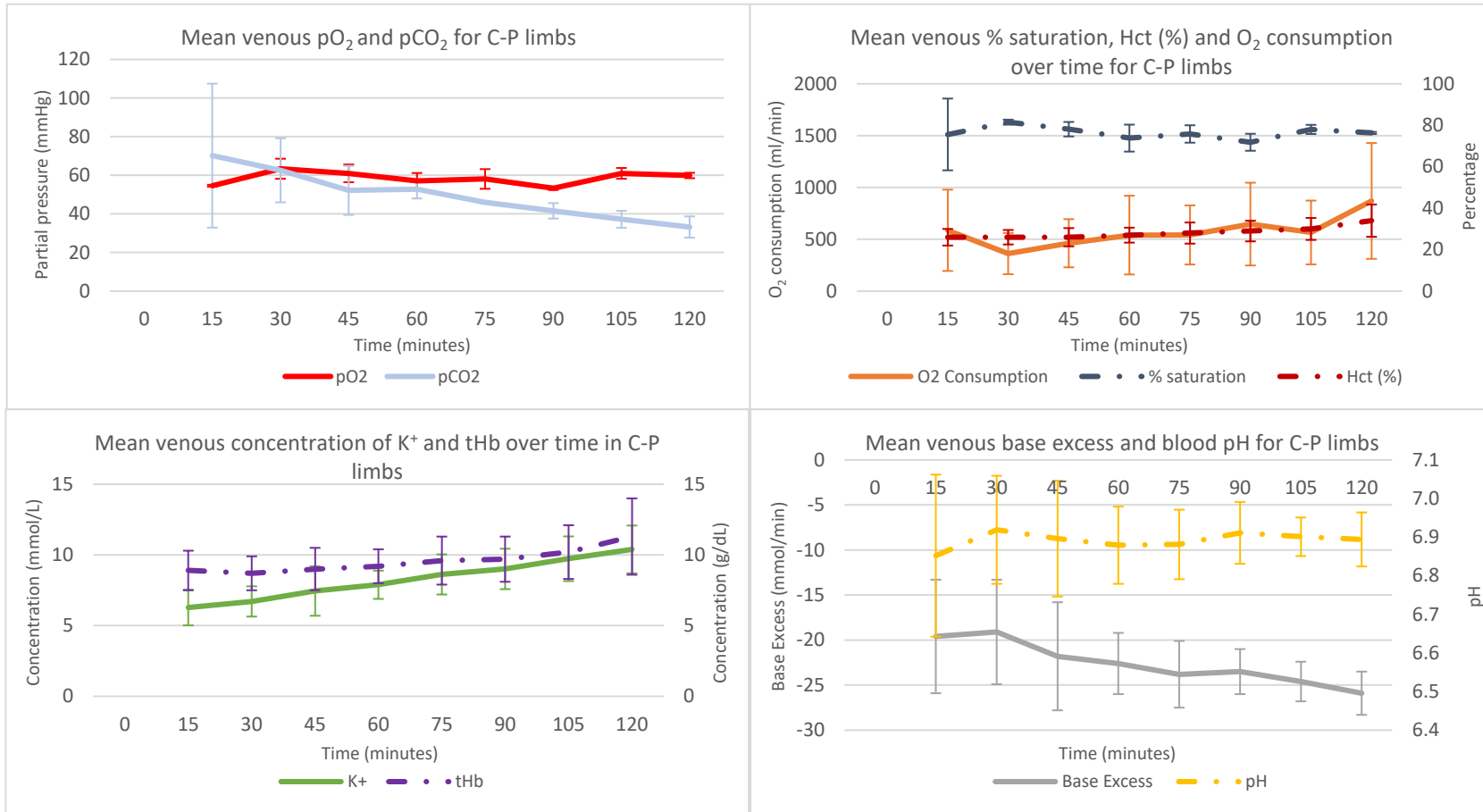


Figure 7-7: Mean venous blood gas data for C-P limbs

7.3.1.1.1. Thermal Imaging

The thermal photographs in Figure 7-9 and Figure 7-10 were taken during the C-P 3 test. The photographs show that the limb warmed up during the test shown by the brighter yellow colour of the muscle tissue at the top of the limb. The tube taking blood into the artery which came directly from the point of heat exchange can clearly be seen on all photographs. Additionally, the dark purple area on the limbs indicates the presence of the damp muslin which was used to keep the limb moist in between sampling points.

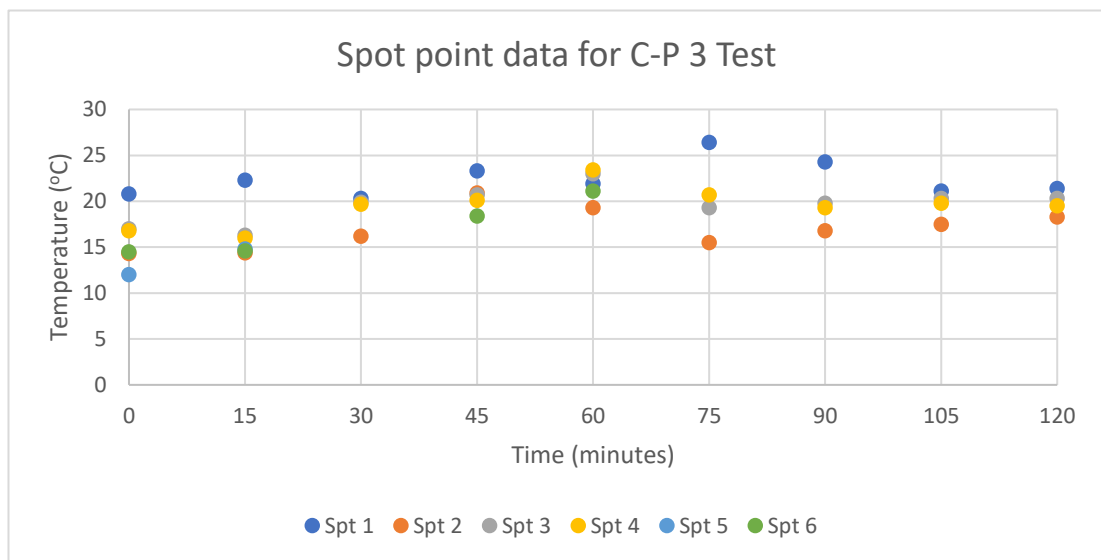


Figure 7-8: Example thermal camera spot point data for C-P 3 test



0 minutes

15 minutes

30 minutes



45 minutes

60 minutes

75 minutes

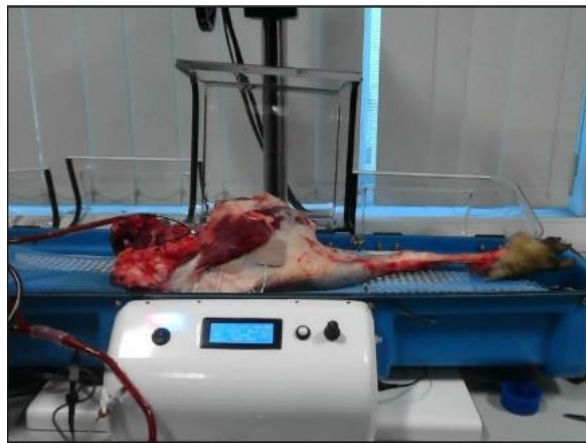
Figure 7-9: Example thermal camera images from C-P 3 0-75 minutes



90 minutes

105 minutes

120 minutes



Anatomical photograph

Figure 7-10: Example thermal camera images from C-P 3 continued (90-120 minutes)

7.3.1.1.2. LDI Imaging

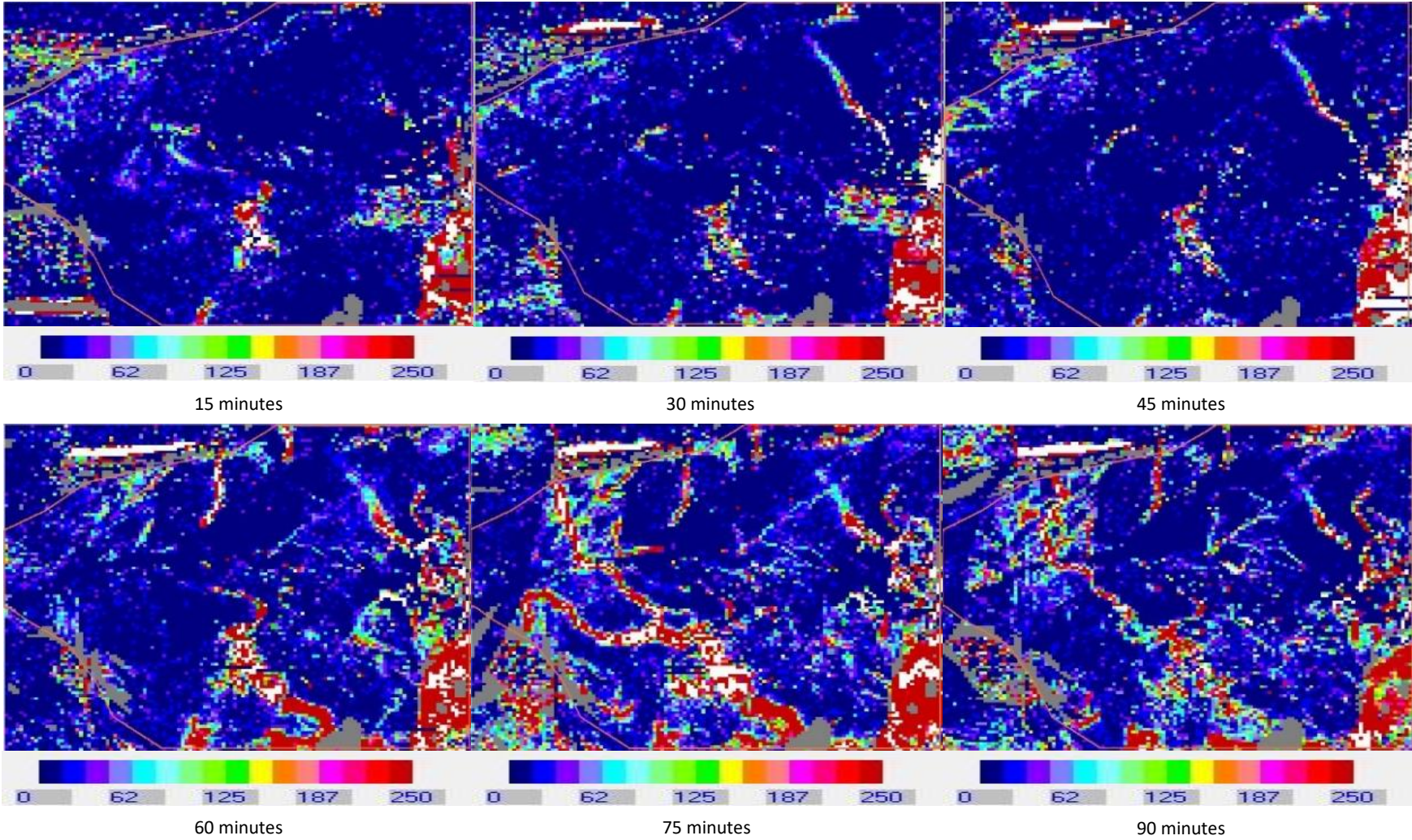


Figure 7-11: Example LDI data for C-P 3 (15-90 minutes)

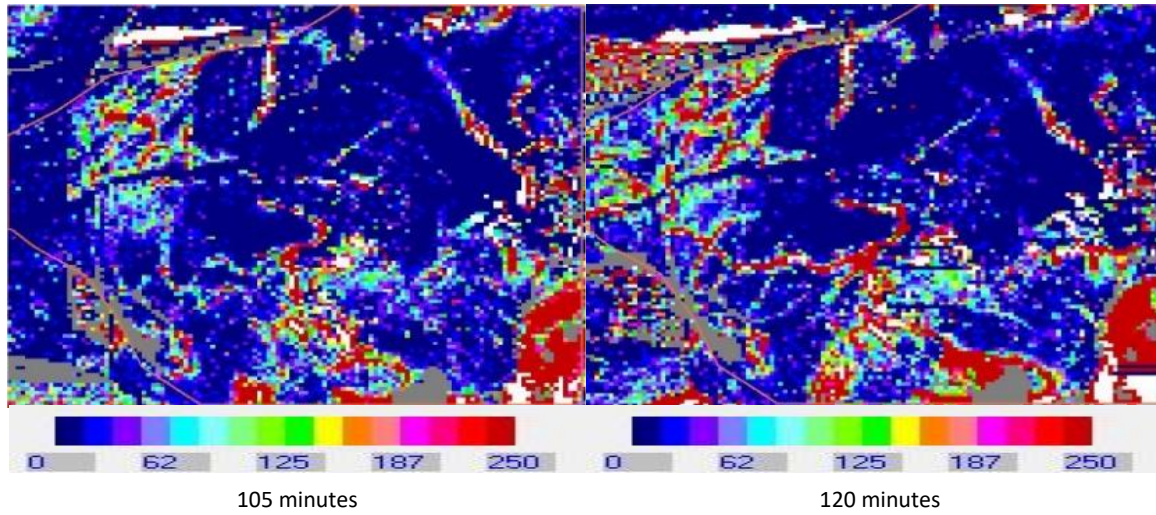


Figure 7-12: Example LDI data for C-P 3 continued (105 and 120 minutes)

Figure 7-11 and Figure 7-12 show the LDI data from test C-P 3, the same test as the thermal camera images in Figure 7-9 and Figure 7-10. The LDI images clearly show the opening up of blood vessels as perfusion continued as evidenced by the lines of red and white appearing as the test progressed. The lighter blue colour which developed over the 120 minutes shows that blood was returning to the capillary bed. However, at 120 minutes there were still patches of dark blue showing that there was little movement of blood in these areas. This is not unexpected.

7.3.1.1.3. Histology

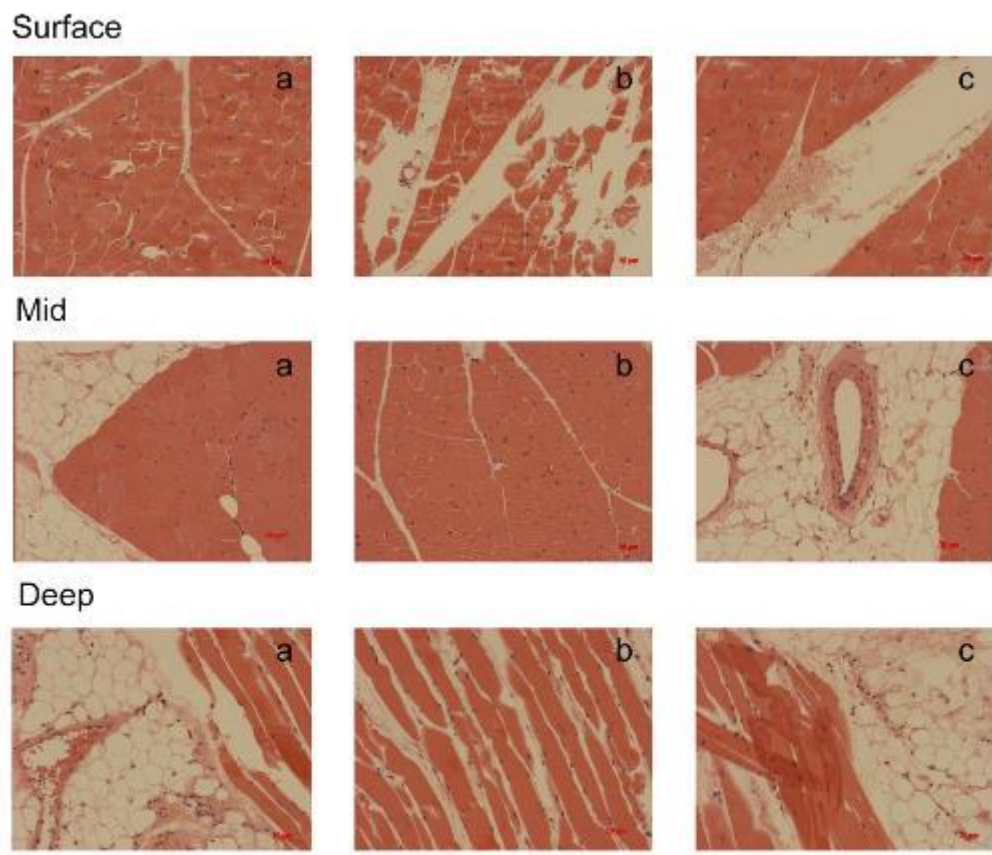


Figure 7-13: Example histology data for C-P 1. Images a, b and c are 3 slices of the tissue samples taken at each depth.

Histologists notes

<i>Table 7-7: Histologist's notes for C-P 1</i>		
C-P 1 EP Superficial	19/2697	Myofibres appear viable; multifocal moderate artifactual fragmentation.
C-P 1 EP Mid	19/2698	Myofibres appear viable; only rare isolated myofibres with condensed sarcoplasm and minimal artifactual fragmentation Rare scattered parasitic cysts (Sarcocystis); focal minimal lymphocytic infiltrate in the endomysium
C-P 1 EP Deep	19/2699	Myofibres appear viable; multifocal mild increased eosinophilia with segmental contraction of the sarcoplasm with sparse minimal artifactual fragmentation. Mild separation of myofibres (possible mild oedema); rare granulocytes and lymphocytes sparse in the endomysium. Single focal parasitic cyst (Sarcocystis).

Figure 7-13 shows the histology data collected for C-P 1. As the histologist's notes state, the myofibres appeared to be viable. The deep tissue had more signs of oedema and increase of eosinophils whilst the mid tissue had more parasitic cysts present in the tissue. There was artifactual fragmentation present at all tissue depths.

7.3.2. Non-cooled – perfused limbs:

<i>Table 7-8: Mean and standard deviation for weight, temperature and nerve stimulation data for non-cooled - perfused limbs</i>	
Collection weight (kg)	4.38 ± 1.99
Temperature of deep tissue at collection (°C)	32.65 ± 10.53
Transport duration (minutes)	59 ± 1.73
Temperature of deep tissue on arrival (°C)	29.29 ± 7.34
Temperature change in deep tissue (°C)	3.36 ± 3.24
Baseline nerve stim (mA)	85
Time from collection to start of perfusion (minutes)	77.33 ± 17.79
End perfusion weight (kg)	3.33
Change in limb weight during perfusion (kg)	0.66
Percentage change in weight during perfusion (%)	24.72
End perfusion nerve stim (mA)	22 ± 13.50
Time since collection for EP nerve stim (minutes)	206 ± 25.42

Table 7-8 shows that the mean weight of the limbs in the NC-P tests was less than that of the C-P limbs. However, there was a greater variation in the limb weights. The mean temperature change in the NC-P limbs was 3.36°C which is smaller than that achieved by actively cooling the limbs in the C-P tests. There was a shorter time period after collection before perfusion

began for the NC-P limbs compared to the C-P limbs. Due to only having one data point for the baseline nerve stimulation, the mean result for the EP nerve stimulation suggests that twitch was achieved at a lower amplitude. Furthermore, there was only one result for the EP weight in the NC-P limbs. This result does indicate that there was an increase in limb weight during perfusion.

Table 7-9 shows that the mean pH of the blood was below normal range in the NC-P tests. Additionally, the base excess and $p_a\text{CO}_2$ were lower than what would be expected. Moreover, as was seen in the C-P limbs, hyperkalaemia was present. The arterial saturation was still within the normal range. The haematocrit was at the higher end of the range that would be expected for blood within an isolated perfusion system. For example, for cardiopulmonary bypass the range would be between about 20-30%. The pressure in the NC-P limb tests was much lower than in the C-P limb tests. In fact, the mean pressure was lower than the 80mmHg which was being aimed for. Again, the temperature and the gas flow rate did not fluctuate much when looking at the standard deviation.

Table 7-9: Mean and standard deviation for perfusion data for non-cooled - perfused limbs

Arterial			Venous		
	Measured value	Normal range		Measured value	Normal range
pO₂ (mmHg)	130.5 ± 6.27	75-100	pO₂ (mmHg)	65.0 ± 8.24	25-40
pCO₂ (mmHg)	27.6 ± 10.98	35-45	pCO₂ (mmHg)	36.1 ± 16.45	41-50
pH	7.160 ± 0.08	7.35-7.45	pH	7.092 ± 0.10	7.33-7.44
Base Excess (mmol/L)	-16.8 ± 4.43	-2 - +1	Base Excess (mmol/L)	-18.5 ± 1.70	-2 - +1
O₂ Consumption (ml/min)	190.20 ± 89.11	250	O₂ Consumption (ml/min)	190.20 ± 89.11	250
K⁺ (mmol/L)	6.4 ± 0.55	3.5-5.0	K⁺ (mmol/L)	6.4 ± 0.45	3.5-5.0
Hct (%)	29 ± 5.70	37-52	Hct (%)	30 ± 6.11	37-52
tHb (g/dL)	10.0 ± 1.97	12-17	tHb (g/dL)	10.2 ± 2.06	12-17
A-Sat (%)	98.4 ± 0.45	>95	V-Sat (%)	87.5 ± 5.12	72-75

<i>Table 7-10: Mean and standard deviation of perfusion parameters for the NC-P limbs</i>	
Pressure (mmHg)	71 ± 8.32
Temperature (°C)	36.47 ± 0.94
Perfusion Flowrate (ml/min)	166 ± 58.30
Gas Flowrate (ml/min)	66 ± 14.73

Table 7-12 shows the arterial blood sample results in more detail. Starting with the $p_a\text{CO}_2$ the values started within normal range. However, by 45 minutes the values had decreased to below the normal range. The blood pH was lower than would be expected. Nevertheless, unlike the C-P limb tests, the arterial pH did not decrease much as the experiment progressed. Moreover, the pH did increase for a while, though not into the normal range. The base excess decreased over the course of the experiment detailing a developing base deficit. Both the K^+ and haematocrit increased as perfusion continues. This was also reflected in the venous blood results as shown in Table 7-13. The arterial saturation stayed around 98%, well within the expected range.

Table 7-11 shows the mean perfusion flowrate increased until 60 minutes at which point it started to be reduced again. This is not reflected in the mean perfusion pressure which continued to rise until 75 minutes even after the blood flow was reduced. In fact, the pressure began to reduce when the flow rate increased again.

Table 7-11: Mean and standard deviation of perfusion parameters at each time point for NC-P limbs

Time (min)	Pressure (mmHg)	Temperature (°C)	Perfusion Flowrate (ml/min)	Gas Flowrate (ml/min)
0	68 ± 5.2	34.97 ± 0.5	167 ± 63	78 ± 16
15	65 ± 13.9	35.90 ± 1.0	169 ± 60	63 ± 3
30	66 ± 7.6	36.11 ± 1.0	178 ± 61	78 ± 16
45	70 ± 12.5	37.04 ± 0.3	204 ± 52	78 ± 16
60	73 ± 8.5	36.84 ± 0.3	164 ± 25	68 ± 14
75	81 ± 4.6	36.92 ± 0.3	143 ± 68	68 ± 14
90	74 ± 3.0	36.92 ± 0.2	144 ± 73	57 ± 15
105	74 ± 5.5	36.69 ± 0.2	167 ± 87	57 ± 15
120	72 ± 5.5	37.22 ± 0.4	170 ± 107	57 ± 15

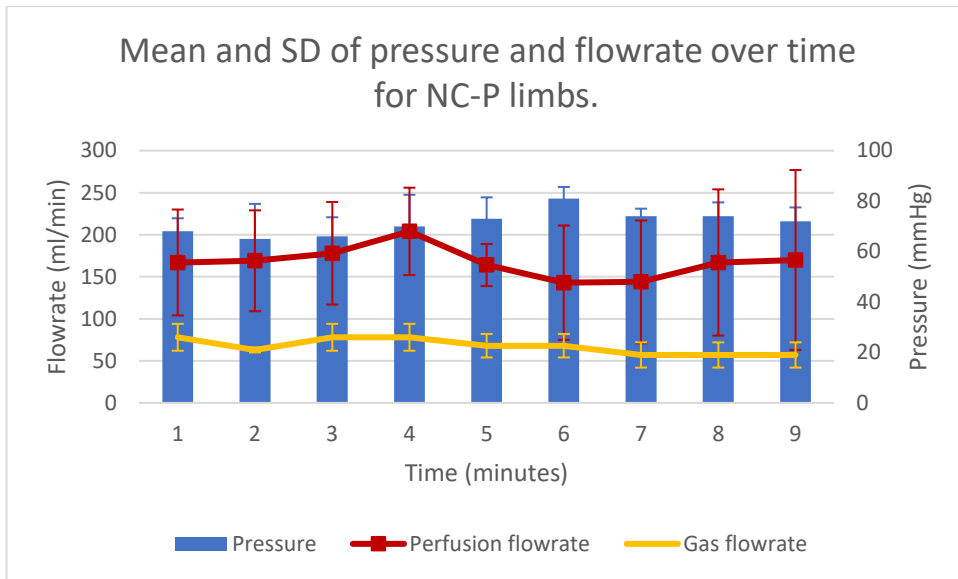


Figure 7-14: Mean pressure and flowrate over time for NC-P limb

Table 7-12: Mean and standard deviation of arterial perfusion data at each time point for non-cooled - perfused limbs

Time (min)	pO₂ (mmHg)	pCO₂ (mmHg)	pH	Base Excess (mmol/L)	O₂ Consumption (ml/min)	K⁺ (mmol/L)	Hct (%)	tHb (g/dL)	A-Sat (%)
0									
15	122.3 ± 9.3	43.2 ± 1.5	7.124 ± 0.04	-14.4 ± 1.2	182.1 ± 67.54	5.4 ± 0.18	23.0 ± 4.24	7.7 ± 1.4	97.9 ± 0.4
30	132.0 ± 5.7	35.6 ± 3.1	7.086 ± 0.02	-18.1 ± 0.1	204.2 ± 101.12	6.1 ± 0.28	23.5 ± 2.12	8.0 ± 0.8	98.3 ± 0.1
45	125.9 ± 2.7	28.3 ± 7.2	7.091 ± 0.06	-20.0 ± 0.1	222.2 ± 212.09	6.6 ± 0.55	26.5 ± 0.71	9.1 ± 0.1	98.0 ± 0.4
60	131.9	25.6 ± 6.8	7.173 ± 0.02	-17.8 ± 1.3	130.6	6.3 ± 0.35	29.0 ± 1.41	9.9 ± 0.5	98.2 ± 0.1
75	133.8 ± 2.9	21.0 ± 7.7	7.232 ± 0.01	-17.1 ± 2.6	114.0 ± 29.25	6.4 ± 0.58	33.0 ± 4.24	11.3 ± 1.4	98.9 ± 0.1
90	132.6 ± 5.4	22.2 ± 14.1	7.209 ± 0.10	-17.9 ± 1.0	143.0 ± 52.38	6.7 ± 0.46	35.0 ± 2.83	11.9 ± 1.1	98.8 ± 0.2
105	134.2 ± 4.7	21.9 ± 16.5	7.190 ± 0.13	-19.1 ± 0.8	278.3 ± 89.78	6.5 ± 0.23	32.0 ± 8.49	11.0 ± 2.8	98.8 ± 0.1
120	132.1 ± 11.0	23.0 ± 17.0	7.180 ± 0.17	-10.3 ± 0.6	217.3 ± 22.59	7.1 ± 0.08	33.5 ± 7.78	11.5 ± 2.7	98.6 ± 0.7

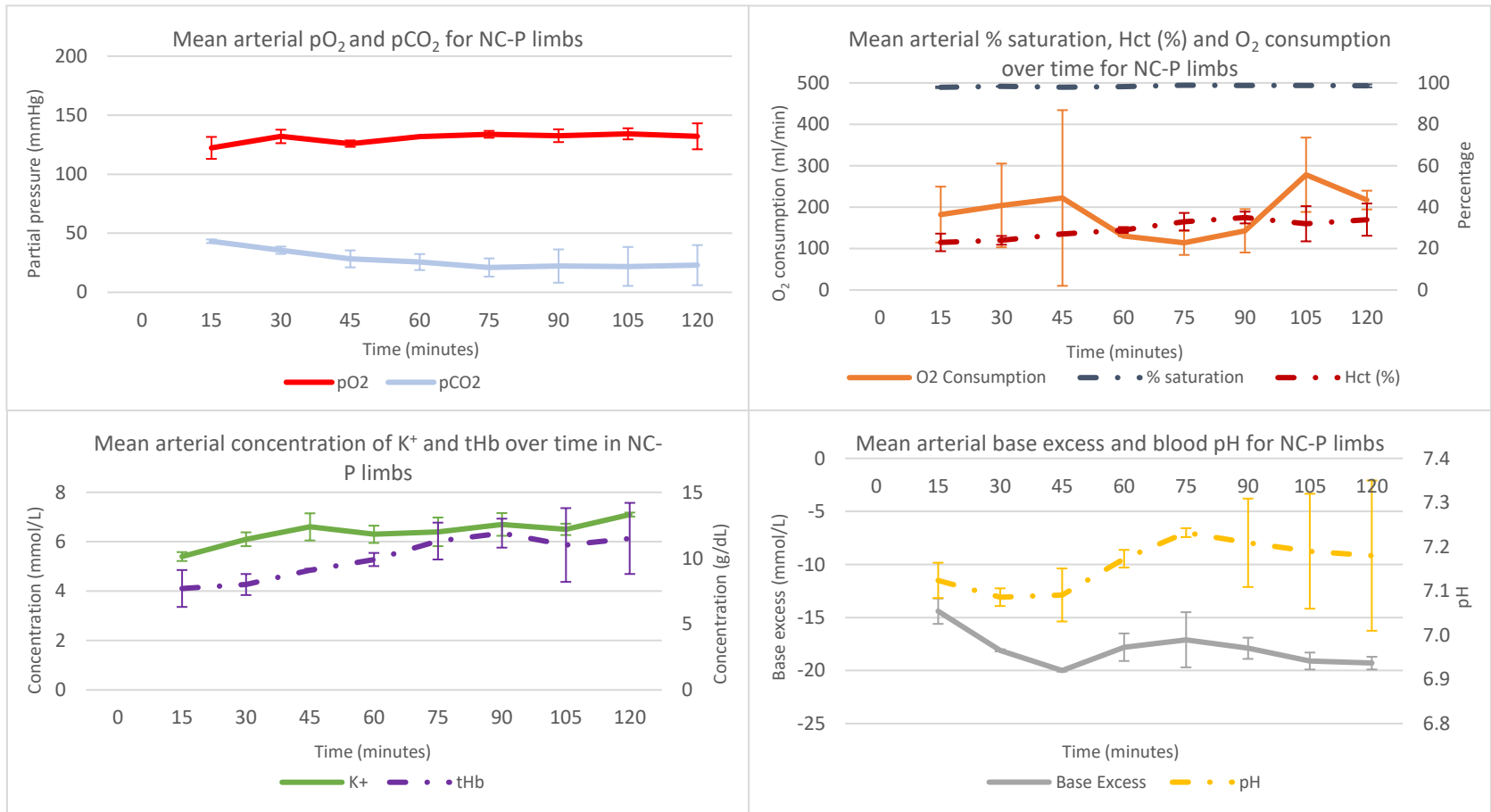


Figure 7-15: Mean arterial blood gas data for C-P limbs

Table 7-13: Mean and standard deviation of venous perfusion data at each time point for non-cooled - perfused limbs

Time (min)	pO₂ (mmHg)	pCO₂ (mmHg)	pH	Base Excess (mmol/L)	O₂ Consumption (ml/min)	K⁺ (mmol/L)	Hct (%)	tHb (g/dL)	V-Sat (%)
0									
15	45.9 ± 12.3	59.0 ± 10.7	7.010 ± 0.02	-15.8 ± 1.2	182.1 ± 67.54	5.7 ± 0.01	23 ± 4.24	7.8 ± 1.4	87.8 ± 5.2
30	46.5 ± 11.0	46.5 ± 15.9	7.006 ± 0.09	-19.0 ± 0.3	204.2 ± 101.12	6.2 ± 0.29	24 ± 2.83	8.2 ± 0.8	86.5 ± 7.9
45	47.7 ± 10.7	34.4 ± 10.9	7.029 ± 0.10	-20.8 ± 0.9	222.2 ± 212.09	6.5 ± 0.69	27 ± 1.41	9.2 ± 0.6	88.0 ± 7.4
60	43.7 ± 9.1	32.3 ± 10.9	7.120 ± 0.04	-18.0 ± 1.2	130.6	6.4 ± 0.21	30 ± 1.41	10.1 ± 0.6	88.6 ± 5.4
75	42.1 ± 3.5	32.2 ± 19.8	7.147 ± 0.08	-17.3 ± 2.4	114.0 ± 29.25	6.5 ± 0.42	35 ± 4.95	11.8 ± 1.5	88.9 ± 5.2
90	41.4 ± 6.6	27.1 ± 18.0	7.161 ± 0.13	-18.4 ± 0.4	143.0 ± 52.38	6.7 ± 0.45	36 ± 2.83	12.3 ± 0.9	88.0 ± 6.3
105	40.4 ± 1.1	28.5 ± 21.2	7.126 ± 0.16	-19.4 ± 0.4	278.3 ± 89.78	6.5 ± 0.06	33 ± 9.19	11.0 ± 3.1	85.7 ± 7.0
120	38.6 ± 13.0	28.8 ± 24.0	7.135 ± 0.19	-19.6 ± 0.6	217.3 ± 22.59	7.0 ± 0.11	35 ± 7.78	11.7 ± 2.6	86.9 ± 9.3

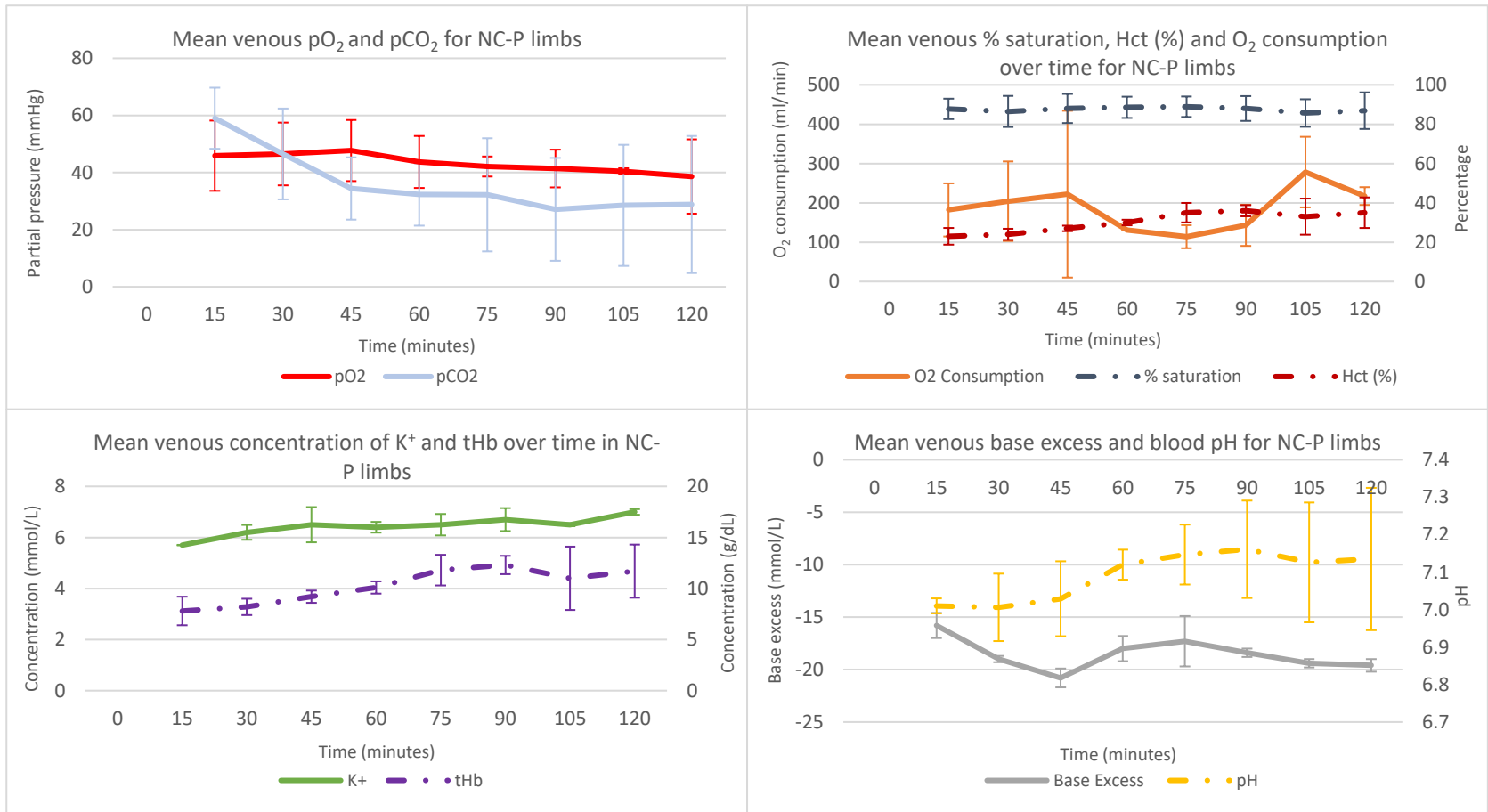


Figure 7-16: Mean venous blood gas data for C-P limbs

7.3.2.1.1. Thermal Imaging

Figure 7-18 and Figure 7-19 shows the thermal camera data from the NC-P 4 test. Again, the blood supply lines could clearly be seen in these images. The limb muscular tissue at the top of the limb got brighter and a more even yellow showing the tissue was warming up. The muslin used to keep the limb moist can also be seen with the purple colour at the distal end of the limb.

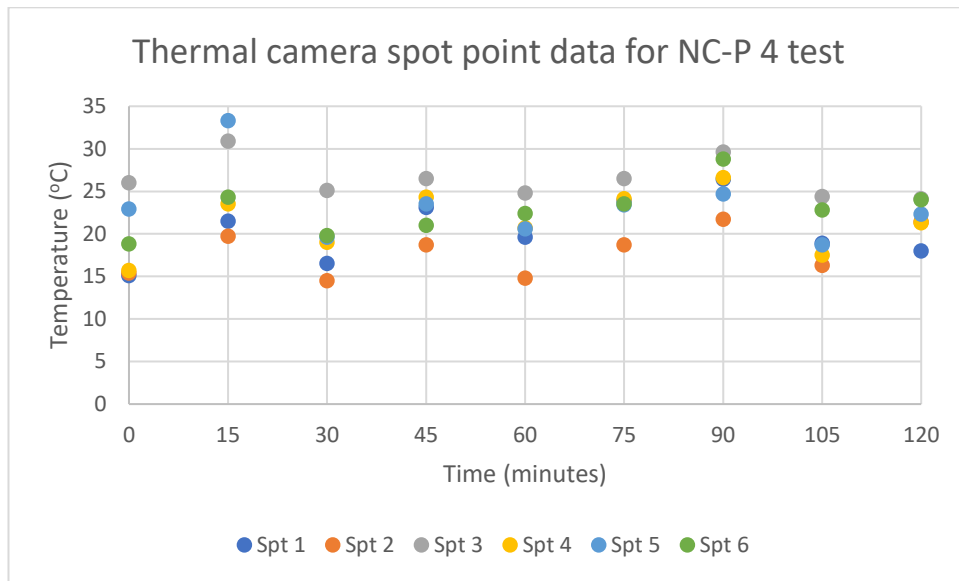


Figure 7-17: Example thermal camera spot point data for NC-P 4 test

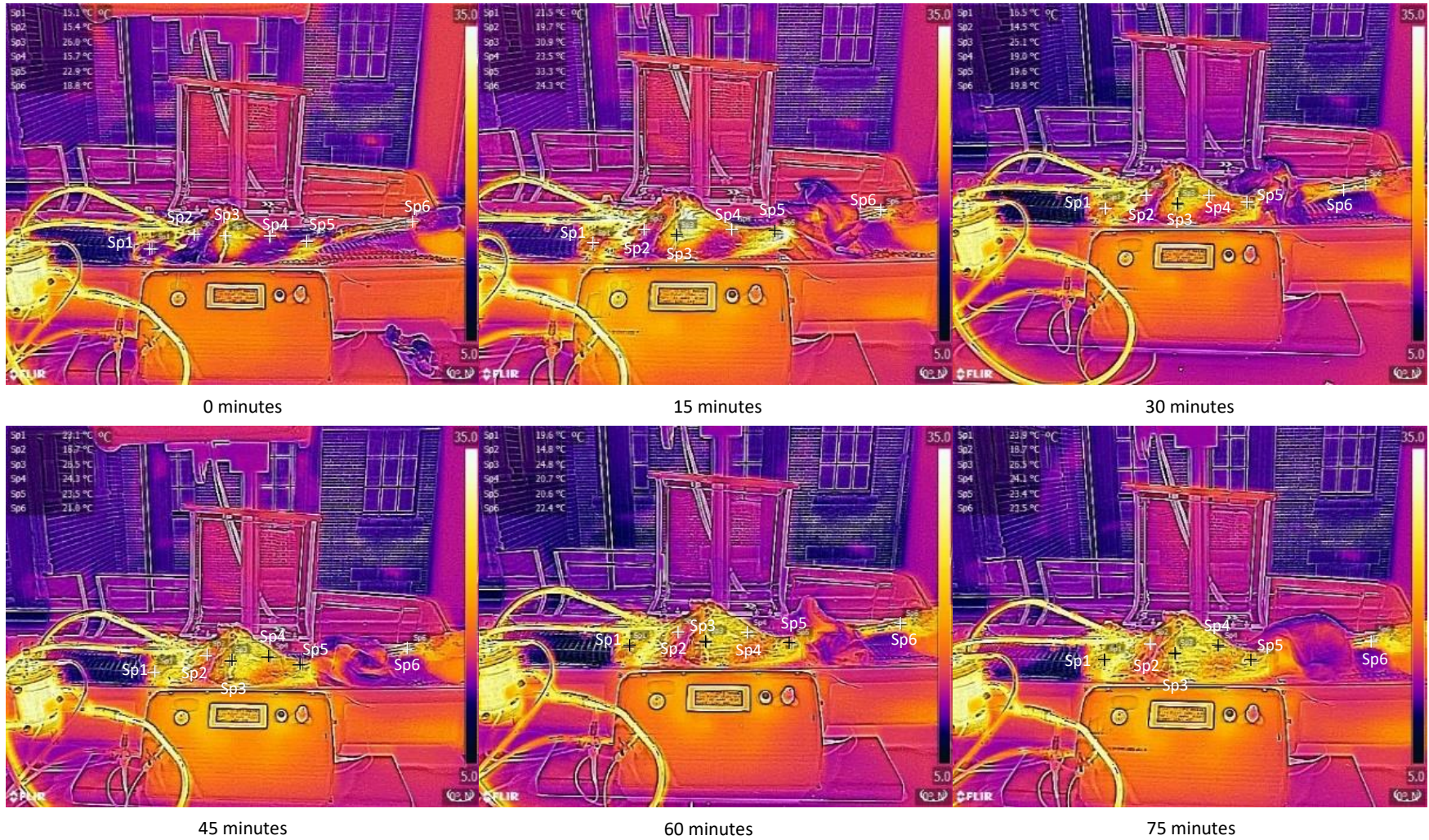


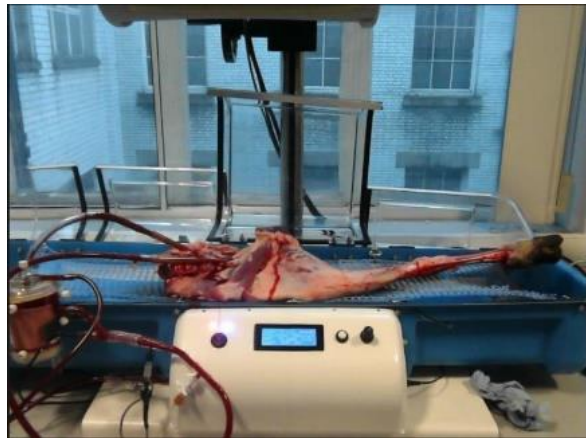
Figure 7-18: Example thermal camera images from NC-P 4 test (0-75 minutes)



90 minutes

105 minutes

120 minutes



Anatomical photograph

Figure 7-19: Example thermal images from NC-P 4 test continued (90-120 minutes)

7.3.2.1.2. LDI Imaging

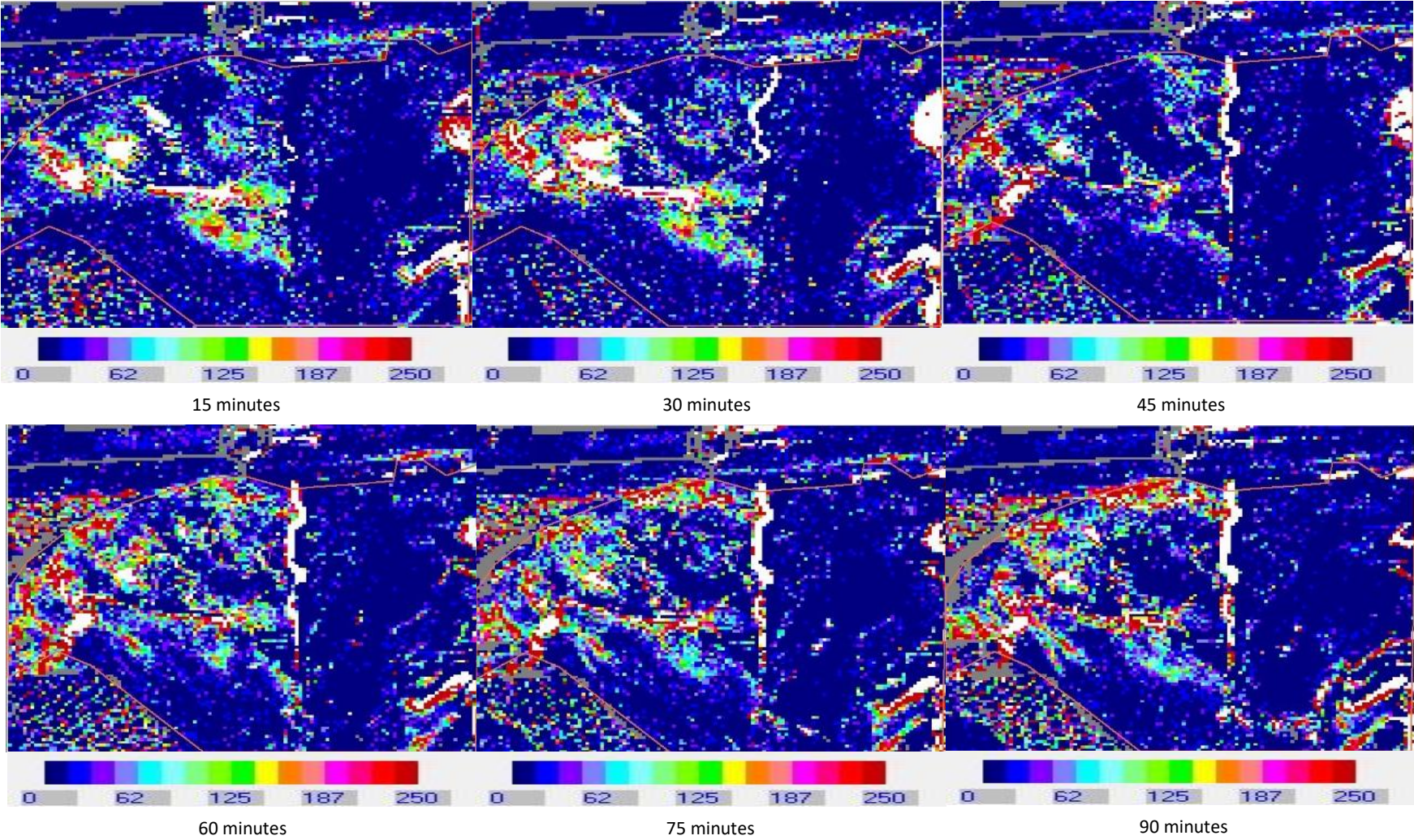


Figure 7-20: Example LDI data for NC-P 4 (15-90 minutes)

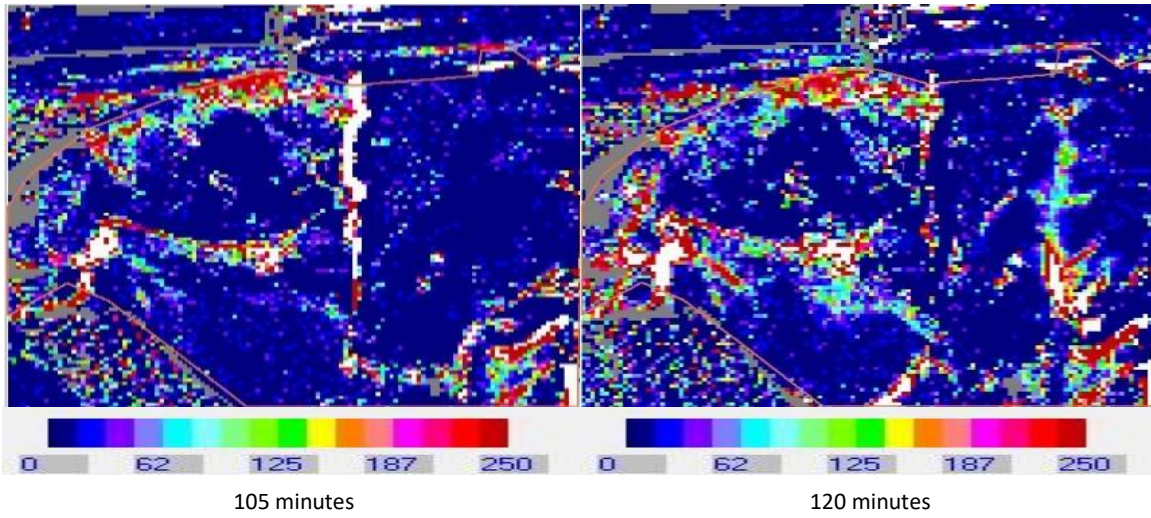
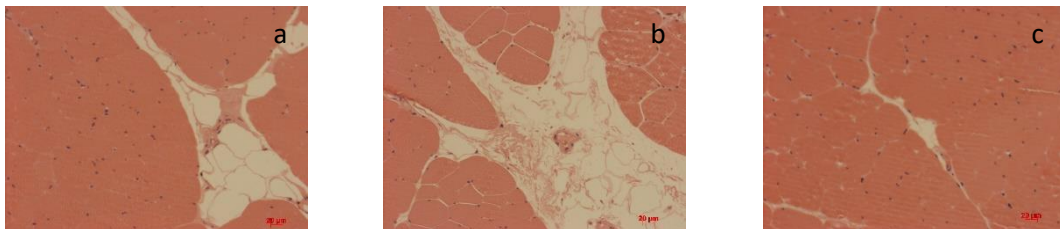


Figure 7-21: Example LDI data for NC-P 4 continued (105 and 120 minutes)

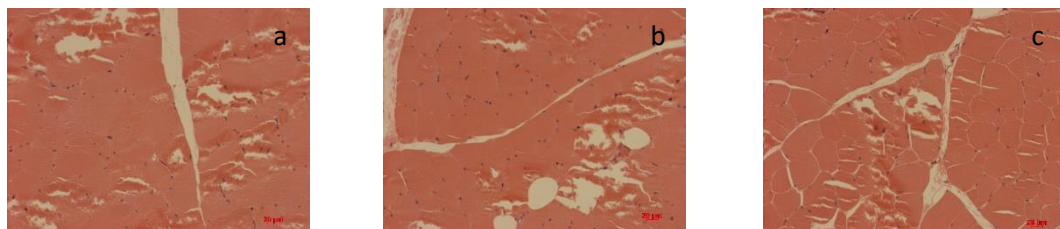
Figure 7-20 and Figure 7-21 show the LDI data from the NC-P 4 test. The laser doppler was positioned at further down the limb so the hammock supporting the limb can be seen in the bottom left corner of the LDI images. The white lines suggesting blood vessels could be seen developing from the first scan at 15 minutes. The increase in light blue across the 8 images points to the resumption of blood flow into the capillary bed. Interestingly, the areas of white which show the highest detected movement of blood cells appeared and disappeared between time points. This suggests that the areas with the highest blood movement were not consistent.

7.3.2.1.3. Histology:

Superficial



Mid



Deep

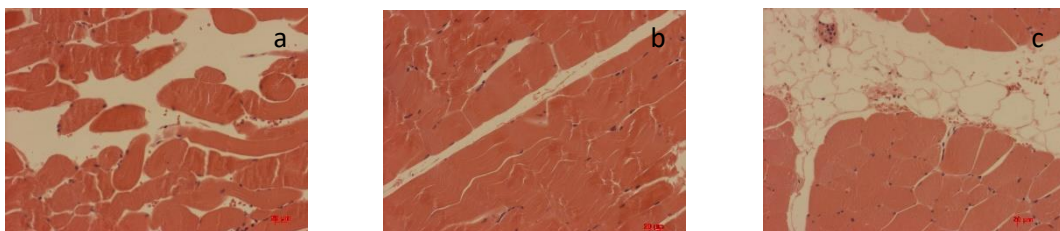


Figure 7-22: Example histology for NC-P 1

<i>Table 7-14: Histologist's notes for NC-P 1</i>		
NC-P 1 EP Superficial	19/2694	Myofibres appear viable; multifocal mild artifactual fragmentation. Few scattered parasitic cysts (Sarcocystis).
NC-P1 EP Mid	19/2695	Myofiber appear viable but with slightly indistinct borders; multifocal mild artifactual fragmentation, and scattered myofibres with slight condensation of the sarcoplasm.
NC-P1 EP Deep	19/2696	Myofibres appear viable; multifocal artifactual myofibre condensation with mild contraction and fragmentation. Few scattered parasitic cysts (Sarcocystis) and a single focal mild infiltrate of lymphocytes in the endomysium.

Figure 7-22 shows example histology data from the NC-P 1 test. As stated in the histologist's notes the myofibres appear viable. There is mild artifactual fragmentation in the superficial and mid tissues with artifactual myofiber condensation in the deep tissue. Similar to C-P 1 there is mild infiltrate of lymphocytes into the endomysium of the deep tissue and parasitic cysts scattered throughout the tissue.

7.3.3. Cooled – non-perfused limbs:

<i>Table 7-15: Mean and standard deviation of weight, temperature and nerve stimulation data for cooled - non-perfused limbs</i>	
Collection weight (kg)	3.61 ± 1.22
Temperature of deep tissue at collection (°C)	30.29 ± 3.66
Transport duration (minutes)	60 ± 0.00
Temperature of deep tissue on arrival (°C)	23.11 ± 2.87
Temperature change in the deep tissue (°C)	7.18 ± 3.26
Baseline nerve stim (mA)	65/ No twitch observed even at 130mA
End experiment (non-perfused) nerve stim (mA)	No twitch observed even at 130mA
Time since collection for EE nerve stim (minutes)	190 ± 0.00

The mean weight of the C-NP limbs shown in Table 7-15 was lighter than the mean weight of the C-P limbs. The mean deep tissue temperature of the C-NP limbs at collection was also lower than the C-P limbs. However, the temperature change in the deep tissue was greater in the C-NP tests than the C-P limbs. The mean temperature change in the C-NP tests was 7.18°C which was much closer to the target 10°C temperature change. Only two tests undertook a baseline nerve stimulation assessment. One of these tests achieved twitch at 65mA, the other could not produce a twitch at all even with 130mA. By the end of the experiment neither limb was able to twitch in response to the stimulation.

Figure 7-23 shows the thermal camera images taken during the C-NP 3 test. These images show the limb was getting cooler as evidenced by the dulling of the yellow colour in the muscular tissue.

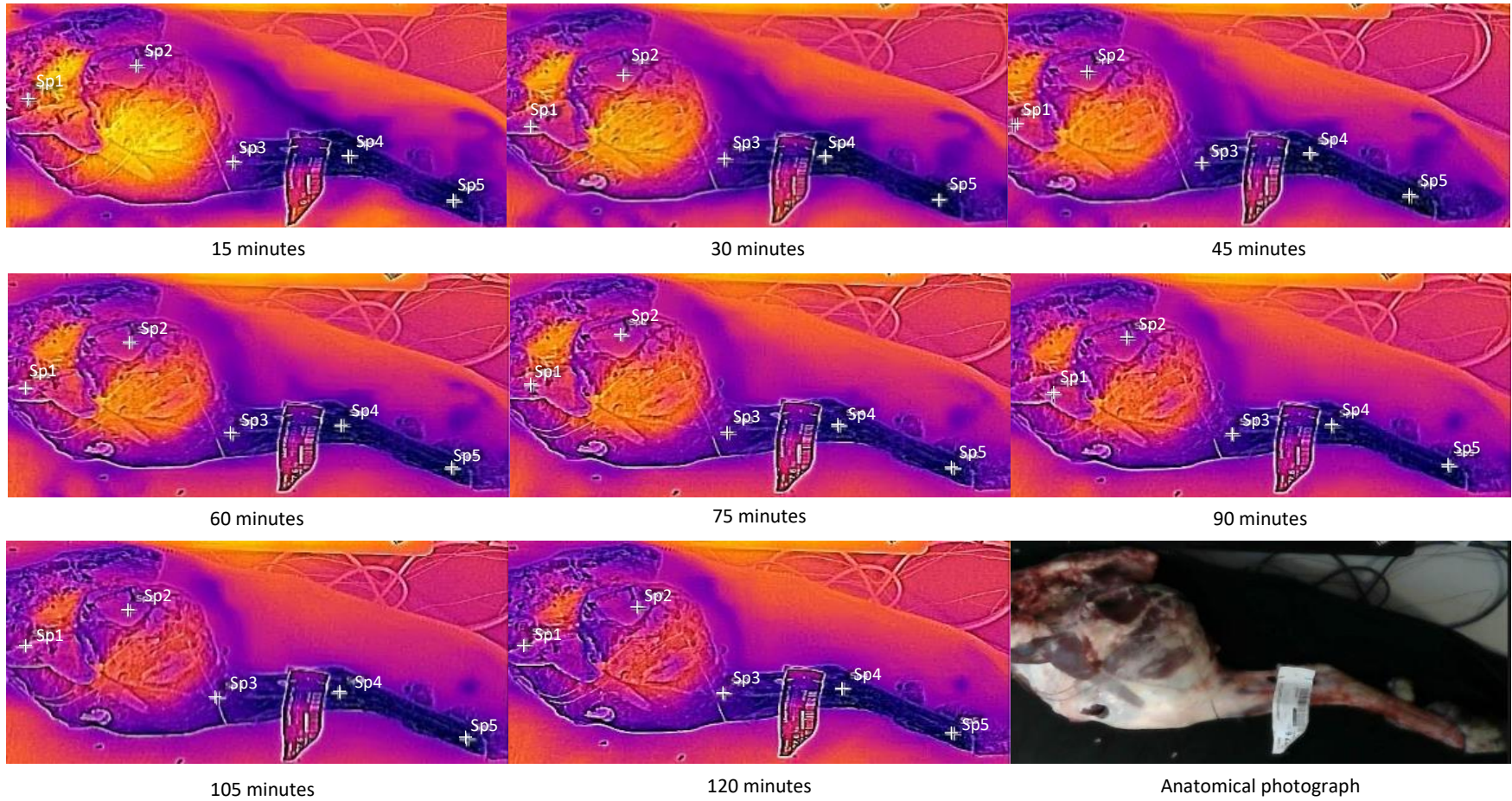


Figure 7-23: Example thermal camera data for C-NP 3 test

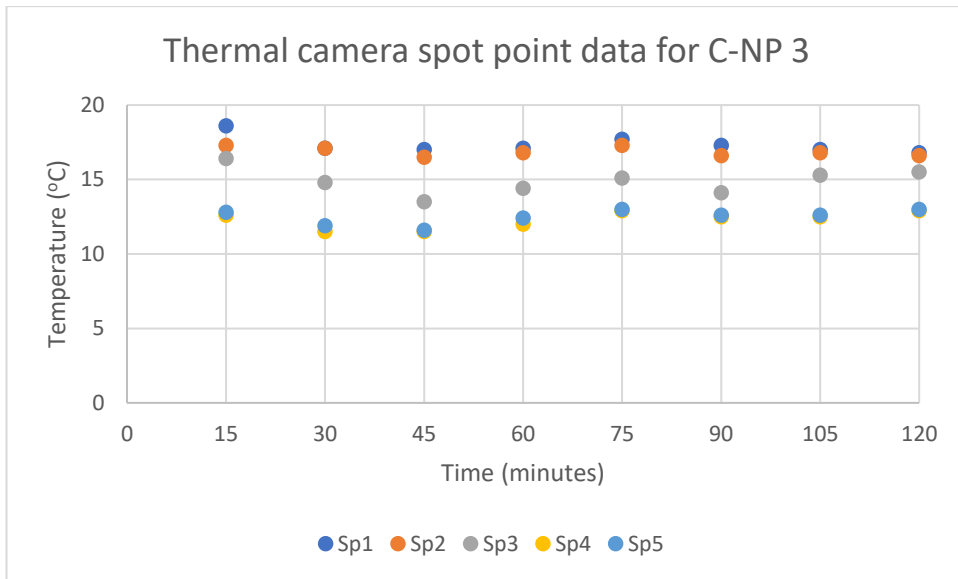


Figure 7-24: Example thermal camera spot point data for C-NP 3 test

7.3.4. Non-cooled – non-perfused limbs:

<i>Table 7-16: Mean and standard deviation of weight, temperature and nerve stimulation data for non-cooled - non-perfused limbs</i>	
Collection weight (kg)	3.96 ± 0.59
Temperature of deep tissue at collection (°C)	N/A
Transport duration (minutes)	59 ± 1.34
Temperature of deep tissue on arrival (°C)	N/A
Baseline nerve stim (mA)	33 ± 26.46
End experiment nerve stim (mA)	No twitch seen even at 130mA
Time since collection for EE nerve stim (minutes)	215 ± 37.16

Table 7-16 shows that the baseline nerve stimulation tests were associated with a twitch at a mean of 33mA stimulation. However, by the end of the test period there was no measurable response in any of the experimental preparations irrespective of stimulation amplitude (130mA maximum)



Figure 7-25: Anatomical picture of NC-NP 5 limb

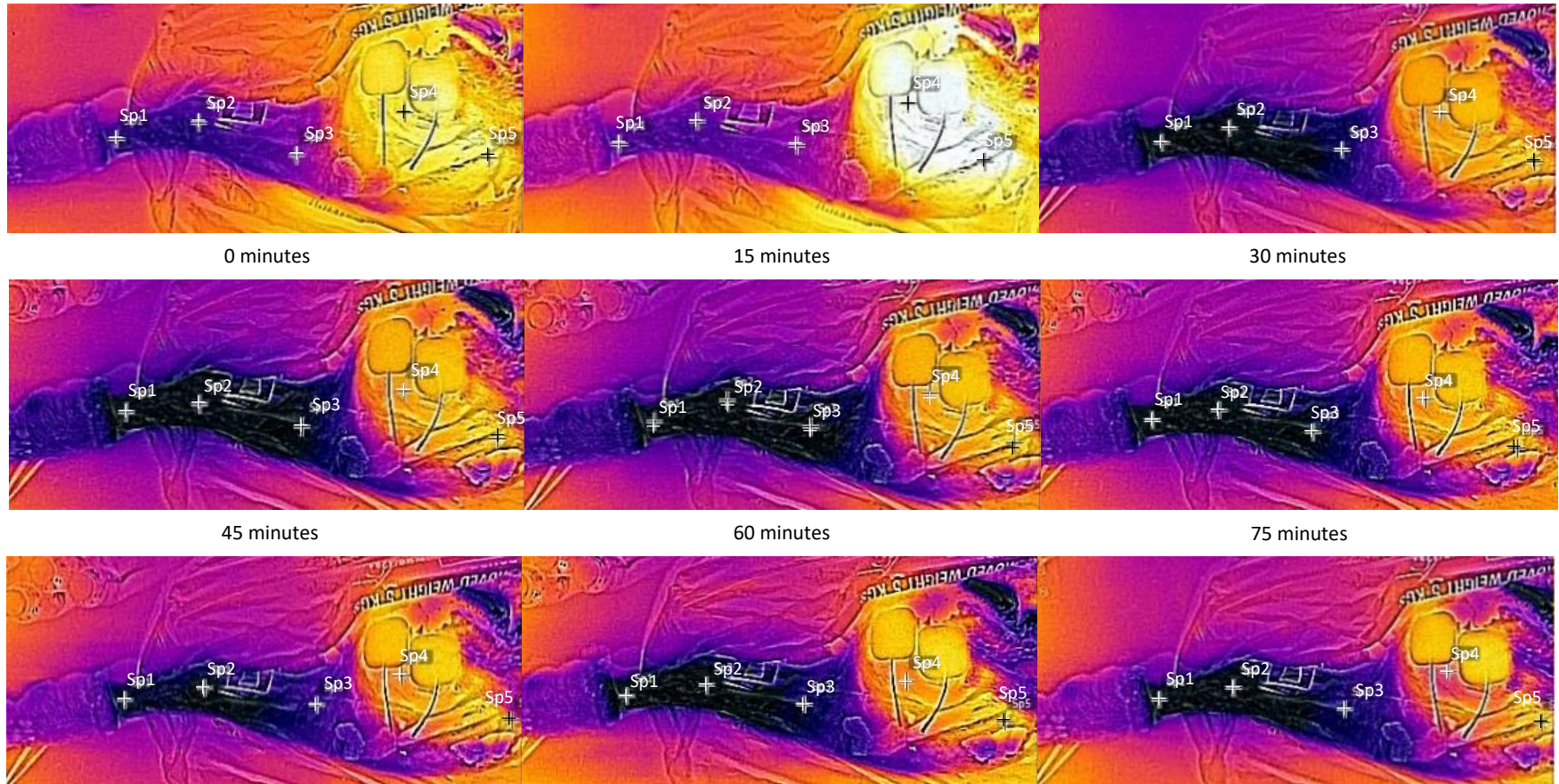


Figure 7-26: Example thermal camera data for NC-NP 5 test

Figure 7-26 shows the thermal camera photographs taken during the NC-NP 5 test. The nerve stimulation pads can be seen on the muscle in these photographs. The photos show the limb was cooling down as the distal end of the limb turned black and the muscle changed from a bright yellow to purple.

The thermal photographs clearly show the difference in limb temperature when perfused as seen in Figure 7-9, Figure 7-10, Figure 7-18, Figure 7-19 compared to no perfusion as seen in Figure 7-23 and Figure 7-26.

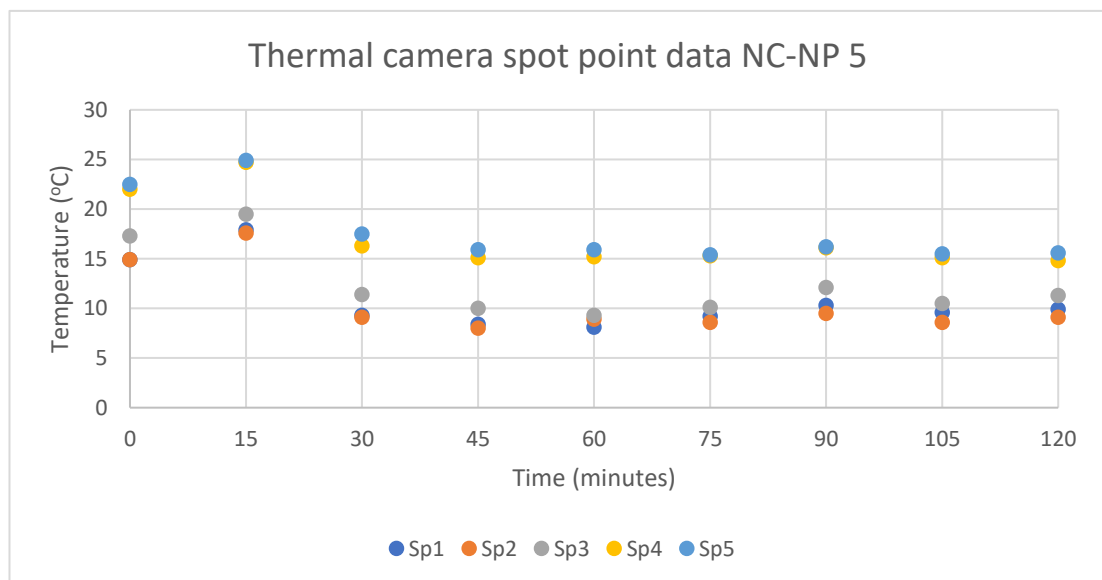


Figure 7-27: Example thermal camera spot point data for NC-NP 5 test

7.3.5. Cooling data:

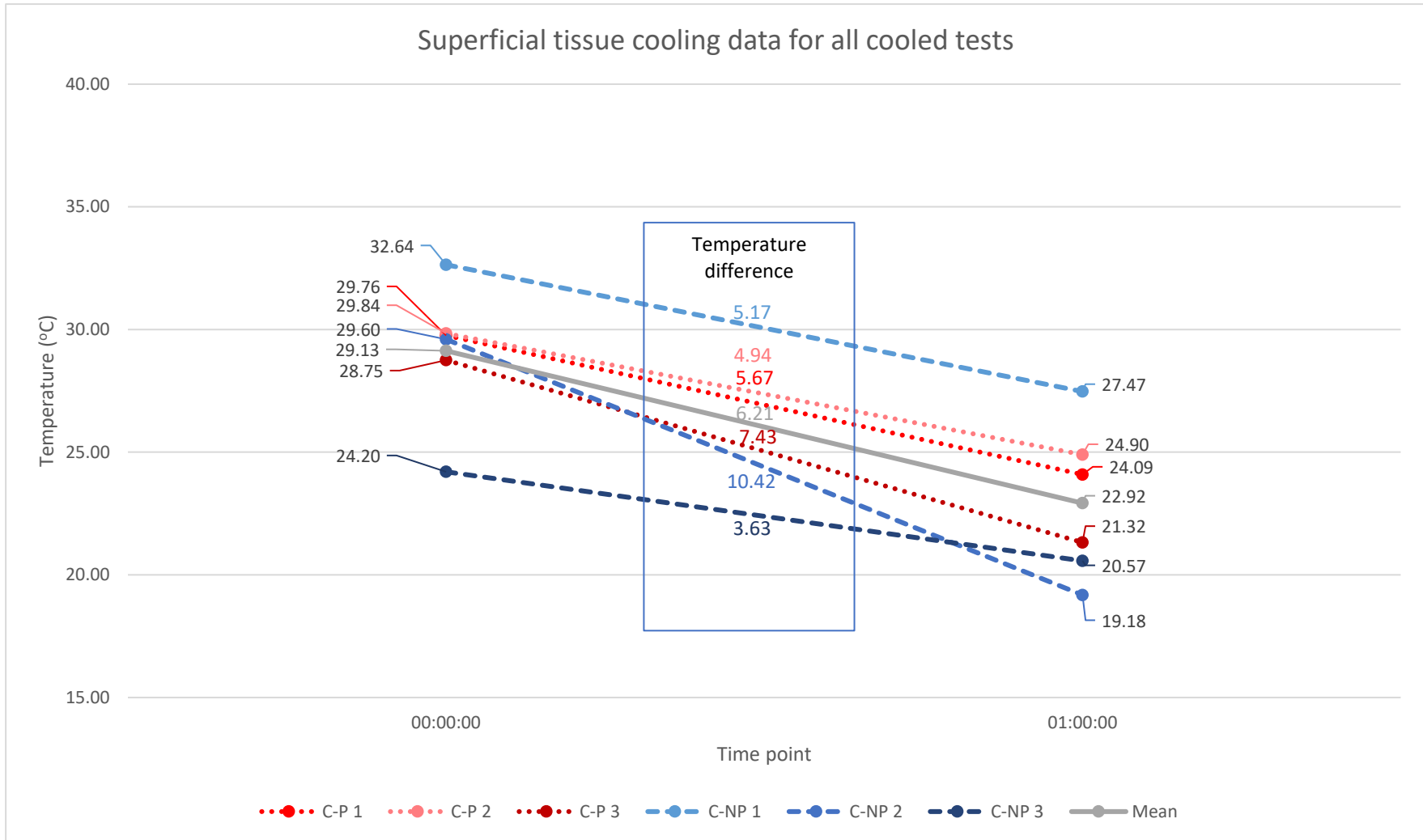


Figure 7-28: Start and end temperatures in the superficial tissue for all cooled tests

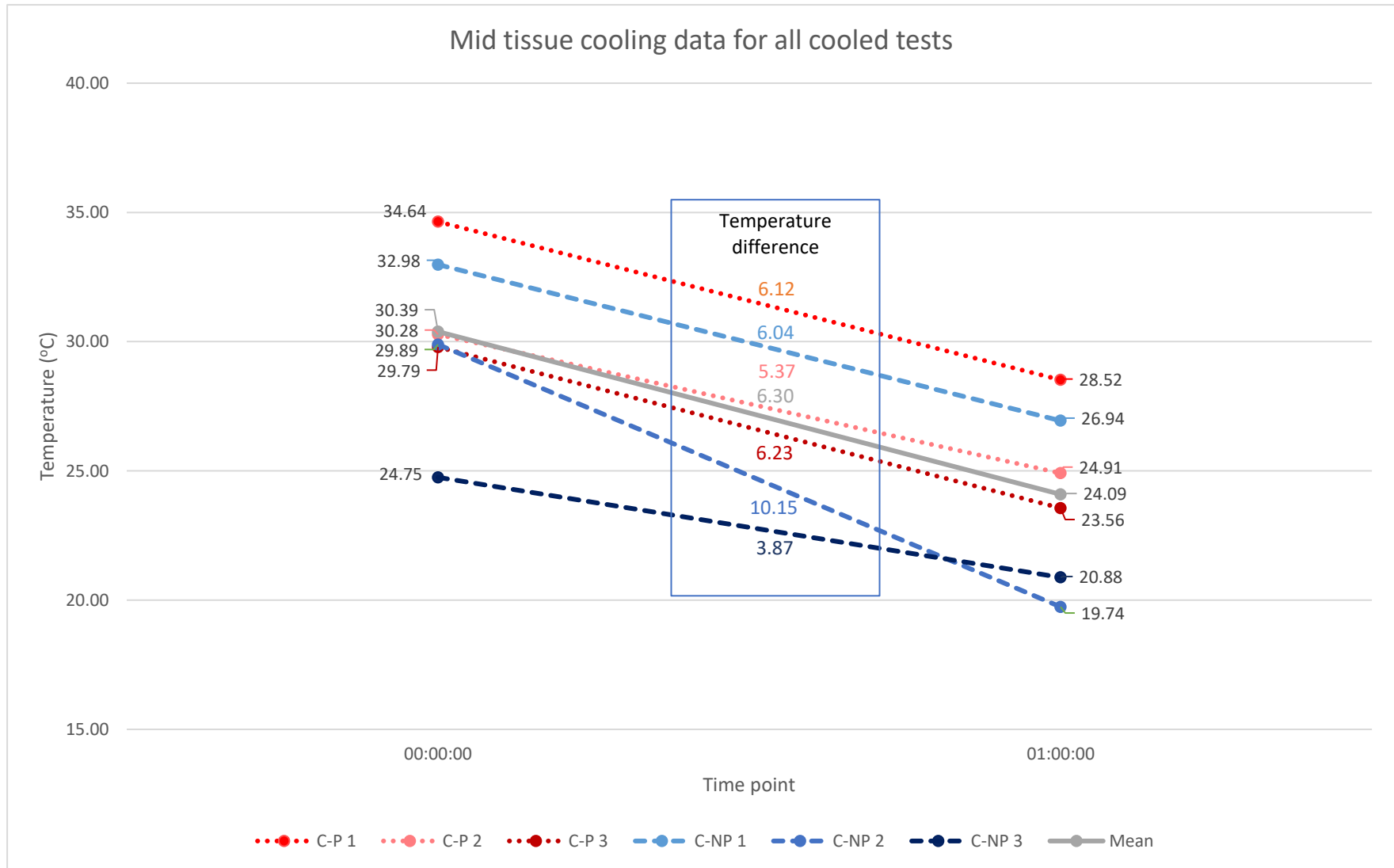


Figure 7-29: Start and end temperatures in the mid tissue for all cooled tests

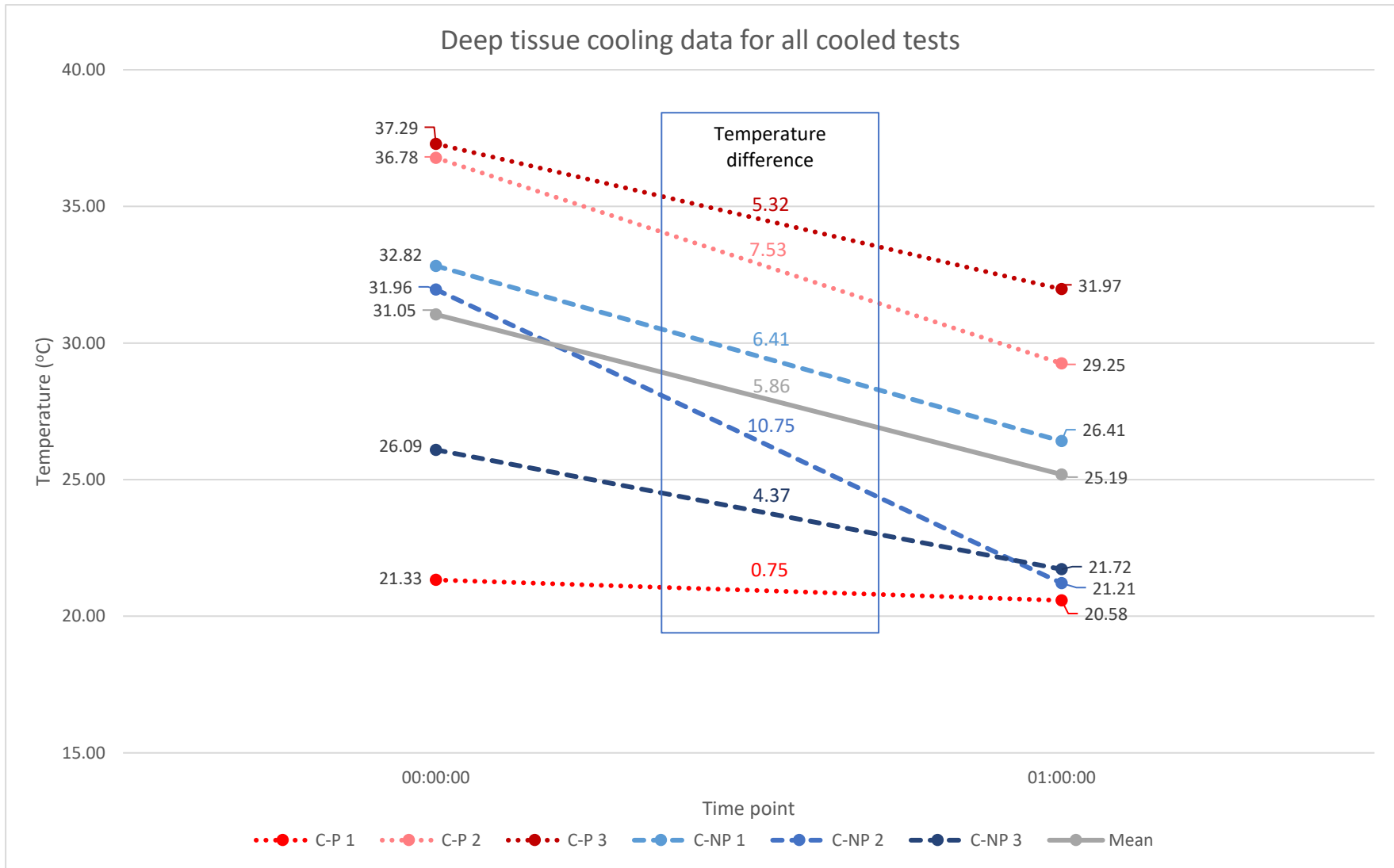


Figure 7-30: Start and end temperatures in the deep tissue for all cooled tests

Table 7-17: Mean temperature change for cooled and non-cooled tests		
<i>Tissue depth</i>	<i>Cooled tests (°C)</i>	<i>Non-cooled tests (°C)</i>
Superficial	6.21 ± 2.40	1.39 ± 0.97
Mid	6.30 ± 2.08	3.64 ± 1.84
Deep	5.86 ± 3.34	5.23 ± 0.28

Figure 7-28, Figure 7-29 and Figure 7-30 show the temperature change at each tissue depth produced during the transportation period. As these graphs show, there was a wide variety in the temperature of the tissue upon collection. Interestingly, the test which had the lowest starting deep tissue temperature (C-P 1) had the warmest starting temperature in the mid tissue. Other than in test C-P 1 and C-NP 1 the deep tissue started off with the warmest temperature. In test C-NP 1 the 3 tissue depths were at a very similar temperature with only 0.34°C separating them. Test C-NP 2 was the only time when the temperature of the deep tissue was reduced by the target 10°C. This temperature reduction was also achieved in the mid and superficial tissue during this test. The mean temperature reduction in the deep over all tests was 5.86°C. C-NP 2 had a much faster rate of cooling compared to the other tests and C-NP 1 had a much slower rate of cooling. However, other than this the steepness of the line for the other tests was similar suggesting the rate of cooling was similar.

7.4. Results analysis:

As has already been mentioned, only one test was able to reduce the temperature in the deep tissue by the target 10°C during active cooling. Nevertheless, 4 of the 6 tests did end up with a deep tissue temperature drop of over 5°C which should give rise to a 25% reduction in metabolic activity. However, 2 of the 3 non-cooled tests also produced a drop in temperature of 5°C (data not shown). In fact, when the temperature reduction in the cooled tests is compared to the non-cooled tests, there is not a significant difference ($p=0.809$) in the temperature decrease observed in the deep tissue, as shown in Table 7-17.

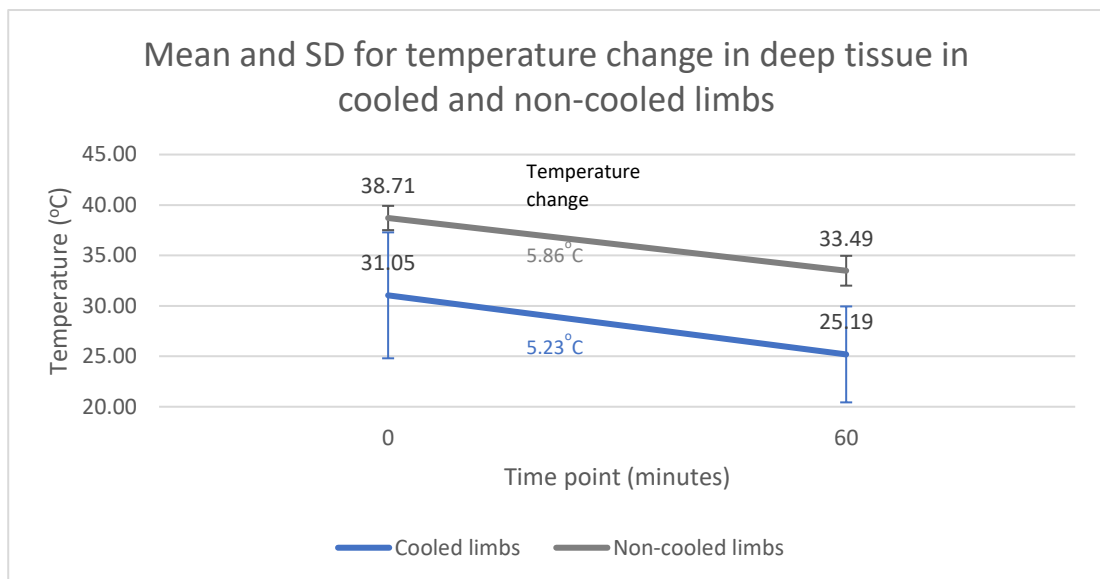


Figure 7-31: Mean temperature change in deep tissue for C and NC limbs

This suggests that by the level of the deep tissue, the combination of topical CO₂ and coolant fluid was not able to achieve cooling. This is contrary to the results from the small-scale tissue tests in Chapter 5 where it was found that the deep tissue temperatures were statistically colder at the end of the experiment compared to tissues with no cooling ($p=0.036$). The main reason for this difference in inability to achieve cooling could be explained by the separation

of the CO₂ into 16 different streams in the cooling sock. By distributing the gas over the limb, the heat transfer is decreased due to a smaller volume of gas being available for heat exchange in any one area. Thereby, the heat removed by using 6 bottles of CO₂ will be less with the cooling sock, even if the coolant fluid is added. Moreover, the mean weight of the ovine limb upon collection was 4.22kg which is much greater than the weight of the tissue sample used in the small-scale tests. Therefore, the same amount of CO₂ is being split into 16 streams and is being used to cool something with a much greater mass. Understandably, the temperature change is not as large.

As has been mentioned in previous chapters, the speed at which the CO₂ was released will have an effect on how rapidly the tissue cools. This is likely to have factored during the ovine limb tests. However, the slight change in the speed of CO₂ release is unlikely to be responsible for the 10°C difference in temperature change in the deep tissue between test C-P 1 and C-NP 2. Although both of these tests were outliers compared to the temperature change produced during the other cooling tests, other factors may have had an impact to alter the temperature change so greatly. The environmental temperature on both days was 13.5°C so this would not have made a difference to the rate of heat loss if the deep tissue started off at the same temperature. The starting temperature for C-P 1 was much lower so the temperature gradient between the deep tissue and ambient temperature was less which will have result in a slower heat exchange from the tissues.

Another factor which is likely to have had a big effect on end temperature in the deep tissue is the location of the thermocouple in comparison to the output nozzles of the cooling sock. The further the tissue was from the CO₂ outlet nozzle, the less the tissue will have cooled as

the CO₂ will have warmed up as it passed over the tissue in between. Therefore, since the C-NP 2 test consistently had the greatest tissue temperature change across all 3 tissue depths, it is possible that the thermocouples were inserted into the muscle directly beneath one of the cooling nozzles. When the limbs were harvested they were skinned down to the ankle, as is likely to be standard practice at the abattoir. However, this meant that there was no skin and fatty tissue over the muscle. The fatty tissue will provide insulation against topical cooling. The lack of fatty tissue should be taken into consideration when analysing the temperature results as removing this insulation will have made topical cooling more effective.

The thermocouples were inserted into the tissue using a needle in these tests. This enabled the thermocouple to be placed in the middle of a muscle rather than the top of the leg as was the case in the porcine limb tests. The benefit of placing the thermocouple into the centre of the muscle was that you can see how the muscle is cooled by the topical cooling alone. However, the thermocouples were still not placed directly into the deep tissue, as demonstrated in Figure 7-32 on the next page (image not to scale). This meant that the temperature, and thereby the cooling, of the very deep tissue could not be monitored. The indications are that fairly peripheral tissue was cooled by around 5°C, it's reasonable to assume therefore that the very deep tissue is likely to experience cooling to a lesser degree. This requires further investigation.

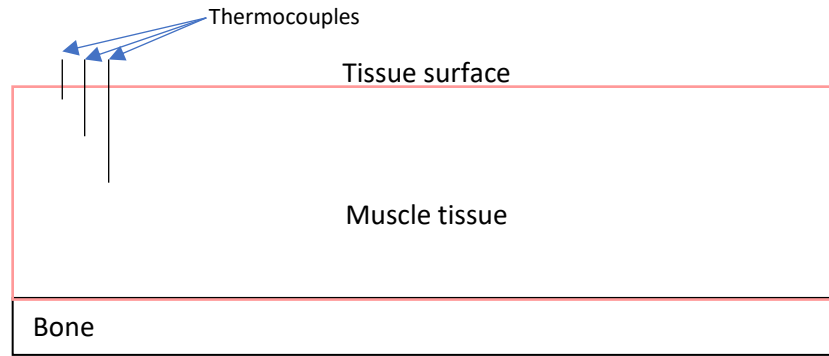


Figure 7-32: Demonstration of thermocouple location compared to muscle tissue depth. (Image not to scale)

As shown in Figure 7-28 - 7-30 the temperature change at all 3 tissue depths was similar between the 6 cooled tests, except for C-P 1 where there was 5°C difference in the temperature change. Furthermore, the starting temperatures in all the C-NP tests were similar across all 3 depths, in tests C-P 2 and C-P 3, the deep tissue was much warmer. However, the temperature change was still similar at each depth. On the other hand, in C-P 1 the mid tissue was the warmest to start off with but had a similar temperature change to the superficial tissue. This suggests that there was a fault in the thermocouple placed in the deep tissue and it wasn't recording the temperatures correctly. In fact, after this test, the input ports used for the thermocouples were changed.

Table 7-5 and Table 7-12 show the mean arterial perfusion data at each sample time point for the C-P and NC-P limbs. There is a lot of interesting information to be drawn from these tables. The first is the K^+ values. The mean K^+ value at 15 minutes for the C-P limbs was within the normal range ($3.5-5.0\text{mmolL}^{-1}$). At every time point after the K^+ value increased to a point of severe hyperkalaemia from 60 minutes as illustrated in Figure 7-33. For the NC-P limbs, the mean K^+ value did start off showing signs of mild hyperkalaemia. Again, at each time

point the value of K^+ increased until severe hyperkalaemia at 120 minutes. The C-P limbs reached a point of severe hyperkalaemia 60 minutes before the NC-P limbs.

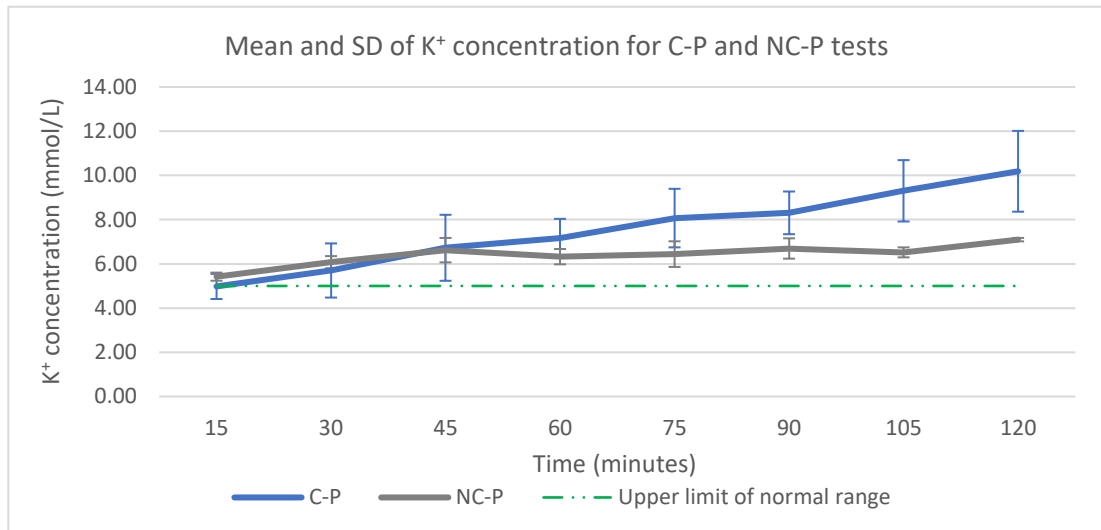


Figure 7-33: Mean potassium concentration for C-P and NC-P tests

When the data was statistically analysed using a one-way ANOVA, the value of arterial K^+ at 120 minutes for the C-P limbs was statistically higher than the NC-P limbs ($p = 0.005$). Furthermore, at 120 minutes the K^+ value for the NC-P limbs was not statistically different from both the C-P limbs and the NC-P limbs at 15 minutes. This shows that the C-P limbs had a very large influx of K^+ into the bloodstream. One possible reason for the hyperkalaemia is haemolytic events associated with high flow, high pressure and shear in combination with a fragile blood product.

Some amount of tissue destruction would be expected within the limbs, they had not had perfusion for at least 60 minutes when the perfusion began. The collection temperature of the C-P and NC-P limbs were statistically similar suggesting that the warm ischaemic time, and thereby tissue destruction, for both would be about the same. Furthermore, as perfusion progressed and blood returned to the dying tissues, more K^+ would enter the blood as the K^+ would need to be carried away from these points. This can account for a small increase in the

K⁺ value seen in the NC-P limbs. Especially since the limbs were not actively cooled so the rate of enzyme action would not be decreased. The large increase in the K⁺ value over perfusion for the C-P limbs is not expected as this suggests greater tissue destruction.

There are a few things that could have caused the increased tissue destruction in the C-P limbs. The first is the cannulation time. The time taken to cannulate the NC-P limbs was 14.33±12.5 minutes, for the C-P limbs it was 39±20.3 minutes. This extra cannulation time provided an extra 25 minutes of ischaemia for the C-P limbs which would have given rise to further tissue damage. Additionally, there could be rhabdomyolysis in response to the insult of cooling the limbs. Although cryotherapy and therapeutic hypothermia are used frequently in medicine with little effect on the tissues, the method of cooling used in this technology has not been tested. Although the coolant fluid is not cytotoxic it has not been certified as biocompatible. Moreover, atmospheric CO₂ concentrations are obviously not cytotoxic. The histology results will help to establish if the method of cooling itself is damaging the limbs in any way.

The C-P limbs had a 12.22±6.23% increase in weight from the collection limb weight. This was in contrast to the 24.72% increase from collection weight seen in NC-P 4 (the only NC-P test with both collection and end perfusion weight). There was an increase in arterial haematocrit throughout perfusion in both the C-P and NC-P limbs. An increase in hct indicates that fluid was being lost somewhere in the circulatory circuit. The fluid was likely to have been passing out of the small vessels into the interstitial space leading to an increase in oedema. This theory could be backed up by the increase in weight of the limbs over the course of perfusion. However, the increase in weight will not have been entirely due to oedema, the limbs will

have been drained of most of the blood at the abattoir. After perfusion there will have been residual blood left in the limbs.

The arterial base excess decreased during perfusion for both the C-P and NC-P limbs. Nonetheless, the base excess decreased by a bigger amount in the C-P limbs. The mean base excess at 120 minutes was significantly lower ($p=0.005$) in the C-P limbs than the NC-P limbs at the same point. The mean base excess value in the NC-P limbs at 120 minutes was not significantly different from the starting values of both the C-P and NC-P limbs. The change in base excess corresponded to a decreasing pH in the arterial blood during the C-P tests. The arterial pH in the NC-P limbs had minor fluctuations during perfusion but ultimately the values stayed steady. However, the pH value was not significantly different between the C-P and NC-P limbs at either 15 minutes or 120 minutes. A low base excess indicated metabolic acidosis and the addition of acid into the blood.

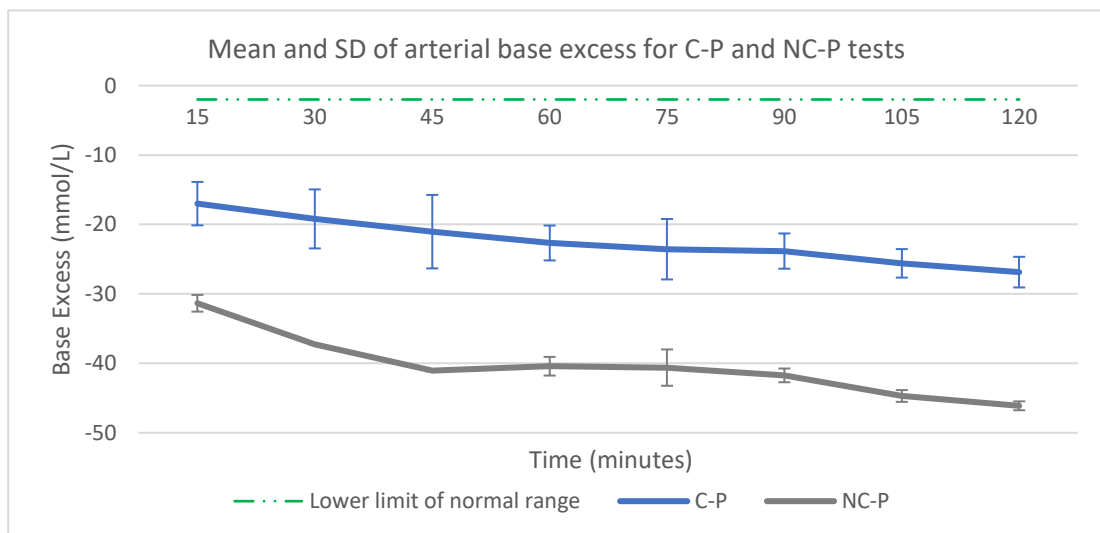


Figure 7-34: Mean arterial base excess for C-P and NC-P limbs

The acid could have been the result of a few causes. The first is from the production of lactic acid. The ischaemic limbs would have had to perform anaerobic respiration to maintain

energy production due to the lack of O₂. This will have resulted in the formation of lactic acid as a by-product of this reaction. When the blood returns to the tissues the lactic acid would have been excreted into the blood to be carried away as a waste product resulting in a lower blood pH. The lactate values for all the perfusion tests started off at least 6 times higher than the normal range and got higher throughout perfusion which supports this theory.

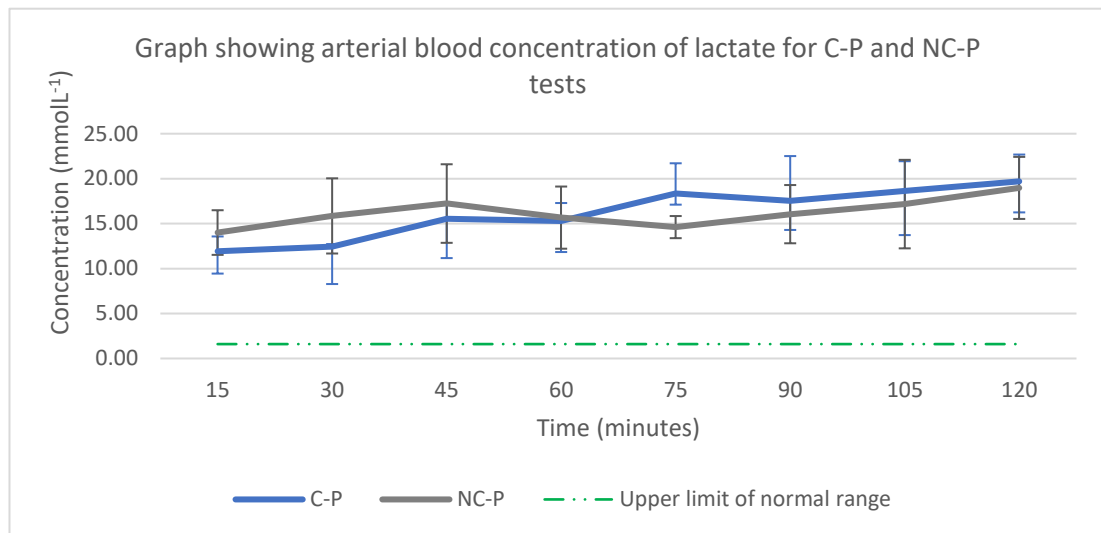


Figure 7-35: Mean arterial lactate concentration for C-P and NC-P limbs

Thus far the histology samples taken were only analysed for C-P 1 and NC-P 1. This means that no full conclusions can be drawn from the histological data so far. However, the results for C-P 1 do suggest that the myofibers were still viable meaning that the technology had preserved the tissue and at this point the tissue could be salvaged. Interestingly the histological results for NC-P 1 were similar in terms of the preservation of tissue viability. However, the nerve stimulation suggested that the tissue is no longer viable. It will be interesting to see if this variation between nerve stimulation and histology persists in the other samples.

The artifactual fragmentation present in all 3 tissue depths in the C-P 1 sample was likely to be from the sample acquisition or processing. C-P 1 had a few parasitic cysts present in the mid and deep tissue. The presence of these cysts shows that more samples were needed because there are other factors which could have affected how well the tissue is able to be withstand the novel technology. The mild eosinophilia present in the deep tissue was most likely an increased immune response triggered by the presence of parasitic cysts rather than in response to the technology. However, it is still possible that the increased immune response was triggered by the technology. Histological analysis of the other samples will help to determine this. The histology samples which have been analysed thus far suggest that the increase in K^+ was not due to rhabdomyolysis as there are few signs of tissue destruction. Therefore, the K^+ was more likely to be associated with haemolysis. However, more histological samples need to be analysed to be able to determine the relationship between the blood results and tissue viability.

Analysis of data suggests that the NC-NP limbs were more responsive at the end of transport than the C-NP limbs. The results from the ovine limb tests show that perfusing the limbs had a direct result on the ability to produce twitch at the end of the 2-hour perfusion period. At the end of the tests with no perfusion no twitch could be achieved even with 130mA. This suggests a complete loss of tissue viability. The complete loss of a twitch at the end of the test period in the NC-NP limbs showed that there was greater tissue degradation in the non-perfusion period compared to the C-NP limbs as demonstrated by the reduction of the twitch threshold of the NC-NP limbs by an additional 32mA over the test period. The fact no end perfusion twitch could be achieved in the NP limbs is unsurprising. By this point the limbs would have been under ischaemic conditions for at least 3 hours, longer than the maximum

warm ischaemic time indicated in the data whereby tissue viability will remain (Perkins *et al.*, 2012). Nonetheless, the aim of cooling the tissues was to preserve tissue viability. Judging by the ability to produce twitch, even the C-NP limbs were no longer viable. This is contrary to expected results. One possible explanation for this is that the tissue was not cooled at a great enough depth to be able to preserve the muscle viability. Another explanation is that, as discussed previously, the CO₂ actually had a damaging effect on the tissues, which combined with the ischaemia resulted in the loss of viability. Nevertheless, it should be born in mind that muscle twitch alone is not a reliable indicator of muscle viability.

Another factor that could have affected the twitch seen in the non-perfused limbs at the end of the test was the amount of Ca²⁺ available to the muscle cells. The limbs were being stimulated many times, especially if twitch could not be seen as the muscle was stimulated at increasing amplitudes. The Ca²⁺ could not be replaced after the initial stimulation seeing as perfusion was not present. Therefore, excessive stimulation may have exhausted the supply of Ca²⁺ so the muscle could not contract even if it was still viable. The Ca²⁺ in both the C-P and NC-P limbs was at a similar concentration in the blood (mean C-P 0.89±0.03mmol/L and mean NC-P 0.91±0.01mmol/L). This is greatly below the normal range of Ca²⁺ in the blood which is 2.2-2.7mmol/L (Goldstein, 1990). Therefore, it is feasible that the Ca²⁺ was at the same concentration in the non-perfused limbs so the supply in the static blood would quickly have become exhausted.

The mean threshold for EP nerve stimulation for the C-P tests was 50 ± 69.31 mA compared to 22 ± 13.50 mA for the NC-P tests. The baseline stimulation threshold value for the NC-P limbs was 85mA (NC-P4) compared to 21 ± 20.51mA for the C-P limbs. However, the C-P 2

test had a nerve twitch threshold of 130mA. This experiment had a very high perfusion pressure and a jelly like substance was seen in the tissue when histology samples were taken suggesting that the limb tissue had been damaged which would reduce the chance of twitch. When the mean for the C-P tests was calculated without C-P 2 it is 10 ± 2.83 mA. This data shows that the NC-P limbs had a much wider range of EP twitch threshold than C-P1 and C-P3 due to the larger standard deviation. The C-P limbs also had a lower twitch threshold when the data for C-P 2 is removed. This suggests that cooling the limbs did help to preserve tissue viability to some extent.

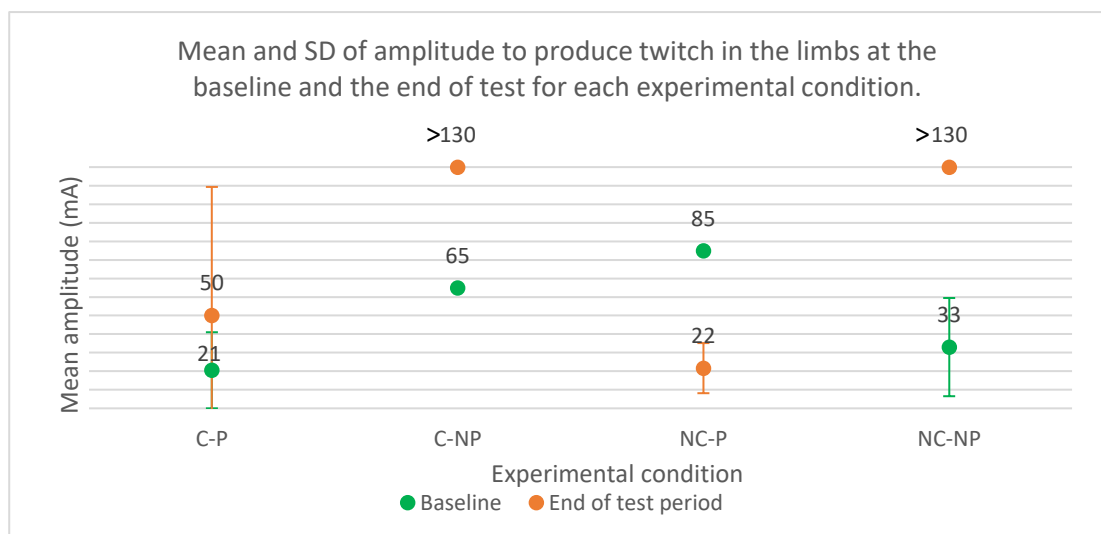


Figure 7-36: Mean baseline and end of test amplitude needed to initiate twitch for each experimental condition

The neural stimulation baseline values suggest that cooling the limb before perfusion did have an effect on tissue viability. The mean baseline amplitude to produce twitch in the cooled limbs was 35 ± 29.50 mA whilst in the non-cooled limbs it was 43 ± 32.65 mA. One limb in both the cooled and non-cooled limbs could not be stimulated to produce twitch and was discounted from the mean. Although the cooled limbs had a lower mean amplitude to produce stimulation, the amplitude required for all the baseline stimulations was very varied, as evidenced by the wide standard deviations. The baseline amplitude did not correlate to the collection temperature of the tissues. For this reason, it was not really possible to draw

any concrete conclusions from the data. One factor which will have changed the threshold needed for twitch was the position of the electrodes on the muscle. It is possible that the electrodes were not always placed on the belly of the muscle. Furthermore, the electrodes were being placed on a muscle whose primary function is stabilisation. Thus, the movements produced when twitch occurred may be small and less obvious to see compared to a muscle that is responsible for movement of the limb.

One interesting thing to note about the neural stimulation tests is the fact that the threshold for twitch decreased during the only NC-P test which had both baseline and end perfusion nerve stimulation data. This was not seen during any of the C-P tests with both B and EP neural stimulation data. The decrease in the threshold for twitch in NC-P 4 was from 85mA baseline to 22mA at end of perfusion. Although, it is possible that the re-warming of the limb during perfusion made it more responsive to stimulation, another potential explanation for this reduction is that the EP electrodes were placed in a better position on the muscle, thus, eliciting a response at a lower amplitude.

The ROM of the limbs was examined both at collection and at the end of perfusion. This was only a visual assessment; no goniometer was used to measure movement of the joints. However, the difference of movement in the limbs was very noticeable. At collection the limbs were pliable and could easily be manipulated. By the end of the perfusion period, the limbs which had been perfused were still able to move but were not as pliable as upon collection. On the other hand, the limbs which were not perfused could not be moved at all. This shows that the limbs had stiffened up completely which is to be expected. A lack of perfusion meant that the ATP needed for movement of the limbs could not be replenished

and therefore the muscles remained fixed in position. Additionally, damage to the muscle tissue could have prevented movement of the limb. Furthermore, the cold could have caused the joints to stiffen up slightly making it more difficult to move the limb. This can be seen to a certain extent when comparing the ROM videos taken at the abattoir compared to the end of the cooling period.

The limbs collected from the abattoir varied in temperature, as evidenced by the cooling graphs in the results section. This is important as the limbs with a cooler collection temperature could have been harvested earlier. This means that there was an unknown period of warm ischaemia which cannot be controlled for. The unknown warm ischaemia time could have led to extensive muscle necrosis before the limbs were even collected. This would have affected the results as the limbs would not perform as well during testing. However, the extent of tissue death at the baseline could be assessed from the histology samples.

The limbs were only perfused for 2 hours during these experiments. Whilst this is longer than the porcine limbs in the previous set of experiments, it is not long enough to suggest that the perfusion system is suitable to use long term. Moreover, nothing was done to ensure the cells had enough energy to function properly. The glucose level was below the range of the blood gas machine at 15 minutes for all but 2 of the limb tests (data not shown). However, no glucose was added into the circulation. This means that the cells would have had to rely on the internal supplies of glucagon for respiration which would have already be depleted from the hour of anaerobic respiration over the transportation period. Therefore, the cells

would not have been able to produce enough ATP to function normally, leading to cell death. This limits our ability to assess how well the technology was able to preserve tissue viability.

Overall, this set of experiments testing the technology in a simulated combat setting using ovine limbs has showed that the deep muscle tissue was able to be cooled by 0.75-10.75°C (mean of 5.86±3.34°C) when using the topical cooling technology developed during this project. However, this was a very similar temperature change to that which is seen in the non-cooled limbs (mean 5.23±0.28°C). The similarity in temperature change means that the technology was not able to sufficiently cool the limbs to an extent which will prevent tissue damage over a long transfer to hospital. However, the deep tissue in the C-P limbs started at a lower temperature (mean 31.05±6.24°C) compared to the NC-P limbs (mean 38.71±1.20°C). The lower starting temperature in the C-P limbs will have meant a smaller temperature gradient which would have in turn resulted in a lesser temperature change.

The experiments showed that perfusing the limbs for 2 hours preserved muscle twitch. This muscle twitch could not be seen in limbs which had not been perfused indicating that perfusion had maintained tissue viability. Furthermore, the limbs which were cooled before perfusing seemed to show a lower EP twitch threshold suggesting that the cooling helped to preserve the tissue viability.

7.5. Future considerations:

The studies carried out demonstrate that the limb salvage technology that forms the basis of this work does indeed function to preserve tissue. As discussed in previous chapters, the use of therapeutic hypothermia is wide spread in clinical settings. Additionally, the perfusion system developed for this study is based on well described principles with a new focus on automated control for limb salvage purposes. For this reason, the technology could be successful at preserving tissue viability. There are some changes to the protocol and further investigations that need to be done to hopefully achieve this.

The first of these is to examine the effect on the tissues of the coolant fluid and the high concentrations of CO₂ used in this experiment. The coolant fluid has not yet undergone biocompatibility testing, if this fluid is toxic to tissues then another more suitable coolant fluid needs to be found and tested. Furthermore, although CO₂ has many attributes that make it an ideal gas to use in these experiments, i.e. inert, inflammable, the high concentrations used might be detrimental to tissue health. It may be worthwhile carrying out toxicology studies of both aspects of the cooling to determine if it is damaging the tissues.

Furthermore, the cooling period should be extended. Perfusion was starting on the limbs in less than 2 hours from the point of collection. Extending the cooling time will show if the limbs could be salvaged for those who cannot reach a medical facility in this time. Moreover, the limb should be perfused for longer. If the final aim is to perfuse the injured limb on an

isolated system for up to 100 days, perfusing the ovine limbs for just 2 hours will not be long enough to observe the long-term effects.

Though the use of bovine blood may only have a small effect on the results, using blood from the correct species when perfusing for prolonged periods should provide better results. This being said, the blood is unlikely to be matched by blood type so the chance of a transfusion reaction may be higher when using blood from the same species as there is a higher probability that the residual white blood cells will have antibodies against the antigens on mis-matched ovine blood.

The temperature data is not sampled from the very deep tissue, as has already been mentioned. To see how this tissue is affected by topical cooling, the thermocouples should be placed much deeper into the muscle tissue. Given that the limbs are disarticulated then this will be possible without the risk of causing long term damage. In addition, the histology samples should be taken from the same depth to examine how the tissue viability is affected at this level as the current study has not done this.

Chapter 8. Conclusions:

The objective of this thesis was to develop technology to improve chances of limb salvage at each stage of the journey from point of injury to the hospital stay. The new technology was designed to be implemented to improve haemorrhage control, preserve tissue viability through topical cooling and to support the limb tissues during staged limb reconstruction.

The first of these objectives was partially met. A dual-bladder pneumatic tourniquet was designed and tested. The wider bladder designed for the thigh could effectively stop blood flow when tested on the HapMed. However, the width of both bladders combined renders the tourniquet somewhat unsuitable for use on the arm. Further development of the bladders is entirely possible with a view to developing a bladder suitable for use on the arm. We have successfully developed a technology which is suitable for use on the lower limbs which was the primary objective of this work given that the vast majority of battlefield blast injuries occur on the lower limb.

The second objective, developing a system that can effectively reduce deep tissue temperature during transit, has been partially met. Primary testing on a small-scale tissue sample showed that it was possible for CO₂ to reduce the temperature of the deep tissue to the same extent as ice, the current method for cryotherapy after injury. This meant that the technology could be designed to test this method on larger limbs. Various iterations of cooling sock were developed to find the most efficient distribution of gas over the limb. These

iterations were tested to monitor the temperature recorded on the surface of the mannequin limb.

Once a design was determined the cooling sock was tested on porcine limbs. This showed that the cooling sock was able to reduce the temperature of the deep tissue by a mean of 13.21°C and did not produce dangerously low temperatures within the trotter injury. The results of this testing prompted further testing on larger limbs. The cooling sock was then tested on ovine limbs. It was found that the temperature of the deep tissue could be reduced by a mean of 5.86°C when using a combination of CO₂ and FLUTEC PP80 coolant fluid. However, this was not significantly different from the mean deep tissue temperature change of 5.23°C in the non-cooled limbs.

The third and most complex intervention point identified at the start of this thesis was during the casualty's stay in hospital. A limb support system was designed to permit injured limbs to be perfused and supported whilst the casualty is recovering in hospital in order that staged salvage surgery could be carried out. This objective has been met. Perfusion of the porcine limbs via the cannulation of the artery showed signs of blood flow returning to the limb as warmth was seen reaching the toes of the limb on the thermal camera images. The LDI images also showed the opening up of blood vessels. Rudimentary nerve stimulation showed that muscle twitch was retained in the perfused limbs and was absent in the non-perfused limbs.

Perfusion of the ovine limbs via cannulation of the artery and vein again showed warmth and blood flow returning to the limb through LDI scans and thermal imaging. The neural

stimulation showed that twitch was maintained in perfused limbs but not in non-perfused ones confirming that perfusion was preserving limb function and supporting the tissues. No definitive conclusions can be drawn from the blood data alone so histology is required to confirm the impact of the techniques on tissues. Histological analysis suggests the preservation of tissues associated with the perfusion rationale. The aim has been met as demonstrated by preservation of muscle function and structure.

Overall, the results of this work confirm that the technology developed works in terms of the primary objectives, the preservation of tissue function and structure. It is clear from this work however that further development of the tissue cooling technology is required to obtain optimum tissue protection. However, it is also clear that there is a lack of clarity in relation to the practical importance of tissue cooling during the transit period and it would seem entirely possible that the optimum benefit in terms of tissue preservation is associated with the perfusion regime instead of the cooling.

References:

Abou-Chebl, A. *et al.* (2011) 'Local Brain Temperature Reduction Through Intranasal Cooling With the RhinoChill Device'. *Stroke*, 42 (8), pp. 2164.

Adams-Chapman, I. and Stoll, B.J. (2001) 'Systemic inflammatory response syndrome'. *Seminars in Pediatric Infectious Diseases*, 12 (1), pp. 5-16.

Alam, H.B. and DiMusto, P.D. (2015) 'Management of Lower Extremity Vascular Trauma'. *Current Trauma Reports*, 1 (1), pp. 61-68.

Alam, H.B. *et al.* (2009) 'Surviving blood loss without blood transfusion in a swine poly-trauma model'. *Surgery*, 146 (2), pp. 325-333.

All Wales Military Prosthetics Working Group (2013) 'Improved Prosthetic Services for Military Veterans'. Available at: http://www.monmouthshire.gov.uk/app/uploads/2014/02/Report_of_the_Military_Prosthetics_Advisory_Group_-_2013_Version_1_October2.pdf.

AnaesthesiaUK (2005) *Intravenous regional anaesthesia*. Available at: <http://www.frca.co.uk/article.aspx?articleid=100447>.

Anand, T. and Skinner, R. (2012) 'Arginine vasopressin: The future of pressure-support resuscitation in hemorrhagic shock'. *Journal of Surgical Research*, 178 (1), pp. 321-329.

Baker, S.P. *et al.* (1974) 'The injury severity score: A method for describing patients with multiple injuries and evaluating emergency care'. *Journal of Trauma and Acute Care Surgery*, 14 (3), pp. 187-196.

Balazs, G.C. *et al.* (2015) 'Blurred front lines: triage and initial management of blast injuries'. *Current Reviews in Musculoskeletal Medicine*, 8 (3), pp. 304-311.

- Belmont, P., Schoenfeld, A.J. and Goodman, G. (2010) 'Epidemiology of combat wounds in Operation Iraqi Freedom and Operation Enduring Freedom: orthopaedic burden of disease'. *J Surg Orthop Adv*, 19 (1), pp. 2-7.
- Bevevino, A.J. *et al.* (2014) 'A Model to Predict Limb Salvage in Severe Combat-related Open Calcaneus Fractures'. *Clinical Orthopaedics and Related Research*[®], 472 (10), pp. 3002-3009.
- Bilmes, L. (2007) 'Soldiers returning from Iraq and Afghanistan: The long-term costs of providing veterans medical care and disability benefits'.
- Bogert, J.N., Harvin, J.A. and Cotton, B.A. (2014) 'Damage Control Resuscitation'. *Journal of Intensive Care Medicine*, 31 (3), pp. 177-186.
- Bouglé, A., Harrois, A. and Duranteau, J. (2013) 'Resuscitative strategies in traumatic hemorrhagic shock'. *Annals of Intensive Care*, 3 (1), pp. 1.
- Bricknell, M. (2003) 'The Evolution Of Casualty Evacuation In The 20th Century (Part 5)-Into The Future'. *Journal of the Royal Army Medical Corps*, 149 (4), pp. 357-363.
- Bridges, E. and Evers, K. (2009) 'Wartime critical care air transport'. *Military medicine*, 174 (4), pp. 370-375.
- Brown, D. (2012) 'In Afghan war, rate of post-injury survival rises'. *The Washington Post*, 30.01.2012, p.
- Brown, K.V. *et al.* (2012) 'Modern military surgery'. *Journal of Bone & Joint Surgery, British Volume*, 94-B (4), pp. 536.
- Burns, G.P. (2014) 'Arterial blood gases made easy'. *Clinical medicine (London, England)*, 14 (1), pp. 66-68.
- Cannon, J.W. *et al.* (2016) 'Dismounted Complex Blast Injuries: A Comprehensive Review of the Modern Combat Experience'. *Journal of the American College of Surgeons*, 223 (4), pp. 652-664.e658.

- Carr Jr, M.E. (2004) 'Monitoring of hemostasis in combat trauma patients'. *Military medicine*, 169 (12), pp. 11.
- Causey, M.W. *et al.* (2015) 'Pharmacologic attenuation of the hyperdynamic response to supraceliac aortic clamping'. *Journal of Vascular Surgery*, 61 (1), pp. 224-230.
- Cave, D.A. and Finegan, B.A. (2007) 'Complications of Intravenous Regional Anesthesia'. In: Finucane, B.T. (ed.) *Complications of Regional Anesthesia*. New York, NY: Springer New York, pp. 211-223.
- Chandler, H., MacLeod, K. and Penn-Barwell, J.G. (2017) 'Extremity injuries sustained by the UK military in the Iraq and Afghanistan conflicts: 2003–2014'. *Injury*, 48 (7), pp. 1439-1443.
- Chauhan, R., Copeland, C.C. and Murray, M. (2018) 'Improvised Explosive Devices: Anesthetic Implications'. *Current Anesthesiology Reports*, 8 (1), pp. 71-77.
- Checketts, M.R. (2013) 'Intravenous regional anaesthesia'. *Anaesthesia & Intensive Care Medicine*, 14 (4), pp. 159-160.
- CHI Systems Inc (2019) *HapMed Tourniquet Training*. Available at: <https://www.hapmedtraining.com/> (Accessed: 14/11/2019).
- Connolly, M., Ibrahim, Z.R. and Johnson, O.N. (2016) 'Changing paradigms in lower extremity reconstruction in war-related injuries'. *Military Medical Research*, 3 (1), pp. 9.
- Cowley, N.J., Owen, A. and Bion, J.F. (2013) 'Interpreting arterial blood gas results'. *BMJ : British Medical Journal*, 346 f16.
- Cpl Dan Bardsley RLC (2009) 'Troops carry casualty to Blackhawk helicopter'. In: 45150649.jpg (ed.) Defenceimagery.mod.uk: MOD.
- Cracowski, J.-L. *et al.* (2006) 'Methodological issues in the assessment of skin microvascular endothelial function in humans'. *Trends in Pharmacological Sciences*, 27 (9), pp. 503-508.
- Davis, B.L., Martin, M.J. and Schreiber, M. (2017) 'Military Resuscitation: Lessons from Recent Battlefield Experience'. *Current Trauma Reports*, 3 (2), pp. 156-163.

de Waard, M.C. *et al.* (2013) 'Automated peritoneal lavage: an extremely rapid and safe way to induce hypothermia in post-resuscitation patients'. *Critical Care*, 17 (1), pp. R31.

Deloughry, J.L. and Griffiths, R. (2009) 'Arterial tourniquets'. *Continuing Education in Anaesthesia Critical Care & Pain*, 9 (2), pp. 56-60.

Dharm-Datta, S. *et al.* (2011) 'The outcome of British combat amputees in relation to military service'. *Injury*, 42 (11), pp. 1362-1367.

Dismounted Complex Blast Injury Task Force (2011) 'Dismounted complex blast injury'. Fort Sam Houston, TX: Office of the Army Surgeon General. <http://armymedicine.mil/Documents/DCBI-Task-Force-Report-Redacted-Final.pdf>.

Dougherty, A.L. *et al.* (2009) 'Battlefield extremity injuries in Operation Iraqi Freedom'. *Injury*, 40 (7), pp. 772-777.

Dougherty, P.J. *et al.* (2014) 'Bilateral Transfemoral/Transtibial Amputations Due to Battle Injuries: A Comparison of Vietnam Veterans with Iraq and Afghanistan Servicemembers'. *Clinical Orthopaedics and Related Research*®, 472 (10), pp. 3010-3016.

Dunn, J.C. *et al.* (2016) 'US service member tourniquet use on the battlefield: Iraq and Afghanistan 2003–2011'. *Trauma*, 18 (3), pp. 216-220.

Edwards, D.S. *et al.* (2015) 'What Is the Magnitude and Long-term Economic Cost of Care of the British Military Afghanistan Amputee Cohort?'. *Clinical Orthopaedics and Related Research*®, 473 (9), pp. 2848-2855.

Ejaz, A. *et al.* (2014) 'Faster recovery without the use of a tourniquet in total knee arthroplasty'. *Acta Orthopaedica*, 85 (4), pp. 422-426.

Engineering ToolBox (2003a) *Human Body and Specific Heat [Online]*. Available at: https://www.engineeringtoolbox.com/human-body-specific-heat-d_393.html (Accessed: 21/05/18).

Engineering ToolBox (2003b) *Specific Heat and Individual Gas Constant of Gases [Online]*. Available at: http://www.engineeringtoolbox.com/specific-heat-capacity-gases-d_159.html (Accessed: 21/05/2018).

Engineering Toolbox (2018) *Carbon Dioxide - Thermophysical properties [Online]*. Available at: https://www.engineeringtoolbox.com/CO2-carbon-dioxide-properties-d_2017.html (Accessed: 25/09/2020).

Estebe, J.-P., Davies, J.M. and Richebe, P. (2011) 'The pneumatic tourniquet: mechanical, ischaemia–reperfusion and systemic effects'. *European Journal of Anaesthesiology (EJA)*, 28 (6), pp. 404-411.

Evrivades, D. *et al.* (2010) 'Shaping the military wound: issues surrounding the reconstruction of injured servicemen at the Royal Centre for Defence Medicine'. *Philosophical Transactions of the Royal Society B: Biological Sciences*, 366 (1562), pp. 219.

Ewington, I. (2016) 'Aeromedical Evacuation and Transfer of the Critically Injured Patient'. In: Hutchings, S.D. (ed.) *Trauma and Combat Critical Care in Clinical Practice*. Cham: Springer International Publishing, pp. 489-507.

Farrokhi, S. *et al.* (2018) 'Incidence of Overuse Musculoskeletal Injuries in Military Service Members With Traumatic Lower Limb Amputation'. *Archives of Physical Medicine and Rehabilitation*, 99 (2), pp. 348-354.e341.

FDA (2015) *FDA clears military traumatic wound dressing for use in the civilian population [Press release]*.

FLIR Systems *How Do Thermal Cameras Work?* Available at: <https://www.flir.co.uk/discover/rd-science/how-do-thermal-cameras-work/> (Accessed: 29/09/2020).

Flor, H. (2002) 'Phantom-limb pain: characteristics, causes, and treatment'. *The Lancet Neurology*, 1 (3), pp. 182-189.

Forsyth, A.L. *et al.* (2012) 'The effect of cooling on coagulation and haemostasis: Should "Ice" be part of treatment of acute haemarthrosis in haemophilia?'. *Haemophilia*, 18 (6), pp. 843-850.

Fox, C.J. *et al.* (2010) 'Popliteal Artery Repair in Massively Transfused Military Trauma Casualties: A Pursuit to Save Life and Limb'. *Journal of Trauma and Acute Care Surgery*, 69 (1), pp. S123-S134.

Fukudome, E.Y. *et al.* (2010) 'Pharmacologic Resuscitation Promotes Survival and Attenuates Hemorrhage-Induced Activation of Extracellular Signal-Regulated Kinase 1/21'. *Journal of Surgical Research*, 163 (1), pp. 118-126.

Ganster, F. *et al.* (2010) 'Effects of hydrogen sulfide on hemodynamics, inflammatory response and oxidative stress during resuscitated hemorrhagic shock in rats'. *Critical Care*, 14 (5), pp. R165.

Gawande, A. (2004) 'Casualties of War — Military Care for the Wounded from Iraq and Afghanistan'. *New England Journal of Medicine*, 351 (24), pp. 2471-2475.

Gillani, S. *et al.* (2012) 'The effect of ischemia reperfusion injury on skeletal muscle'. *Injury*, 43 (6), pp. 670-675.

Gillies, M.A. *et al.* (2010) 'Therapeutic hypothermia after cardiac arrest: A retrospective comparison of surface and endovascular cooling techniques'. *Resuscitation*, 81 (9), pp. 1117-1122.

Glick, C.P.T.Y. *et al.* (2018) 'Comparison of Two Tourniquets on a Mid-Thigh Model: The Israeli Silicone Stretch and Wrap Tourniquet vs. The Combat Application Tourniquet'. *Military Medicine*, 183 (suppl_1), pp. 157-161.

Godfrey, B.W. *et al.* (2017) 'Patients with multiple traumatic amputations: An analysis of operation enduring freedom joint theatre trauma registry data'. *Injury*, 48 (1), pp. 75-79.

Goldstein, D.A. (1990) 'Serum Calcium'. In: Walker HK, H.W., Hurst JW (ed.) *Clinical Methods: The History, Physical, and Laboratory Examinations*. 3rd Edition edn. Boston: Butterworths, pp. 677-679.

Gonzalez-Ibarra, F., Varon, J. and Lopez-Meza, E. (2011) 'Therapeutic Hypothermia: Critical Review of the Molecular Mechanisms of Action'. *Frontiers in Neurology*, 2 (4), pp.

Gordon, W. *et al.* (2015) 'Challenges in definitive fracture management of blast injuries'. *Current Reviews in Musculoskeletal Medicine*, 8 (3), pp. 290-297.

Guler, O. *et al.* (2016) 'Comparison of quadriceps muscle volume after unilateral total knee arthroplasty with and without tourniquet use'. *Knee Surgery, Sports Traumatology, Arthroscopy*, 24 (8), pp. 2595-2605.

Hannon, M. *et al.* (2016) 'Venous thromboembolism after traumatic amputation: an analysis of 366 combat casualties'. *The American Journal of Surgery*, 212 (2), pp. 230-234.

Harmsen, A.M.K. *et al.* (2015) 'The influence of prehospital time on trauma patients outcome: A systematic review'. *Injury*, 46 (4), pp. 602-609.

Harsten, A. *et al.* (2015) 'Tourniquet versus no tourniquet on knee-extension strength early after fast-track total knee arthroplasty; a randomized controlled trial'. *The Knee*, 22 (2), pp. 126-130.

Hassoun, H.T. *et al.* (2002) 'Intraischemic hypothermia differentially modulates oxidative stress proteins during mesenteric ischemia/reperfusion'. *Surgery*, 132 (2), pp. 369-376.

Hayman, J. and Oxenham, M. (2016) 'Chapter 1 - Supravital Reactions in the Estimation of the Time Since Death (TSD)'. In: Hayman, J. and Oxenham, M. (eds.) *Human Body Decomposition*. Academic Press, pp. 1-12.

Hildebrand, F. *et al.* (2004) 'Pathophysiologic changes and effects of hypothermia on outcome in elective surgery and trauma patients'. *The American Journal of Surgery*, 187 (3), pp. 363-371.

Holcomb, J. *et al.* (2007) 'Causes of death in US Special Operations Forces in the global war on terrorism: 2001-2004'. *US Army Med Dep J*, 24-37.

Holcomb, J.B. and Mitchell, T.A. (2017) 'Principles for Damage Control in Military Casualties'. In: Pape, H.-C. *et al.* (eds.) *Damage Control Management in the Polytrauma Patient*. Cham: Springer International Publishing, pp. 273-281.

Hooper, T.J. *et al.* (2014) 'Implementation and Execution of Military Forward Resuscitation Programs'. *Shock*, 41.

Hoyt, B.W. *et al.* (2015) 'Rehabilitation of Lower Extremity Trauma: a Review of Principles and Military Perspective on Future Directions'. *Current Trauma Reports*, 1 (1), pp. 50-60.

Hubbard, W.B. *et al.* (2015) 'Steroid-Loaded Hemostatic Nanoparticles Combat Lung Injury after Blast Trauma'. *ACS Macro Letters*, 4 (4), pp. 387-391.

Ibrahim, A. and Oneisi, A. (2017) 'Lower Extremity Reconstruction'. In: Abu-Sittah, G.S., Hoballah, J.J. and Bakhach, J. (eds.) *Reconstructing the War Injured Patient*. Cham: Springer International Publishing, pp. 79-88.

Jacobi, U. *et al.* (2007) 'Porcine ear skin: an in vitro model for human skin'. *Skin research and technology : official journal of International Society for Bioengineering and the Skin (ISBS) [and] International Society for Digital Imaging of Skin (ISDIS) [and] International Society for Skin Imaging (ISSI)*, 13 (1), pp. 19-24.

Jafarian, A.A. *et al.* (2016) 'Simple Arm Tourniquet as an Adjunct to Double-Cuff Tourniquet in Intravenous Regional Anesthesia'. *Anesthesiology and Pain Medicine*, 6 (3), pp. e29316.

Jeffery, S. (2009) 'Advanced wound therapies in the management of severe military lower limb trauma: a new perspective'. *ePlasty: Open Access Journal of Plastic Surgery*, 9.

Kochanek, P.M. (2004) 'Novel Resuscitation From Lethal Hemorrhage Suspended Animation for Delayed Resuscitation, Year 7'.

Kohlhauer, M. *et al.* (2016) 'Therapeutic hypothermia to protect the heart against acute myocardial infarction'. *Archives of Cardiovascular Diseases*, 109 (12), pp. 716-722.

Kolluru, G.K. *et al.* (2016) 'Oxygen tension, H₂S, and NO bioavailability: is there an interaction?'. *Journal of Applied Physiology*, 120 (2), pp. 263.

Korompilias, A.V. *et al.* (2009) 'The mangled extremity and attempt for limb salvage'. *Journal of Orthopaedic Surgery and Research*, 4 (1), pp. 4.

Kotwal, R.S. *et al.* (2016) 'The Effect of a Golden Hour Policy on the Morbidity and Mortality of Combat Casualties'. *JAMA Surgery*, 151 (1), pp. 15-24.

Kovesdy, C.P. (2015) 'Management of Hyperkalemia: An Update for the Internist'. *The American Journal of Medicine*, 128 (12), pp. 1281-1287.

Kragh, J.J.F. *et al.* (2011) 'The Military Emergency Tourniquet Program's Lessons Learned With Devices and Designs'. *Military Medicine*, 176 (10), pp. 1144-1152.

Kragh Jr, J.F. and Dubick, M.A. (2016) 'Battlefield Tourniquets: Lessons Learned in Moving Current Care Toward Best Care in an Army Medical Department at War'. *US Army Medical Department Journal*.

Kragh Jr, J.F. *et al.* (2011) 'Battle Casualty Survival with Emergency Tourniquet Use to Stop Limb Bleeding'. *The Journal of Emergency Medicine*, 41 (6), pp. 590-597.

Kragh Jr, J.F. *et al.* (2012) 'Historical review of emergency tourniquet use to stop bleeding'. *The American Journal of Surgery*, 203 (2), pp. 242-252.

Kragh Jr, J.F. *et al.* (2014) 'Emergency tourniquet effectiveness in four positions on the proximal thigh'.

Kragh Jr, J.F. *et al.* (2008) 'Practical use of emergency tourniquets to stop bleeding in major limb trauma'. *Journal of Trauma and Acute Care Surgery*, 64 (2), pp. S38-S50.

Kragh Jr, J.F. *et al.* (2009) 'Survival with emergency tourniquet use to stop bleeding in major limb trauma'. *Annals of surgery*, 249 (1), pp. 1-7.

Krug, E. *et al.* (2011) 'Evidence-based recommendations for the use of Negative Pressure Wound Therapy in traumatic wounds and reconstructive surgery: Steps towards an international consensus'. *Injury*, 42, Supplement 1 S1-S12.

Kumar, K., Railton, C. and Tawfic, Q. (2016) 'Tourniquet application during anesthesia: "What we need to know"'. *Journal of Anaesthesiology Clinical Pharmacology*, 32 (4), pp. 424-430.

Kumar, N. *et al.* (2015) 'Evaluation of pain in bilateral total knee replacement with and without tourniquet; a prospective randomized control trial'. *Journal of Clinical Orthopaedics and Trauma*, 6 (2), pp. 85-88.

Köstler, W., Strohm, P.C. and Südkamp, N.P. (2004) 'Acute compartment syndrome of the limb'. *Injury*, 35 (12), pp. 1221-1227.

Lashof-Sullivan, M. *et al.* (2016) 'Hemostatic Nanoparticles Improve Survival Following Blunt Trauma Even after 1 Week Incubation at 50 °C'. *ACS Biomaterials Science & Engineering*, 2 (3), pp. 385-392.

Lashof-Sullivan, M.M. *et al.* (2014) 'Intravenously administered nanoparticles increase survival following blast trauma'. *Proceedings of the National Academy of Sciences*, 111 (28), pp. 10293-10298.

Lawrence, T. (2009) 'The nuclear factor NF-kappaB pathway in inflammation'. *Cold Spring Harbor perspectives in biology*, 1 (6), pp. a001651-a001651.

Lehman, C. (2008) 'Mechanisms of Injury in Wartime'. *Rehabilitation Nursing*, 33 (5), pp. 192-205.

'limb salvage'. (2002) *McGraw-Hill Concise Dictionary of Modern Medicine*. The McGraw-Hill Companies, Inc.

Liu, D. *et al.* (2014) 'Effects of tourniquet use on quadriceps function and pain in total knee arthroplasty'. *Knee Surgery and Related Research*, 26 (4), pp. 207-213.

- Lord, J.M. *et al.* (2014) 'The systemic immune response to trauma: an overview of pathophysiology and treatment'. *The Lancet*, 384 (9952), pp. 1455-1465.
- Manring, M.M. *et al.* (2009) 'Treatment of War Wounds: A Historical Review'. *Clinical Orthopaedics and Related Research*[®], 467 (8), pp. 2168-2191.
- Martini, W.Z. (2007) 'The effects of hypothermia on fibrinogen metabolism and coagulation function in swine'. *Metabolism*, 56 (2), pp. 214-221.
- Mathieu, L. *et al.* (2011) 'Damage control orthopaedics in the context of battlefield injuries: The use of temporary external fixation on combat trauma soldiers'. *Orthopaedics & Traumatology: Surgery & Research*, 97 (8), pp. 852-859.
- Mathieu, L. *et al.* (2014) 'Combat-related upper extremity injuries: Surgical management specificities on the theatres of operations'. *Chirurgie de la Main*, 33 (3), pp. 174-182.
- McDowell, M.A. *et al.* (2008) 'Anthropometric reference data for children and adults: United States, 2003–2006'. *National health statistics reports*, 10 (1-45), pp. 5.
- Millet, C. *et al.* (2011) 'Comparison between laser speckle contrast imaging and laser Doppler imaging to assess skin blood flow in humans'. *Microvascular Research*, 82 (2), pp. 147-151.
- Moore, E.M. *et al.* (2011) 'Therapeutic hypothermia: Benefits, mechanisms and potential clinical applications in neurological, cardiac and kidney injury'. *Injury*, 42 (9), pp. 843-854.
- Moore, L.J. *et al.* (2015) 'Implementation of resuscitative endovascular balloon occlusion of the aorta as an alternative to resuscitative thoracotomy for noncompressible truncal hemorrhage'. *Journal of Trauma and Acute Care Surgery*, 79 (4), pp.
- Mooyaart, E.A.Q. *et al.* (2016) 'Outcome after hydrogen sulphide intoxication'. *Resuscitation*, 103 1-6.
- Morrison, J.J. *et al.* (2012) 'Associated injuries in casualties with traumatic lower extremity amputations caused by improvised explosive devices'. *British Journal of Surgery*, 99 (3), pp. 362-366.

- Mullenix, P.S. *et al.* (2006) 'Limb salvage and outcomes among patients with traumatic popliteal vascular injury: An analysis of the National Trauma Data Bank'. *Journal of Vascular Surgery*, 44 (1), pp. 94-100.
- Murray, A.K., Herrick, A.L. and King, T.A. (2004) 'Laser Doppler imaging: a developing technique for application in the rheumatic diseases'. *Rheumatology*, 43 (10), pp. 1210-1218.
- National Trauma Institute *Hemorrhage*. Available at: <http://www.nationaltraumainstitute.org/home/hemorrhage.html> (Accessed: 06.04.2017).
- Niemann, C.U. *et al.* (2015) 'Therapeutic Hypothermia in Deceased Organ Donors and Kidney-Graft Function'. *New England Journal of Medicine*, 373 (5), pp. 405-414.
- Ning, J. *et al.* (2016) 'Therapeutic Whole-body Hypothermia Protects Remote Lung, Liver, and Kidney Injuries after Blast Limb Trauma in Rats'. *The Journal of the American Society of Anesthesiologists*, 124 (6), pp. 1360-1371.
- Ning, J. *et al.* (2013) 'Sodium Hydrosulphide Alleviates Remote Lung Injury Following Limb Traumatic Injury in Rats'. *PLOS ONE*, 8 (3), pp. e59100.
- Oh, S.H. *et al.* (2015) 'An observational study of surface versus endovascular cooling techniques in cardiac arrest patients: a propensity-matched analysis'. *Critical Care*, 19 (1), pp. 85.
- Olivecrona, C. *et al.* (2013) 'Tourniquet time affects postoperative complications after knee arthroplasty'. *International Orthopaedics*, 37 (5), pp. 827-832.
- Ostadal, P. *et al.* (2013) 'Mild therapeutic hypothermia is superior to controlled normothermia for the maintenance of blood pressure and cerebral oxygenation, prevention of organ damage and suppression of oxidative stress after cardiac arrest in a porcine model'. *Journal of Translational Medicine*, 11 (1), pp. 124.
- Owens, B.D. *et al.* (2008) 'Combat Wounds in Operation Iraqi Freedom and Operation Enduring Freedom'. *Journal of Trauma and Acute Care Surgery*, 64 (2), pp. 295-299.

Pasquina, P.F. and Fitzpatrick, K.F. (2006) 'The Walter Reed Experience: Current Issues in the Care of the Traumatic Amputee'. *JPO: Journal of Prosthetics and Orthotics*, 18 (6), pp. P119-P122.

Pasquina, P.F. et al. (2014) 'Special Considerations for Multiple Limb Amputation'. *Current Physical Medicine and Rehabilitation Reports*, 2 (4), pp. 273-289.

Patel, M.B., Richter, K.M. and Shafi, S. (2015) 'Mangled Extremity: Amputation Versus Salvage'. *Current Trauma Reports*, 1 (1), pp. 45-49.

Penn-Barwell, J.G. et al. (2014) 'Acute bilateral leg amputation following combat injury in UK servicemen'. *Injury*, 45 (7), pp. 1105-1110.

Penn-Barwell, J.G. et al. (2011) 'Use of topical negative pressure in British servicemen with combat wounds'. *Eplasty*, 11 e35.

Perkins, Z.B. et al. (2012) 'Factors affecting outcome after traumatic limb amputation'. *British Journal of Surgery*, 99 (S1), pp. 75-86.

Plagenhoef, S., Evans, F.G. and Abdelnour, T. (1983) 'Anatomical Data for Analyzing Human Motion'. *Research Quarterly for Exercise and Sport*, 54 (2), pp. 169-178.

Pohlman, T.H. et al. (2015) 'Damage control resuscitation'. *Blood Reviews*, 29 (4), pp. 251-262.

Polderman, K.H. (2004a) 'Application of therapeutic hypothermia in the ICU: opportunities and pitfalls of a promising treatment modality. Part 1: Indications and evidence'. *Intensive Care Medicine*, 30 (4), pp. 556-575.

Polderman, K.H. (2004b) 'Application of therapeutic hypothermia in the intensive care unit'. *Intensive Care Medicine*, 30 (5), pp. 757-769.

Potter, B.K. et al. (2007) 'Heterotopic Ossification Following Traumatic and Combat-Related Amputations: Prevalence, Risk Factors, and Preliminary Results of Excision'. *JBJS*, 89 (3), pp. 476-486.

- Prasarn, M.L., Helfet, D.L. and Kloen, P. (2012) 'Management of the mangled extremity'. *Strategies in Trauma and Limb Reconstruction*, 7 (2), pp. 57-66.
- Ramasamy, A. *et al.* (2009) 'A review of casualties during the Iraqi insurgency 2006–A British field hospital experience'. *Injury*, 40 (5), pp. 493-497.
- Rappold, J.F. and Bochicchio, G.V. (2016) 'Surgical adjuncts to noncompressible torso hemorrhage as tools for patient blood management'. *Transfusion*, 56 S203-S207.
- Rattan, R., Jones, K.M. and Namias, N. (2015) 'Management of Lower Extremity Vascular Injuries: State of the Art'. *Current Surgery Reports*, 3 (11), pp. 35.
- Rawal, N. (2000) 'Intravenous regional anesthesia'. *Techniques in Regional Anesthesia and Pain Management*, 4 (1), pp. 51-53.
- Rigal, S. (2012) 'Extremity amputation: how to face challenging problems in a precarious environment'. *International Orthopaedics*, 36 (10), pp. 1989-1993.
- Robbins, C.B. *et al.* (2009) 'A review of the long-term health outcomes associated with war-related amputation'. *Mil Med*, 174 (6), pp. 588-592.
- Robertson, C.M. and Coopersmith, C.M. (2006) 'The systemic inflammatory response syndrome'. *Microbes and Infection*, 8 (5), pp. 1382-1389.
- Rosenberry, C., Stone, F. and Kalbfleisch, K. (2009) 'Rhabdomyolysis-induced severe hyperkalemia'. *The western journal of emergency medicine*, 10 (4), pp. 302-302.
- Royal College of Physicians (2011) *The Armed Forces Covenant in Action? Part 1: Military Casualties - Defence Committee*. Available at: <https://www.publications.parliament.uk/pa/cm201012/cmselect/cmdfence/762/762we12.htm> (Accessed: 20.12.2016).
- Satterly, S.A. *et al.* (2015) 'Hydrogen sulfide improves resuscitation via non-hibernatory mechanisms in a porcine shock model'. *Journal of Surgical Research*, 199 (1), pp. 197-210.

- Sayer, N.A. *et al.* (2008) 'Characteristics and Rehabilitation Outcomes Among Patients With Blast and Other Injuries Sustained During the Global War on Terror'. *Archives of Physical Medicine and Rehabilitation*, 89 (1), pp. 163-170.
- Schrager, J.J., Branson, R.D. and Johannigman, J.A. (2012) 'Lessons From the Tip of the Spear: Medical Advancements From Iraq and Afghanistan'. *Respiratory Care*, 57 (8), pp. 1305.
- Schreckengaust, R., Littlejohn, L. and Zarow, G.J. (2014) 'Effects of Training and Simulated Combat Stress on Leg Tourniquet Application Accuracy, Time, and Effectiveness'. *Military Medicine*, 179 (2), pp. 114-120.
- Seiyama, A. *et al.* (1996) 'Effect of Hypothermia on Skeletal Muscle Metabolism in Perfused Rat Hindlimb'. *Cryobiology*, 33 (3), pp. 338-346.
- Shackelford, S.A. *et al.* (2014) 'Optimizing the use of limb tourniquets in tactical combat casualty care: TCCC guidelines change 14-02'.
- Sharma, J.P. and Salhotra, R. (2012) 'Tourniquets in orthopedic surgery'. *Indian Journal of Orthopaedics*, 46 (4), pp. 377-383.
- Shoffstall, A.J. *et al.* (2012) 'Intravenous Hemostatic Nanoparticles Increase Survival Following Blunt Trauma Injury'. *Biomacromolecules*, 13 (11), pp. 3850-3857.
- Simkhovich, B.Z., Hale, S.L. and Kloner, R.A. (2004) 'Metabolic Mechanism by Which Mild Regional Hypothermia Preserves Ischemic Tissue'. *Journal of Cardiovascular Pharmacology and Therapeutics*, 9 (2), pp. 83-90.
- Soar, J. *et al.* (2010) 'European Resuscitation Council Guidelines for Resuscitation 2010 Section 8. Cardiac arrest in special circumstances: Electrolyte abnormalities, poisoning, drowning, accidental hypothermia, hyperthermia, asthma, anaphylaxis, cardiac surgery, trauma, pregnancy, electrocution'. *Resuscitation*, 81 (10), pp. 1400-1433.
- Spinella, P.C. and Holcomb, J.B. (2009) 'Resuscitation and transfusion principles for traumatic hemorrhagic shock'. *Blood Reviews*, 23 (6), pp. 231-240.

- Stewart, L. *et al.* (2016) 'Microbiological Profile of Combat-Related Extremity Wound Infections: Trauma Infectious Disease Outcomes Study 2009–2012'. *Open Forum Infectious Diseases*, 3 (suppl_1), pp. 1158-1158.
- Summerfield, A., Meurens, F. and Ricklin, M.E. (2015) 'The immunology of the porcine skin and its value as a model for human skin'. *Molecular Immunology*, 66 (1), pp. 14-21.
- Swindle, M.M. *et al.* (2011) 'Swine as Models in Biomedical Research and Toxicology Testing'. *Veterinary Pathology*, 49 (2), pp. 344-356.
- Szabo, C. (2007) 'Hydrogen sulphide and its therapeutic potential'. *Nat Rev Drug Discov*, 6 (11), pp. 917-935.
- Tai, T.-W. *et al.* (2012) 'Effects of tourniquet use on blood loss and soft-tissue damage in total knee arthroplasty'. *J Bone Joint Surg Am*, 94 (24), pp. 2209-2215.
- Tarwala, R. *et al.* (2014) 'Tourniquet Use During Cementation Only During Total Knee Arthroplasty: A Randomized Trial'. *Clinical Orthopaedics and Related Research*®, 472 (1), pp. 169-174.
- Tatum, J.B. (2008a) '6.1 The Ideal Gas Equation'. *Heat and Thermodynamics*. Online: LibreTexts, pp. 7242.
- Tatum, J.B. (2008b) '8.4 Reversible Adiabatic Expansion of an Ideal Gas'. *Heat and Thermodynamics*. Online: LibreTexts, pp. 7259.
- Taylor, C. and Jeffery, S. (2009) 'Management of military wounds in the modern era'. *Wounds UK*, 5 (4), pp. 50-58.
- Teichman, P.G., Donchin, Y. and Kot, R.J. (2007) 'International Aeromedical Evacuation'. *New England Journal of Medicine*, 356 (3), pp. 262-270.
- Testori, C. *et al.* (2013) 'Rapid induction of mild therapeutic hypothermia by extracorporeal veno-venous blood cooling in humans'. *Resuscitation*, 84 (8), pp. 1051-1055.

Tien, C.H. *et al.* (2015) 'Advances in damage control resuscitation and surgery: implications on the organization of future military field forces'. *Canadian Journal of Surgery*, 58 (3 Suppl 3), pp. S91.

Tribble, D.R. and Rodriguez, C.J. (2014) 'Combat-Related Invasive Fungal Wound Infections'. *Current Fungal Infection Reports*, 8 (4), pp. 277-286.

Valerio, I.L. *et al.* (2015) 'The use of urinary bladder matrix in the treatment of trauma and combat casualty wound care'. *Regen Med*, 10.

Valerio, I.L. *et al.* (2016) 'A Case Report of the First Nonburn-related Military Trauma Victim Treated with Spray Skin Regenerative Therapy in Combination with a Dermal Regenerate Template'. *Plastic and Reconstructive Surgery – Global Open*, 4 (12), pp. e1082.

Valerio, I.L. *et al.* (2013) 'Sequential free tissue transfers for simultaneous upper and lower limb salvage'. *Microsurgery*, 33 (6), pp. 447-453.

Van der Spuy, L. (2012) 'Complications of the arterial tourniquet'. *Southern African Journal of Anaesthesia and Analgesia*, 18 (1), pp. 14-18.

Wall, P.L., Sahr, S.M. and Busing, C.M. (2015) 'Different width and tightening system: emergency tourniquets on distal limb segments'. *J Spec Oper Med*, 15 (4), pp. 28-38.

Wallace, D. (2012) 'Trends in traumatic limb amputation in Allied Forces in Iraq and Afghanistan'. *Journal of Military and Veterans Health*, 20 (2), pp. 31.

Wally Santana, G.I. (2002) 'Army medics and soldiers carry a wounded soldier onto an Air Force C-17 at Bagram Air Field'. *The Christmas Rush: Getting Wounded Soldiers Home: National Public Radio*.

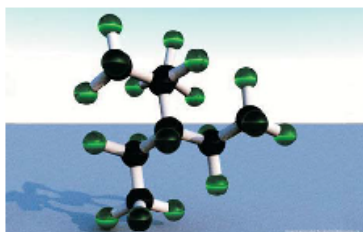
Wang, K. *et al.* (2016) 'The effects of tourniquet use in total knee arthroplasty: a randomized, controlled trial'. *Knee Surgery, Sports Traumatology, Arthroscopy*, 1-9.

Wardell, K., Jakobsson, A. and Nilsson, G.E. (1993) 'Laser Doppler perfusion imaging by dynamic light scattering'. *IEEE Transactions on biomedical Engineering*, 40 (4), pp. 309-316.

- Wayne, B.A. (2004) 'Medical Aspects of Air Evacuation from a Tactical Environment'. *Journal of Special Operations Medicine*, 4 (1), pp. 31-39.
- Wenzel, V., Raab, H. and Dünser, M.W. (2008) 'Arginine vasopressin: a promising rescue drug in the treatment of uncontrolled haemorrhagic shock'. *Best Practice & Research Clinical Anaesthesiology*, 22 (2), pp. 299-316.
- Wojcik, B.E. *et al.* (2010) 'Traumatic Brain Injury Hospitalizations of U.S. Army Soldiers Deployed to Afghanistan and Iraq'. *American Journal of Preventive Medicine*, 38 (1, Supplement), pp. S108-S116.
- Wolf, S.J. *et al.* 'Blast injuries'. *The Lancet*, 374 (9687), pp. 405-415.
- Wolf, S.J. *et al.* (2009) 'Blast injuries'. *The Lancet*, 374 (9687), pp. 405-415.
- Wong, S. and Irwin, M.G. (2015) 'Procedures under tourniquet'. *Anaesthesia & Intensive Care Medicine*, 16 (3), pp. 93-96.
- Youngson, R.M. (2004, 2005) 'exsanguination'. *Collins Dictionary of Medicine*. The Free Dictionary [Internet].
- Zan, P.F. *et al.* (2015) 'Releasing of Tourniquet Before Wound Closure or not in Total Knee Arthroplasty: A Meta-Analysis of Randomized Controlled Trials'. *The Journal of Arthroplasty*, 30 (1), pp. 31-37.
- Zhang, W. *et al.* (2014) 'The effects of a tourniquet used in total knee arthroplasty: a meta-analysis'. *Journal of Orthopaedic Surgery and Research*, 9 (1), pp. 13.
- Zouris, J.M. *et al.* (2006) 'Wounding patterns for US Marines and sailors during Operation Iraqi Freedom, major combat phase'. *Military medicine*, 171 (3), pp. 246.



F2 Chemicals Ltd



FLUTEC™ PP80

Synonyms: Perfluoro-2-methyl-3-pentane

CAS Number: 354-97-2

Description & Characteristics

Flutec PP80, C8F18, is a fully-fluorinated, odourless, colourless liquid with the following characteristics:

- Compatibility with most construction materials
- Excellent chemical and thermal stability
- Non flammability
- Practically non-toxic¹

Applications

Flutec PP80 is used for heat transfer and cooling applications but can be used in many different applications

Safety & Handling

Although Flutec PP80 is considered biologically and chemically inert, good laboratory practices should be observed when handling. Flutec PP80 has an indefinite shelf life if properly stored in its original sealed container. Safety data sheets are available on request.

Typical Physical Properties

Boiling Point °C	103.2
Pour Point °C	-70
Molecular Weight	438
Density, g/l	1.839
Specific Heat, kJ/kg °C	1.0019
Viscosity, (dynamic), mPas	2.95
Kinematic Viscosity	1.604
Critical Temperature, °C	K
Vapour Pressure	4.5 kPa
Vapour Density	ca. 0.012 g/ml

* Estimated value

The above typical physical properties, in no way form or represent product specification.